AD_____

GRANT NUMBER DAMD17-94-J-4054

TITLE: Novel Cytochrome P4501B1 as a Mammary Cancer Risk Factor

PRINCIPAL INVESTIGATOR: Colin R. Jefcoate, Ph.D.

CONTRACTING ORGANIZATION: University of Wisconsin
Madison, Wisconsin 53706-4880

REPORT DATE: July 1998

TYPE OF REPORT: Final

PREPARED FOR: Commander
U.S. Army Medical Research and Materiel Command
Fort Detrick, Maryland 21702-5012

REPORT DOCUMENTATION PAGE

Form Approved
OMB No. 0704-0188

1. AGENCY USE ONLY *(Leave blank)*	2. REPORT DATE	3. REPORT TYPE AND DATES COVERED
	July 1998	Final (1 Jul 94 - 30 Jun 98)

4. TITLE AND SUBTITLE
Novel Cytochrome P4501B1 as a Mammary Cancer Risk Factor

5. FUNDING NUMBERS
DAMD17-94-J-4054

6. AUTHOR(S)
Colin R. Jefcoate, Ph.D.

7. PERFORMING ORGANIZATION NAME(S) AND ADDRESS(ES)
University of Wisconsin
Madison, Wisconsin 53706-4880

8. PERFORMING ORGANIZATION REPORT NUMBER

9. SPONSORING/MONITORING AGENCY NAME(S) AND ADDRESS(ES)
Commander
U.S. Army Medical Research and Materiel Command
Fort Detrick, MD 21702-5012

10. SPONSORING/MONITORING AGENCY REPORT NUMBER

11. SUPPLEMENTARY NOTES

19990301000

12a. DISTRIBUTION / AVAILABILITY STATEMENT
Approved for public release; distribution unlimited

12b. DISTRIBUTION CODE

13. ABSTRACT *(Maximum 200*

We have recently documented the expression of CYP1A1 and CYP1B1, both of which are inducible by many environmental pollutants via the Ah receptor [AhR], in human breast cells. The expression of CYP1B1 and CYP1A1 has been quantitated in primary human breast luminal and basal epithelial cells [LEC and BEC, respectively], in BF, and in estrogen receptor positive and negative (ER^+ and ER^-, respectively) breast tumor cell lines. CYP1B1 is constitutively expressed in LEC, BEC, and BF, whereas constitutive expression of CYP1A1 is almost undetectable. Following 2,3,7,8-tetrachlorodibenzo(p)dioxin [TCDD]-induction, similar levels of CYP1B1 and CYP1A1 are expressed in LEC and BEC. Additionally, these cytochromes (CYPs) demonstrate widely different linkages to the estrogen receptor and to increased progression of tumorigenesis. We have shown that BF exhibit CYP1B1 activity and, most significantly, have shown that these cells also express functional ER. We have shown that CYP1B1, indeed, mediates 4-hydroxylation in normal HBEC, but at low rates unless induced by environmental AhR agonists. The examination of PAH-DNA adduct formation in primary cultures of three donors has demonstrated substantial dose-dependent DNA adduct formation in the breast epithelia following exposure to dibenzo(a)pyrene, a prevalent environmental contaminant.

14. SUBJECT TERMS	15. NUMBER OF PAGES
Cytochrome P450, Estradiol, Fibroblast, Environmental Chemicals, Oxidative Stress, Inhibition, Breast Cancer	230
	16. PRICE CODE

17. SECURITY CLASSIFICATION OF REPORT	18. SECURITY CLASSIFICATION OF THIS PAGE	19. SECURITY CLASSIFICATION OF ABSTRACT	20. LIMITATION OF ABSTRACT
Unclassified	Unclassified	Unclassified	Unlimited

FOREWORD

Opinions, interpretations, conclusions and recommendations are those of the author and are not necessarily endorsed by the U.S. Army.

Non Where copyrighted material is quoted, permission has been obtained to use such material.

Non Where material from documents designated for limited distribution is quoted, permission has been obtained to use the material.

✓ Citations of commercial organizations and trade names in this report do not constitute an official Department of Army endorsement or approval of the products or services of these organizations.

✓ In conducting research using animals, the investigator(s) adhered to the "Guide for the Care and Use of Laboratory Animals," prepared by the Committee on Care and use of Laboratory Animals of the Institute of Laboratory Resources, national Research Council (NIH Publication No. 86-23, Revised 1985).

N/A For the protection of human subjects, the investigator(s) adhered to policies of applicable Federal Law 45 CFR 46.

✓ In conducting research utilizing recombinant DNA technology, the investigator(s) adhered to current guidelines promulgated by the National Institutes of Health.

✓ In the conduct of research utilizing recombinant DNA, the investigator(s) adhered to the NIH Guidelines for Research Involving Recombinant DNA Molecules.

✓ In the conduct of research involving hazardous organisms, the investigator(s) adhered to the CDC-NIH Guide for Biosafety in Microbiological and Biomedical Laboratories.

PI - Signature Date

Table of Contents
for
Grant No. DAMD17-94-J-4054

Final Progress Report **DAMD17-94-J-4054**

Goals of this Research:

In 1994, at the beginning of this grant period, this laboratory had just cloned a novel mouse cytochrome P450 [CYP], CYP1B1, resulting from the previous purification and characterization of the protein in mouse embryo fibroblast and rat adrenal (1-3) cells. Human CYP1B1 was also cloned in 1994, isolated as one of several 2,3,7,8-tetrachlorodibenzo(*p*)dioxin [TCDD]-inducible genes in human keratinocytes (4). This proposal aimed to show that CYP1B1 and CYP1A1 were both functional in normal human breast cells and were responsive to environmental chemicals that accumulate in human breast fat. We also aimed to test the hypothesis that CYP1B1 was responsible for estradiol 4-hydroxylation in normal human breast epithelial cells [HBEC]. We, additionally, recognized that the expression of CYP1B1 in human breast fibroblasts [BF] may modulate the signaling produced by estrogens that are locally synthesized in these same cells.

Introduction:

CYP1B1 is involved in the metabolism of environmental chemicals, particularly polycyclic aromatic hydrocarbons [PAHs], as well as playing an important role in normal physiological function. For example, a role for CYP1B1 in developmental regulation has been shown whereby a deficiency in CYP1B1 leads to congenital glaucoma which results from a failure to develop an adult trabecula network in the anterior chamber of the eye (5). Recent work from this laboratory with CYP1B1(-/-) fibroblasts indicates a role in the differentiation to adipocytes. Furthermore, a role for CYP1B1 in the physiological functioning of the breast is suggested by the selective expression in steroidogenic tissues under hormonal control as well as in embryonic tissues and fibroblastic outgrowth (2, 6). CYP1B1 mediates the conversion of estradiol to 4-catechol estrogen, a steroid which undergoes redox cycling (7-8). This conversion is higher in breast and uterine tumors relative to surrounding tissue (9). The donor-dependent regulation of CYP expression in various mammary epithelia is dependent on the presence of differentiating factors [extracellular matrix (ECM), hormones]. These factors stimulate expression of CYPs in rat luminal epithelia, while also stimulating formation of ductal structures and differentiation, as recognized by markers such as ß-casein (10-11). CYP1A1 is detectable in invasive breast carcinomas (12), and a mutation in the 3'-UTR may be a risk factor [odds ratio of 7] for breast cancer in African Americans (13).

Carcinogenesis may be initiated through the CYP-mediated conversion PAHs to polycyclic aromatic hydrocarbon dihydrodiol epoxide [PAHDE] metabolites (14) [Fig. 1].

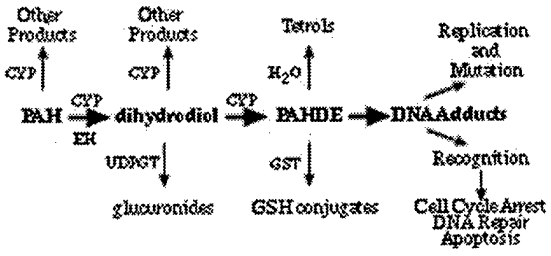

Fig. 1. Formation of PAHDE-DNA adducts depends on the partitioning between activation and inactivation steps.

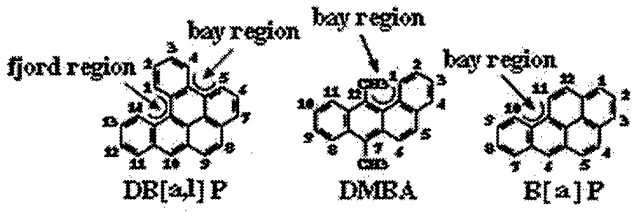

Fig. 2. PAH Chemical Structures.

CYP-mediated epoxidation of precursor dihydrodiols [PAHDH] generates PAHDE which react with and modify DNA bases. For most PAHs [e.g., benzo(a)pyrene (BP)], these PAHDE are only effective in forming DNA adducts and in initiating tumorigenesis when located adjacent to a bay region of the PAH [benzo[*a*]pyrene 7,8-diol-9,10-epoxide (BPDE)] [Fig. 2] (15). However, recent work has shown that benzo[*c*]phenanthrene-derived PAHs, such as dibenzo(a,l)pyrene [diBP], which contain a "fjord" configuration are far more potent carcinogens [Fig. 2] (16). DiBP has been shown to be 25-fold more potent than BP in a rat mammary cancer assay (17), and syn- and anti-diBPDE were 100 times more potent than anti-BPDE in V79 mutagenesis assays.

In this research, we have set out to measure the expression of CYP1B1 in relation to the better characterized CYP1A1, notably to assess basal expression and inducibility by many environmental pollutants [TCDD, polychlorinated biphenyls (PCBs), PAHs] via the Ah receptor [AhR], in human breast cells. We have assessed the capacity of CYP1B1 in comparison to CYP1A1 to activate PAHs to carcinogenic PAHDE (16). In order to assess the role of CYP1B1 and CYP1A1 in breast cancer, we have quantitated their expression in primary human breast luminal and basal epithelial cells [LEC and BEC, respectively] and in estrogen receptor positive and negative [ER^+ and ER^-, respectively] breast tumor cell lines. This work shows that CYP1B1 exhibits a very different pattern of expression from that of CYP1A1, demonstrating widely different linkages to the ER and to changes in cell type. We have shown that CYP1B1, indeed, mediates 4-hydroxylation in normal HBEC, but at low rates unless induced by environmental AhR agonists. We have correlated this activity with 7,12-dimethylbenz(a)anthracene [DMBA] metabolism at CYP1B1-regioselective positions [5,6- and 10,11-dihydrodiol formation] which provides a marker of functional CYP activity. We have assessed whether the substrate selectivity of the human CYPs is different from the rodent forms. To test the role of BF in mediating signaling to LEC or BEC, we have measured levels of ER, its functionality, and the expression of CYP1B1 in these cells. In order to determine whether CYP1B1, CYP1A1, or the AhR provide markers of breast cancer progression, we have quantitated expression in a set of eight cell lines which exhibit differences in the state of tumor progression. We aim to relate these model systems to measurements of normal breast tissue and tumors.

Body:

Specific Studies:

1. Cytochrome P450 expression in cultured human breast cells.

We have shown that cultured HBEC demonstrate a CYP1B1 predominance in mediating basal DMBA metabolism, a marker of functional CYP activity [Table 1]. Nevertheless, several donors expressed sufficient CYP1A1, albeit at very low levels, to contribute substantially to basal activities. The analysis of the recombinant proteins demonstrated that CYP1B1 is six times less active than CYP1A1 in the metabolism of DMBA. Those donors exhibiting measurable levels of basal CYP1A1 activity may be expected to show an enhanced capability for the bioactivation of PAHs. TCDD-induced DMBA metabolism exceeded basal levels by >100-fold. CYP1A1 contributes 75-85% of the induced activity, and CYP1B1 contributes 15-25% of the activity. This difference is consistent with turnover numbers of the recombinant CYPs. We have noted substantial variability in CYP expression among eight donors, although this is greater for CYP1A1 [as much as 21-fold] than for CYP1B1 [as much as 7-fold] [Figs. 3 and 4]. Quantitation of AhR and aryl hydrocarbon nuclear translocator [ARNT] protein expression, proteins which mediate CYP expression, indicate inter-individual variation [up to 3-fold], compatible with a variability in AhR levels seen in the lungs from multiple donors (18). AhR levels did not appear to correlate with variation in the level of expression of either of the CYPs. This is not surprising since AhR and ARNT protein levels in the breast cells

were extremely high [50-100 times higher than MCF-7 cells] and were probably not limiting factors in the regulation of CYP expression [Appendix, *Cancer Res.* **58**, 2366-2374, 1998].

TABLE 1. Antibody Inhibition of Microsomal DMBA Dihydrodiol Formation in Primary HMEC.

Treatment / IgG Addition	Dihydrodiols 5,6-	8,9-	10,11-	3,4-	Total Dihydrodiol Formation (pmol/mg/hr)	% Inhibition
PRIMARY HMEC						
Constitutive						
Donor D						
(+) pre-immune	0.29	0.34[d]		0.19	**0.82**	**0**
(+) anti-1A1[a]	0.29	0.35		0.12	**0.76**	**7**
(+) anti-1B1[b]	0.07	0.05		0.01	**0.13**	**84**
Donor E						
(+) pre-immune	0.21	1.96[d]		0.14	**2.31**	**0**
(+) anti-1A1[a]	0.32	1.25		0.10	**1.48**	**36**
(+) anti-1B1[b]	0.13	1.01		0.19	**1.52**	**34**
TCDD-Induced[c]						
(+) pre-immune	17	68	12	7	**104**	**0**
(+) anti-1A1[a]	6	10	4	2	**22**	**79**
(+) anti-1B1[b]	10	55	8	5	**78**	**25**
(+) anti-1A1+anti-1B1[ab]	2	5	2	1	**10**	**90**
RECOMBINANT HUMAN CYTOCHROMES P450						
CYP1B1[e]	50	33	27	17	**127**	
CYP1A1[f]	189	870	73	80	**1212**	

[a]10mg IgG/mg microsomal protein.
[b] 5mg IgG/mg microsomal protein.
[c]Metabolism demonstrated by donor D.
[d]8,9-+10,11- DMBA dihydrodiols, peaks were poorly resolved at this low level of activity.
[e]Recombinant human CYP1B1 expressed in lymphoblast microsomes (Gentest Corp.), 74-pmol/mg.
[f]Recombinant human CYP1A1 expressed in lymphoblast microsomes (Gentest Corp.), 104-pmol/mg.

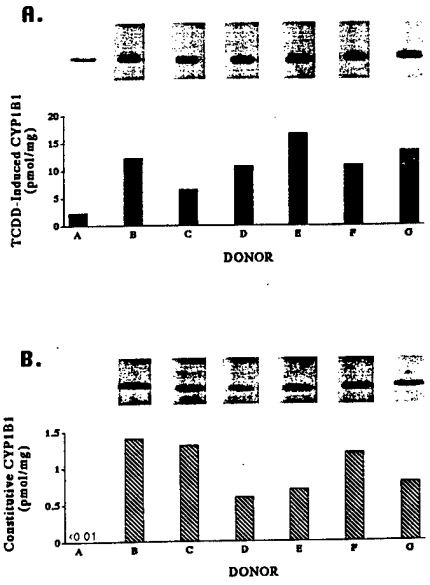

Fig. 3. Quantitative immunoblot analysis of TCDD-induced [A] and constitutive [B] CYP1B1 expression in cultured HBEC. Recombinant human CYP1B1 [74 pmol/mg; Gentest Corp.] was utilized for the generation of standard curves for the quantitation of CYP expression by soft laser scanning densitometry.

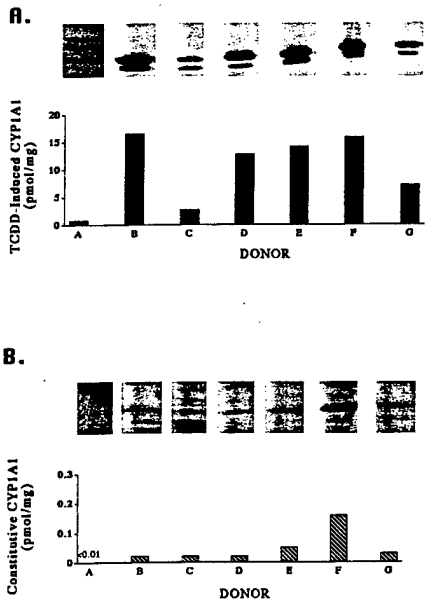

Fig. 4. Quantitative immunoblot analysis of TCDD-induced [A] and constitutive [B] CYP1A1 expression in cultured HBEC. Recombinant human CYP1A1 [104 pmol/mg; Gentest Corp.] was utilized for the generation of standard curves for the quantitation of CYP expression by soft laser scanning densitometry.

Heterogeneous HBEC populations undergo a phenotypic change under serum-free conditions, in which LEC express BEC characteristics in response to hormones present in the media (19-20). We have found that TCDD-inducible CYP1A1 expression peaks early in passage 2 and then declines [concomitant with a decrease in LEC], while CYP1B1 expression is largely unchanged. Separation of LEC and BEC was achieved using the method of Chang (20-21). We found that CYP1A1 induction was over 10-fold lower in BEC, relative to LEC, while CYP1B1 was expressed at similar levels in the BEC and LEC [Fig. 5].

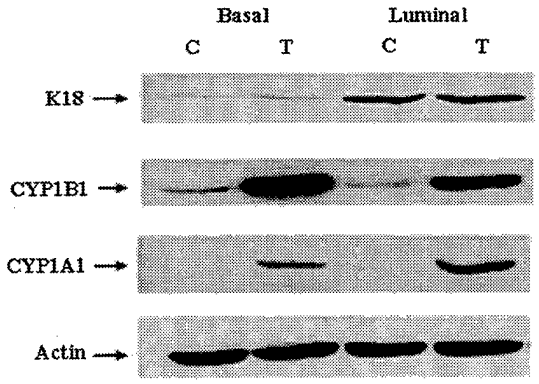

Fig. 5. Immunoblot analysis of CYP expression in separated BEC and LEC of one representative donor.

In order to assess the impact of tumor cell progression on CYP expression, we have examined eight human mammary epithelial cell lines. These range from the spontaneously immortalized MCF10A to the aggressive and dedifferentiated MDA-MB-231 [MB-231] and MDA-MB-468 [MB-468] cells.

Four lines which differ in their expression of the ER [T47D, ER^+ and ER^-; MB-231, ER^+ and ER^-] established that basal CYP1B1 expression is elevated in ER^- cells, while the induction of CYP1A1 is suppressed when compared to their ER^+ counterparts [Fig. 6]. The ER antagonist, ICI 182,780, failed to produce an ER^- phenotype for CYP1B1 or CYP1A1 expression when introduced to ER^+ clones, establishing that the ER does not directly regulate CYP expression in human breast cells [Appendix, Carcinogenesis, Submitted]. The basal expression of CYP1B1 was highly variable among the eight lines, but TCDD-induction resulted in similar levels of expression in most lines. This suggests that activation of the AhR by TCDD achieves a maximum induction which is independent of cell-specific factors that modulate basal expression.

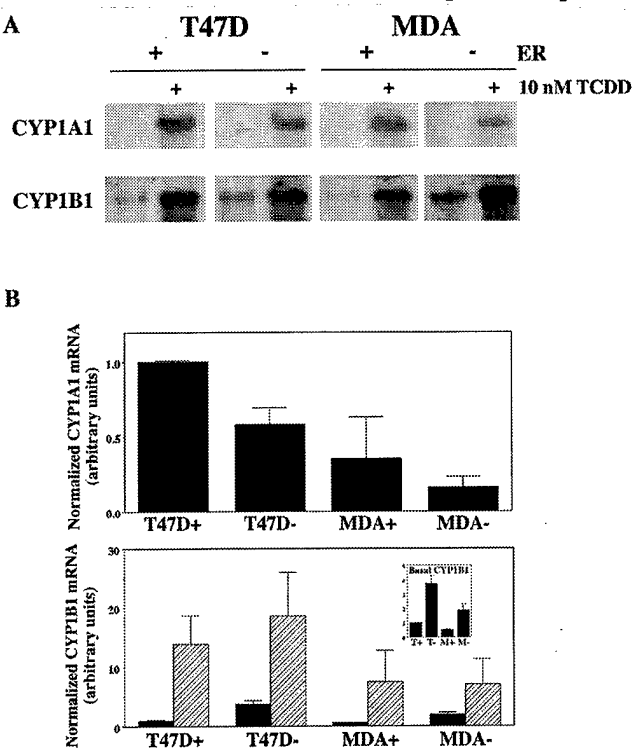

Fig. 6 Northern blot of CYP1A1 and CYP1B1 expression in estrogen receptor positive and negative clones of T47D and MDA-MB-231 cells (T47D+/-, MDA +/-, respectively) exposed to TCDD for 24 hours (A). B) Relative levels of CYP mRNA normalized to T47D+, DMSO-treated.

Surprisingly, the level of AhR expression was generally inversely proportional to the level of CYP1A1 and CYP1B1 expression, and the AhR levels were generally higher with increased stage of progression of the line.

One line, Hs578T, displayed the highest level of AhR, but demonstrated impaired AhR responsiveness, as measured through the minute induction of CYP1A1 and failure to induce CYP1B1 by TCDD [Fig. 7]. Nuclear extracts from these cells, following TCDD treatment, produced comparable gel shifts on xenobiotic response elements to those seen

with T47D cells, indicating that the lack of AhR responsiveness was not due to a defect in AhR-DNA binding or heterodimerization with ARNT.

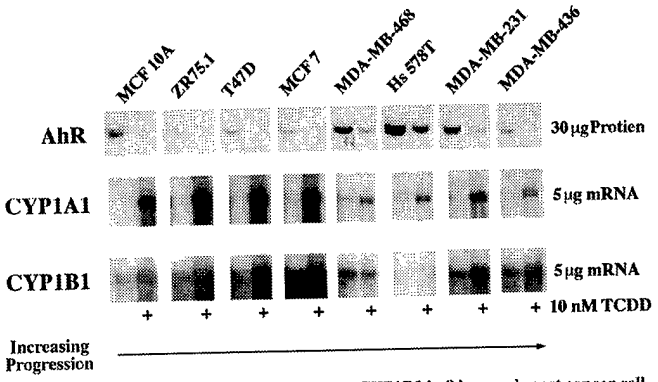

Fig. 7 Expression of Ah receptor, CYP1A1 and CYP1B1 in 8 human breast cancer cell lines of increasing progessive nature. Top: Western blot of Ah receptor expression. Center and Bottom: Northern blot of CYP1A1 and CYP1B1 expression. The general trend is for decreased CYP expression and increased Ah receptor expression with increasing progression.

We have addressed the issue of whether fibroblasts from different tissue sources would show different CYP expression characteristics. Human BF [tumors and peripheral] and human skin fibroblasts, from multiple donors, have been characterized with respect to CYP expression, DMBA metabolism, and the level of AhR and ARNT expression. We have observed variable inter-donor expression of constitutive and TCDD-induced CYP1B1 expression [Fig. 8]. However, the level of expression was relatively similar in fibroblasts from three sources within the same individual that should, otherwise, be clearly distinct [tumor, breast distal to tumor, and skin]. CYP1A1 was not detectable in any of the BF examined. Levels of CYP1B1 and associated DMBA metabolism, as well as AhR and ARNT expression were lower in the HMF than in the HBEC. The regioselective profile of DMBA metabolism in the HMF, even when TCDD-induced was consistent with a predominance of CYP1B1-mediated activity [Appendix, *Carcinogenesis* 19, In Press]. We have identified the expression of low levels of normal ER in HMF [Fig. 9]. Interestingly, the growth of HMF from both normal tissues and tumors was stimulated by estradiol and inhibited by ICI 182,780, while skin fibroblasts were unresponsive, even though expressing similar receptor levels. This finding for HMF contrasts that of the epithelia, where we detected a 58 kDa splice-variant of the normal ER.

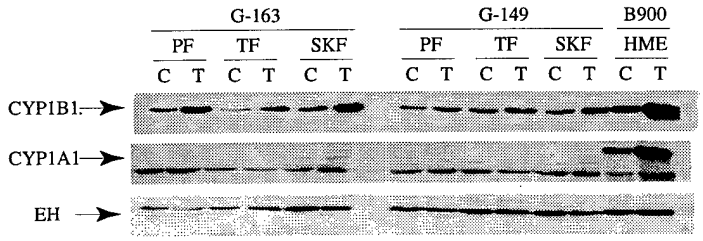

Fig. 8 Expression of CYP1B1and CYP1A1 in primary cultures of matched human mammary fibroblasts derived from normal peripheral (PF), tumor (TF), or skin (SKF) of two patients (G-163 & G-149). Epoxide hydrolase(EH) was used as a loading control.

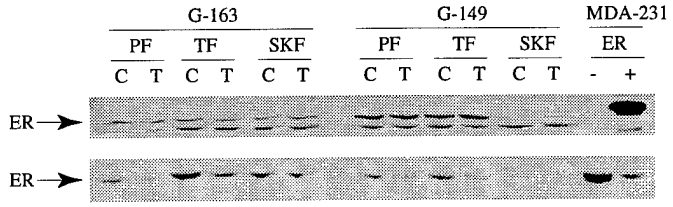

Fig. 9 Expression of Ah receptor (AhR) and estrogen receptor (ER) in primary cultures of matched human mammary fibroblasts derived from normal peripheral (PF), tumor (TF) or skin (SKF) of two patients (G-163 & G-149). Total cellular proteins were isolated from Trizole® lysates of these cells after they were treated with 10 nM TCDD for 24 h. Extracts from MB-MDA-231 human breast carcinoma cell lines (the wild type which is ER-negative, and its ER-transfected variant S30) were used as controls.

2. Cytochrome P450 expression in human breast tissue.

In addition to the characterizations of CYP expression in the cultured breast cells described above, we examined the levels of ER, CYP1B1, and CYP1A1 expression in 13 breast tissue samples by reverse transcriptase polymerase chain reaction [rtPCR] [Table 2]. We were interested in the possibility that endogenous PCBs might induce CYP1A1. Two ER^+ tumors expressed CYP1B1 at a 5-fold higher level than found in normal tissue, while one tumor [ER^-] expressed extremely low levels. In all remaining samples, the level of CYP1B1 expression in the tumor tissue was not significantly different from the level of expression observed in the normal tissues. CYP1A1 was only detectable in one tumor, at much lower levels than CYP1B1. This work requires completion of quantitation with DNA mimics for CYP1B1 and CYP1A1. This study will be completed in the next six months with the analysis of a larger pool of ER^+ and ER^- tumors.

Table 2. rtPCR analysis of CYP1B1 and estrogen receptor [ER] expression in normal and tumor-derived human breast tissue.

	Relative Expression	
Tissue Sample	**ER**	**CYP1B1**
Tumor Tissue		
1	3.9	2.2
2	3.8[a]	2.3
3	3.5	2.7
4	3.5	2.0
5	3.5[a]	5.0
6	1.8	0.4
7	1.7	5.3
8	1.2	2.6
9	0.9	2.2
10	0.8[b]	2.9
11	0.9[b]	2.8
Normal Tissue		
12	2.4	2.2
13	1.0	1.1

[a] Tissue was clinically diagnosed as ER^+.
[b] Tissue was clinically diagnosed as ER^-.

3. Metabolism-based inhibition of human CYP1B1 and CYP1A1.

Metabolism-based inhibitors provide a means to resolve CYP1B1- or CYP1A1-mediated activities. We have analyzed a series of mechanism-based ethynyl-substituted PAH inhibitors, provided by Dr. Alworth (Tulane) (22) [Fig.10], for their selectivity in inhibiting DMBA metabolism by recombinant CYP1B1 and CYP1A1 [expressed in V79 cells; Table 3]. The effectiveness of three of these inhibitors was also examined in TCDD-induced MDA-MB-231 [express predominantly CYP1B1] and T47D [express predominantly CYP1A1] human breast tumor cell lines [Fig. 11]. The majority of the compounds examined were more potent inhibitors of human CYP1B1 than CYP1A1. Notably, 2-ethynylphenanthrene [2EPH] (2.5 μM) reduced recombinant CYP1B1 activity by 53%, while stimulating CYP1A1-mediated metabolism. This inhibition by 2EPH was shown to be irreversible. At the other extreme, methyl-1-ethynylpyrene [M1EP] (0.5 μM; 2 hr pretreatment) inhibited recombinant CYP1A1 by 65% and CYP1B1 by 52%. The inhibition of human CYP1B1 by these inhibitors was typically at least 10-fold weaker than the equivalent mouse forms and exhibited less dramatic differences of selectivity of inhibition with respect to the two CYPs. This is consistent with much lower effectiveness of human CYP1B1 in the metabolism of many PAHs. Nevertheless, the ratio of inactivation effected by these inhibitors, by for example 1EP versus M1EP, provides a useful diagnostic of the involvement of CYP1B1 or CYP1A1 in human cellular metabolism.

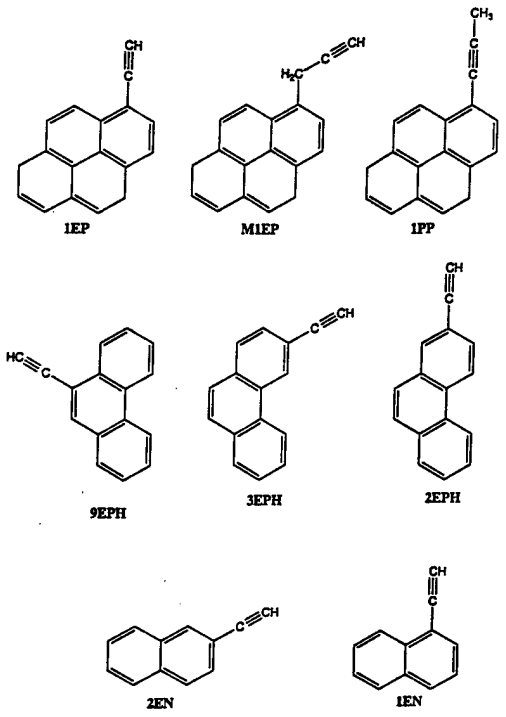

Fig. 10. Chemical structures of ethynyl-substituted PAH inhibitors analyzed for their selectivity in the inhibition of CYP1B1 and CYP1A1 functional activity.
[1EP, 1-ethynylpyrene; M1EP, methyl-1-ethynylpyrene; 1PP, 1-propynylpyrene pyrene; 9EPH, 9-ethynylphenanthrene; 3EPH, 3-ethynylphananthrene; 2-EPH, 2-ethynylphenanthrene; 2EN, 2-ethynylnapthalene; 1EN, 1-ethynylnaphthalene].

Table3. Inhibition of cellular human recombinant CYP1B1 and CYP1A1 DMBA metabolism.

		% Remaining Activity[a]	
Inhibitor	[μM]	CYP1B1[b]	CYP1A1[c]
1EP	[2.5]	30	74
M1EP	[0.5]	48	35
2EPH	[2.5]	47	148
9EPH	[2.5]	81	92
1PP	[0.5]	16	14

[a]Percent of DMBA metabolism relative to control [untreated] cells. Inhibitors were incubated with the cells for 120 min., media was removed, and DMBA [10 μM] added for 60 min.

[b]Analyses completed in V79 cells expressing recombinant human CYP1B1.

[c]Analyses completed in V79 cells expressing recombinant human CYP1A1.

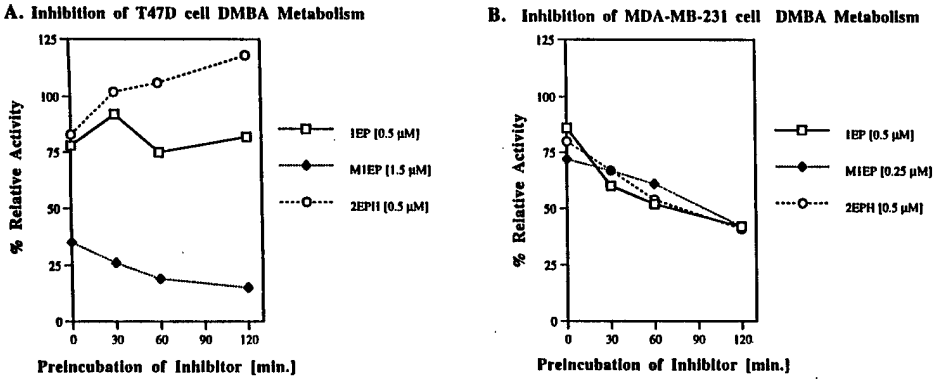

Fig. 11. Inhibition of CYP1B1- and CYP1A1-mediated DMBA metabolism in T47D and MDA-MB-231 human breast tumor cell lines. Data is normalized relative to uninhibited, control DMBA metabolism.

4. PAH-DNA adduct formation and cellular response in primary human breast epithelial cells.

We have measured the formation of DNA adducts in primary HBEC, treated with either diBP or diBP-11,12-dihydrodiol [diBPDH] [with and without prior treatment with 3,4,5,3',4',5'-hexachlorobiphenyl (HCB)], from three different donors for which we have characterized CYP1B1, CYP1A1, p53, and p21 expression. DiBP, diBPDH, and 3,4,5,3',4',5'-HCB elevated the expression of both CYP1B1 and CYP1A1 in the primary HBEC, consistent with AhR activation [Fig. 12].

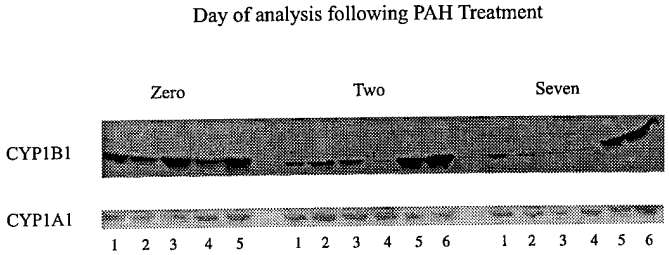

Fig. 12. Immunoblot analysis of CYP1B1 and CYP1A1 expression in primary human breast epithelial cells following exposure to:
(1) solvent control, (2) diBP (0.1 uM; 24 h), (3) diBP (1.0 uM; 24 h),
(4) diBP-11,12-diol (0.1 uM; 2h),
(5) diBP-11,12-diol / 3,4,5,3',4',5'-Hexachlorobiphenyl (24 h pretreatment; acute exposure)
(6) diBP-11,12-diol / 3,4,5,3',4',5'-Hexachlorobiphenyl (24 h pretreatment; chronic exposure).

The induction of CYP1B1 [mRNA and protein] by diBP is much more effective than the induction of CYP1A1, indicating a contribution from an AhR-independent mechanism. The magnitude of total adduct formation varied among the donors, with adduct generation being negligible in the untreated cells and substantially increasing, in a dose-dependent manner, with exposure to diBP.

DiBPDH also generated significant levels of adducts which were increased by TCDD pretreatment but were surprisingly obliterated by pretreatment with the 3,4,5,3',4',5'-HCB [Fig. 13]. This suggests CYP1B1-specific inhibition by HCB. Indeed, Spink and coworkers have shown a similar potent inhibition of CYP1B1-mediated estradiol metabolism by this PCB (23).

We recognize that initiation of the cancer process results from a mutational event that requires replication of DNA which has been modified by the metabolite. The surveillance processes typically prevent this event by preventing replication [cell cycle arrest], by stimulating repair, and by diverting damaged cells towards apoptosis. We are, therefore, interested in characterizing the response of the cells to chemical insult [PAH-DNA adduct formation] by measuring the expression of specific markers of cell cycle arrest and apoptosis. Preliminary FAC-Scan analysis shows a predominant arrest in G2 two days after diBP treatment [Fig. 14]. The expression of p53 was detectable in all confluent cultures and increased substantially 48 hr after exposure to diBP. Levels of diBPDH that produced comparable levels of PAHDE adducts, although with a different distribution, did not produce this response. This elevation of p53 diminished substantially after a further 6 days of culture. Conversely, p21 expression was high in early confluent cultures, presumably as a consequence of confluent arrest, and then declined after a further 48 hr. On day 7, when p53 was declining, p21 became elevated in cultures treated with either diBP or diBPDH [Fig. 15]. Thus, 24 hr after the peak level of adduct formation p53 rises, apparently not as a general response to adducts, but rather as a more selective response to diBP. The late p21 increase appears to be distinct from the early p53 response and more generally proportional to the relative levels of PAHDE adducts.

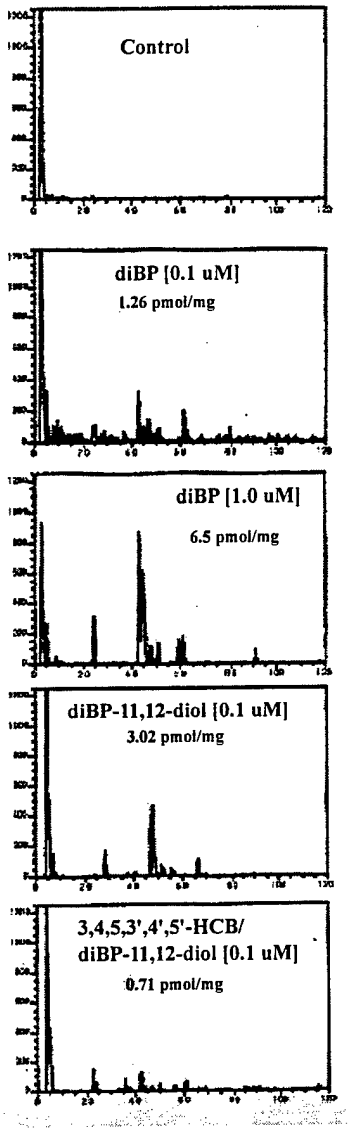

Fig. 13. DNA adduct formation in primary human breast epithalia from one representative donor.

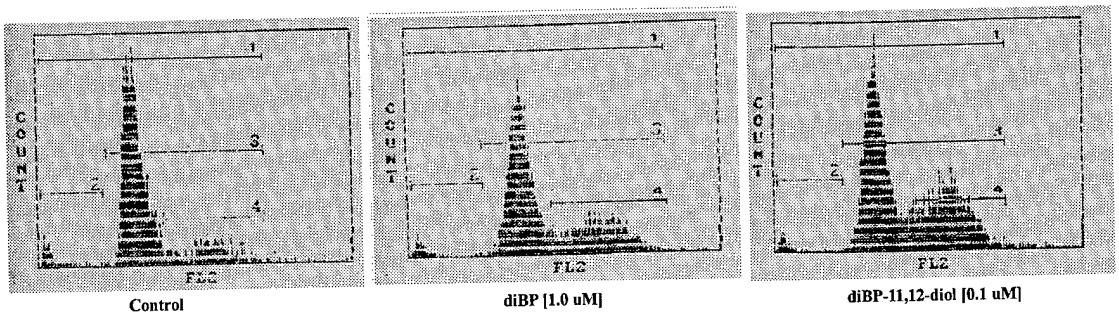

Fig. 14. FACS cell cycle analysis of primary human breast epithelia treated with diBP [24 h], diBP-11,12-diol [2 h], or solvent control [data from one representative donor].

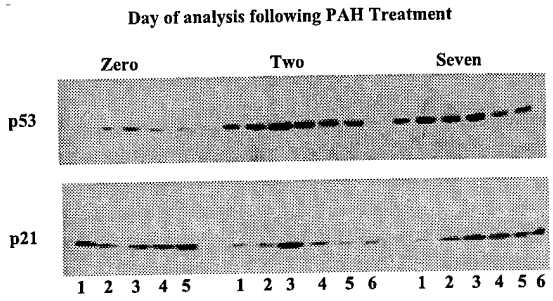

Fig. 15. Immunoblot analysis of the cellular response in primary human breast epithelia following exposure to: [1] solvent control, [2] diBP [0.1 uM; 24hr], [3] diBP [1.0 uM; 24hr], [4] diBP-11,12-diol [0.1 uM; 2hr], [5]diBP-11,12-diol/3,4,5,3',4',5'-HCB [24hr pretreatment; acute exposure], [6] diBP-11,12-diol/ 3,4,5,3',4',5'-HCB [24hr pretreatment; chronic exposure]. [Data obtained from one donor. Two other donors showed more dramatically enhanced p53 response to diBP (conditions 3) at day 2].

5. Estradiol metabolism in cultured primary human breast epithelial cells.

Breast cancer has been linked to heightened cellular estrogen activity (24). We have collaborated with Dr. Joachim Liehr to show that uterine mesenchymal tissues expressed estradiol 4-hydroxylase activity to a much larger extent than surrounding non-tumor tissue. Anti-CYP1B1 antibodies inhibited this activity by 70% consistent with our measurements with this antibody in HBEC. This activity was also blocked by 9-ethynylanthracene, which we have shown to selectively inhibit CYP1B1, but not CYP1A1 [Appendix, *Proc. Natl. Acad. Sci. USA* **92**, 9220-9224, 1995]. We have quantitated estradiol metabolism [constitutive and TCDD-induced] in cultured HBEC from four donors for which we have quantitated CYP1B1 and CYP1A1 expression and their contributions to DMBA metabolism, relative to human recombinant CYP1B1 and CYP1A1 [expressed in V79 cells]. The ratio of 4-OH/2-OH of estradiol generated by recombinant CYP1B1 and CYP1A1 was 3.7 and 0.5, respectively. The primary HBEC demonstrated variable levels of basal CYP1B1-mediated metabolism [4-OH], ranging from 0.04-0.27 pmol/mg/min, which was induced 8-to 23-fold by treatment with TCDD [Table 4]. CYP1A1-mediated metabolism [2-OH] was characterized by low levels of basal activity [0.01-0.05 pmol/mg/min] which increased by as much as 100-fold upon TCDD-induction. These analyses verify that the oxidative metabolism of estradiol at the 4- and 2-positions strongly correlates with levels of CYP1B1 [r^2=0.900] and CYP1A1 [r^2=0.999] protein expression, respectively, for these donors and that only the CYP1B1-mediated 4-hydroxylation was observable in absence of an inducer.

Table 4. Estrodiol metabolism in primary human breast epithelial cells.

Sample / Donor	2-OH E_2		4-OH E_2	
	Control[a]	TCDD[b]	Control[a]	TCDD[b]
	(pmol/mg/min)			
hCYP1A1[c]	1.67		0.78	
hCYP1B1[d]	0.27		1.01	
Donor E	0.01	0.54	0.06	0.85
Donor F	0.02	0.56	0.10	1.11
Donor H	0.01	1.05	0.04	0.90
Donor I	0.05	0.60	0.27	2.07

[a] Cells remained untreated.
[b] Cells were treatedwith 10^{-9} M TCDD.
[c] Human recombinant CYP1A1 expressed in V79 cells.
[d] Human recombinant CYP1B1 expressed in V79 cells.

6. TCDD and growth factor signaling in human breast cells.

TCDD may potentially affect the regulation of CYP expression via effects on growth factor signaling. We have found that the expression of the membrane tyrosine kinase, c-erbB2, is elevated in ER^+ cell lines exposed to TCDD. In the T47D cell line TCDD treatment [24 hr, 10^{-8}M] increased c-erbB2 and c-erbB3 mRNA expression 4-fold and proportionate increases in the receptor proteins, including phosphotyrosine forms [Fig. 16]. Thus, TCDD enhanced a set of signaling responses to heregulin, and erbB3 agonist. This included a 4-fold increase in the expression of MAPK, increased phosphorylation of the p85 subunit of PI3K, and stimulation of cell proliferation.

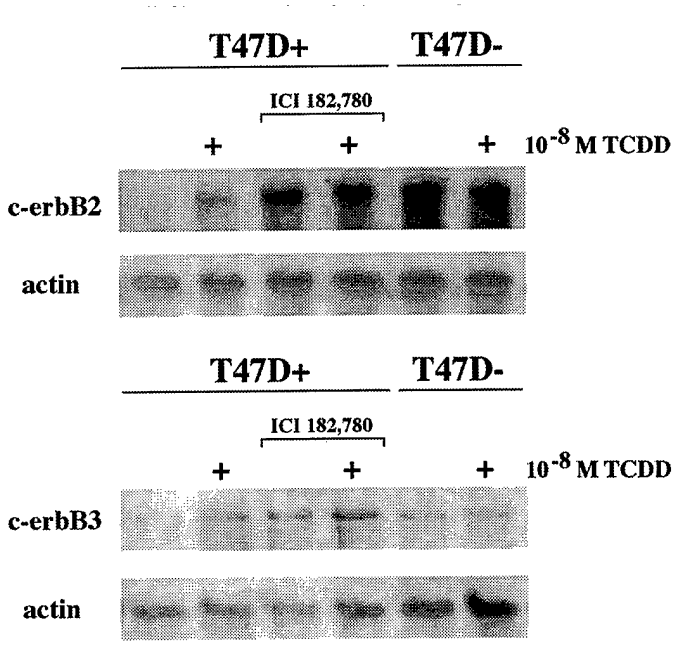

Fig. 16 Northern blot of c-erbB2 and c-erbB3 expression in estrogen receptor positive and negative T47D cells (T47D+, T47D-, respectively) exposed to TCDD for 48 hours. Antiestrogen ICI 182,780 maximally induces c-erbB2 and c-erbB3 in T47D+ cells. In T47D- cells, c-erbB2 is expressed at a high level, and c-erbB3 expression is repressed.

These data suggest that TCDD can also produce signaling responses in breast cells via indirect effects of AhR activation [Appendix, Submitted to *Oncogene*].

7. Cytochrome P450 regulation in cultured rat mammary epithelial cells.

We have shown that cultured rat epithelia, express elevated levels of CYP1B1 and CYP1A1 when grown on the ECM, Matrigel, but not on plastic. In addition, the expression of CYP1A1 and CYP1B1 differs dramatically between Wistar Furth and Wistar Kyoto rat strains. WF rats are highly susceptible to chemically induced mammary cancer while the WK strain is highly resistant. ß-Napthoflavone-induced CYP1A1 expression was 5-fold higher in WK cells relative to the WF strain, while CYP1B1 expression was 5-fold higher in the WF strain [Fig. 17].

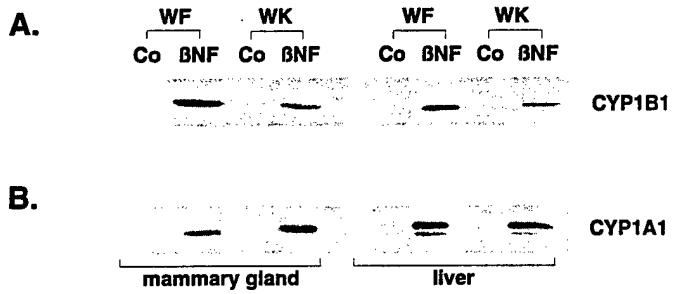

Fig. 17. Immunoblot analysis of tissue-specific CYP1B1 and CYP1A1 expression in Wistar Furth [WF] and Wistar Kyoto [WK] rats. Female WF and WK rats were injected with vehicle control or 60 mg/kg β–naphthaflavone [βNF] prior to sacrifice.

Interestingly, this strain-specific CYP expression was not demonstrated in hepatic tissues. This tissue-specificity in CYP expression may reflect differences in mammary nuclear regulatory factors that are linked to AhR activity [Appendix, Carcinogenesis, In Press pending minor corrections]. Rat BF were shown to express AhR-inducible CYP1B1, but not CYP1A1, and this induction is blocked by glucocorticoids, acting via the CYP1B1 upstream enhancer element [Fig. 18] [Appendix, Mol. Pharmacol., In Press].

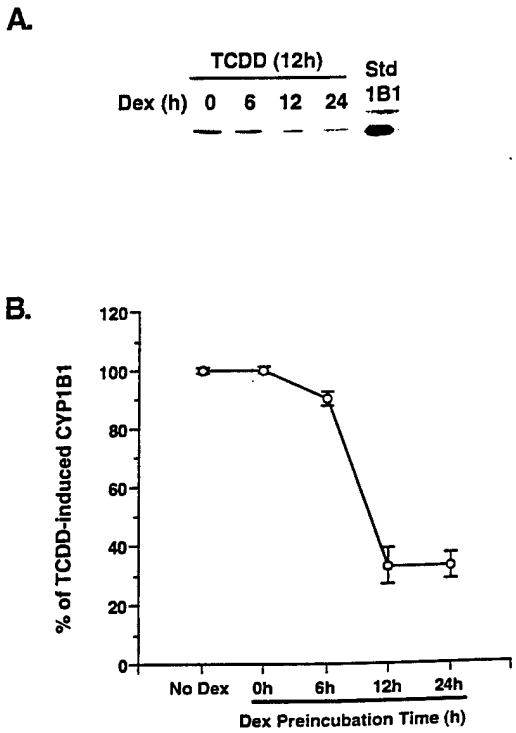

Fig. 18. Immunoblot analysis of the effect of dexamethasone [Dex] on TCDD induction of microsomal CYP1B1 protein. Rat mammary fibroblasts were isolated and cultured to 75-80% confluence, preincubated with 10^{-7} M Dex for 0, 6, 12, or 24 h, as indicated, followed by treatment with 10^{-9} M TCDD for 12 h prior to analysis.

Experimental Methods:

Cell Culture

All cell lines were maintained in monolayer culture in 6 well dished, 75 cm^2 or 175 cm^2 flasks in a humidified 5% CO_2 atmosphere. Cell lines were passaged using 0.5% trypsin at 80-90% confluence.

Mammary Organoid Preparation:

Human mammary organoid preparations were provided by Dr. Michael Gould and the UW Comprehensive Cancer Center Cell Bank. The mammary tissue was processed and organoids isolated in the Gould laboratory, according to previously published procedures

(25). Primary organoids were plated ($2x10^4$ cells/cm^2) on plastic and cultured in mammary epithelial growth media (MEGM; Clonetics) supplemented with penicillin-streptomycin (50 U/ml penicillin, 0.05 mg/ml streptomycin). Cells were grown at 37°C in a humidified environment of 5% CO_2 and 95% air. Confluent cells (7-10 days post-plating) were passaged by differential trypsinization, plated at $1.7x10^4$ cells/cm^2, and subsequently analyzed 6 days later. Cells either remained untreated or were treated with TCDD (10 nM) for a period of 24 h prior to analysis. Cells utilized for microsomal preparations were harvested by trypsinization and washed three times with ice cold 1X PBS.

Hybridization analysis of mRNA:

Cells from various lines were cultured in 150 mm plates, then were harvested and poly A^+ RNA isolated according to the technique of Badley et al., 1988 (26). Briefly, cells were washed with PBS (0.01 M phosphate buffer in 2.7 mM KCl and 137 mM NaCl, pH 7.4) containing 20 μM ATA and lysed in a buffer consisting of 0.2 M NaCl, 0.2 M Tris-HCl, pH 7.5, 0.15 mM $MgCl_2$ 2% SDS, 200 μg/ml Proteinase K, and 20 μM ATA. Lysates were sheared with a 23 gauge needle and incubated for 2 hours at 45 C°, then agitated with oligo dT, eluted in DEPC-treated water and precipitated with ethanol. The RNA was resuspended in sterile DEPC-treated H_2O and quantitated by reading absorbance at 260 nm.

Poly A^+ RNA was electrophoresed through a formaldehyde-containing 1% agarose gel. Capillary action was used to transfer the RNA to nylon membrane, and RNA was crosslinked to the membrane by UV. Membranes were prehybridized in a buffer of 6X SSC, 5X Denhardt's reagent, 0.1% SDS, 10 μg/ml salmon sperm DNA, and 50% formamide at 42 C° for at least 2 hours. Membranes were prehybridized, then incubated with probes for various indicated genes. Probes were randomly labeled using [α-^{32}P] dCTP (50 μCi) following the manufacturer's instructions for the Prime-It II kit. Specific activity was 10^6 cpm or greater per ml of probe. Nonspecific hybridization was removed by sequential washing with 2X SSPE + 0.5% SDS, 1X SSPE + 0.5% SDS, 0.5X SSPE + 0.5% SDS, and 0.25X SSPE + 0.25% SDS at hybridization temperature for 15 min. Signals were visualized by autoradiography and quantitated by densitometry on a laser scanner.

A 1046 bp cDNA probe from the 3' end of the human CYP1A1 was obtained from Dr. Lynne Allen-Hoffman (University of Wisconsin). The CYP1B1 cDNA probe was a 3.1 Kb fragment encoding the open reading frame of human CYP1B1, and was obtained from Dr. William Greenlee (University of Massachusetts). The probes used for c-erbB2 were a 50:50 mixture of a 1.4 Kb *neu* fragment (HP-125) from Oncogene Research Products, and an 882 bp fragment of the *c*-erbB2 cDNA obtained from Dr. M. X. Sliwkowski (Genentech, Inc. South San Francisco, CA) cut using Hind III and EcoR I. The *c*-erbB3 probe was excised from the cDNA obtained from Dr. G. Plowman (Sugen, Inc., Redwood City, CA) using Xba I and Bgl II, and was 1.3 Kb long.

Measurement of mRNA by rt-PCR:

cDNA templates for PCR were synthesized as follows: total RNA (2 μg) and the random 9-mer primer mix (1 μg), in a total volume of 31 μl, were heated to 60°C for 5 min. The samples were allowed to cool slowly to room temperature followed by the addition of the reverse transcription master mix composed of 1.0 mM of each dNTP, 40 U RNasin, 10.0 mM DTT, and 200 U M-MLV reverse transcriptase, to total of 50 μl. The samples were incubated at 40°C for 1 h followed by denaturation for 5 min at 100°C.

Primers specific to CYP1B1 (fp: 5'-CGTACCGGCCACTATCACTG-3'; rp: 5'-GCAGGCTCATTTGGGTTGGC-3') and CYP1A1 (fp: 5'-AAGCACGTTGCAGGAGCTGATG-3'; rp: ACATTGGCGTTCTCATCCAGCTGCT-3') were synthesized using an Applied Biosystems 380A synthesizer. All PCR amplifications were completed in a Perkin Elmer Cetus model 480 DNA thermocycler. CYP1B1 amplifications were composed of 2 µg cDNA template, 0.22 mM of each dNTP, 0.625 U Taq DNA polymerase, and 0.56 µM of each primer, and H_2O to a final volume of 22.5 µl. The reaction was initiated under "hot start" conditions whereby, the samples were heated to 94°C for 3 min followed by the addition of 2.78 mM $MgCl_2$. The samples were cycled for 1 min at 94°C, 1.5 min at 60°C, and 2.0 min at 72°C for a total of 30 cycles. CYP1A1 amplifications were composed of 2 µg cDNA template, 0.6 mM of each dNTP, 2.5 mM $MgCl_2$, 0.625 U Taq DNA polymerase, and 0.5 µM of each PCR primer and H_2O to a total volume of 25 µl. Cycle parameters were 1 min at 94°C, 1.5 min at 57°C, and 2.0 min at 72°C for a total of 30 cycles. PCR products were analyzed by agarose gel (1.6% agarose) chromatography and visualized by staining in ethidium bromide.

Microsomal metabolism of DMBA:

Microsomes were generated by differential centrifugation as previously described (27). Microsomal DMBA metabolism was analyzed as previously described (27). Briefly, microsomal incubations were composed of 0.2 and 1.0 mg/ml microsomal protein for induced and basal metabolism, respectively, 14.2 mM glucose 6-phosphate, 0.06 U glucose 6 phosphate dehydrogenase, 1.2 mM NADP, 6 mM $MgCl_2$, and 0.1 M potassium phosphate (pH 7.6) to a total reaction volume of 1 ml. The reaction was initiated by the addition of 1.5 µM DMBA (HPLC purified) and allowed to incubate for 15 min at 37°C, under conditions of subdued lighting. The analysis of the human recombinant CYP1B1 and CYP1A1 microsomal standards, 0.075- and 0.050 mg microsomal protein/ml, respectively, were assayed, as above, with the addition of 0.5 mg/ml human epoxide hydratase. Metabolites were extracted and the microsomal DMBA metabolic profiles were examined by reverse phase HPLC analysis. Reverse-phase HPLC separation of DMBA metabolites was accomplished using a Phenomonex Ultrasphere ODS column [5m, 4.6 mm x 25 cm] employing a gradient of 53-70% methanol gradient over the initial 30 min, 70-100% over the next 25 min, and holding at 100% for an additional 30 min. Metabolites were detected using a Waters 470 scanning fluorescence detector [excitation = 268 nm, emission = 395 nm for the 5,6-, 8,9-, and 10,11-diols; excitation = 268 nm, emission = 478 nm for 3,4-diol; excitation = 269, emission = 415 for the phenols]. The internal standard was added prior to metabolite extraction and was detected by a Beckman UV Detector Module 166, monitoring absorbance at 254 nm. Fluorescence and UV data were analyzed using Beckman System Gold Software [version 310].

Antibody Inhibition Analysis:

Antibody inhibition of microsomal DMBA metabolism was analyzed by the addition of anti-CYP1B1 (chicken; IgY, 5 mg Ab/mg microsomal protein) and anti-CYP1A1 (rabbit; IgG, 10 mg Ab/mg microsomal protein), concentrations previously determined to optimally inhibit CYP1B1- and CYP1A1-specific activities in constitutive and TCDD-induced MCF-7 cells. The corresponding pre-immune IgY or IgG was added at equivalent concentrations to serve as controls. All reaction mixtures were incubated for 45 min at room temperature prior to assaying DMBA metabolism (28).

Cellular DMBA Metabolism:

For the cellular analyses, the inhibitors were preincubated with the cells [2 h, V79 cells expressing recombinant human proteins and T47D and MDA-MB-231 tumor cell lines] in the growth media of each respective cell type, at 37°C under conditions of subdued lighting. Following the preincubation, the media was removed and replaced with the growth media containing DMBA (10 μM) and incubated for an additional 1 h at 37°C. This media was removed and treated 1:1 with β-glucuronidase solution (2000 units/ml β-glucuronidase, 0.5 M sodium acetate, pH 5.0) for 4 h at 37°C to recover the β-glucuronide conjugated DMBA metabolites. The DMBA metabolites were extracted with ethylacetate:acetone (2:1), dried under N_2, and resuspended in HPLC-grade methanol for HPLC analysis. Turnover values were normalized to cell number in the individual assay wells. Cell number was determined for each sample by trypsinizing cells and counting on a hemocytometer.

Cell lysates and Western Immunoblots:

Cellular proteins were obtained by several methods. In some studies, proteins were obtained from cells using the protein fraction of the TRIzol reagent (GIBCO) was utilized, as per the manufacturer's instructions. In other studies, cells were harvested using a lysis buffer consisting of 150 mM NaCl, 50 mM TRIS-HCl, pH 7.4, 1 mM EDTA, 1% NP-40, 0.25% deoxycholate, 0.05% SDS, 1 mM Na_3VO_4, 1 mM PMSF, 1 mM molybdate, 40 mM NaF, and 10 μl/ml protease inhibitor cocktail. Protein samples were kept frozen at -80 °C.

Cellular proteins were separated on SDS-PAGE containing 7.5% acrylamide as per Laemmli (1970) (29, 30), and transferred to nitrocellulose or PVDF membrane. Membranes were probed for various proteins, as indicated. Reactive proteins were visualized using the ECL procedure according to manufacturer's instructions.

Protein levels in cellular extracts and microsomal preparations were determined using the BCA method as per manufacturer's instructions using bovine serum albumin as a standard.

Antibodies for immunoblots were obtained as follows: CYP1A1 was generated in this laboratory, human CYP1B1 (Dr. Craig Marcus, University of New Mexico), c-erbB2 and c-erbB3 (NeoMarkers, Inc., Freemont, CA), Ah receptor (Dr. Gary Perdew, Penn State University), p53 [AB-6] and p21 [WAF-1; AB-1] (Calbiochem).

Microsomal Estrogen Metabolism:

Microsomal estrogen metabolism analyses were completed in collaboration with Dr. Joachim Liehr, as previously described (31). Briefly, microsomal proteins [200 μg TCDD-induced (10^{-9} M for 24 h); 1000 μg constitutive], 5 mM NADPH, 10 μM [^{3}H]-estradiol were incubated in 0.1 M Tris-HCl/HEPES buffer [pH 7.4] containing 5 mM ascorbic acid in a final volume of 500 μl at 30°C for 30 min. The reactions were terminated by rapid freezing followed by analysis by thin-layer chromatography.

DNA Adduct Analysis:

PAH-DNA adduct formation was analysis was completed in collaboration with Dr. William Baird. HBEC cultures were treated with diBP, diBP-11,12-dihydrodiol, and HCB as indicated in the figure legends. Cells were lysed with TRIzol reagent and the DNA isolated according to manufacturer's protocols. DNA adduct quantitation was completed as previously described (32). Briefly, 10 μg DNA was digested with Nuclease P1 and prostatic acid phosphatase, postlabeled with [γ-^{33}P]ATP [3500 Ci/mmol], cleaved to adducted mononucleotides with snake venom phosphodiesterase I, and prepurified with Sep-Pak C_{18} cartridge, and analyzed by C_{18} reverse-phase HPLC.

To be completed:

A number of papers remain to be completed. Notably, rtPCR studies of breast tumor RNA and estrogen regulation of human breast fibroblasts.

Conclusions:

This research has addressed the level and selectivity of expression of a novel cytochrome P450, CYP1B1, which is present in breast cells. We have established that CYP1B1 is present in LEC, BEC, BF, and in a broad range of breast tumor cells. We have compared this expression pattern with a related CYP isoform, CYP1A1. This form shows a very different expression selectivity with detection of constitutive levels only in more metastatic breast tumor lines. Each form is inducible by chemicals [PAHs, PCBs, dioxins] that bind to the cytosolic protein, the AhR. We have shown that each form metabolized estrogen to catecholestrogens and PAHs to carcinogenic dihydrodiols. The products formed by each form are different. Thus, CYP1A1 produces 2-hydroxyestradiol while CYP1B1 produces 4-hydroxyestradiol. Induction of these forms by dioxin [TCDD] is paralleled by a potent anti-estrogen effect demonstrated by elevation of c-erbB2, a protein that is over-expressed in many breast tumors. This anti-estrogen effect may be due to enhanced depletion of estrogens by the increased levels of P450 or due to a direct intervention by the activated AhR. Each CYP also produces a different set of products from a PAH, such as DMBA, and shows a different substrate selectivity. These reactions generate carcinogenic metabolites [dihydrodiol epoxides that bind to DNA bases]. Constitutive levels of CYP1B1 and CYP1A1 may certainly be predictors of risk from exposure to these chemicals.

While these CYPs were highly induced by polycyclic environmental chemicals in cell culture, rtPCR quantitation of normal breast tissue and breast tumor tissue indicated that this environmental activation is essentially absent *in vivo*. CYP1B1 mRNA was always expressed, was not elevated in tumors, and varied between individuals in cultured breast epithelia. Constitutive CYP1A1 was absent in most samples, but was occasionally seen at very low levels in some 'normal' breast epithelia and in breast tumor tissue. This level was lower than was seen in some highly metastatic tumor cell lines and probably represents endogenous rather than xenobiotic signaling [independent of media changes].

There is considerable interest in the role of BF as mediators of estrogen signaling to epithelia, particularly as estrogens are synthesized in these cells under cytokine stimulus. We have shown that human BF contain low levels of estrogens and exhibit a growth response to estradiol. These cells also express inducible CYP1B1 that potentially could determine the responsiveness of these cells to estradiol.

References:

1. Savas, U., Bhattacharyya, K.K., Brake, P.B., Eltom, S.E., Otto, S.A., and Jefcoate, C.R. (1994) Mouse cytochrome P450EF, representative of a new 1B subfamily of cytochromes P450s. Cloning, sequence determination, and tissue expression. *J. Biol. Chem.* **269**, 14905-14911.
2. Pottenger, L.H., Christou, M., and Jefcoate, C.R. (1991) Purification and immunological characterization of a novel cytochrome P450 from C3H10T1/2 cells. *Arch. Biochem. Biophys.* **286**, 488-497.
3. Otto, S.A., Marcus, C., Pidgeon, C., and Jefcoate, C.R. (1991) A novel adrenocorticotropin-inducible cytochrome P450 from rat adrenal microsomes catalyzes polycyclic aromatic hydrocarbon metabolism. *Endocrinol.* **129**, 970-982.

4. Sutter, T.R., Tang, Y.M., Hayes, C.L., Wo, Y.Y.P., Jabs, E.W., Li, X., Yink, H., Cody, C.W., and Greenlee, W.F. (1994) Complete cDNA sequence of a human dioxin-inducible mRNA identifie a new gene subfamily of cytochrome P450 that maps to chromosome 2. *J. Biol. Chem.* **269**, 13092-13099.
5. Stoilov, I., Akarsu, A.N., and Sarfarazi, M. (1997) Identification of three different truncating mutations in cytochrome P4501B1 (CYP1B1) as the principal cause of primary congenital glaucoma (Buphthalmos) in families linked to the GLC3A locus on chromosome 2p21. *Human Mol. Genetics* **6**, 641-647.
6. Bhattacharyya, K.K., Brake, P.B., Eltom, S.E., Otto, S.A., and Jefcoate, C.R. (1995) Identification of a rat adrenal cytochrome P450 active in polycyclic aromatic hydrocarbon metabolism as rat CYP1B1: Demonstration of a unique tissue-specific pattern of hormonal and aryl hydrocarbon receptor-linked regulation. *J. Biol. Chem.* **270**, 11595-11602.
7. Spink, D.C., Hayes, C.L., Young, N.R., Christou, M., Sutter, T.R., Jefcoate, C.R., and Gierthy, J.F. (1994) The effects of 2,3,7,8-tetrachlorodibenzo(p)dioxin on estrogen metabolism in MCF-7 breast cancer cells: Evidence for induction of a novel 17β-estradiol 4-hydroxylase. *J. Steroid Biochem. Mol. Biol.* **51**, 251-258.
8. Hayes, C.L., Spink, D.C., Spink, B.C., Cao, J.Q., Walter, N.J., and Sutter, T.R. (1996) 17 Beta-estradiol hydroxylation catalyzed by human cytochrome P4501B1. *Proc. Natl. Acad. Sci. U.S.A.* **93**, 9776-9781.
9. Liehr, J.G., and Ricci, M.J. (1996) 4-Hydroxylation of estrogens as marker of human mammary tumors. *Proc. Natl. Acad. Sci. U.S.A.* **93**, 3294-3296.
10. Darcy, K.M., Black, J.D., Hamh, H.A., and Ip, M.M. (1991) Mammary organoids from immature virgin rats undergo ductal and alveolar morphogenesis when grown within a reconstituted basement membrane. *Exper. Cell Res.* **196**, 49-65.
11. Blum, J.L., Zeigler, M.E., and Wicha, M.S. (1989) Regulation of mammary differentiation by the extracellular matrix. *Env. Health Perspective* **80**, 71-83.
12. Murray, G.I., Weaver, R.J., Paterson, P.J., Ewen, S.W.B., Melvin, W.T., and Burke, M.D. (1993) Expression of xenobiotic metabolizing enzymes in breast cancer. *J. Pathology* **169**, 347-353.
13. Crofts, F., Cosma, G.N., Currie, D., Taioli, E., Toniolo, P., and Garte, S.J. (1993) A novel CYP1A1 gene polymorphism in African-Americans. *Carcinogenesis* **14**, 1729-1731.
14. Dipple, A., Peltonen, K., and Cheng, S.C. (1993) Chemistry of DNA adduct formation by dihydrodiol epoxides of polycyclic aromatic hydrocarbons. In Hydrocarbons: Synthesis, Properties, Analytical Measurments, Ocurrence and Biological Effects (Garigues, P. and Lamotte, M., eds), pp. 807-816.
15. Conney, A.H., Chang, R.L., Jerina, D.M., and Wei, S.-J.C. (1994) Studies on the metabolism of benzo[*a*]pyrene and dose-dependent differences in the mutagenic profile of its ultimate carcinogenic metabolite. *Drug Metabolism Rev.* **26**, 125-163.
16. Ralston, S.L., Lau, H.H.S., Seidel, A., Luch, A., Platt, K.L., and Baird, W.M. (1994) The potent carcinogen dibenzo[*a,l*]pyrene is metabolically activated to fjord-region 11,12-diol 13,14-epoxides in human mammary carcinoma MCF-7 cell cultures. *Cancer Res.* **54**, 887-890.
17. Amin, S., Krzeminski, J., Rivenson, A., Kurtzke, C., Hecht, S., and El-Bayoumy, K. (1995) Mammary carcinogenicity in female CD rats of fjord region diol epoxides of benzo[*c*]phenanthrene, benzo[*g*]chrysene and dibenzo[*a,l*]pyrene. *Carcinogensis* **16**, 1971-1974.
18. Hayashi, S., Watanabe, J., Nakachi, K., Eguchi, H., Gotoh, O., and Kawajiri, K. (1994) Interindividual difference in expression of human Ah receptor and related P450 genes. *Carcinogenesis* **15**, 801-806.

19. Ethier, S.P., Mahacek, M.L., Gullick, W.J., Frank, T.S., and Weber, B.L. (1993) Differential isolation of normal luminal mammary epithelial cells and breast cancer cells from primary and metastatic sites using selective media. *Cancer Res.* **53**, 627-635.
20. Kang, K., Morita, I., Cruz, A., Jeon, Y.J., Trosko, J.E., and Chang, C. (1997) Expression of estrogen receptors in a normal human breast epitheial cell type with luminal and stem cell characteristics and its neoplasically transformed cell lines. *Carrcinogenesis* **18**, 251-257.
21. Kao, C., Nomata, K., Oakley, C.S., Welsch, C.W., and Chang, C. (1995) Two types of normal human breast epithelial cells derived from reduction mammoplasty phenotypic characterization and response to SV40 transfection. *Carcinogenesis* **16**, 531-538.
22. Foroozesh, M., Primrose, G., Guo, Z., Bell, L.C., Alworth, W.L., and Guengerich, F.P. (1997) Aryl acetylenes as mechanism-based inhibitors of cytochrome P450-dependent monooxygenase enzymes *Chem. Res. Toxicol.* **10**, 91-102.
23. Pang, S., Cao, J.Q., Hayes, C.L., Sutter, T.R., and Spink, D.C. (1997) Coplanar polycyclic aromatic biphenyls as inducers and inhibitors of human cytochromes P450 1A1 and 1B1. *Toxicologist* **36** (2), 158.
24. Feigelson, H.S. and Henderson, B.E. (1996) Estrogens and breast cancer. *Carcinogenesis* **17**, 2279-2284.
25. Gould, M. N., Cathers, L. E., and Moore, C. J. Human breast cell-mediated mutagenesis of mammalian cells by polycyclic aromatic hydrocarbons. Cancer Res., 42: 4619-4624, 1982.
26. Bradley, J. E., Bishop, G. A., St. John, T., and Frelinger, J. A. A simple, rapid method for the purification of poly A^+ RNA. Biotechniques, 6: 114-116, 1988.
27. Pottenger, L. H. and Jefcoate, C. R. Characterization of a novel cytochrome P450 from the transformable cell line, C3H/10T1/2. Carcinogenesis, 11: 321-327, 1990.
28. Christou, M., Savas, U., Spink, D. C., Gierthy, J. F., and Jefcoate, C. R. Co-expression of human CYP1A1 and a human analog of cytochrome P450-EF in response to 2,3,7,8-tetrachloro-dibenzo-p-dioxin in the human mammary carcinoma-derived MCF-7 cells. Carcinogenesis, 15: 725-732, 1994.
29. Laemmli, U. K. Cleavage of structural proteins during the assembly of the head of bacteriophage T4. Nature, 227: 680-685, 1970.
30. Towbin, H., Staehlin, T., and Gordon, J. Electrophoretic transfer of proteins from polyacrylamide gels to nitrocellulose sheets: procedure and some applications. Proc. Natl. Acad. Sci., 76: 4350-4354, 1979.
31. Liehr, J.G., Ricci, M.J., Jefcoate, C.R., Hannigan, E.V., Hokanson, J.A., and Zhu, B.T. (1995) 4-Hydroxylation of estradiol by human uterine myometrium and myoma microsomes: Implications for the mechanism of uterine tumorigenesis. *Proc. Natl. Acad. Sci. USA* **92**, 9220-9224.
31. Einolf, H.J., Story, W.T., Marcus, C.B., Larsen, M.C., Jefcoate, C.R., Greenlee, W.F., Yagi, H., Jerina, D.M., Amin, S., Park, S.S., Gelboin, H.V., and Baird, W.M. (1997) Role of cytochrome P450 enzyme induction in the metabolic activation of benzo[c]phenanthrene in human cell lines and mouse epidermis. *Chem. Res. Toxicol.* **10**, 609-617.

Personnel receiving pay from this effort:

Colin R. Jefcoate
Michele L. Larsen
Irina Artemenko
Xin Shen
Paul B. Brake
Kristine A. Sukow
Leonardo Ganem
Leying Zhang
William G.R. Angus
Carsten-Peter Carstens
Fidelis Ikegwuonu
Uzen Savas
Sakina E. Eltom

Published or submitted work resulting from the project:

Christou, M., Savas, Ü., Schroeder, S., Shen, X., Thompson, T., Gould, M.N., and Jefcoate, C.R. (1995) Cytochromes CYP1A1 and CYP1B1 in the rat mammary gland: Cell-specific expression and regulation by polycyclic aromatic hydrocarbons and hormones. *Mol. Cell. Endocrinol.* **115**, 41-50.

Liehr, J.G., Ricci, M.J., Jefcoate, C.R., Hannigan, E.V., Hokanson, J.A., and Zhu, B.T. (1995) 4-Hydroxylation of estradiol by human uterine myometrium and myoma microsomes: Implications for the mechanism of uterine tumorigenesis. *Proc. Natl. Acad. Sci. U.S.A.* **92**, 9220-9224.

Einolf, H.J., Story, W.T., Marcus, C.B., Larsen, M.C., Jefcoate, C.R., Greenlee, W.F., Yagi, H., Jerina, D.M., and Baird, W.M. (1997) Role of cytochrome P450 enzyme induction in the metabolic activation of benzo[*c*]phenanthrene in human cell lines and mouse epidermis. *Chem. Res. Toxicol.* **10**, 609-617.

Larsen, M.C., Angus, W.G.R., Brake, P.B., Eltom, S.E., Sukow, K.A., and Jefcoate, C.R. (1998) Characterization of CYP1B1 and CYP1A1 expression in human mammary epithelial cells: Role of the aryl hydrocarbon receptor in polycyclic aromatic hydrocarbon metabolism. *Cancer Res.* **58**, 2366-2374.

Eltom, S.E., Larsen, M.C., and Jefcoate, C.R. (1998) Expression of CYP1B1 but not CYP1A1 in primary cultured human mammary stromal fibroblasts constitutively and in response to dioxin exposure: Role of the Ah receptor. *Carcinogenisis* **19**, (In Press).

Angus, W.G.R., Larsen, M.C., and Jefcoate, C.R. (1998) Expression of CYP1A1 and CYP1B1 depends on cell-specific factors in human breast cancer cell lines: Role of estrogen receptor status (Submitted to *Carcinogenesis*).

Angus, W.G.R. and Jefcoate, C.R. (1998) TCDD elevates erbB2, erbB3, and heregulin signaling in T47D human mammary epithelial cells. (Submitted to *Oncogene*).

Brake, P.B., Larsen, M.C., Hanlon, P.R., and Jefcoate, C.R. (1998) Cell- and developmental-specific expression of cytochrome P4501B1 in the rat mammary gland. (In press pending minor modifications;*Carcinogenesis*).

Brake, P.B., Zhang, L., and Jefcoate, C.R. (1998) Ah-receptor regulation of cytochrome P4501B1 in rat mammary fibroblasts: Evidence for transcriptional repression by glucocorticoids. (In press; *Molec. Pharmacol.*).

Luch, A., Coffing, S.L., Jefcoate, C.R., Seidel, A., Greenlee, W.F., Baird, W.M., and Doehmer, J. (1998) Stable expression of human cytochrome P450 1B1 in V79 chinese hamster cells and metabolically catalyzed DNA adduct formation of dibenzo(a,l)pyrene. (In press; *Crit. Res. Toxicol.*).

Manuscripts in preparation:

Larsen, M.C., Somasunderam, A., Hanlon, P., Doehmer, J., Liehr, J., and Jefcoate, C.R. (1998) Estradiol hydroxylation in primary breast epithelia: Constitutive 4-hydroxylation correlates with CYP1B1; 2-hydroxylation requires induction of CYP1A1.

Larsen, M., Schild, L., Hanlon, P., Baird, W., and Jefcoate, C.R. (1998) CYP1B1 selectively mediates bioactivation of diBP and diBP-11,12-diol in primary human breast epithelia: DNA adduct formation and cellular responses.

Larsen, M., Alexander, D., Brake, P., Angus. W., Hanlon, P., Alworth, W., and Jefcoate, C.R. (1998) Mechanism based aryl acetylenic compounds discriminate between CYP1B1 and CYP1A1 in inhibiting DMBA metabolism in cultured cells: Species differences in potency and selectivity.

Eltom, S.E., and Jefcoate, C.R. (1998) Identification of a functional estrogen receptor in primary cultured human mammary stromal fibroblasts.

Appendix

ABSTRACT INFORMATION

FOR OFFICE USE ONLY
ADG No. _____
SOT No. _____
Fee $ _____
Check No. _____ (group)

1998 SOT Annual Meeting Abstract Form

[Any correspondence regarding your abstract must reference this number]

16858

Carefully read the Abstract Submission Guidelines and Instructions. Return this form by October 1, 1997, to: Program Committee, c/o Executive Director, Society of Toxicology, 1767 Business Center Drive, Suite 302, Reston, VA 20190. Submit original abstract form, two copies of this page, and non-refundable abstract submission fee of $30 (US) PER ABSTRACT. Payment must be made by check or credit card. Abstract submitters are still required to register and pay the registration fee for the Annual Meeting. No cash or purchase orders will be accepted. *Submission Questions?* Please contact SOT Headquarters, (703) 438-3115; fax: (703) 438-3113, e-mail: nelld@toxicology.org.

☐ Check ☐ Credit Card:
☐ Amex ☐ Diners Card ☐ MasterCard ☐ Visa: Credit Card #: _____ Exp. Date: _____

Signature: _____ Name on Card: _____

AUTHOR INFORMATION:
Please type an X in the appropriate spaces.

1. Name and address of contact author: Persons can be first author for only one abstract for the meeting and are expected to present the abstract at the meeting.

Name: WILLIAM ANGUS
Department: PHARMACOLOGY
Organization: UNIVERSITY of WISCONSIN
Address: 1300 UNIVERSITY AVE
City: MADISON State: WI Zip: 53706
Country: USA
Telephone: 608/263-3128
Fax: 608/262-1257
E-mail: wganguS@facstaff.wisc.edu

2. Membership status of contact author:

☒ SOT member ☐ Non-member

3. If none of the authors is a member of SOT, an SOT member (not a student) must sign below as a sponsor.

_____
Sponsor Signature
[illegible]
Typed Sponsor Name

4. SOT members ONLY: Would any author be willing to serve as Chairperson or Co-Chairperson of a session?

☐ Yes ☒ No

If Yes _____ (name)

5. Please indicate your preference and whether you wish to withdraw your abstract if your choice cannot be met. The Program Committee reserves the right to move a platform choice into a poster session.

☐ Platform ☒ Poster

☐ Withdraw if choice cannot be met

TYPE OR CUT & PASTE ABSTRACT TEXT HERE
STAY WITHIN BORDERS OF RECTANGLE

TCDD INDUCES THE EXPRESSION OF THE RECEPTOR TYROSINE KINASE ERBB2 IN T47D BREAST CANCER CELLS. WGR Angus and CR Jefcoate. Department of Pharmacology and Environmental Toxicology Center, The University of Wisconsin, Madison, WI, USA.

The receptor tyrosine kinase (RTK) ErbB2 (HER2/neu) is overexpressed in a large percentage of breast cancers. ErbB2 can heterodimerically pair with the EGF receptor (ErbB1) and two other family members, ErbB3 and ErbB4. Different signalling pathways, including the mitogen activated protein kinase (MAPK) and phosphatidyl inositol 3 kinase (PI3K), can be activated depending upon which ErbB proteins dimerize. Estrogen (E2) is reported to downregulate ErbB2. Since 2,3,7,8-tetrachlorodibenzo-p-dioxin (TCDD) is considered an antiestrogen and downregulates the ER, we examined the possibility that TCDD could increase ErbB2 by releasing the E2-induced downregulation. TCDD , 10 nM, more than doubled the expression of ErB2 and ErbB3 in T47D breast cancer cells by 24 hours. PCR analysis of ErbB2 and ErbB3 message also indicated an induction by 10 nM TCDD at 24 hours. These data suggest that TCDD could play an important role in the etiology of breast cancer by altering the expression of RTKs, which may lead to altered cellular signalling. Supported by grants DAMD17-94-J-4054 (CRJ) and NRSA 1-F32-ES05733-01 (WA)

Abstract Dimensions: 10.7 cm x 14.5 cm

6. ☐ Authors: please check this box if you wish to have your abstract considered for presentation in a special visiting student poster session IN ADDITION to your other scientific presentation.

7. Select three topic numbers that best describe your paper from the list on the reverse side of this form. The Program Committee will use this information to direct your abstract to the appropriate session.

1. 3 2. 35 3. 42

8. Type three keywords that best describe the research presented in your paper. The information you provide will be used to prepare a keyword index and to assist Specialty Sections with their award selection process.

1. TCDD 2. ErbB2 3. Breast cancer

In many epithelial cancer cells epidermal growth factor (EGF) enhances apoptosis induced by DNA-damaging agents, such as cisplatin, UV-B- and γ-radiation. The role of specific EGF receptor (EGFR) domains in mediating EGF-induced sensitization to cisplatin was determined in NR6 fibroblast clones transduced with signaling-restricted EGFR constructs. EGF sensitized cells expressing a wild-type EGFR by 2–4-fold, whereas cells expressing a kinase-inactive mutant were not sensitized. Truncation of the EGFR at residue 991, abolishing carboxyterminal autophosphorylation on tyrosine residues, also prevented sensitization. A construct truncated at position 1000, with one tyrosine in position 992, retained sensitization. A similar construct, in which tyrosine 992 was replaced by phenylalanine, did not mediate sensitization. We conclude that signals dependent on EGFR kinase activity and autophosphorylation of at least one tyrosine residue in position 992 are required for sensitization to cisplatin-induced apoptosis. The pattern of the sensitization is similar to the requirements for activation of phospholipase C and suggests independence from the mitogen-activated protein-kinase pathway.

#2968 Suppression of EGF-mediated tyrosine phosphorylation by pretreatment of breast cancer cells with oncostatin M. Spence, M.J., Vestal, R.E., and Liu, J. *Mountain States Medical Research Institute and Department of Veterans Affairs Medical Center, Boise, ID 83702*

H3922 is a breast cancer cell line derived from an infiltrating ductal carcinoma. Incubation of H3922 cells with EGF increases cellular proliferation to 3–4 fold higher than that observed in untreated cells. Simultaneous treatment of these cells with oncostatin M (OM) causes a dose-dependent antagonistic effect on EGF-stimulated cell growth. Through propagation of an isolated single cell, H3922–8 cells were subcloned from the H3922 parental cell population. H3922–8 cells exhibit virtually no proliferative response to EGF. Receptor binding assays using ^{125}I-EGF revealed the presence of both the high and low affinity EGF receptor components on H3922 cells. In contrast, only the low affinity binding sites were detected on the clonal cells. In order to investigate the impact of OM on EGF-mediated signal transduction, tyrosine phosphorylation events were examined in H3922 and H3922–8 cells. Incubation of H3922 cells with EGF induced rapid tyrosine phosphorylation of several cellular proteins including the EGF receptor. Pretreatment of H3922 cells with OM for 3 days abolished these EGF-mediated events. Although EGF has no effect on H3922–8 cellular proliferation, a moderate degree of EGF-stimulated tyrosine phosphorylation was detected in these cells. OM pretreatment abolished this activity as it did in the parental cells. These results suggest that EGF signaling components may be key targets for the antagonistic activity of OM. It is also apparent that the moderate degree of EGF-mediated tyrosine phosphorylation in H3922–8 cells is insufficient to trigger cellular proliferation.

#2969 ErbB2 is induced by TCDD in ER-positive and ER-negative human breast epithelial cell lines. Angus, W., and Jefcoate, C. *Univ. of Wisconsin, Madison, WI 53706*

ErbB2 is overexpressed in many human breast cancers. The ubiquitous environmental contaminant tetrachlorodibenzo-p-dioxin (TCDD), a reported antiestrogen, interacts with the aryl hydrocarbon receptor (AhR) leading to induction or inhibition of expression of numerous genes, including decreased levels of the estrogen receptor (ER). Estrogen is reported to down regulate ErbB2, while heregulin decreases ER. As TCDD is reported to be an antiestrogen, we hypothesize that exposure of cells to TCDD results in increased ErbB2 expression by attenuation of the negative regulatory influence of estrogen on ErbB2. In these studies, 3 paired ER+/ER- cell lines [ER+ (ZR75.1, T47D:A18, S30) and ER- (MCF10A, T47D:C4:2W, MDA-MB-231)] were exposed for 24 hours to 10 nM TCDD, and expression of message and proteins were determined by PCR and immunoblot, respectively. TCDD increased protein and message expression of ErbB2 by at least 2-fold in the 3 ER+ lines examined. Surprisingly, the ER- lines also showed induction of ErbB2 by TCDD, suggesting that TCDD increases ErbB2 through a non-ER related mechanism. ErbB4 expression displayed a trend toward inhibition by TCDD, while ErbB3 expression was unaffected by TCDD exposure. These data suggest that TCDD plays an important role in the etiology of breast cancer by increasing the expression of ErbB2. Supported by grants DAMD17–94-J-4054 (CJ) and NRSA 1-F32-ES05733–01 (WA).

#2970 Ribotoxic stress response: Activation of the stress-activated protein kinase JNK1 and of immediate-early gene expression by anisomycin and by sequence-specific RNA damage to the alpha-sarcin/ricin loop in the 28S ribosomal RNA. Iordanov, M.S., Pribnow, D., Magun, J.L., Pearson, J.A., Dinh, T.H., Chen, S.L.Y., and Magun, B.E. *Department of Cell and Developmental Biology, Oregon Health Sciences University, Portland, OR 97201*

Inhibition of protein synthesis does not *per se* potentiate the stress-activated protein kinases (SAPKs, also known as cJun NH_2-terminal kinases, JNKs). The protein synthesis inhibitor anisomycin, however, is a potent activatior of SAPKs/JNKs. The mechanism of this activation is unknown. We provide evidence that the anisomycin-activated signal transduction cascade to SAPK/JNK1 is initiated in the ribosome, suggesting the presence of a ribosomal anisomycin-sensing component. Both genetic evidence and footprinting data indicate that 28S rRNA is the ribosomal target for anisomycin. Therefore, we hypothesized that changes (e.g. damage) in the 28S rRNA may act as recognition signal to activate SAPK/JNK1. Two ribotoxic enzymes, ricin A-chain and alpha-sarcin, catalyze sequence-specific RNA damage within a single site in the 28S rRNA, the alpha-Sarcin/Ricin loop (S/R loop). Consistent with our hypothesis, ricin A-chain and alpha-sarcin appeared to be strong agonists of SAPK/JNK1 and of its upstream activator SEK1/MKK4, as well as to induce the expression of the immediate-early genes c-fos and c-jun. Interestingly, only active 80S ribosomes are able to initiate and subsequently transduce the signal from the damaged 28S rRNA to SAPK/JNK1. Our study defines a novel function of the translational apparatus, namely participation in signaling to the nucleus in response to ribotoxic stress.

#2971 Co-expression of *DRT* receptor kinase gene and *LERK* ligand genes in neuroblastoma and small cell lung carcinoma cell lines. Ikegaki, N., Tang, X.X., and Pleasure, D.E. *The Children's Hospital of Philadelphia, Philadelphia, PA 19104, Department of Pediatrics, University of Pennsylvania, School of Medicine, Philadelphia, PA 19104*

We previously isolated and characterized cDNA clones of a human EPH-related gene, *DRT*, that encodes a receptor type protein-tyrosine kinase. It was found that *DRT* is expressed in neuroblastoma (NB) and small cell lung carcinoma (SCLC) cell lines. It has been shown that ECK, another *EPH*-related receptor kinase, and its ligand, *LERK*-1, are frequently co-expressed in melanoma cells, suggesting auto-activation of ECK by *LERK*-1 in these cells. We examined the mRNA expression of potential ligands for DRT *(LERK-2, LERK-5,* and *LERK-8)* in NB and SCLC cell lines to see if a similar situation exists in these cells. *LERK-5* and *LERK-8* were found to be expressed in several NB cell lines. Little expression of *LERK-2* mRNA was found among NB cell lines tested. Several SCLC cell lines were found to express *LERK-2* and *LERK-8* mRNA. These results suggest that there is auto activation of the DRT receptor kinase in NB and SCLC cells co-expressing LERK ligands, contributing to the pathogenesis of NB and SCLC.

#2972 Mitogen-activated protein kinase (MAPK) signaling cascade properties associated with growth factor-stimulated cell invasion. Zeigler, M.E., Chi, Y., and Varani, J. *University of Michigan, Ann Arbor, MI 48109*

In a skin explant model, hepatocyte growth factor/scatter factor (HGF/SF) or epidermal growth factor (EGF) converts non-invasive epidermal cells to an invasive phenotype. Neither insulin-like growth factor-1 (IGF-1) nor keratinocyte growth factor (KGF) has this effect. We performed a time course analysis to detect changes in signaling properties of two components of the MAPK cascade, i.e., mitogen-activated protein kinase kinase (MEK1) and its substrate MAPK2. Equivalent amounts of lysate protein prepared from keratinocyte cultures treated with these growth factors for 2 to 60 minutes or with no growth factor were western blotted with anti-phospho-specific-MEK1 or anti-phospho-specific-MAPK2 antibody. In cells stimulated by HGF/SF and EGF, peak MEK1 activation occured at 2 minutes, while peak MAPK2 activation was seen by 10 minutes and was sustained through 60 minutes. In contrast, IGF-1 and KGF either did not activate MEK1 or only transiently activated MEK1. Cells stimulated with IGF-1 did not activate MAPK; only a transient profile of MAPK activation was seen in cells stimulated by KGF. These results suggest 1) peak MEK1 activation occurs prior to peak MAPK2 activation, consistent with the role of MEK1 as an effector of MAPK activation, 2) a correlation exists between duration of the MEK1/MAPK2 activation signal and induction of an invasive response in epidermal cells.

#2973 Epidermal growth factor receptor-mediated phosphorylation of C-MET. Jo, M., Stolz, D.B., Shima, N., Michalopoulos, G.K., and Strom, S.C. *Dept. of Pathology, University of Pittsburgh, Pittsburgh, PA 15213*

Previous reports from our laboratory have indicated that there is constitutive phosphorylation of the HGF receptor, c-met, in cells that overexpress TGF-alpha (TGF-a). We have now determined that blocking antibodies to TGF-a and/or the EGF-receptor (EGF-r) decrease the constitutive c-met phosphorylation by more than 50%. Additionally, the EGF-r-specific tyrosine kinase inhibitor, Tyrphostin AG1478, inhibits the constitutive phosphorylation of c-met by more than 70% at concentration of the inhibitor which do not interfere with hepatocyte growth factor (HGF) mediated c-met phosphorylation. In cultures of normal human hepatocytes and human hepatoma cell lines, addition of TGF-a or EGF did not increase c-met phosphorylation. However, when TGF-a or EGF was added to cultures with HGF (50ng/ml), there was significantly greater phosphorylation of c-met over that observed from the HGF alone. These results indicate that there is cross-talk between the HGF and the EGF receptor signaling pathways in the liver. This cross-talk may have important implications for the amplification of the growth factor signals involved in normal liver growth or neoplastic transformation.

#2974 Cripto 1 induces tyrosine phosphorylation of erbB4 and fibroblast growth factor-receptor 1 in mouse and human mammary epithelial cells. Bianco, C., Kannan, S., De Santis, M., Martinez-Lacaci, I., Ciardiello, F., and Salomon, D. *Tumor Growth Factor Section, Laboratory of Tumor Immunology and Biology, NCI, NIH, Bethesda, MD 20892*

The human Cripto 1 (CR-1) gene encodes for a 188 amino acid protein related to the EGF-family of peptides. A full length recombinant human CR-1 protein was expressed in SF9 insect cells with a baculovirus expression vector. We showed that CR-1 protein interacts with a specific high affinity, saturable receptor in HC-11 mouse mammary epithelial cells,whereas it does not bind directly to any member of the erbB receptor family. To evaluate if CR-1 could modulate the phosphorylation of members of the erbB receptor and fibroblast growth factor

<SPONSOR> 13880
<CATEGORY> BL3-01
<TITLE> ErbB2 is induced by TCDD in ER-positive and ER-negative human breast cancer epithelial cell lines
<LAST> Angus
<INIT> W
<LAST> Jefcoate
<INIT> C
<AFFIL> University of Wisconsin, Madison, WI 53706
<ABSTRACT> ErbB2, a heterodimeric binding partner of ErbB3, ErbB4, and the EGF receptor (EGFR), is overexpressed in many human breast cancers, and is a poor prognostic indicator. Tetrachlorodibenzo-p-dioxin (TCDD), a toxic, antiestrogenic xenobiotic, interacts with the aryl hydrocarbon receptor (AhR) leading to induction or inhibition of expression of numerous genes, including inhibition of the EGFR and estrogen receptor (ER). Exposure of breast epithelial cells to estrogen is reported to result in down regulation of ErbB2, while exposure to heregulin leads to decreased ER. Since TCDD is reported to be an antiestrogen, exposure of cells to TCDD could result in increased ErbB2 expression by attenuation of the negative regulatory influence of estrogen on ErbB2. In these studies, ER+ (ZR75.1, T47D:A18, S30) and ER- (MCF10A, T47D:C4:2W, MDA-MB-231) human breast epithelial cell lines were exposed for 24 hours to 10 nM TCDD. ErbB2 was induced at least two-fold at both the message and protein levels, as determined by PCR and immunoblot, respectively. ErbB4 message and protein expression displayed a trend toward inhibition by TCDD, while ErbB3 expression was unaffected by TCDD exposure. These data suggest that TCDD, and perhaps other xenobiotic agents acting through the AhR, plays an important role in the etiology of breast cancer by increasing the expression of ErbB2. Supported by grants DAMD17-94-J-4054 (CJ) and NRSA 1-F32-ES05733-01 (WA).

P450 and activities of microsomal ethoxyresorufin *O*-deethylase (EROD), methoxyresorufin *O*-demethylase (MROD), pentoxyresourfin *O*-dealkylase (PROD), a representative activity of P4501A1, P4501A2 and P4502B1/2, respectively, with dose-dependent manner. In contrast there was no effect on the P4502E1 catalyzed aniline hydroxylase. In the time-course experiment, methoxsalen exhibited a biphasic effect on EROD, MROD, and PROD activities, an initial inhibitory phase was followed by a phase of induction following a single treatment. Immunoblot analysis using anti-rat liver P4501A and P4502B revealed that increase in the apoprotein levels of P4501A1/2 and P4502B1/2 by methoxsalen was consistent with those in enzyme activity levels. Levels of mRNA of P4501A1/2 and P4502B1/2 were also increased by methoxsalen in Northern blot analysis. These results demonstrated that methoxsalen act as an inducer of the hepatic microsomal mixed function oxidase, selectively inducer of P4501A and P4502B families involved increases in mRNA levels. [Supported by KOSEF Grant 961-0505-117-2.]

677 MURINE *Cyp1a-1* INDUCTION IN MOUSE HEPATOMA HEPA-1C1C7 CELLS BY MYRISTICIN.

S S Lee[1], H G Jeong[2], and K H Yang[1]. [1]*Dept. of Bio. Sci., KAIST, Taejon,* [2]*Dept. of Environ. Sci., Chosun University, Kwangju, Korea.*

Mouse hepatoma Hepa-1c1c7 (Hepa-1) cells were treated with myristicin to assess the role of myristicin in the process of the Cyp1a-1 induction. Treatment of Hepa-1 cells with myristicin increased the *Cyp1a-1* transcription in a dose-dependent manner as indicated by analysis of 7-ethoxyresorufin O-deethylase activity and Cyp1a-1 protein level and Cyp1a-1 mRNA. Myristicin, however, did not competitively displace [^{3}H]2,3,7,8-tetrachlorodibenzo-*p*-dioxin from the Hepa-1 cytosolic aryl hydrocarbon (Ah) receptor in a competitive Ah receptor binding analysis using sucrose density gradient sedimentation and did not effect formation of DNA-protein complexes between the Ah receptor and its DRE target in a gel mobility shift assays using oligonucleotides corresponding to DRE 3 of the *Cyp1a-1*. These results suggest that the induction of the *Cyp1a-1* gene expression by myristicin in Hepa-1 cells might occur through an Ah receptor-independent pathway. [Supported by KOSEF Grant 961-0505-117-2.]

678 ROLE OF P450 4B1 IN 1,3-BUTADIENE (BD) AND BUTADIENE MONOXIDE (BMO) OXIDATIONS IN MOUSE TISSUES.

R J Krause[1], R M Philpot[2] and A A Elfarra[1]. [1]*Dept. of Comp. Biosci., Univ. of Wisconsin, Madison, WI and* [2]*NIEHS, RTP, NC.*

Previously, we have shown that P450 2E1 is a major catalyst of BD oxidation to BMO in human liver microsomes, and that it is a major catalyst of BMO oxidation to diepoxybutane (DEB) in mouse liver microsomes. To further assess the role of 2E1 in BD and BMO oxidations in the mouse, we correlated BMO and DEB formations in male and female mouse liver, lung and kidney microsomes with the 2E1 marker activity, chlorzoxazone 6-hydroxylase. Because the results indicated no such correlation, the involvement of other P450s in BD and BMO oxidations in extrahepatic tissues was indicated. The BD oxidation pattern in male and female mouse kidney and lung microsomes was similar to 4B1 levels expressed in these tissues, as reported by Imaoka *et al.* To confirm the role of 4B1 in BD and BMO metabolism, inhibition experiments were conducted using antiserum to rabbit 4B1. When the antibody was used at a 2 mg IgG/mg microsomal protein in male mouse kidney and male and female lung, BMO formation was inhibited by 86%, 35%, and 40%, respectively. However, with male liver microsomes which have catalytic activity similar to those of male and female lung and male kidney, no inhibition was observed; the liver activity was only inhibited by 10% when the antibody concentration was doubled. Nearly complete inhibition of DEB formation from BMO was observed when the 4B1 antibody (2 mg IgG/mg protein) was included in kidney microsomal incubations. These results show that 4B1 is the major catalyst of BD and BMO oxidations in the male mouse kidney and that 4B1 also contributes to BD activation in male and female mouse lung. (Supported by NIH grant ES 06841).

679 SUPPRESSION OF CONSTITUTIVE AND INDUCIBLE CYTOCHROME P4501B1 BY GLUCOCORTICOIDS IN ISOLATED RAT MAMMARY CELLS.

P B Brake and C R Jefcoate. *Department of Pharmacology and the Environmental Toxicology Center, University of Wisconsin, Madison, WI.*

Cytochrome P4501B1 (CYP1B1) is expressed and regulated in a cell-specific manner by endogenous steroid and peptide hormones and ubiquitous environmental contaminants. We have demonstrated the presence of CYP1B1 in the rat and human mammary gland as the major constitutive polycyclic aromatic hydrocarbon (PAH)-metabolizing species. CYP1B1 and CYP1A1 exhibit cell-type specific expression in cultures of isolated rat mammary cells. A constitutively expressed CYP1B1 is stimulated by agonists of the Ah receptor in isolated rat mammary fibroblasts (RMF). In isolated rat mammary epithelial cells (RMEC), CYP1A1 is induced by TCDD; the presence of CYP1B1 in RMEC may be due to stromal contamination and is currently under investigation. Corticosterone and dexamethasone suppress both constitutive and TCDD-induced levels of CYP1B1 (50-60%) in both RMF and rat embryo fibroblasts (REF). This suppression is relieved by the glucocorticoid antagonist, RU486, suggesting a possible role for the glucocorticoid receptor. PAH induction of CYP1A1 is similarly suppressed in RMEC by a hormonal mixture containing progesterone and glucocorticoids. Glucocorticoid treatment does not affect translocation of the Ah receptor to the nucleus upon stimulation by TCDD. The activity of a luciferase construct containing the enhancer region of the mouse CYP1B1 promoter and transiently transfected into RMF and REF, was similarly suppressed (>50%) by glucocorticoids. Experiments are presented which document the steroid regulation of CYP1B1. Notably, we address whether steroid regulation is mediated through changes in Ah receptor expression and activity or through distinct *cis*-acting suppression elements in the CYP1B1 promoter. (PB Brake supported by NRSA Grant T32 ES07015 from the NIEHS. Supported by NIH Grant P30 CA14520 and DAMD Grant 17-94-J-4054).

680 ANALYSES OF THE 5'-FLANKING REGION OF THE MOUSE CYP1B1 GENE.

L- Y Zhang, Ü Savas, and C R Jefcoate. *Department of Pharmacology, University of Wisconsin, Madison, WI.*

Transcriptional activation of cytochrome CYP1B1 in rodents is stimulated by both polycyclic aromatic hydrocarbons and cAMP. It is expressed in steroidogenic tissues and embryonic cell lines with preferential expression in stromal fibroblasts relative to epithelial cells. *CYP1B1* is transcribed from a very compact gene that has two introns and three exons of which exon 2 is the start of the open reading frame. 1.75 kb upstream of the iniation codon ATG of a mouse genomic clone were subjected to DNA sequencing and deletion analyses linked to the reporter gene luciferase. DNA sequencing revealed 11 putative xenobiotic responsive elements (TnGCGTG) or (GCGTG), 4 GC-rich sequences that resemble DXE elements, in addition to 5 E-box elements and 3 steroidogenic factor-1 motifs. Primer extension identified a starting domain defining an exon 1 of 372 bp, substantially smaller than reported for human exon1 of CYP1B1. Segments containing exon 1 and 5'-flanking region were cloned upstream of the reporter gene luciferase. In transient transfection assays, TCDD induced the expression of luciferase 5-fold in the mouse C3H10T1/2 (express predominantly CYP1B1) when the CYP1B1 insert comprised exon 1 and 1 kb of 5'-flanking region. Similar induction was seen in Hepa1c1c7 cells (express predominantly CYP1A1) indicating the absence of the elements that confer the *in vivo* cell-specific expression. A 200 bp basal promoter region for mouse CYP1B1 has been identified that includes 2 putative Sp-1 sites, a TATA-box like site, and XRE sequences adjacent to the start site. TCDD induction is primarily dependent on positive regulatory elements present between -1193 and -1436 where three XREs are localized. An in vivo TCDD-induced hypersensitive site has been identified immediately on the 3'-side of this XRE cluster. A 30 bp oligomer containing one putative XRE (-1262 to -1231) was found to form complexes from nuclear extracts of C3H10T1/2 and Hepa1c1c7 cells. Negative regulatory elements have been identified in exon 1 (+1 to -300) and between the promoter and TCDD enhancer regions. Supported by NIH grant P30 CA 14520.

681 REGULATION OF CYP2B EXPRESSION BY SQUALESTATIN 1, AN INHIBITOR OF SQUALENE SYNTHASE, IN PRIMARY CULTURED RAT HEPATOCYTES.

T A Kocarek and A B Reddy. *Institute of Chemical Toxicology, Wayne State University, Detroit, MI.*

We recently reported that several inhibitors of 3-hydroxy-3-methylglutaryl-coenzyme A (HMG-CoA) reductase, the rate-limiting step in the biosynthesis of sterols and other isoprenoids, induced CYP2B, CYP3A and CYP4A mRNA and immunoreactive protein when incubated with primary cultures of rat hepatocytes. To examine the effects of inhibition of only sterol biosynthesis on P450 expression, we have utilized the drug squalestatin 1 (SQ1), a potent inhibitor of squalene synthase, the first committed step in sterol biosynthesis.

FOR OFFICE USE ONLY
ADG No. _____
SOT No. _____
Fee $ _____
Check No. _____ (group)

1997 SOT Annual Meeting Abstract Form

[Any correspondence regarding yc abstract must reference this numc

182718

Carefully read the Abstract Submission Guidelines and Instructions. Return this form by **October 1, 1996**, to: Program Committee Executive Director, Society of Toxicology, 1767 Business Center Drive, Suite 302, Reston, VA 22090. Submit original abstract form. copies of this page, and non-refundable abstract submission fee of $30 (US) PER ABSTRACT. Check must be drawn on a U.S. ba Abstract submitters are still required to register and pay the registration fee for the Annual Meeting. No cash or purchase orders will accepted. *Submission Questions?* Please contact SOT Headquarters. (703) 438-3115; fax: (703) 438-3113, E-mail: sothq@toxicc gy.org.

AUTHOR INFORMATION:
Please type an X in the appropriate spaces.

1. Name and address of contact author: Persons can be first author for only one abstract for the meeting and are expected to present the abstract at the meeting.

Name: Michele L. Larsen
Department: Environmental Toxicology Center
Organization: University of Wisconsin
Address: 1300 University Ave.
City: Madison State: WI Zip: 53706
Country: USA
Telephone: (608) 263-3128
Fax: (608) 262-1257
E-mail: mllarsen@facstaff.wisc.edu

2. Membership status of contact author:
☐ SOT member ☒ Non-member

3. If none of the authors is a member of SOT, an SOT member (not a student) must sign below as a sponsor.

_____
Sponsor Signature

_____
Typed Sponsor Name

4. SOT members ONLY: Would any author be willing to serve as Chairperson or Co-Chairperson of a session?
☐ Yes ☐ No
If Yes _____(name)

5. The Program Committee reserves the right to assign abstracts to either a platform or poster session. Please indicate your preference and whether you wish to withdraw your abstract if your choice cannot be met
☐ Platform ☒ Poster ☐ Either
☐ Withdraw if choice cannot be met

TYPE OR CUT & PASTE ABSTRACT TEXT HERE
STAY WITHIN BORDERS OF RECTANGLE

CYP1B1 REPRESENTS THE MAJOR PAH-RESPONSIVE P45 CYTOCHROME CONSTITUTIVELY EXPRESSED IN NORMA PRIMARY HMEC. M Larsen, W G R Angus, P Brake, S Eltom, an C R Jefcoate. Department of Pharmacology and the Environmenta Toxicology Center. University of Wisconsin, Madison, WI.

CYP1B1 and CYP1A1, the major PAH metabolizing P45 cytochromes, have been shown to metabolically activate 7,12-dimethylbenz(a)anthracene (DMBA) in a cell-type selective manner in rat mammary fibroblasts and rat mammary epithelial cells, respectively [Christou *et al.* (1995) *Molec. Cell. Endocrinol.* 115: 41-50.]. Conversely, constitutive CYP1B1 as well as 2,3,7,8-tetrachlorodibenzo-p-dioxin (TCDD)-inducible CYP1B1 and CYP1A1 expression has been identified in the transformed human mammary MCF-7 carcinoma cell line [Christou *et. al.* (1994) *Carcinogenesis* 15: 725-732.]. We have characterized CYP1B1 and CYP1A1 expression in early passage normal primary human mammary epithelial cells (HMEC) isolated from seven individuals. The primary cells demonstrated low constitutive levels of microsomal DMBA metabolism, which were highly inducible by TCDD. The regioselective distribution of DMBA metabolites generated by basal microsomes is consistent with human CYP1B1-mediated metabolism, while the profile of TCDD-induced metabolism suggests CYP1A1 activity. rtPCR and Northern analysis of RNA and immunoblot analysis of microsomal proteins each demonstrated low constitutive and increased TCDD-inducible expression of CYP1B1 in the normal primary HMEC. Constitutive CYP1A1 was only detectable in induced cell populations. CYP1B1 was expressed in two ER positive as well as two ER negative primary tumors by rtPCR, while CYP1A1 expression was essentially undetectable. AhR immunoblot analysis suggests that constitutive CYP1B1 expression parallels AhR expression in the HMEC. (Supported by NIEHS 144EN46)

(Supported by DAMDI7-94-J-4054)

Abstract Dimensions: 10.7 cm x 14.5 cm

6. ☐ Authors: please check this box if you wish to have your abstract considered for presentation in a special visiting student poster session IN ADDITION to your other scientific presentation.

7. Select three topic numbers that best describe your paper from the list on the reverse side of this form. The Program Committee will use this information to direct your abstract to the appropriate session.
1. Cytochrome P450 (7) 2. Hydrocarbons, polycyclic (19) 3. Carcinogenesis (3)

8. Type three keywords that best describe the research presented in your paper. The information you provide will be used to prepare a keyword index and to assist Specialty Sections with their award selection process.
1. CYP1B1 2. Human Mammary 3. CYP1A1

FOR OFFICE USE ONLY
ADG No. _____
SOT No. _____
Fee $ _____
Check No. _____ (group)

1997 SOT Annual Meeting Abstract Form

[Any correspondence regarding your abstract must reference this number:
182502

Carefully read the Abstract Submission Guidelines and Instructions. Return this form by **October 1, 1996**, to: Program Committee, c/o Executive Director, Society of Toxicology, 1767 Business Center Drive, Suite 302. Reston, VA 22090. Submit original abstract form, two copies of this page, and non-refundable abstract submission fee of $30 (US) PER ABSTRACT. Check must be drawn on a U.S. bank. Abstract submitters are still required to register and pay the registration fee for the Annual Meeting. No cash or purchase orders will be accepted. *Submission Questions?* Please contact SOT Headquarters, (703) 438-3115; fax: (703) 438-3113, E-mail: sothq@toxicology.org.

AUTHOR INFORMATION:
Please type an X in the appropriate spaces.

1. Name and address of contact author: Persons can be first author for only one abstract for the meeting and are expected to present the abstract at the meeting.
   Name: WILLIAM ANGUS
   Department: PHARMACOLOGY
   Organization: U. WISCONSIN
   Address: 3770 MSC, 1300 UNIVERSITY
   City: MADISON State: WI Zip: 53706
   Country: USA
   Telephone: 608/263-3128
   Fax: 608/262-1257
   E-mail: wgangus@facstaff.wisc.edu
2. Membership status of contact author:
   ☒ SOT member ☐ Non-member
3. If none of the authors is a member of SOT, an SOT member (not a student) must sign below as a sponsor.

   _____
   Sponsor Signature

   _____
   Typed Sponsor Name
4. SOT members ONLY: Would any author be willing to serve as Chairperson or Co-Chairperson of a session?
   ☐ Yes ☒ No
   If Yes _____(name)
5. The Program Committee reserves the right to assign abstracts to either a platform or poster session. Please indicate your preference and whether you wish to withdraw your abstract if your choice cannot be met
   ☐ Platform ☒ Poster ☐ Either
   ☐ Withdraw if choice cannot be met

TYPE OR CUT & PASTE ABSTRACT TEXT HERE
STAY WITHIN BORDERS OF RECTANGLE

THE ESTROGEN RECEPTOR DOES NOT DIRECTLY MODULATE INDUCTION OF CYP1A1 OR CYP1B1 EXPRESSION IN TWO HUMAN BREAST EPITHELIAL CELL LINES. W G R Angus, M Larsen, and C R Jefcoate. Department of Pharmacology and Environmental Toxicology Center, University of Wisconsin, Madison, WI.

The estrogen receptor (ER) has been implicated in the induction of CYP1A1 by TCDD. Using a quartet of complementary ER+/ER- cell lines representing earlier (T47D) and later (MDA-MB) stages of tumorigenesis and the "pure" antiestrogen ICI 182,780 (ICI), the role of the ER in TCDD induced expression of CYP1A1 and CYP1B1 message and protein was examined. T47D:A18 (ER+) represents a clonal expansion of T47D; T47D:C4:2W (ER-) was selected from A18 by growth in estrogen deficient media; MDA-MB-231 (ER-) is a classical model of ER- breast cancer; and MDA-MB-231/S30 (ER+) results from stable transfection of the wt hER into MDA-MB-231 cells. TCDD induced mRNA and protein expression of CYP1A1 and CYP1B1 to similar levels in both ER+ and ER- cells within a cell type, either in the presence or absence of ICI. The overall levels of expression were lower in MDA-MB-231 cells compared to T47D. Basal protein expression of CYP1B1 was greater in ER- cells than ER+ cells, while ICI treatment elevated the expression of basal CYP1B1 protein over that of vehicle alone in ER+ cells. ICI had no effect on ER- cells. These data indicate that ER does not directly influence TCDD induction of CYP1A1 or CYP1B1 at the mRNA or protein level. ER, however, plays an inhibitory role in the basal expression of CYP1B1 protein in these cells. Supported by grants DAMD17-94-J-4054 (CRJ) and NRSA 1-F32-ES05733-01 (WGRA).

Abstract Dimensions: 10.7 cm x 14.5 cm

6. ☐ Authors: please check this box if you wish to have your abstract considered for presentation in a special visiting student poster session IN ADDITION to your other scientific presentation.
7. Select three topic numbers that best describe your paper from the list on the reverse side of this form. The Program Committee will use this information to direct your abstract to the appropriate session.
   1. CYTOCHROME P450 2. TCDD 3. CARCINOGENESIS
8. Type three keywords that best describe the research presented in your paper. The information you provide will be used to prepare a keyword index and to assist Specialty Sections with their award selection process.
   1. CYTOCHROME P450 2. ESTROGEN RECEPTOR 3. TCDD

1997 AACR

CYP1B1 REPRESENTS THE MAJOR PAH-RESPONSIVE P450 CYTOCHROME CONSTITUTIVELY EXPRESSED IN NORMAL PRIMARY HMEC and TUMOR-DERIVED TISSUES. M Larsen, W G R Angus, P Brake, S Eltom, and C R Jefcoate. Department of Pharmacology and the Environmental Toxicology Center, University of Wisconsin, Madison, WI.

CYP1B1 and CYP1A1, the major PAH metabolizing P450 cytochromes, have been shown to metabolically activate 7,12-dimethylbenz(a)anthracene (DMBA) in a cell-type selective manner in rat mammary fibroblasts and rat mammary epithelial cells, respectively [Christou *et al.* (1995) *Molec. Cell. Endocrinol.* 115: 41-50.]. Conversely, constitutive CYP1B1 as well as 2,3,7,8-tetrachlorodibenzo-p-dioxin (TCDD)-inducible CYP1B1 and CYP1A1 expression has been identified in the transformed human mammary MCF-7 carcinoma cell line [Christou *et. al.* (1994) *Carcinogenesis* 15: 725-732.]. We have characterized CYP1B1 and CYP1A1 expression in early passage normal primary human mammary epithelial cells (HMEC) isolated from seven individuals. The primary cells demonstrated low constitutive levels of microsomal DMBA metabolism, which were highly inducible by TCDD. The regioselective distribution of DMBA metabolites generated by basal microsomes is consistent with human CYP1B1-mediated metabolism, while the profile of TCDD-induced metabolism is representative of CYP1A1 activity. rtPCR and Northern analysis of RNA and immunoblot analysis of microsomal proteins each demonstrated low constitutive and increased TCDD-inducible expression of CYP1B1 in the normal primary HMEC which correlates with protein expression. Constitutive CYP1A1 was only detectable in induced cell populations. CYP1B1 was expressed in two ER positive as well as two ER negative primary tumors by rtPCR, while CYP1A1 expression was essentially undetectable. AhR immunoblot analysis suggests that constitutive CYP1B1 expression parallels AhR expression in the HMEC.
(Supported by NIEHS 144EN46)

(Supported by DAMDI7-94-J-4054)

Sakina E. Eltom and Colin R. Jefcoate. Upregulation of the Ah receptor in human breast carcinoma cell lines in proportional to their malignancy. Presented in a poster-discussion session at the 50th Annual Symposium on Fundamental Cancer Research: Molecular Determinants of Cancer Metastasis. October 28-31, 1997. Houston, Texas

ABSTRACT:

The Ah receptor (AhR), a ligand-activated helix loop helix transcription factor, binds environmental polyhalogenated aromatic hydrocarbons (PAHs), e.g., dioxin, and mediates their toxic effects. AhR is a cytosolic protein and binding of PAHs leads to its activation to a nuclear transcription factor and subsequent down-regulation by proteolysis. This study was designed to investigate the expression of AhR and its possible role in breast carcinogenesis, using MDA-MB231 and T47D series of breast carcinoma cell lines and Sager's 21T series which are closely matched pairs of mammary carcinoma cell lines characterized by exhibiting gradient order of malignancy (21MT> 21NT> 21PT). Cells were maintained in culture at the optimal recommended conditions, and at 80% confluence they were treated with 10 nM TCDD or DMSO (vehicle) for 18 h. Cells were then lyzed in Trizol® reagent which allows simultaneous isolation of total cellular RNAs and proteins. The human AhR (huAhR) protein was detected (as 104 kDa) by Western immunoblotting. The AhR mRNA transcript was detected on Northern using a 1422 bp *Spe1* fragment of huAhR cDNA as a probe. The MT lines showed the highest expression of AhR (~10 fold higher than PT), and NT was medium between MT and PT which expressed >20 fold higher than normal mammary tissues. MDA-MB231 expressed higher AhR levels than T47D series and MCF-7, irrespective of their estrogen receptor (ER) status. Although TCDD treatment in all cases resulted in lowering AhR levels, the 21T series were less responsive than the other lines. TCDD treatment on the other hand resulted in ~5-fold induction of urokinase plasminogen activator (u-PA) in MB231 while dramatically lowering it in MCF-7. The plasminogen activator inhibitor-2 (PAI-2) was induced by TCDD in MB231 and ER-negative T47D with the opposite effect in the ER-positive lines. The PAI-2 level in 21T series was consistently high in all three lines and was less sensitive to TCDD treatment. In conclusion, these data have demonstrated a strong link between the AhR expression and development of breast cancer malignancy, and suggest a role for AhR in mammary tumor progression. While the AhR activation by environmental chemicals is associated with induction of some components of U-PA system, the lack of this response in the 21T series suggests that the receptor over-expression and its PAH-dependent activation are probably different pathways. Currently, the mechanisms underlying these pathways are under investigation. (This work was supported by US Army grant DMAD 17-94-J14054).

Key words: 1. Sager's 21T series breast carcinoma cell lines. 2. Increased metastatic potential. 3. Ah receptor up-regulation. 4. Dioxin (TCDD). 5. Induction of urokinase-plasminogen activator system.

ORIGINAL ABSTRACT FORM FOR POSTER PRESENTATIONS

Furnish the information requested (below) and submit the abstract on the form provided (type the abstract within the 12 c
cm area: please see sample abstract for details). Please submit the unfolded original form and 5 photocopies which must a
your conference registration and housing forms. The deadline for receipt is March 29, 1996.

Presenting Author Michele Larsen

Organization/Institution University of Wisconsin Title Research Ass

Address 1300 University Ave

City/State Madison, WI Zip Code 53706 Country USA

Business Telephone 608 263 3125 FAX 608 262 1257 E-Mail mllarsen@facstaf

Submitted: XI International Symposium on Microsomes and Drug Oxidations
(Los Angeles, CA, July 21, 1996)

Please select one of the categories below.

- ☐ Roles of cytochrome P450s & phase II enzymes in endogenous metabolic pathways
- ☐ Drug metabolizing enzymes in the nervous system
- ☐ Mechanisms of toxicity & cell death manifested by substrates of drug metabolizing enzymes
- ☐ Biological significance of non-mammalian P450s
- ☒ Chemical carcinogenesis, mutagenesis & teratogenesis
- ☐ Phase II enzymes
- ☐ Pharmacogenetics in clinical pharmacology & toxicity
- ☐ Chemical & enzymological characterization of cytochrome P450 reactions
- ☐ Nitric oxide synthase & cytochrome P450 - a comparison
- ☐ P450 models & mechanisms
- ☐ Site-directed mutagenesis & protein structure/activity relationships
- ☐ Inhibitors of drug metabolizing enzymes
- ☐ Three-dimensional analysis of drug metabolizing enzymes
- ☐ Targeting & localization of cytochrome P450 systems
- ☐ Barbiturate-mediated induction of drug metabolizing enzymes
- ☐ Use of transgenic mice to study the function & regulation of drug-metabolizing enzymes
- ☐ Ah receptor
- ☐ Enzyme induction by peroxisome proliferators, fatty acids & prostaglandins
- ☐ Modulation of drug-metabolizing enzymes by oxidant stress

CHARACTERIZATION OF CYP1B1 AND CYP1A1 EXPRESS
NORMAL PRIMARY AND TUMOR-DERIVED HMEC

M. Larsen, K. Sukow, S. Eltom, W. Angus, and C. Jefcoate, *Enviro*
Toxicology Center and the Department of Pharmacology, Unive
Wisconsin (Madison, WI, USA).

CYP1B1 and CYP1A1, the major PAH metabolizing P450 cytoch
have been shown to metabolically activate
dimethylbenz(a)anthracene (DMBA) in a cell-type selective manner
mammary fibroblasts and rat mammary epithelial cells, respec
[Christou *et al.* (1995) *Molec. Cell. Endocrinol.* **115**: 41-50.]. Conve
constitutive CYP1B1 as well as 2,3,7,8-tetrachlorodibenzo-p-di
(TCDD)-inducible CYP1B1 and CYP1A1 expression has been identifie
the transformed human mammary MCF-7 carcinoma cell line [Christo
al. (1994) *Carcinogenesis* **15**: 725-732.]. We have characterized CYP
and CYP1A1 expression in early passage normal primary human mamm
epithelial cells (HMEC) from six individuals and in the 21T cell line se
(21PT, 21NT, and 21MT-2), isolated from an ER-/PR- tumor, representi
HMEC of different stages of tumor development [Band *et al.* (1990) *Canc*
Res. **50**: 7351-7357.]. The primary cells and the 21T cell lin
demonstrated low constitutive levels of DMBA metabolism which we
highly inducible by TCDD. The tumor-derived cell lines exhibited
substantially higher rate of induced metabolic activity (2- to 3-fold
relative to the normal cells. rtPCR analysis of RNA and immunoblo
analysis of microsomal proteins each demonstrated lower constitutive and
increased TCDD-inducible expression of CYP1B1 in the normal primary
HMEC as compared to the tumor cell lines. Similar levels of TCDD-
inducible CYP1A1 expression were observed in the normal and tumor-
derived cell populations, while constitutive CYP1A1 was undetectable in
all of the cells. The 21PT, 21NT, and 21MT-2 cell lines exhibited variable
levels of ER expression which correlated with TCDD-responsive CYP1B1
and CYP1A1 expression, whereby increased P450 expression was observed
in cells exhibiting elevated levels of ER. The normal primary HMEC
failed to express detectable ER by PCR methodologies despite showing
extensive TCDD induction. Comparisons of cellular AhR expression are
being completed by immunoblot and PCR analyses in all cell populations.
This data suggests a complex mechanism of regulation of CYP1B1 and
CYP1A1 expression which differs between primary and immortalized
HMEC.

(Supported by DAMD17-94-J-4054)

ELSEVIER

Molecular and Cellular Endocrinology 115 (1995) 41–50

Molecular and Cellular Endocrinology

Cytochromes CYP1A1 and CYP1B1 in the rat mammary gland: Cell-specific expression and regulation by polycyclic aromatic hydrocarbons and hormones

Maro Christou[a], Uzen Savas[a], Shelly Schroeder[a], Xin Shen[a], Todd Thompson[b], Michael N. Gould[b], Colin R. Jefcoate*[a]

[a]*Department of Pharmacology, University of Wisconsin, 1300 University Avenue, 3770 Medical Science Center Madison, WI 53705, USA*
[b]*Department of Human Oncology, University of Wisconsin, Madison, WI 53706, USA*

Received 18 May 1995; accepted 28 August 1995

Abstract

Cultured rat mammary cells express both CYP1A1 and CYP1B1 in response to polycyclic aromatic hydrocarbons (PAH) and 2,3,7,8-tetrachlorodibenzo-*p*-dioxin (TCDD) in a cell type-specific manner. The expression of each P450 was determined functionally (regioselective PAH metabolism), as apoprotein (immunoblots) and as mRNA (Northern hybridization). The epithelial rat mammary cells (RMEC) expressed CYP1A1, however only after PAH or TCDD treatment. CYP1B1 protein was scarcely detected in these induced RMEC but was surprisingly active as a participant in 7,12-dimethylbenz[*a*]anthracene (DMBA) metabolism shown through selective antibody inhibition (40% of total activity). CYP1B1 was selectively expressed in the stromal fibroblast population of rat mammary cells to the exclusion of CYP1A1. In the rat mammary fibroblasts (RMF), CYP1B1 protein and associated activity were each present at low levels constitutively and were highly induced by benz[*a*]anthracene (BA) to a greater extent than by TCDD (12- versus 6-fold). However, BA (10 μM) and TCDD (10 nM) stimulated the 5.2-kb CYP1B1-specific mRNA equally. These increases are consistent with the involvement of the aryl hydrocarbon (Ah) receptor in the transcription of the CYP1B1 gene and with the additional stabilization of CYP1B1 protein by BA, previously observed in embryo fibroblasts. Exactly this regulation of CYP1B1-dependent activity was seen in RMEC suggesting that this arises from exceptionally active CYP1B1 in a small proportion (5%) of residual RMF. The constitutive expression and PAH inducibility of CYP1B1 and CYP1A1 proteins in RMF and RMEC, respectively, were each substantially decreased ($\sim$75%) by a hormonal mixture (17β-estradiol (0.2 μM) progesterone (1.5 μM) cortisol (1.5 μM) and prolactin (5 μg/ml)). Progesterone and cortisol, added singly to RMF suppressed CYP1B1 protein expression ($\sim$80%) in both untreated and BA-induced cells, while cortisol also suppressed the 5.2-kb CYP1B1 mRNA. In contrast, 17β-estradiol stimulated constitutive expression of CYP1B1 protein (50–75%) and mRNA level (2- to 3-fold), but did not affect CYP1B1 expression in BA-treated RMF. The expression of CYP1A1 and CYP1B1 is therefore highly cell specific even though each is regulated through the Ah receptor. Each P450 exhibits a surprisingly similar pattern of hormonal regulation even though expressed in different cell types.

Keywords: CYP1B1; Rat mammary gland; Stromal fibroblast; Steroid

1. Introduction

Human breast cancer depends on a complex array of developmental endocrine, nutrition, genetic, and environmental factors. It is unclear how these various factors interplay in the multiple stages of the cancer process [1]. Human breast cancers more often exhibit overexpression of certain proto-oncogenes (HER2/neu) rather than mutation to oncogenes such as H-*ras* [2]. A

Abbreviations: Ah receptor, aryl hydrocarbon receptor; BA, benz[*a*]anthracene; CHM, complete hormonal media; DMBA, 7,12-dimethylbenz[*a*]anthracene; DMSO dimethylsulfoxide; PAH, polycyclic aromatic hydrocarbons; RMEC rat mammary epithelial cells; 10T1/2, C3H10T1 2 mouse embryo fibroblasts; RMF, rat mammary stromal fibroblasts; TCDD 2,3,7,8-tetrachlorodibenzo-*p*-dioxin.

* Corresponding author.

SSDI 0303-7207(95)03668-W

substantial proportion of breast cancers are linked to a gene located on chromosome 17 [3]. Thus, the role of metabolic activation of environmental chemicals has not been established. Recent studies however show that chemically induced rat mammary tumors which express mutated H-*ras* oncogenes do not show elevated mutation levels in the original tissue [4]. This suggests that reactive chemicals may cause epigenetic selection of these cells. An epidemiological linkage to elevated levels of organochlorine compounds in serum and breast fat has been reported [5]. In rats, polycyclic aromatic hydrocarbons (PAH) such as 7,12-dimethylbenz[*a*]-anthracene (DMBA) are proven mammary carcinogens [6] presumably through metabolic activation to a mutagenic dihydrodiol epoxide metabolite [7]. Rat mammary epithelial cells (RMEC) convert DMBA to metabolites capable of generating mutations in co-cultured Chinese hamster V-79 fibroblasts [8]. Metabolism of DMBA by microsomes from these cells generates a variety of dihydrodiol, hydroxymethyl, and phenolic metabolites [9]. The cells also generate DNA adducts compatible with addition of DMBA 3,4-dihydrodiol 1,2-oxide to DNA bases, notably adenine [10].

Cytochrome P450 (P450) is required for this activation process in two separate steps along with epoxide hydrolase. We have previously shown that one contributor is CYP1A1 which is inducible in RMEC by PAH [9], probably mediated by the aryl hydrocarbon receptor (Ah receptor). In these studies, we also showed that there was a second P450 which contributed equally to PAH metabolism in rat mammary epithelial microsomes. This form which was then unidentified, exhibited a different product selectivity but was also inducible by PAH, presumably via the Ah receptor. Recently, this laboratory has purified and cloned two related P450s from, respectively, C3H10T1/2 mouse embryo fibroblasts (10T1/2) and rat adrenal glands [11–13]. Sequence analyses show that these forms are probably rat and mouse orthologs of a new CYP1B1 subfamily [14]. Both proteins have 543 amino acids residues translated from an unusually large 5.2-kb mRNA which show a 92% amino acid and even higher nucleotide sequence identity. We have also shown that CYP1B1 and not CYP1A1 is selectively induced through the Ah receptor in several fibroblast cell types [15, 16]. A human ortholog has been cloned [17] and we have shown co-expression of CYP1A1 and CYP1B1 in two human breast carcinoma cell lines [18].

Stromal fibroblasts probably play a key role in regulating growth and differentiation of epithelia and myoepithelia which form the ductal structures of the mammary gland [19,20]. Thus rat embryo mesenchyme induces mammary ductal growth, even from adult epidermis [21,22]. Interactions between these cell types are demonstrable in vitro and fibroblasts mediate at least some of the estrogenic control of the mammary development [23]. This growth promotion may therefore be a key part of the cancer process. The PAH metabolism within these fibroblasts may also play an important role in determining the regulatory activity of these cells that almost certainly involves release of multiple growth factors [22].

In this study, we show that PAH metabolism in microsomes from rat mammary cells is indeed carried out by CYP1A1 and CYP1B1 in a cell-selective manner. Notably, CYP1B1 but not CYP1A1 is activated by the Ah receptor in mammary fibroblasts. We also show that the expression of these P450 isoforms is highly susceptible to hormones which affect both growth of these cells and mammary development.

2. Materials and methods

2.1. Materials

Unlabeled DMBA, benz[*a*]anthracene (BA) dimethylsulfoxide (DMSO), Tween 20 and reaction cofactors were purchased from Sigma Chemical Co. (St. Louis, MO). 2,3,7,8-Tetrachlorodibenzo-*p*-dioxin (TCDD) dissolved in toluene was purchased from Chemsyn Science Laboratories (Lenexa KS). HPLC grade methanol was from Baker/Mallinckrodt; nitrocellulose and materials for SDS-PAGE were from Bio-Rad Laboratories (Richmond, CA); enhanced chemiluminescence (ECL) detection kit was from Amersham Corporation (Arlington Heights IL). BCA protein reagents were obtained from Pierce (Rockford IL).

2.2. Cells and cell culture

Mammary tissue was obtained from mature virgin female Sprague–Dawley rats (6–8 weeks old). Mammary cells were prepared as previously described [11,24]. Briefly, minced mammary tissue was digested with 25 volumes of collagenase type III (2 mg/ml; Worthington Biochemical Corp., Freehold, NJ) and 0.002% DNase. The digested tissue was washed and suspended in serum-containing Dulbecco's modified Eagle's/F12 (DME/F12 (1:1) Gibco supplemented with 10% fetal bovine serum (Gemini), 2 mM L-glutamine (Sigma) and gentamicin sulfate with or without hormonal additives. The complete hormonal media (CHM) consisted of the above media supplemented with the following hormones: 17β-estradiol (0.2 μM), progesterone (1.5 μM) cortisol (1.5 μM) and prolactin (5 μg/ml). The cell suspension was then distributed in plastic tissue culture dishes and incubated at 37°C for 90 min. The adherent surfaces of the dishes were washed twice with serum-containing media to remove ductal fragments and cell clumps. This adherent cell population has been shown to consist primarily of monodispersed fibroblast-like cells [25]. The fragments containing the majority of the mammary epithelial cells

were separated by low-speed cenrifugation, redigested in 0.075% pronase and 0.002% DNase and resuspended in serum-containing media with or without complete hormonal additives. These cultures were ~95% epithelial as determined by immunohistological staining for keratin [26]. 3-Methylcholanthrene-transformed 10T1/2 mouse embryo fibroblasts (MCA cells) [27] were also cultured in DME/F12 (1:1) supplemented as previously described [18].

2.3. Cell treatments and preparation of microsomes

RMEC were cultured for 24–48 h after initial plating in serum-containing media (5% FBS) either without or with hormonal supplements (CHM). Identical fresh serum-containing medium containing either dimethylsulfoxide (DMSO) alone (1 μl/ml) or BA in DMSO (10 μM) or TCDD (10 nM), was then added to the cells for a period of 18–22 h. Cells were then washed and harvested in ice-cold phosphate-buffered saline. Microsomes were prepared from cell pellets as previously described [9]. Rat mammary stromal fibroblasts (RMF) were also cultured in media similar to those described for RMEC containing 10% FBS except without CHM. Unlike RMEC, RMF were rapidly proliferating cells and were passaged at subconfluence. RMF were completely free of RMEC contamination by passage 4. In experiments with RMF investigating the effects of single hormonal additives 17β-estradiol (0.2 μM) or progesterone (1.5 μM), or cortisol (1.5 μM) or prolactin (5 μg/ml) or a mixture of all four (CHM) were added 24 h prior to the addition of the inducing agents to RMF from passages 4–8 which were grown to confluence in DME/F12 (1:1). RMF microsomes were prepared as described above for RMEC.

2.4. Antibodies

Chicken anti-mouse CYP1B1 and anti-CYP1A1 IgGs were isolated in our laboratory from eggs of chickens immunized with partially pure CYP1B1 and pure CYP1A1, as described previously [11,15]. Rabbit anti-rat CYP1B1 was prepared in our laboratory, as previously described [12].

2.5. DMBA metabolism and antibody inhibition studies

DMBA metabolite profiles were determined for untreated, BA- and TCDD-treated RMEC and RMF cell microsomes. Typical incubations were carried out with 0.5–1.0 mg microsomal protein/ml reaction and a standard cofactor mixture [15]. Reverse-phase HPLC separation of DMBA metabolites was accomplished using a C-18 column (Alltech) and a linear gradient from 50–100% methanol. Metabolites were detected using a time-programmable variable-wavelength Waters 470 scanning fluorescence detector (Millipore) that enabled optimization of conditions for maximum sensitivity of detection of each DMBA metabolite. The conditions used were as follows: the excitation wavelength was set at 268 nm for the duration of the gradient. The emission wavelength was set at 395 nm for the first 30 min of the gradient and changed to 478 nm between 30 and 38 min (for detection of DMBA 3,4-dihydodiol), and then to 415 nm between 38 and 50 min. Fluorescence data was analyzed using System Gold Software via a System Gold Analog Interface Module 406 (Beckman). UV data was generated by a Beckman System Gold programmable Detector Module 166.

Inhibition of metabolism by chicken antibodies to CYP1B1 and both chicken and rabbit antibodies to CYP1A1 was studied by addition of IgG concentrations that effected maximal inhibition of each enzymatic activity relative to pre-immune IgG. These concentrations were pre-determined by dose-response studies and were as follows: for chicken anti-mouse CYP1B1, 2–5 mg/mg; for chicken anti-CYP1A1, 2–5 mg/mg; and for rabbit anti-CYP1A1, 1 mg/mg.

2.6. Immunoblotting

Microsomal proteins were separated by SDS-PAGE using 7.5% gels of 0.75 mm thickness according to Laemmli [28]. Proteins were then transferred to nitrocellulose using a Hoeffer TE51 Transfer Apparatus at a setting of 300 mA for 2 h. Visualization of immunoreactive proteins was accomplished using the ECL detection method (Amersham), as described by the manufacturer. Immunoreactive proteins were quantified by scanning with a Zeineh model SL-504 Soft Laser densitometer.

2.7. RNA hybridization analyses

The isolation of total RNA from untreated and induced cultured RMF was performed according to standard protocols, using the guanidinium isothiocyanate method [29]. Binding of total RNA to activated oligo (dT)-cellulose, type 3 (Collaborative Research Inc., Bedford, MA) and elution of mRNA were performed in Eppendorf tubes following standard protocols [30]. mRNA samples were electrophoresed through 1% formaldehyde-containing agarose gels, transferred by capillary action to Nytran membrane (Schleicher & Schuell) and immobilized by UV-induced covalent linkage to the membrane (UV-Stratalinker with a setting of 1900 Joule × 100 for 30 s). Hybridization was carried out using either the *Sma*I fragment of CYP1B1 cDNA 1028-bp [13] or a full-length CYP1A1 cDNA probe or a gyceraldehyde-3-phosphate dehydogenase probe. Each probe was labelled by the random-primed labeling method using [α-^{32}P]dCTP (3000 Ci/mmol) (Amersham Corp.) following the Boehringer-Mannheim labeling protocol. Pre-hybridization and hybridization conditions were as previously described [13].

3. Results

3.1. Regioselectivity of DMBA metabolism in uninduced and BA and TCDD-induced RMEC and RMF

DMBA metabolism has been used to characterize the expression of functional CYP1B1 and CYP1A1 in separated RMEC and RMF. Previous work has shown that high proportions of 3,4- and 10,11-dihydrodiols characterize CYP1B1-mediated metabolism while these dihydrodiols are almost undetectable for CYP1A1. High proportions of 5,6-dihydrodiol (~ 20%), 8,9-dihydrodiol (~ 30%) and 7-hydroxy products are characteristic of metabolism by CYP1A1. Data in Tables 1 and 2 show that microsomal metabolism in both cell types is inducible by BA (10 μM) and TCDD (10 nM), with BA producing higher maximum activity in each case. This difference was consistently more marked in RMF (BA induction/TCDD induction = 2.0) than in RMEC preparations (BA induction/TCDD induction = 1.4), while the induction factor was 2–3-times less in RMF. The profile of products in these RMF was fully consistent with CYP1B1 metabolism seen in rodent embryo fibroblasts [15]. In induced RMEC the higher proportions of 5,6-dihydrodiol and 7-hydroxy products concomitant with lower proportions of 3,4- and 10,11-dihydrodiols point to substantial contributions of CYP1A1.

3.2. Antibody inhibition studies

We have shown that antibodies raised against, respectively CYP1B1 and CYP1A1, are completely selective in distinguishing reactions due to these two enzymes [12,17]. We have used these antibodies to quantitate the proportions of CYP1B1 and CYP1A1 contributing to DMBA metabolism in these cell types. Fig. 1 establishes that DMBA metabolism is exclusively due to CYP1B1 in RMF. However, CYP1A1 contributes almost equally in the RMEC although the ratio of contributions is more favorable to CYP1A1 after TCDD induction. Each antibody was selective for metabolites in proportion to the selectivity shown by the corresponding P450. Thus, all the 10,11- and 3,4-dihydrodiols formed by RMEC microsomes were removed by anti-CYP1B1 (data not shown). All the DMBA metabolizing activity was accounted for by these two activities.

Table 1
Regioselective DMBA metabolism in rat mammary epithelial cells in the presence and absence of complete hormonal media (CHM)

Cell treatment[b]	DMBA Metabolite (pmol/mg/h)[a]							
	Dihydrodiols					Phenols		Total
	5,6-	8,9-	10,11-	3,4-	7HO	A[c]	B[c]	
DMSO	5	12	3	3	<0.5	8	<0.5	31 ± 3.0
+ CHM	2	5	1	1	<0.5	4	<0.5	13 ± 2.8
BA	60	218	57	73	45	250	60	758 ± 62
+ CHM	18	70	16	23	15	84	15	241 ± 18
TCDD	65	175	33	42	52	135	34	536 ± 35
+ CHM	20	56	11	12	15	45	8	167 ± 12

[a]Data represents the mean ± range of two separate experiments. Each experiment utilized microsomes prepared from separate cell cultures.
[b]Cells were treated either with 0.1% DMSO (DMSO) or 10 μM BA (BA) or 10 nM TCDD (TCDD). CHM refers to addition of a complete hormonal mixture consisting of 17β-estradiol (0.2 μM), progesterone (1.5 μM), cortisol (1.5 μM) and prolactin (5 μg/ml).
[c]A and B correspond to two HPLC peaks consisting of mixtures of unresolved DMBA phenols. Peak comprises mostly DMBA 3- and 4-phenols [9,11,32].

Table 2
Regioselective DMBA metabolism in rat mammary fibroblasts in the presence and absence of complete hormonal media (CHM)

Cell treatment[b]	DMBA metabolite (pmol/mg/h)[a]							
	Dihydrodiols					Phenols		Total
	5,6-	8,9-	10,11-	3,4-	7HO	A[c]	B[c]	
DMSO	<0.5	8	3	5	<0.5	20	2	38 ± 3
BA	7	70	29	56	<0.5	148	52	362 ± 32
+ CHM	1.5	14	6	7	<0.5	38	5	72 ± 5
TCDD	3	35	15	28	<0.5	95	14	190 ± 14
+ CHM	1	7	3	5	<0.5	18	2	36 ± 4

[a]Data represents the means ± SEM of three separate experiments. Each experiment utilized microsomes prepared from separate cell cultures.
[b]Cells were treated either with 0.1% DMSO (DMSO) or 10 μM BA (BA) or 10 nM TCDD (TCDD). CHM refers to addition of a complete hormonal mixture consisting of 17β-estradiol (0.2 μM), progesterone (1.5 μM), cortisol (1.5 μM) and prolactin (5 μg/ml).
[c]A and B correspond to two HPLC peaks consisting of mixtures of unresolved DMBA phenols. Peak comprises mostly DMBA 3- and 4-phenols [9,11,32].

3.3. Immunological detection of CYP1A1 and CYP1B1-effects of complete hormonal media

Immunoblots have been carried out with the respective antibodies to assess the levels of protein expression in each cell type. Fig. 2A establishes that P450 expression is highly selective in the two cell types. CYP1B1 is seen in induced RMF (BA ≫ TCDD) but is barely detectable in BA-induced epithelial cells inspite of the clearly measurable CYP1B1 activity in these cells. CYP1A1 was undetectable in the RMF but was induced in epithelial cells (TCDD > BA) (Fig. 2B). When RMEC are cultured, a complete hormonal mix (containing prolactin, 17β-estradiol, cortisol and progesterone) was added to limit fibroblast growth. Treatment of the cells for 24 h with this mix suppressed DMBA metabolism in epithelial cells by 3-fold for each induction while the corresponding treatment of RMF pro-

duced decreases of over 5-fold for each induction condition (Tables 1 and 2). However, product ratios remained exactly the same for both RMEC and RMF microsomes during this suppression. Most notably, there was no selective effect of the hormones on CYP1A1 relative to CYP1B1 in the RMEC preparation. In addition, induced and basal activities were decreased to the same extents. Addition of the same hormonal mix to 10T1/2 mouse embryo cells caused a 2.5-fold stimulation of basal metabolism but no effect on induced metabolism, indicating that these effects are specific to the source of fibroblasts (data not shown).

Immunoblots also confirmed the effects of the hormonal mix (Fig. 3): that is a 4- to 5-fold suppression of BA-induced CYP1B1 expression in both RMF and RMEC preparations. Suppression of induced CYP1A1 protein by the hormonal mix was comparably effective in RMEC to suppression of CYP1B1 in RMF.

The individual components of the hormonal mix produced comparable effects in RMF on DMBA metabolism (Fig. 4A) and CYP1B1 protein expression (Fig. 4B). In the basal microsomes 17β-estradiol produced a 1.5- to 2-fold increase in DMBA metabolism and CYP1B1 expression, but had no effect after BA-induction. Prolactin produced small stimulatory effects while progesterone and cortisol decreased basal and induced CYP1B1 protein levels and DMBA metabolism by 5- to 10-fold. These inhibitions were not significantly different from the effect of the hormonal mix. The concentrations of each hormone were maintained in excess of physiological concentrations to allow for inactivation during the prolonged treatment. Protein and activity data suggest that cortisol and progesterone did not differ in effectiveness between basal and BA-induced states. Cortisol was only slightly more inhibitory than progesterone with both basal and BA-induced cells (80–90% inhibition).

Epithelial preparations typically contained only about 5% fibroblast cells based on keratin staining of RMEC and proliferation of fibroblasts was prevented by the addition of the hormonal mixture. When the fibroblast content was allowed to increase to about 20%, we found that the activity attributable to CYP1A1 remained relatively constant while the CYP1B1 activity increased 3-fold in proportion to the fibroblast content. Remarkably, the increase in DMBA metabolizing activity was greater than that obtained by pure fibroblasts under the same conditions. The CYP1B1 contribution to activity was also far higher than expected from the very small level of CYP1B1 expression in the preparations. Based on the ratios of DMBA metabolism to protein expression, CYP1B1 activity in these epithelial cell preparations is increased by about 10-fold relative to ratios in a mammary fibroblast preparation.

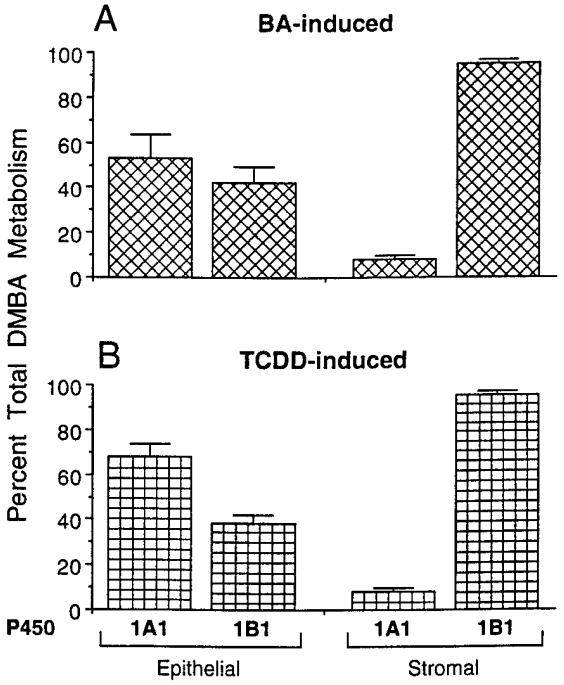

Fig. 1. Relative effects of anti-CYP1B1 and anti-CYP1A1 on DMBA metabolism induced RMEC and RMF microsomes. Total DMBA metabolism was determined following HPLC analysis of DMBA metabolites from BA- (10 μM) and TCDD- (10 nM) induced cell microsomes as described in the Methods section. Reported data represent the mean $\pm$ range of duplicate incubations.

3.4. Steady state mRNA levels in RMF-effects of cortisol and 17β-estradiol

CYP1B1 is transcribed as an unusually long 5.2-kb mRNA [13]. Quantitation of CYP1B1 steady-state mRNA levels in RMF under these various conditions established that the above reported effects on protein expression were also seen at the level of steady-state mRNA (Fig. 5). BA and TCDD stimulated mRNA levels to the same extent contrasting with the much greater stimulations of both protein and activity by BA. This exactly parallels effects seen previously with rodent embryo cells [15] uterine [16], and prostate fibroblasts [31]. The TCDD-induced increases in mRNA (12-fold) and activity (5-fold) were fully compatible with the involvement of the Ah receptor in this induction process. 17β-Estradiol produced a small 2-fold basal stimulation of CYP1B1 mRNA, but did not affect BA-induced expression, again paralleling protein and activity changes. Cortisol lowered BA-induced transcription back to basal expression levels. CYP1A1 mRNA expression was not detectable in RMF under any of these conditions.

4. Discussion

Evidence from several sources has been presented establishing that CYP1A1 and CYP1B1 are induced by

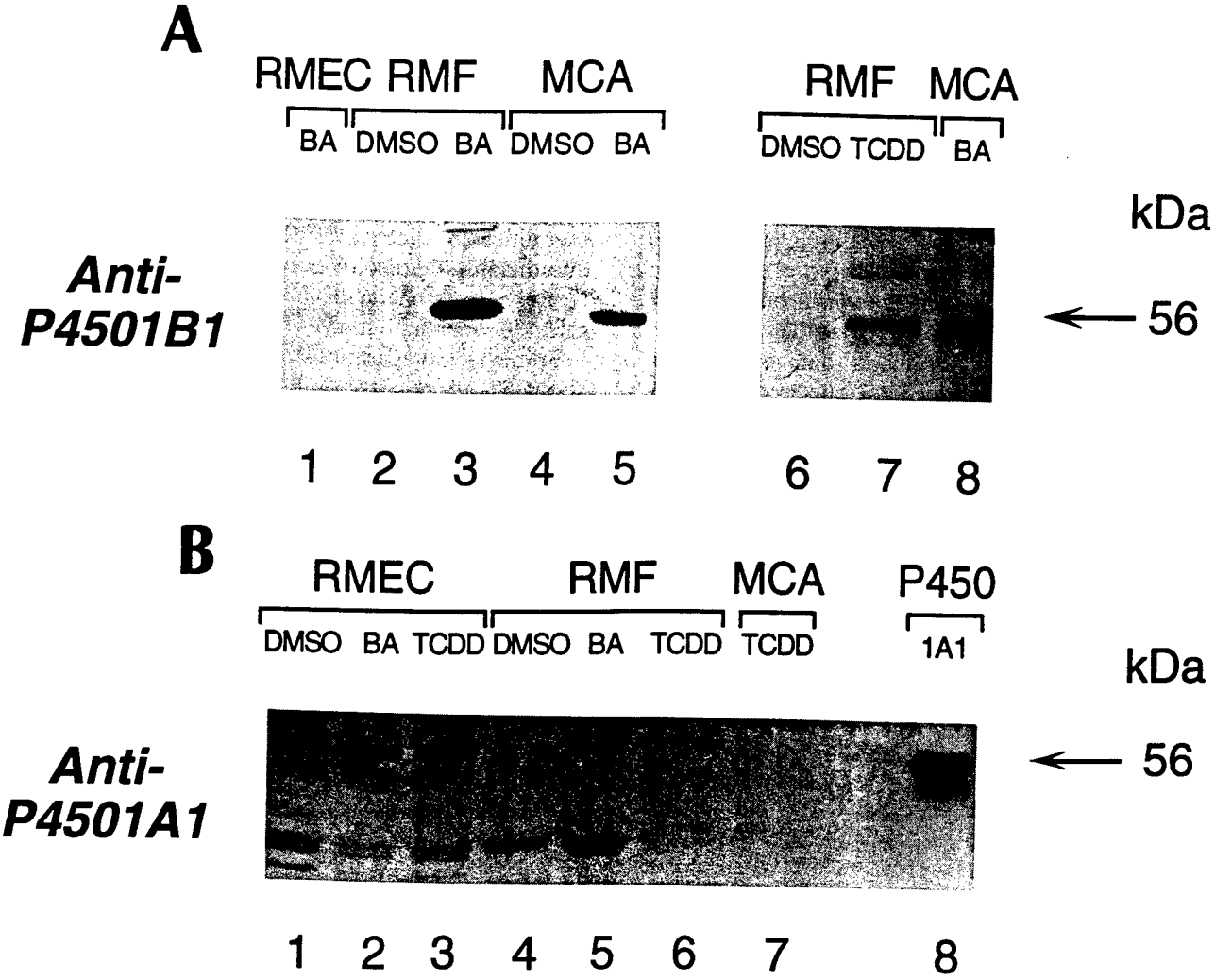

Fig. 2. Selective expression of CYP1B1 and CYP1A1 protein in RMF as compared to RMEC. Both RMF and RMEC were treated with BA (10 μM) or TCDD (10 nM). Microsomal proteins were separated by SDS-PAGE and immunoreactive proteins were visualized using the ECL method as described in the Methods section. The microsomal protein loads were as follows: (A) lanes 1–3 (15 μg); lane 4 (12 μg); lane 5 (2 μg); lanes 6 and 7 (15 μg); and lane 8 (2 μg); (B) lanes 1–7 (12 μg); lane 8 (3 ng of pure CYP1A1).

TCDD and PAHs in the rat mammary gland in a cell-specific manner. CYP1A1 is absent constitutively but is induced in epithelia but not stromal fibroblasts. Conversely, CYP1B1 is expressed at low constitutive levels in fibroblasts and is substantially induced. In epithelial preparations CYP1B1 protein is scarcely detectable even after induction but, nevertheless, based on the regioselectivity of DMBA metabolism and the extent of metabolite selective inhibition by anti-CYP1B1 antibodies, this isoform contributes nearly half of the metabolism. The specific activity of CYP1B1 in terms of immunodetectable protein is evidently at least 10-times higher than in the pure fibroblast population. We cannot rigorously establish whether this activity is due to a small proportion of fibroblasts associated with the epithelia or to low level expression of CYP1B1 in the epithelial cells. However, the CYP1B1 contribution approximately paralleled the estimated fibroblast content of preparations suggesting that this is the source. This would imply that the specific activity of CYP1B1 is many times higher in fibroblasts associated with epithelia than in separated fibroblasts. The isolated fibroblasts show about 10-fold lower specific activities for DMBA metabolisms relative to expressed protein than are seen in 10T1/2 mouse embryo fibroblasts while specific activities are comparable in the epithelial preparations.

The regulation of CYP1B1 also supports the view that even in epithelial preparations, CYP1B1 is being expressed in fibroblasts. In the pure fibroblast preparations we show that 5.2-kb CYP1B1 mRNA, 56-kDa immunoreactive protein, and DMBA metabolism are hormonally regulated in closely correlated manner. CYP1B1 expression is stimulated by 17β-estradiol (2-fold) and suppressed almost completely by glucocorticoids and to a lesser extent by progesterone. This suppression was similar for both basal and induced CYP1B1 but estrogen stimulation was only apparent

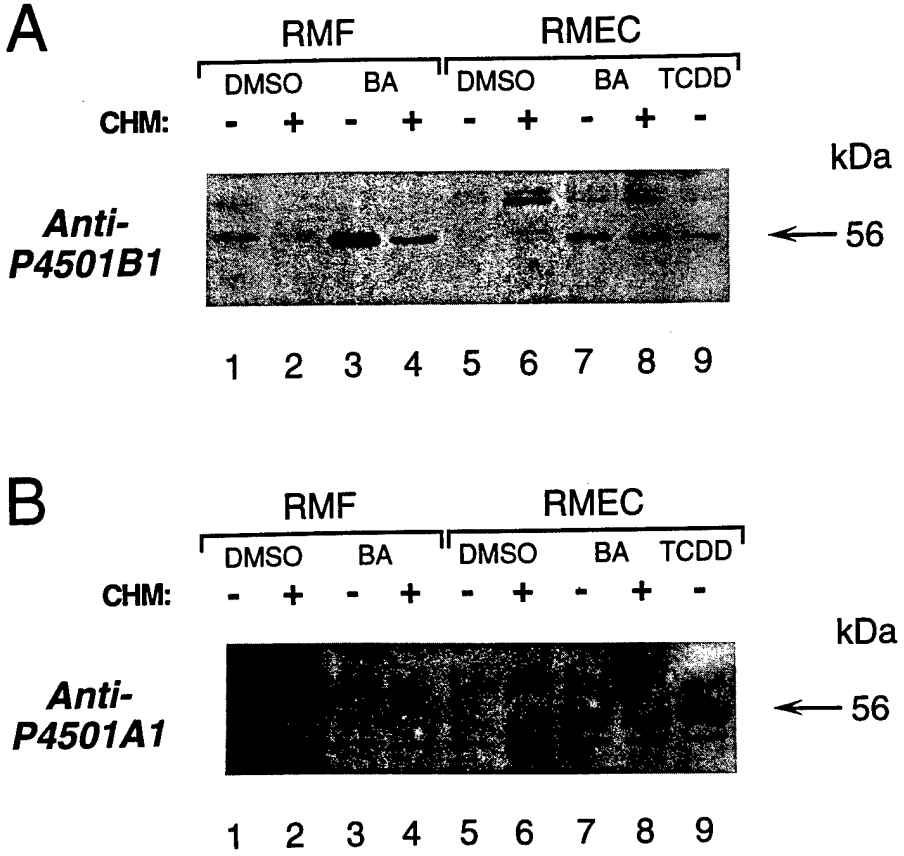

Fig. 3. Effects of a growth regulating hormonal mixture on the constitutive and BA-induced expression of CYP1B1 (A) and CYP1A1 (B) in RMF and RMEC. Both RMF and RMEC were treated with either DMSO (0.1%) or BA (10 μM) and in half of the culture dishes with complete hormonal media (CHM), which inhibits fibroblast growth. RMEC were also treated with TCDD (10 nM) in the absence of CHM. Culture conditions without CHM were as follows: DME/F12 media with normal supplements of 10% FBS and antibiotics. Culture conditions with CHM were as follows: Cells were seeded in CHM-media supplemented with a mixture of the following hormones: 17β-estradiol (0.2 μM), progesterone (1.5 μM), cortisol (1.5 μM) and prolactin (5 μg/ml). Microsomal proteins were separated by SDS-PAGE and immunoreactive proteins were visualized by the ECL method. Microsomal protein loads were 12 μg per lane.

for basal expression. As in embryo fibroblasts [32], BA was about twice as effective in elevating CYP1B1 protein and activity as the prime Ah receptor agonist TCDD while this preference was not seen for 5.2-kb mRNA. This anomalously high expression in the presence of BA may be due to stabilization of a labile CYP1B1 protein by PAH as we reported previously for mouse 10T1/2 fibroblasts [32]. The same preference for stimulation of CYP1B1 by BA relative to TCDD was observable in the DMBA metabolizing activities of the epithelial preparations together with suppression by the hormonal mixture. Retention of these unusual regulatory characteristics again suggest that CYP1B1 is mostly present in the residual fibroblasts. However, in these preparations epithelial cells must in some way increase the specific activity of CYP1B1 in these residual fibroblasts. A higher proportion of fibroblasts increased the CYP1B1 activity proportionally while maintaining the higher turnover based on protein content.

Comparison with DMBA metabolism in mouse and rat embryo fibroblasts indicates that turnover of CYP1B1 is very low in pure fibroblasts and is restored to more typical levels in the epethelial preparations. This change in specific activity could be attributable to several causes including changes in heme content or in the effectiveness of oxidoreductase. There is now substantial evidence that factors released from epithelial cells modulate the function of fibroblasts in mammary gland and prostate, while the reverse regulation also plays an important role [21,33].

The expression of CYP1A1 in epithelial preparations was suppressed by a mixture of the active steroids to exactly the same extent as CYP1B1 as evidenced by maintenance of DMBA product ratios derived from both P450s. The absence of CYP1A1 from fibroblasts ensures that this expression is only in epithelial cells. Thus, the suppression in epithelial preparations matches the hormonal suppression of CYP1B1 pure fibroblasts. The data from these epithelial preparations suggest that CYP1A1 and CYP1B1 in, respectively,

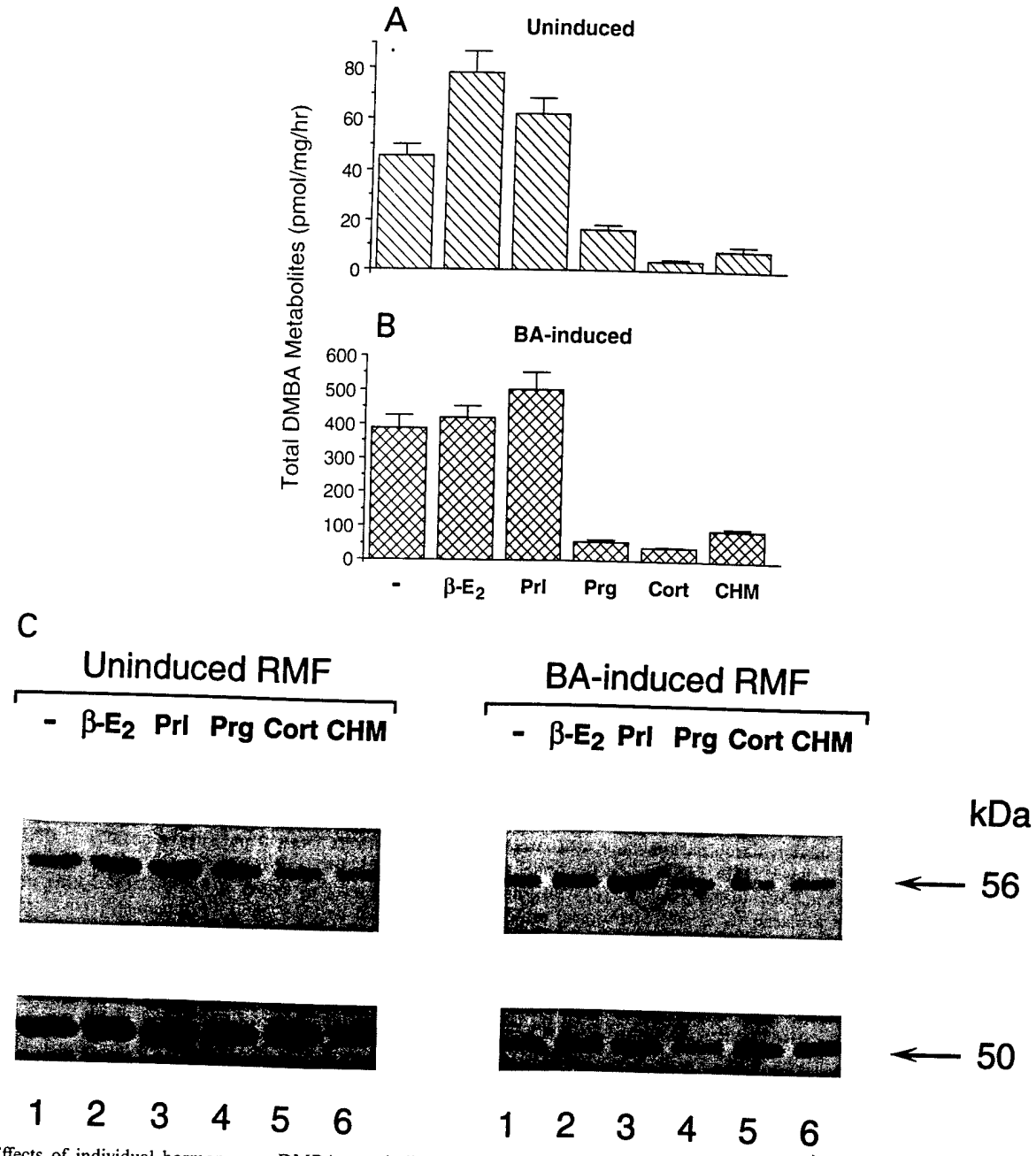

Fig. 4. Effects of individual hormones on DMBA metabolism and immunodetectable protein by uninduced and BA-induced RMF. A and B represent DMBA metabolism by uninduced and BA-induced RMF. These cells were maintained in DME/F12 media with normal supplements of 10% FBS and antibiotics (no hormonal supplement); β-E2 (17β-estradiol, 0.2 μM); Prl (bovine prolactin, 5 μg/ml); Prg (progesterone, 1.5 μM); Cort (cortisol, 1.5 μM); CHM (a mixture of all four hormones at the concentrations indicated). The total DMBA metabolites are reported as the mean $\pm$ range of duplicate incubations from two separate experiments. C shows the effect of individual hormones on immunodetectable CYP1B1 protein on constitutive and BA-induced RMF microsomes. Microsomal protein loads were 20 μg per lane for uninduced and 5 μg per lane for BA-induced RMF.

epithelia and fibroblasts are regulated by steroids through a common mechanism that could be provided by epithelia and residual fibroblasts functioning as an interactive unit. The hormonal mix that suppresses these activities was originally used because of a selective inhibitory effect on fibroblast growth in these preparations, which may also parallel release of growth factors and matrix proteins from these cells.

There is now extensive evidence that fibroblasts modulate hormonal responses in organs such as the uterus [34], prostate [35] and mammary gland [22]. The common mechanism is the release of growth factors and extracellular matrix from fibroblasts in response to hormonal stimulation of the fibroblasts. For example, fibroblasts mediate estradiol stimulation of DNA synthesis and progesterone receptors in mouse mammary

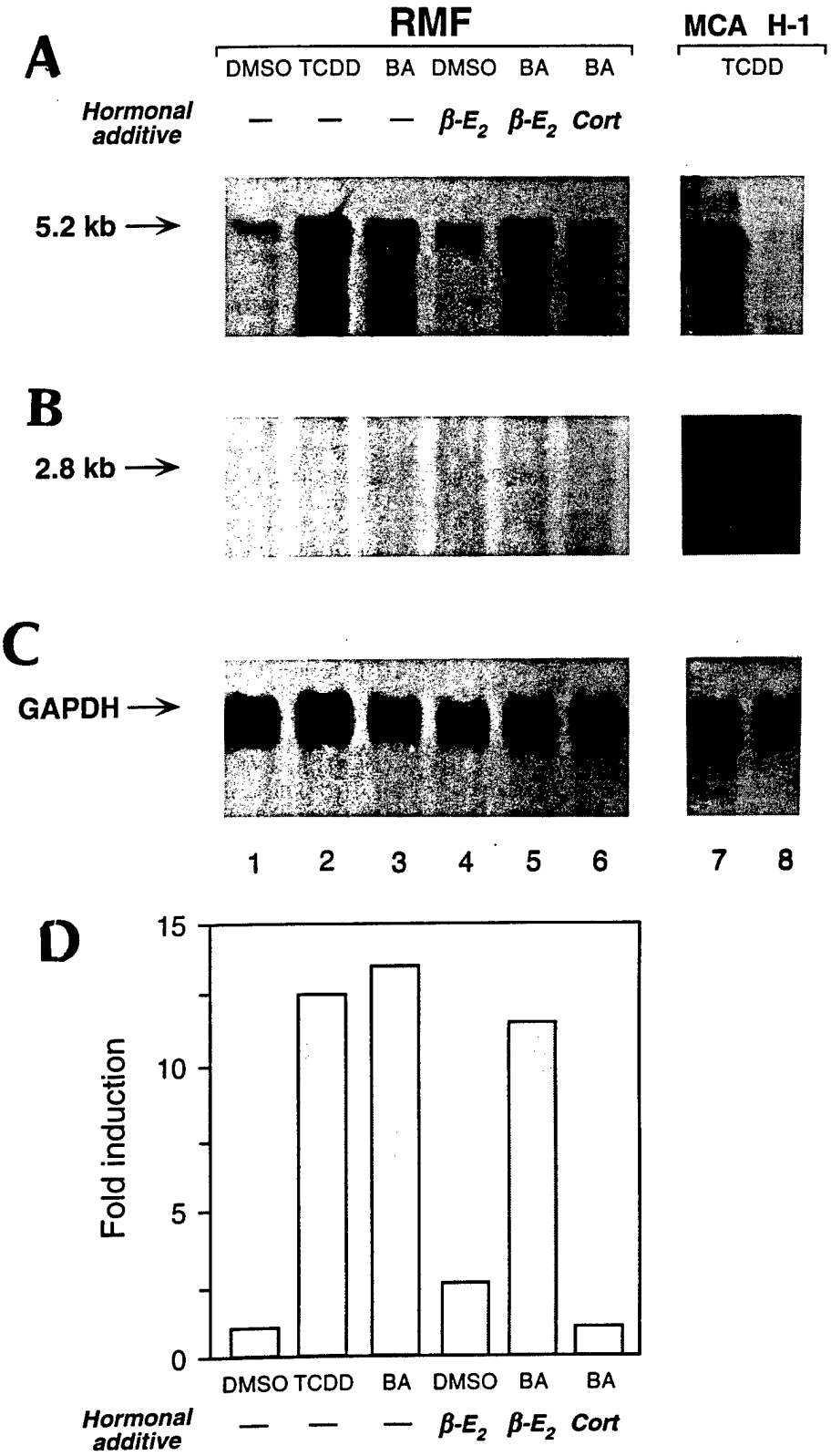

Fig. 5. Effect of steroids on the expression of CYP1B1 mRNA in uninduced, BA- and TCDD-treated RMF. RMF were treated with either DMSO (0.1%) or BA (10 μM) or TCDD (10 nM) for 6 h. Two subsets of RMF were cultured in the presence of 17β-estradiol (0.05 μg/ml) for 24 h and were then treated with either DMSO or BA. A third subset of RMF were cultured in the presence of cortisol (0.5 μg/ml) for 24 h prior to BA treatment. mRNA was isolated from each cell type as described in the Methods section, electrophoresed on a denaturing agarose gel (5 μg/lane) and transferred to nitrocellulose membrane. The immobilized mRNAs were hybridized either to a *Sma*I 1028-bp fragment of CYP1B1 cDNA (A) or a full-length CYP1A1 cDNA clone (B). The relative quantities of the loaded mRNA were assessed by hybridization of the same membrane to a glyceraldehyde-3-phosphate dehydrogenase probe (C). D illustrates the fold-induction of CYP1B1 mRNA as quantitated by laser densitometric scanning and normalizing for differences in loading.

cells [36]. We hypothesize that the Ah receptor and the elevation of CYP1B1 and CYP1A1 in these cells plays a role in such processes in part through regulation of the hydroxylation of lipophilic mediators. Significantly, CYP1B1 is expressed in a similar way in fibroblasts from the uterus and prostate [16,31].

Acknowledgments

This work was supported by National Institute of Health Grant CA16265 and in part by Council for Tobacco Research USE, Inc. Grant 2963.

References

[1] Petersen, D.W., Ronnov-Iessen, L., Howlett, A.R. and Bissell, M.J. (1992) Proc. Natl. Acad. Sci. USA 89, 9064–9068.
[2] Russel, K.S. and Hung, M.-C. (1992) Cancer Res. 52 6624–6629.
[3] Hall, J.M., Kee, M.K., Newman, B., Morrow, J.E. Anderson, L.A., Huey, B. and King, M.-C. (1990) Science 250 1684–1689.
[4] Cha, B.S., Thilly, W.G. and Zarbl. H. (1994) Proc. Natl. Acad. Sci. 91, USA 3749–3753.
[5] Wolff, M.S., Toniolo, P.G., Lee, E.W., Rivera, M. and Dubin, N. (1993) Reports 85, 648–652.
[6] Huggins, C.B. and Fukunishi, R. (1962) Cancer Res. 11 474–478.
[7] Cooper, C.S., Pal, K., Hewer, A., Grover, P.L. and Sims, P. (1982) Carcinogenesis 3, 203–210.
[8] Gould, M.N., Cather, L.E. and Moore, C.J. (1982) Cancer Res. 42, 4619–4624.
[9] Christou, M., Moore, C.J., Gould, M.N. and Jefcoate C.R. (1987) Carcinogenesis 8, 73–80.
[10] Sawicki, J.T., Moschel, R.C. and Dipple, A. (1983) Cancer Res. 40, 1580–1582.
[11] Pottenger, L.H., Christou, M. and Jefcoate, C.R. (1991) Arch. Biochem. Biophys. 286, 488–497.
[12] Otto, S., Marcus, C., Pidgeon, C. and Jefcoate, C.R. (1991) Endocrinology 129, 970–982.
[13] Savas, Ü., Bhattacharyya, K., Christou, M., Alexander D.L. and Jefcoate, C.R. (1994) J. Biol. Chem. 269, 14905–14911.
[14] Bhattacharyya, K.K., Brake, P.B., Eltom, S.E., Otto S.A. and Jefcoate, C.R. (1995) J. Biol. Chem. 270, 11595–11602.
[15] Pottenger, L.H. and Jefcoate, C.R. (1990) Carcinogenesis 11, 321–327.
[16] Savas, U., Christou, M. and Jefcoate, C.R. (1993) Carcinogenesis 14, 2013–2018.
[17] Sutter, T.R., Tang, Y.M., Hayes, C.L., Wo, Y.P., Jabs E.W., Li, X., Yin, H., Cody, C.W. and Greenlee, W.F. (1994) J. Biol. Chem. 269, 13092–13099.
[18] Christou, M., Savas, U., Spink, D.C., Gierthy, J.F. and Jefcoate, C.R. (1994) Carcinogenesis 15, 725–732.
[19] Lazard, D., Sastre, X., Frid, M.G., Glukhova, M.A. Thiery, J.-P. and Koteliansky, V.E. (1993) Proc. Natl. Acad. Sci. USA 90, 999–103.
[20] Borrelini, F. and Oka, F. (1989) Environ. Health Perspect. 80, 85–99.
[21] Cunha, G.R. (1994) Cancer 74, 1030–1044.
[22] Seslar, S.P., Nakamura, T. and Byers, S.W. (1993) Cancer Res. 53, 1233–1238.
[23] McGrath, C.M. (1983) Cancer Res. 43, 1355–1360.
[24] Moore, C.J., Bachhuber, A.J. and Gould, M.N. (1983) J. Natl. Cancer Inst. 70, 777–784.
[25] Gould, M.N. (1980) Cancer Res. 40, 1836–1841.
[26] Gould, M.N., Grau, D.R., Seidman, L.A. and Moore, C.J. (1986) Cancer Res. 46, 4946–4952.
[27] Reznikoff, C.A., Brankow, D.W. and Heidelberger, C. (1973) Cancer Res. 33, 3231–3238.
[28] Laemmli, U.K. (1970) Nature 227, 680–685.
[29] Sambrook, J., Fritsch, E.F. and Maniatis, T. (1989) Molecular Cloninig: A Laboratory Manual (Spring Harbor Laboratory, Cold Spring Harbor, NY) 2nd Edn.
[30] Badley, J.E., Bishop, G.A., John, T. St. and Frelinger, J.A. (1988) Biotechniques 6 , 114–116.
[31] Gehly, E.B., Fahl, W.E., Jefcoate, C.R. and Heidelberger, C. (1979) J. Biol. Chem. 254, 5041–5048.
[32] Savas, U. and Jefcoate, C.R. (1994) Mol. Pharmacol. 45, 1153–1159.
[33] Inaguma, Y., Kusakabe, M., Mackie, E.J., Pearson, C.A. and Sakaakura, T. (1988) Dev. Biol. 128, 245–255.
[34] Wegner, C.C. and Carson, D.D. (1992) Endocrinology 131, 2565–2572.
[35] Chang, S.-M. and Chung, L.W.K. (1989) Endocrinology 125, 2719–2727.
[36] Haslam, S.Z. (1986) Cancer Res. 46, 310–316.

Proc. Natl. Acad. Sci. USA
Vol. 92, pp. 9220–9224, September 1995
Medical Sciences

4-Hydroxylation of estradiol by human uterine myometrium and myoma microsomes: Implications for the mechanism of uterine tumorigenesis

(2-hydroxyestradiol/4-hydroxyestradiol/estrogen metabolism/cytochrome P450/uterine myoma)

JOACHIM G. LIEHR*†, MARY JO RICCI*, COLIN R. JEFCOATE‡, EDWARD V. HANNIGAN§, JAMES A. HOKANSON¶, AND BAO TING ZHU*‖

Departments of *Pharmacology and Toxicology, §Obstetrics and Gynecology, and ¶Office of Biostatistics, The University of Texas Medical Branch, Galveston, TX 77555-1031; and ‡Department of Pharmacology and Environmental Toxicology Center, University of Wisconsin, Madison, WI 53706

Communicated by Allen H. Conney, Rutgers State University of New Jersey, Piscataway, NJ, June 28, 1995 (received for review March 22, 1995)

ABSTRACT **Estradiol is converted to catechol estrogens via 2- and 4-hydroxylation by cytochrome P450 enzymes. 4-Hydroxyestradiol elicits biological activities distinct from estradiol, most notably an oxidant stress response induced by free radicals generated by metabolic redox cycling reactions. In this study, we have examined 2- and 4-hydroxylation of estradiol by microsomes of human uterine myometrium and of associated myomata. In all eight cases studied, estradiol 4-hydroxylation by myoma has been substantially elevated relative to surrounding myometrial tissue (minimum, 2-fold; mean, 5-fold). Estradiol 2-hydroxylation in myomata occurs at much lower rates than 4-hydroxylation (ratio of 4-hydroxyestradiol/2-hydroxyestradiol, 7.9 ± 1.4) and does not significantly differ from rates in surrounding myometrial tissue. Rates of myometrial 2-hydroxylation of estradiol were also not significantly different from values in patients without myomata. We have used various inhibitors to establish that 4-hydroxylation is catalyzed by a completely different cytochrome P450 than 2-hydroxylation. In myoma, α-naphthoflavone and a set of ethynyl polycyclic hydrocarbon inhibitors (5 μM) each inhibited 4-hydroxylation more efficiently (up to 90%) than 2-hydroxylation (up to 40%), indicating >10-fold differences in K_i (<0.5 μM vs. >5 μM). These activities were clearly distinguished from the selective 2-hydroxylation of estradiol in placenta by aromatase reported previously (low K_m, inhibition by Fadrozole hydrochloride or ICI D1033). 4-Hydroxylation was also selectively inhibited relative to 2-hydroxylation by antibodies raised against cytochrome P450 IB1 (rat) (53 vs. 17%). These data indicate that specific 4-hydroxylation of estradiol in human uterine tissues is catalyzed by a form(s) of cytochrome P450 related to P450 IB1, which contribute(s) little to 2-hydroxylation. This enzyme(s) is therefore a marker for uterine myomata and may play a role in the etiology of the tumor.**

2-Hydroxylation of estradiol (E_2) is the primary metabolic oxidation of this hormone in most mammalian species (1, 2). In human liver, this metabolic oxidation is catalyzed mainly by cytochrome P450 IIIA and, to a lesser extent, IA family enzymes (2, 3). Cytochrome P450 IA enzymes have also been identified as estrogen 2-hydroxylases in extrahepatic tissues and in MCF-7 human breast cancer cells (2, 4, 5). In addition, aromatase has been reported to catalyze the 2-hydroxylation of E_2 in placenta (6). Aromatic hydroxylations of estrogens by these enzymes mainly result in 2-hydroxylated catechol estrogens (CE) accompanied by small amounts of 4-hydroxylated estrogens (<20% of total CE metabolites) (1, 2). Therefore, 4-hydroxyestradiol (4-OH-E_2) has been considered as an unimportant by-product of 2-hydroxyestradiol (2-OH-E_2) formation because rates of its formation by microsomal preparations are low relative to total CE formation (1, 2) and also because urinary concentrations of 4-hydroxylated estrogens are much lower than those of 2-hydroxylated metabolites (7, 8). In contrast, in microsomes of MCF-7 cells induced by 2,3,7,8-tetrachlorodibenzo-*p*-dioxin, a specific E_2 4-hydroxylase activity distinct from the more common 2-hydroxylase activity has been detected by selective inhibition of the latter activity with anti-rat P450 IA IgG (4). Moreover, a specific E_2 4-hydroxylase activity has been identified in rat pituitary and mouse uterus, in which it represents the almost exclusive form of CE formation (9, 10), and in hamster kidney, in which it has been unmasked by inhibitors of E_2 2-hydroxylase activity, such as by Fadrozole hydrochloride (11). A physiological function of this estrogen metabolite and of the form(s) of cytochrome P450 catalyzing its formation is not known.

E_2 induces malignant cancers in hamster kidney (12), mouse uterus (13), and hyperplasia in rat pituitary (14). The expression of a specific E_2 4-hydroxylase activity in these three rodent organs, in which estrogens induce tumors, and also in a human breast cancer cell line has been taken as evidence for a role of 4-OH-E_2 formation in the development of benign and/or malignant E_2-induced tumors (11, 15). This hypothesis was developed because CE, including 4-OH-E_2, are capable of undergoing metabolic redox cycling between the catechol (hydroquinone) and corresponding quinone forms (16). Such redox cycling is a mechanism to generate potentially mutagenic free radicals (17). 4-OH-E_2 may also contribute to carcinogenesis by acting as a mitogen because it is known to be a long-acting estrogen (18). In line with this hypothesis, 4-OH-E_2 was found to be as carcinogenic as E_2 in the hamster kidney tumor model (19).

In this study, 2- and 4-hydroxylase activities have been assayed in microsomes of human uterine myoma and surrounding myometrial tissue to examine the hypothesis that 4-OH-E_2 formation serves as a marker of uterine myomata and plays a role in tumor development. Values were compared to enzyme activities in myometrial microsomes of patients without apparent myomata. For the identification of enzymes catalyzing 2- and 4-hydroxylation, several inhibitors of specific forms of cytochrome P450 were investigated. We also examined CE formation by microsomes of human placenta for the validation

The publication costs of this article were defrayed in part by page charge payment. This article must therefore be hereby marked "*advertisement*" in accordance with 18 U.S.C. §1734 solely to indicate this fact.

Abbreviations: E_2, 17β-estradiol; 2-OH-E_2 and 4-OH-E_2, 2-hydroxyestradiol and 4-hydroxyestradiol, respectively; CE, catechol estrogen(s).

†To whom reprint requests should be addressed at: Department of Pharmacology and Toxicology, The University of Texas Medical Branch, 301 University Boulevard, Galveston, TX 77555-1031.
‖Present address: Department of Chemical Biology and Pharmacognosy, The State University of New Jersey, Rutgers, Piscataway, NJ 08855-0789.

of the assays. In our studies, we identified 4-hydroxylation of E_2 in human tissues as a specific metabolic pathway distinct from the more common 2-hydroxylation.

MATERIALS AND METHODS

Chemicals. Chemicals were obtained from the following sources: E_2, NADPH, ascorbic acid, Hepes, Tris base, and Tris·HCl from Sigma; α-naphthoflavone, a specific inhibitor of cytochrome P450 IA1/IA2 (20), from Aldrich; 2-OH-E2 and 4-OH-E_2 from Steraloids (Wilton, NH); the aromatase inhibitors Fadrozole hydrochloride (CGS 16949A) (21, 22) from A. Bhatnagar, CIBA–Geigy, and ICI D1033 (23) from M. Dukes, ICI; 1-ethynylpyrene, which preferentially inhibits cytochrome P450 IA1 (24), 1- and 2-ethynylnaphthalene, which preferentially inhibit cytochrome P450 IB1 (24), and 2-, 3-, and 9-ethynylphenanthrene, which inhibit both cytochromes P450 IB1 and P450 IA1 (24, 25), from W. L. Alworth, Tulane University (New Orleans); [6,7-^{3}H]estradiol (specific activity, 40–60 Ci/mmol; 1 Ci = 37 GBq) from Amersham; neutral alumina, hydrochloric acid, hexane, and ethyl acetate (HPLC grade) from Fisher Scientific. Anti-cytochrome P450 IB1 antibody was raised in rat as described (26).

Microsome Preparation. Human uterine tissues after excision were immediately transferred to the surgical pathology laboratory, sectioned, placed in ice-cold homogenization buffer (1.14% KCl/10 mM EDTA, pH 7.5), and homogenized with a Tekmar (Cincinnati) Ultra-Turrax homogenizer. Microsomes were prepared by differential centrifugation according to the method of Dignam and Strobel (27). Microsomal pellets were resuspended in storage buffer (0.25 M sucrose/10 mM EDTA, pH 7.5) and frozen in aliquots at −80°C until used. Protein concentrations were determined by the method of Bradford using bovine serum albumin as standard (28).

Portions of placentae from healthy women were obtained within 1 hr of term deliveries. The tissues were rinsed repeatedly in ice-cold homogenization buffer to remove excess blood. Microsomes were prepared as described above (27).

Microsome-Mediated CE Formation. A validated direct product isolation assay was used to determine rates of CE formation. The assay method and its validation have been described in detail (29). Briefly, microsomal protein (750–1500 μg), 5 mM NADPH, and 1–100 μM [^{3}H]E_2 as substrate were incubated in 0.1 M Tris·HCl/Hepes buffer (pH 7.4) containing 5 mM ascorbic acid in a final volume of 500 μl at 30°C for 30 min. After termination of reactions by rapid freezing, trace amounts of ^{14}C-labeled CE were added to correct for procedural losses. The CE were then adsorbed onto neutral alumina and washed to remove residual substrate. The CE were eluted from the neutral alumina with 0.25 M HCl and separated by thin-layer chromatography. Blank values, determined with heat-denatured microsomes or by omitting either enzyme or NADPH, were subtracted. Values >125% of blanks were minimum criteria for acceptance. Product formation was proportional to incubation time for up to 20 min and to protein concentrations for up to 3 mg/ml. Incubations with chemical inhibitors or cytochrome P450 antibody were done as described above, except that inhibitors were dissolved in 2 μl of ethanol and the cytochrome P450 antibody was dissolved in water before addition to the incubation mixture.

Statistical significance was determined by one-way ANOVA for 2- and 4-hydroxylase activities after testing for the homogeneity of variances. For the ratio data, the nonparametric

Table 1. Rates of 2- and 4-hydroxylation of E_2 and ratios of 4-OH-E_2/2-OH-E_2 formation by microsomes of human myoma, myometrium, and placenta

	4-OH-E_2, (pmol/mg of protein) per min			2-OH-E_2, (pmol/mg of protein) per min			4-OH-E_2
Patient no.	Myoma	Myometrium	Placenta	Myoma	Myometrium	Placenta	2-OH-E_2
Myoma							
1	0.88	0.22 (4)		0.10	0.04 (2)		8.8
2	0.24	0.03 (8)		0.02	0.01 (2)		12.0
3	0.36	0.12 (3)		0.06	0.04 (1)		6.0
4	0.11	<0.01 (>11)		0.01	<0.01 (>1)		11.0
5	0.52	<0.01 (>50)		0.06	<0.01 (>6)		8.7
6	0.11	<0.01 (>10)		0.03	<0.01 (>3)		3.7
7	0.09	0.03 (3)		0.01	<0.01 (>1)		9.0
8	0.25	0.13 (2)		0.04	0.02 (2)		6.2
9	0.35	ND		0.05	ND		
Mean ± SD	**0.33** ± 0.26*			**0.04** ± 0.03			**7.9** ± 1.4†
Myometrium							
10		0.22			0.08		2.8
11		0.08			0.03		2.7
12		0.04			0.02		2.0
13		0.07			0.05		1.4
14		0.03			0.02		1.5
15		0.03			0.03		1.0
16		0.04			0.03		1.3
Mean ± SD		**0.08** ± 0.08			**0.03** ± 0.02		**2.6** ± 1.7
Placenta							
17			0.03			0.77	<0.1
18			0.07			1.13	<0.1
19			0.02			0.60	<0.1
20			0.08			0.73	<0.1
Mean ± SD			**0.05** ± 0.03			**0.81** ± 0.23	**<0.1**

Incubations were done by using 5 μM E_2. Numbers in parentheses represent fold difference in myoma/surrounding myometrium. ND, not determined (tissues were not available).

*Rates of 4-hydroxylation of E_2 by myoma microsomes are significantly higher than those of 2-hydroxylation and also higher than those of 4- and 2-hydroxylation by myometrial microsomes as determined by one-way ANOVA analysis followed by a contrast analysis ($P < 0.01$).

†Ratios of rates of 4-OH-E_2/2-OH-E_2 formation by myoma microsomes were significantly higher than those by myometrium microsomes, as determined by the Wilcoxon procedure (33.54, $P < 0.001$).

Wilcoxon procedure was used to account for the possibility that the ratios would not have a normal distribution.

RESULTS

Uterine Myoma. The mean rate of 2-hydroxylation of 5 μM E_2 by nine uterine myoma microsomes was 0.04 ± 0.03 pmol/mg of protein per min (Table 1). In contrast, the mean rate of 4-hydroxylation of E_2 was 8-fold higher than that of 2-hydroxylation. A kinetic analysis of CE formation from E_2 by two representative myoma microsomes indicated comparable K_m values (5.9–9.2 and 13.1–17.8 μM, respectively) but significantly higher mean V_{max} values for 4-hydroxylation than for 2-hydroxylation (0.8–1.7 and 0.2–0.3 pmol/mg of protein per min, respectively; $P < 0.05$) (Fig. 1).

α-Naphthoflavone, an inhibitor of cytochrome P450 IA1/IA2 (20), inhibited 2-hydroxylase activity in myoma microsomes by 43% and potently inhibited 4-hydroxylase activity by almost 90% (Table 2). Fadrozole hydrochloride, previously reported to inhibit aromatase (21–23), did not markedly affect 4-hydroxylation at low inhibitor concentrations (2–20 μM), whereas 50 μM concentrations decreased this reaction by 25%. 2-Hydroxylation of E_2 was enhanced from 46% to 21% with 2 μM to 50 μM Fadrozole concentration, respectively (Table 2 and data not shown). Similar effects were obtained with ICI D1033. 1-Ethynylnaphthalene and 2-ethynylnaphthalene, selective inhibitors of cytochrome P450 IB1 (24), did not affect 2-hydroxylation but inhibited 4-hydroxylation by 38% and 52%, respectively. At higher concentrations, these inhibitors inhibited 2-hydroxylation of E_2 by ≈30% and 4-hydroxylation of E_2 by up to 80% (data not shown). 1-Ethynylpyrene and 2-, 3-, and 9-ethynylphenanthrene, known to affect activities of both cytochromes P450 IA1 and IB1 enzymes (24), inhibited E_2 2-hydroxylase activity in myoma microsomes by 29–38% and 4-hydroxylase by up to 89%.

A partial but specific inhibition of 4-hydroxylase activity of myoma microsomes was obtained with an antibody raised against cytochrome P450 IB1. At a concentration of 1 mg of cytochrome P450 IB1 antibody per mg of microsomal protein, the rate of 4-hydroxylation of 10 μM E_2 was decreased by 34% from the control value, whereas 2-hydroxylation was not affected (Fig. 2). At an antibody concentration of 2 mg per mg of microsomal protein, the rate of E_2 4-hydroxylation was inhibited by 53%, whereas that of 2-hydroxylation was decreased by 17% (Fig. 2).

In summary, 4-hydroxylation of E_2 is the almost exclusive form of CE formation by microsomes of human myoma. Approximately 50% of this 4-hydroxylase activity is catalyzed by form(s) of cytochrome P450 IB1 recognized by an antibody raised against a rodent form of this enzyme. The small amount of 2-hydroxylase activity in myoma microsomes is affected by specific inhibitors of cytochromes P450 IA enzymes.

Uterine Myometrium. The rates of 2-hydroxylation of 5 μM E_2 by 15 myometrium microsomes were not different from those of myoma microsomes (Table 1). However, mean rates of 4-hydroxylation of 5 μM E_2 by myometrium microsomes (0.08 ± 0.08 pmol/mg of protein per min) were significantly lower than those of myoma microsomes ($P < 0.01$). The lower rates of 4-hydroxylation by myometrium compared to myoma microsomes are also reflected by significantly lower ratios of rates of 4-OH-E_2/2-OH-E_2 formation. Variations were much larger in rates of 4-hydroxylation than 2-hydroxylation. For instance, in two myometrium microsomes (patients 1 and 3), a predominant 4-hydroxylation of E_2 was evident, whereas in one other sample (patient 13), 2- and 4-hydroxylation rates were comparable (Table 1).

A kinetic analysis of 2-hydroxylation of E_2 by three myometrium microsomes revealed that the V_{max} and K_m values (0.1–0.3 pmol per mg of protein per min and 10.1–30.3 μM, respectively) did not differ from values observed with myoma

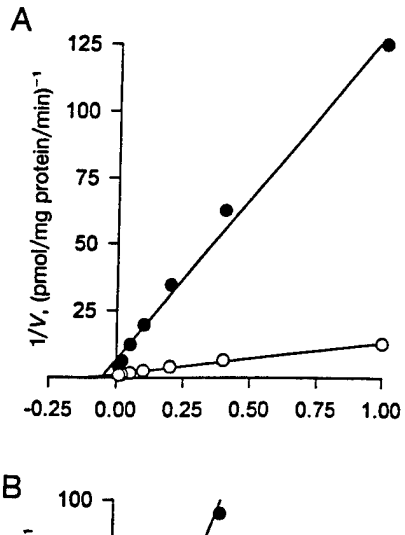

FIG. 1. Double-reciprocal plots of 4-hydroxylation and 2-hydroxylation by two representative myoma microsomes (*A* and *B*). Assays were done as described in text. Each point was the mean of duplicate determinations. Intraassay variations were within 10%. ●, 2-OH-E_2; ○, 4-OH-E_2. (*A*) For 2-OH-E_2 K_m = 13.1 and V_{max} = 0.3; for 4-OH-E_2 K_m = 5.9 and V_{max} = 1.7. (*B*) For 2-OH-E_2 K_m = 17.8 and V_{max} = 0.2; for 4-OH-E_2 K_m = 9.2 and V_{max} = 0.8. *V*, velocity; S, substrate.

Table 2. Inhibition of the conversion of E_2 to CE by uterine myoma and myometrium microsomes

Inhibitor	E_2, μM	CE formation as % of control activity	
		2-OH-E_2	4-OH-E_2
Myoma			
ICI D1033	5	131*	90*
Fadrozole hydrochloride	5	146*	93*
α-Naphthoflavone	10	57	12
2-Ethynylphenanthrene	10	66	15
3-Ethynylphenanthrene	10	67	17
9-Ethynylphenanthrene	10	71	28
1-Ethynylnaphthalene	10	97	62
2-Ethynylnaphthalene	10	93	48
1-Ethynylpyrene	10	62	11
Myometrium			
Fadrozole hydrochloride	5	106	85
α-Naphthoflavone	5	43	18
3-Ethynylphenanthrene	5	65†	17†

Incubations were done as described in the absence of inhibitors to determine E_2 2- and 4-hydroxylase activities (controls) and in the presence of 5 μM inhibitor. Values are expressed as percentage of control activities.
*These values were determined at 2 μM inhibitor concentration.
†These values were determined at 50 μM inhibitor concentration.

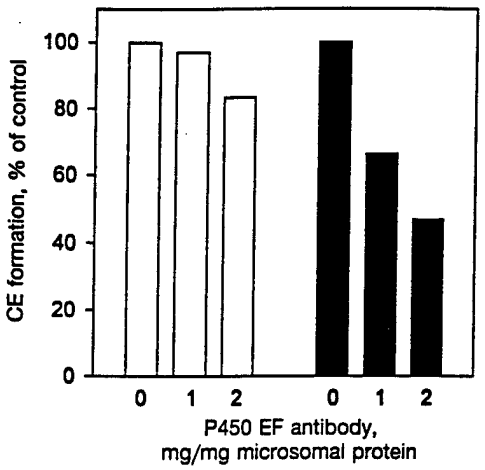

FIG. 2. Inhibition of 4- and 2-hydroxylase activity of human myoma microsomes by an antibody to cytochrome P450 IB1. The assay was done as described in text. Rates of 4-hydroxylation and 2-hydroxylation (black and white bars, respectively) of 10 μM E_2 in the absence of antibody (1.03 and 0.14 pmol/mg of protein per min, respectively) were considered to be 100%. Each point was the mean of duplicate determinations; average intraassay variation was 4.4%. EF, see ref. 33.

microsomes (data not shown). In contrast, V_{max} values for 4-hydroxylation by myometrium microsomes were significantly lower than values for 4-hydroxylation by myoma microsomes (0.5 ± 0.2 and 1.2 ± 0.6, respectively).

As with myoma microsomes, α-naphthoflavone partially inhibited 2-hydroxylation in myometrium (57%) while reducing 4-hydroxylase activity to <20% of controls (Table 2). Fadrozole hydrochloride did not markedly affect the rates of 2- and 4-hydroxylation of E_2 by myometrium microsomes (106 and 85% of control values, respectively, at 5 μM inhibitor concentration (Table 2) and 113 and 85% of control values, respectively, at 50 μM inhibitor concentration; $n = 3$) (data not shown). 1-Ethynylnaphthalene and 2-ethynylnaphthalene inhibited 4-hydroxylation by ≈25% but did not affect 2-hydroxylation (data not shown). 3-Ethynylphenanthrene preferentially inhibited 4-hydroxylation over 2-hydroxylation of E_2.

In summary, human myometrium microsomes predominantly expressed an E_2 4-hydroxylase activity, but the rate of 4-hydroxylation was only ≈20% of that observed with myoma microsomes. 2-Hydroxylation of E_2 did not differ from that in myoma microsomes.

Placenta. Human placenta microsomes converted E_2 almost exclusively to 2-OH-E_2 (Table 1). The mean V_{max} and K_m values for 2-hydroxylation of E_2, calculated from the double-reciprocal plots of four placenta microsomes (data not shown), were 0.98 ± 0.26 pmol/mg of protein per min and 1.4 ± 0.1 μM, respectively. Fadrozole hydrochloride inhibited placental microsome-mediated 2-hydroxylation of 10 μM E_2 by >95% at a 50 μM inhibitor concentration (data not shown). In summary, human placenta microsomes almost exclusively expressed E_2 2-hydroxylase activity. This 2-hydroxylase activity in placenta microsomes is potently inhibited by Fadrozole hydrochloride. Data of CE formation and inhibition are in close agreement with published values (30).

DISCUSSION

Our data identify a specific estrogen 4-hydroxylase activity in human tissues. In uterine myoma, 4-hydroxylation of E_2 is the predominant form of CE formation and occurs at rates 5-fold higher than in surrounding myometrium. Large variations in ratios of 4-OH-E_2/2-OH-E_2 formation seen in uterine myometrium are due to variations in 4-hydroxylase activity, whereas 2-hydroxylase activity varies less and is comparable to that in myoma. This predominance of 4-hydroxylation of E_2 contrasts with CE formation by microsomes of human liver (2, 3, 5) or placenta (Table 1 and ref. 30), which express mainly 2-hydroxylase activity. The conversion of E_2 predominantly to 2-OH-E_2 has been reported to be catalyzed by cytochrome P450 IIIA and aromatase enzymes, respectively (2, 3, 5, 6). In incubations with hepatic or placental enzymes, 4-OH-E_2 is only a minor by-product of the more common formation of 2-OH-E_2.

The enzyme(s) catalyzing this specific 4-hydroxylation of E_2 may be identical or related to cytochrome P450 IB1 {previously identified as EF [for embryo fibroblast (33)]}, a special class of cytochromes P450 previously detected in embryo and uterine endometrial fibroblast cells of mouse and fibroblasts of mammary glands of rats (26, 31–33). This hypothesis is supported by the specific inhibition of ≈50% of 4-hydroxylation of E_2 by an antibody raised against a rodent form of this enzyme. This antibody also inhibits 4-hydroxylation of E_2 in human breast cancer cells such as MCF-7 and T47D, which also express cytochrome P450 IB1 (34). Moreover, inhibition studies by a series of ethynylated hydrocarbon inhibitors suggest that 2-hydroxylation and 4-hydroxylation of E_2 in both myoma and myometrium are catalyzed by distinct enzyme systems.

2-Hydroxylation of E_2 by myoma or myometrium microsomes likely is catalyzed by cytochrome P450 IA and other isozymes. CE formation by aromatase, reported previously for placenta microsomes (6), does not play a role in uterine tissues. This fact has been confirmed here by the inhibition studies using Fadrozole hydrochloride or ICI D1033, which inhibit placental but not uterine conversion of E_2 to catechol metabolites.

The biological role of 4-hydroxylation of E_2 by cytochrome P450 IB1 is unknown. 4-OH-E_2 has been postulated to mediate blastocyst implantation based on physiological studies in the mouse uterus (10). Whether formation of this metabolite is the main function of this form(s) of cytochrome P450 remains to be ascertained. 4-OH-E_2 has also been postulated to participate in E_2-induced tumor formation in hamster kidney (11, 15). This hypothesis is based on the metabolic redox cycling between hydroquinone (CE) and quinone intermediates of CE, including 4-OH-E_2, which may generate potentially mutagenic free radicals (16, 17) and on the decreased dissociation of 4-OH-E_2 from the estrogen receptor complex, which makes this catechol metabolite a long-acting estrogen (18). Consistent with this hypothesis, a specific E_2 4-hydroxylase activity in animals has been identified in hamster kidney (11), mouse uterus (10), and rat pituitary (11), which all serve as animal models of estrogen-induced tumorigenesis. In human tissues, an E_2 4-hydroxylase distinct from the more common 2-hydroxylase has been detected in MCF-7 cells, a breast cancer cell line (4, 34), and in benign and malignant neoplastic mammary tissue (35). In our study, a specific E_2 4-hydroxylase activity has been demonstrated in human uterine myoma and, with lower activity, in surrounding myometrium. The presence of elevated cellular 4-hydroxylase activity in myometrium may predispose to myoma formation. Elevated formation of 4-OH-E_2 in precursor cells could mediate benign tumor formation consistent with a postulated role of this estrogen metabolite in the formation of benign or malignant tumors in rodent models. The postulated development of benign or malignant uterine tumors in women with high E_2 4-hydroxylase activity requires further studies.

In summary, a specific E_2 4-hydroxylase activity has been identified in human uterine myoma and, at lower activity, in uterine myometrium. Elevated 4-OH-E_2 formation in myometrial precursor cells is postulated to mediate benign tumor growth consistent with a role of this estrogen metabolite in estrogen-induced rodent tumors.

We thank Robert J. Hadden, Surgical Pathology, University of Texas Medical Branch, for providing the human tissues, and Rosalba Ortiz and Darlene Coleman for the preparation of the manuscript. This work was supported by the National Cancer Institute Grant CA43233.

1. Slaunwhite, W. R., Jr., Kirdani, R. Y. & Sandberg, A. A. (1973) in *Handbook of Physiology*, eds. Greep, R. O., Astwood, E. B. & Geiger, S. R. (Am. Physiol. Soc., Washington, DC), Sec. 7, Vol. 2, Part 1, pp. 485–523.
2. Martucci, C. P. & Fishman, J. (1993) *Pharmacol. Ther.* **57,** 237–257.
3. Kerlan, V., Dreano, Y., Bercovici, J. P., Beaune. P. H., Floch, H. H. & Berthou, F. (1992) *Biochem. Pharmacol.* **44,** 1745–1756.
4. Spink, D. C., Eugster, H.-P., Lincoln, D. W., II, Eugster, J. P., Schuetz, J. D., Schuetz, E. G., Johnson. J. A., Kaminsky, L. S. & Gierthy, J. F. (1992) *Arch. Biochem. Biophys.* **293,** 342–348.
5. Guengerich, F. P. (1989) *Annu. Rev. Pharmacol. Toxicol.* **29,** 241–264.
6. Osawa, Y., Higashiyama, T., Shimizu, Y. & Yarborough, C. (1993) *J. Steroid Biochem. Mol. Biol.* **44,** 469–480.
7. Adlercreutz, H., Fotsis, T., Höckerstedt, K., Hämäläinen, E., Bannwart, C., Bloigu, S., Valtonen, A. & Ollus, A. (1989) *J. Steroid Biochem.* **34,** 527–530.
8. Adlercreutz, H., Gorbach, S. L., Goldin, B. R., Woods, M. N., Dwyer, J. T. & Hämäläinen, E. (1994) *J. Natl. Cancer Inst.* **86,** 1076–1082.
9. Bui, Q. D. & Weisz, J. (1989) *Endocrinology* **124,** 1085–1087.
10. Paria, B. C., Chakraborty, C. & Dey, S. K. (1990) *Mol. Cell. Endocrinol.* **69,** 25–32.
11. Weisz, J., Bui, Q. D., Roy, D. & Liehr, J. G. (1992) *Endocrinology* **131,** 655–661.
12. Kirkman, H. (1959) *Natl. Cancer Inst. Monogr.* **1,** 1–57.
13. Newbold, R. R., Bullock, B. C. & MacLachlan, J. A. (1990) *Cancer Res.* **50,** 7677–7681.
14. Clifton, K. H. & Meyer, R. K. (1956) *Anat. Rec.* **125,** 65–81.
15. Liehr, J. G. (1994) *Polycyclic Aromat. Compd.* **6,** 229–239.
16. Liehr, J. G., Ulubelen, A. A. & Strobel, H. W. (1986) *J. Biol. Chem.* **261,** 16865–16870.
17. Liehr, J. G. & Roy, D. (1990) *Free Radical Biol. Med.* **8,** 415–423.
18. MacLusky, N. J., Barnea, E. R., Clark, C. R. & Naftolin, F. (1983) in *Catechol Estrogens*, eds. Merriam, G. M. & Lipset, M. B. (Raven, New York), pp. 151–165.
19. Liehr, J. G., Fang, W. F., Sirbasku, D. A. & Ari-Ulubelen, A. (1986) *J. Steroid Biochem.* **24,** 353–356.
20. Murray, M. & Reidy, G. F. (1990) *Pharmacol. Rev.* **42,** 85–101.
21. Wozniak, A., Holman, S. D. & Hutchinson, J. B. (1992) *J. Steroid Biochem. Mol. Biol.* **43,** 281–287.
22. Bhatnagar, S. A., Schieweck, K., Häusler, A., Browne, L. J. & Steele, R. E. (1989) *Proc. R. Soc. Edinburgh* **95B,** 293–303 (abstr.).
23. Dukes, M., Edwards, P. N., Large, M., Frank, R., Yates, R. A., Deberardinis, M. & Plourder, P. Y. (1992) *Proc. Am. Assoc. Cancer Res.* **33,** 1677 (abstr.).
24. Brake, P. B., Alexander, D. L., Otto, S. A., Christou, M. & Jefcoate, C. R. (1993) *Toxicologist* **13,** 150 (abstr.).
25. Allworth, W. L., Wiaje, A., Sandoval, A., Warren, B. S. & Slaga, T. J. (1991) *Carcinogenesis* **12,** 1209–1215.
26. Pottenger, L. H., Christou, M. & Jefcoate, C. (1991) *Arch. Biochem. Biophys.* **286,** 488–497.
27. Dignam, J. D. & Strobel, H. W. (1977) *Biochemistry* **16,** 1116–1123.
28. Bradford, M. M. (1976) *Anal. Biochem.* **72,** 248–254.
29. Hersey, R. M., Williams, K. I. H. & Weisz, J. (1981) *Endocrinology* **109,** 1912–1920.
30. Bui, Q. & Weisz, J. (1988) *Pharmacology* **36,** 356–364.
31. Savas, U., Christou, M. & Jefcoate, C. R. (1993) *Carcinogenesis* **14,** 2013–2018.
32. Sutter, T. R., Tang, Y. M., Hayes, C. L., Wo, Y.-Y. P., Jabs, E. W., Li. X., Yin, H., Cody, C. W. & Greenlee, W. F. (1994) *J. Biol. Chem.* **269,** 13092–13099.
33. Savas, U., Bhattacharya, K. K., Christou, M., Alexander, D. L. & Jefcoate, C. R. (1994) *J. Biol. Chem.* **269,** 14905–14911.
34. Spink, D. C., Hayes, C. L., Young, N. R., Christou, M., Sutter, T. R., Jefcoate, C. R. & Gierthy, J. F. (1994) *J. Steroid Biochem. Mol. Biol.* **51,** 251–258.
35. Ricci, M. J. & Liehr, J. G. (1995) *Proc. Am. Assoc. Cancer Res.* **36,** 255 (abstr.).

Role of Cytochrome P450 Enzyme Induction in the Metabolic Activation of Benzo[c]phenanthrene in Human Cell Lines and Mouse Epidermis

Heidi J. Einolf,[†] William T. Story,[†] Craig B. Marcus,[‡] Michele C. Larsen,[§] Colin R. Jefcoate,[§] William F. Greenlee,[▽] Haruhiko Yagi,[¶] Donald M. Jerina,[¶] Shantu Amin,[⊥] Sang S. Park,[∥] Harry V. Gelboin,[∞] and William M. Baird*,[†]

Department of Medicinal Chemistry & Molecular Pharmacology, Purdue University, West Lafayette, Indiana 47907, Department of Pharmacology & Toxicology, University of New Mexico, Albuquerque, New Mexico 87131-1066, Department of Pharmacology, University of Wisconsin, Madison, Wisconsin 53706, Department of Pharmacology and Molecular Toxicology, University of Massachusetts Medical Center, Worcester, Massachusetts 01655-0126, NIDDK, The National Institutes of Health, Bethesda, Maryland 20892, Naylor Dana Institute for Disease Prevention, American Health Foundation, Valhalla, New York 10595, Laboratory of Comparative Carcinogenesis, NCI–FCRDC, Frederick, Maryland 21702-1201, and Laboratory of Molecular Carcinogenesis, NCI, Bethesda, Maryland 20892

Received October 14, 1996[⊗]

The environmental contaminant benzo[c]phenanthrene (B[c]Ph) has weak carcinogenic activity in rodent bioassays; however, the fjord region diol epoxides of B[c]Ph, B[c]Ph-3,4-diol 1,2-epoxides (B[c]PhDE), are potent carcinogens. To determine the role of cytochrome P450 isozymes in the activation of B[c]Ph in MCF-7 cells and the low activation of B[c]Ph in mouse skin, cells of the MCF-7 and the human hepatoma HepG2 cell lines were treated with the potent Ah receptor agonist 2,3,7,8-tetrachlorodibenzo-*p*-dioxin (TCDD) prior to exposure to B[c]Ph for 24 h. Mice were treated topically with 1 μg of TCDD or vehicle (control) for 73 h and then with 2 μmol of B[c]Ph for 24 h. In MCF-7 cells, TCDD exposure increased B[c]PhDE–DNA adduct levels more than 3-fold with a 10-fold increase in the (−)-B[c]PhDE-2-dA_t adduct. Treatment of HepG2 cells with TCDD prior to B[c]Ph application did not increase B[c]PhDE–DNA binding. Total B[c]PhDE–DNA adducts increased 3-fold in TCDD-treated mouse epidermis: the majority of the increase resulted from (+)-B[c]PhDE-1-dA adducts. Analysis of P450 enzymes by Western blotting detected a large increase of P4501B1 but almost no increase in P4501A1 in MCF-7 cells exposed to 10 μM B[c]Ph for 24 or 48 h. In HepG2 cells, there were no detectable levels of P4501A1 or P4501B1 after treatment with 10 μM B[c]Ph for 24 h. In contrast, topical application of 2 μmol of B[c]Ph to mouse skin for 48 or 72 h increased P4501A1, but no P4501B1 was detected. As a measure of P450 activity, the metabolism of 7,12-dimethylbenz[a]anthracene (DMBA) was analyzed in microsomes prepared from MCF-7 and HepG2 cells exposed to 0.1% DMSO, 10 μM B[c]Ph, or 10 nM TCDD for 24 or 48 h and from mouse epidermis treated with 1 μg of TCDD, or vehicle control for 72 h, or 2 μmol of B[c]Ph for 48 h. The levels of DMBA metabolites were low or undetectable in microsomes from B[c]Ph-treated MCF-7 and HepG2 cells, but a metabolite pattern consistent with P4501A1 metabolism of DMBA was present in B[c]Ph-exposed mouse epidermal microsomes. TCDD-treated MCF-7 cells, HepG2 cells, and mouse epidermis had DMBA metabolism patterns characteristic of P4501A1 activity. Microsomes from TCDD-treated human cells formed a higher proportion of the proximate carcinogenic metabolite DMBA-3,4-dihydrodiol (16% of total identified metabolites) than TCDD-treated mouse epidermis (2%). In mouse epidermis, the weak ability of B[c]Ph to increase hydrocarbon-metabolizing activity and the increase in mainly P4501A1, leading to formation of the less carcinogenic stereoisomer B[c]PhDE-1, may explain the low carcinogenic activity of B[c]Ph. In a human mammary carcinoma cell line, treatment with B[c]Ph increases mainly P4501B1 and results in formation of a higher proportion of the more carcinogenic B[c]PhDE-2. This indicates that cells in which B[c]Ph treatment increases P4501B1 levels effectively activate B[c]Ph to potent carcinogenic metabolites.

Introduction

The polycyclic aromatic hydrocarbon (PAH)[1] benzo[c]-phenanthrene (B[c]Ph) is an environmental pollutant with low mutagenic activity in bacterial mutagenesis assays and low carcinogenic activity in rodent tumor bioassays (*1–4*). The fjord region diol epoxides of B[c]-Ph, B[c]Ph-3,4-diol 1,2-epoxides (B[c]PhDE), however, are among the most mutagenic diol epoxides tested in bacterial and mammalian cells and most carcinogenic in the rat mammary tumor model, on mouse skin, and in newborn mice (*2–10*).

* Author to whom correspondence and reprint requests should be addressed.
[†] Purdue University.
[‡] University of New Mexico.
[§] University of Wisconsin.
[▽] University of Massachusetts Medical Center.
[¶] NIDDK.
[⊥] American Health Foundation.
[∥] NCI–FCRDC.
[∞] NCI.
[⊗] Abstract published in *Advance ACS Abstracts,* April 15, 1997.

S0893-228x(96)00174-9 CCC: $14.00

The bioactivation of B[*c*]Ph relies upon the metabolism of the parent compound by cytochrome P450 (P450) enzymes to form the 3,4-epoxide with subsequent hydrolysis by epoxide hydrase yielding a proximate carcinogenic metabolite *trans*-B[*c*]Ph-3,4-dihydrodiol. The diol is then metabolized by P450 enzymes to form an ultimate carcinogenic metabolite, B[*c*]Ph-3,4-diol 1,2-epoxide. P450 enzymes involved in the bioactivation of PAH have been identified as P4501A1, P4501A2, P4503A4, and recently characterized P4501B1 (*11*–*15*). B[*c*]Ph was an excellent substrate for metabolism by P4501A1 in liver microsomes from 3-methylcholanthrene (3MC)-treated rats (P4501A1 constituted >70% of the total P450 content) (*16*). However, in B[*c*]Ph metabolism assays utilizing rat liver microsomes prepared from control rats or rats treated with phenobarbital (PB) or 3MC, most of the dihydrodiol metabolites formed were from the K-region 5,6-epoxide (77–89% of total metabolites) (*16*). The proximate carcinogenic metabolite of B[*c*]Ph, B[*c*]Ph-3,4-dihydrodiol, was formed only to a small extent (6–17% of the total metabolites) (*16*). The metabolism of B[*c*]Ph was higher by purified rat P4501A1 than by purified rat P4502A1 or P4502B1; however, formation of the 3,4-dihydrodiol was low (3–5% of the total metabolites) (*16*).

Enantiomeric B[*c*]Ph-3,4-dihydrodiols metabolized by a reconstituted rat P4501A1 system with epoxide hydrase formed low amounts of B[*c*]PhDE (1.5–3.4% of the total metabolites) (*17*). However, a higher percentage of diol epoxide was formed from enantiomerically pure or racemic B[*c*]Ph-3,4-dihydrodiols by liver microsomes prepared from control rats and from mice and rats treated with PB than from liver microsomes obtained from 3MC-treated rats (*17*). Liver microsomes from control rats and mice also produced moderately higher percentages of B[*c*]-Ph-3,4-dihydrodiol from B[*c*]Ph (24–29% of total metabolites for rats, 17% for mice) (*17*). Recent studies have shown that human P4501B1 had higher catalytic efficiency than human P4501A1 or P4501A2 for the activation of B[*c*]Ph-3,4-dihydrodiol (*18*). These results suggest that cytochrome P450(s) other than P4501A1, possibly P4501B1, may be important for the formation of the proximate carcinogenic metabolite B[*c*]Ph-3,4-dihydrodiol from the parent compound and the formation of B[*c*]Ph-3,4-diol 1,2-epoxide from B[*c*]Ph-3,4-dihydrodiol.

B[*c*]Ph has also been found to have low monooxygenase induction activity in rat liver as determined by the examination of benz[*a*]anthracene (BA) metabolite profiles of rat liver microsomes from B[*c*]Ph-treated rats (*19*). The low mutagenic activity and carcinogenicity of B[*c*]-Ph and B[*c*]Ph-3,4-dihydrodiol in rodent systems may be due to the low formation of the 3,4-dihydrodiol and B[*c*]-Ph-3,4-diol 1,2-epoxide and a lack of inducibility of the monooxygenases by B[*c*]Ph and B[*c*]Ph-3,4-dihydrodiol (*2, 4, 19*).

The human mammary carcinoma cell line MCF-7 has been shown to bioactivate B[*c*]Ph to B[*c*]Ph-3,4-diol 1,2-epoxide (*20*). However, in mouse skin, only very small amounts of B[*c*]PhDE–DNA adducts are formed with topical B[*c*]Ph treatment (*20*). To explore the possibility that the level of B[*c*]Ph–DNA binding was limited by the levels of P450-metabolizing enzymes, B[*c*]Ph–DNA binding was investigated in MCF-7 cells and in mouse skin treated with the potent aryl hydrocarbon (Ah) receptor agonist 2,3,7,8-tetrachlorodibenzo-*p*-dioxin (TCDD) prior to topical application of B[*c*]Ph. To determine whether the differences in the activation of B[*c*]Ph in MCF-7 cell cultures and mouse skin were due to differences in the effect of B[*c*]Ph on P450 isozyme levels, P4501A1 and P4501B1 proteins in MCF-7 cells as well as in mouse epidermis were measured by Western blotting analyses.

Materials and Methods

Enzymes and Chemicals. Caution: *The PAH and PAH derivatives described in this publication are chemical carcinogens and must be handled with care as outlined in the National Cancer Institute guidelines.*

Cell Culture and Treatment. Human mammary MCF-7 cells were grown in 175-cm^2 flasks with minimal essential medium (MEM), supplemented with 10% fetal calf serum (FCS) (Intergen, Purchase, NY), 1 mM sodium pyruvate, and 0.1 mM nonessential amino acids. Human hepatoma HepG2 cells were grown in 175-cm^2 flasks with MEM, supplemented with 10% FCS. Cells covering about 90% of the flask were refed 24 h prior to treatment. For preinduction studies, cells were treated with 0.1% dimethyl sulfoxide (DMSO) or 10 nM TCDD for 24 h before 10 μM B[*c*]Ph was added for 24 h. Cells for microsomal preparations were treated with 0.1% DMSO, 10 nM TCDD, or 10 μM B[*c*]Ph for 24 or 48 h. The cells were harvested by trypsinization with 0.05% trypsin-EDTA and washed with PBS.

Treatment of Mice and Isolation of Epidermis. Female SENCAR mice (Harlan Sprague–Dawley, Inc., Indianapolis, IN), 6–7 weeks of age and in the resting phase of the hair growth cycle, were shaved on the dorsal side 2 days prior to treatment. For preinduction studies, mice (3/group) were treated topically with either 1 μg of TCDD in 200 μL of acetone:DMSO (9:1, v/v) or the vehicle control for 73 h before applying 2 μmol of B[*c*]Ph in 200 μL of acetone or 200 μL of acetone for 48 h. For microsomal preparations, mice were treated with 1 μg of TCDD in 200 μL of acetone:DMSO (9:1, v/v) or the vehicle control for 72 h or with 2 μmol of B[*c*]Ph in 200 μL of acetone for 48 or 72 h. The mice were sacrificed, and epidermis was harvested by the method of Slaga *et al.* (*21*). For microsomal preparations to be used for *in vitro* metabolism studies, the skins were heated to 50 °C instead of 58 °C. The epidermal tissue from each treatment group was pooled, and the DNA was isolated or microsomes were prepared.

^{33}P-Postlabeling Analysis of DNA Adducts. DNA was isolated by treatment with RNase, proteinase K, and phenol followed by chloroform:isoamyl alcohol (24:1) extraction as described previously (*22*). The DNA was dissolved in H_2O and quantitated by absorbance at 260 nm (1 AU = 50 μg of DNA). The DNA was postlabeled with [γ-^{33}P]ATP (*23*). Cellular DNA samples (10 μg) or B[*c*]PhDE–DNA standards (2 μg) were digested with nuclease P1 and prostatic acid phosphatase and then labeled with [γ-^{33}P]ATP (4 μCi/μL, s.a. 2000 Ci/mmol) and T4 polynucleotide kinase. The labeled adducted dinucleotides were digested to mononucleotides with snake venom phosphodiesterase and separated from other digestion products by Sep-Pak C_{18} column chromatography (*24*).

The B[*c*]Ph–DNA adducts were analyzed by reverse-phase HPLC utilizing a 5-μm Ultrasphere C_{18} column (4.6 mm × 25

[1] Abbreviations: PAH, polycyclic aromatic hydrocarbon; B[*c*]Ph, benzo[*c*]phenanthrene; B[*c*]Ph-3,4-dihydrodiol, (±)-*trans*-3,4-dihydroxy-3,4-dihydrobenzo[*c*]phenanthrene; B[*c*]PhDE, (±)-*trans*-3,4-dihydroxy-1,2-epoxy-1,2,3,4-tetrahydrobenzo[*c*]phenanthrene; (−)-B[*c*]PhDE-2, (4*R*,3*S*)-dihydroxy-(2*S*,1*R*)-epoxy-1,2,3,4-tetrahydrobenzo[*c*]phenanthrene; (+)-B[*c*]PhDE-1, (4*S*,3*R*)-dihydroxy-(2*S*,1*R*)-epoxy-1,2,3,4-tetrahydrobenzo[*c*]phenanthrene; DMBA, 7,12-dimethylbenz[*a*]anthracene; DMBA-5,6-dihydrodiol, (±)-*trans*-5,6-dihydroxy-5,6-dihydro-7,12-dimethylbenz[*a*]anthracene; DMBA-3,4-dihydrodiol, (±)-*trans*-3,4-dihydroxy-3,4-dihydro-7,12-dimethylbenz[*a*]anthracene; DMBA-8,9-dihydrodiol, (±)-*trans*-8,9-dihydroxy-8,9-dihydro-7,12-dimethylbenz[*a*]-anthracene; DMBA-10,11-dihydrodiol, (±)-*trans*-10,11-dihydroxy-10,11-dihydro-7,12-dimethylbenz[*a*]anthracene; 7HOMMBA, 7-(hydroxymethyl)-12-methylbenz[*a*]anthracene; TCDD, 2,3,7,8-tetrachlorodibenzo-*p*-dioxin; dA, deoxyadenosine; dG, deoxyguanosine; PB, phenobarbital; 3MC, 3-methylcholanthrene; B[*a*]P, benzo[*a*]pyrene; B[*a*]PDE, (±)-7,8-dihydroxy-9,10-epoxy-7,8,9,10-tetrahydrobenzo[*a*]pyrene; (+)-B[*a*]PDE-2, (7*R*,8*S*)-dihydroxy-(9*S*,10*R*)-epoxy-7,8,9,10-tetrahydrobenzo[*a*]pyrene; BA, benz[*a*]anthracene; s.a., specific activity; PMSF, (phenylmethyl)sulfonyl; DTT, dithiothreitol; TEMED, tetramethylethylenediamine.

cm; Beckman Instruments Inc., St. Louis, MO) and an on-line radioisotope detector (Radiomatic Flo-ONE BETA, Packard Instruments, Downers Grove, IL). The B[c]Ph–DNA adducts were resolved by elution at 1 mL/min with 50 mM ammonium phosphate and 20 mM tetrabutylammonium phosphate (pH 5.5; solvent A) and 50:50 (v/v) acetonitrile:methanol (solvent B). The elution gradient was as follows: 37–38% solvent B over 20 min, 38–40% solvent B over 20 min, 40–43% solvent B over 20 min, 43–49% solvent B over 20 min, 49–55% solvent B over 10 min, and isocratic elution at 55% solvent B for 20 min. The identities of the B[c]Ph-adducted nucleotides were determined by comparison with adducts from calf thymus-DNA reacted with each enantiomerically pure B[c]PhDE and with standards prepared by reaction of racemic B[c]PhDE-1 and B[c]PhDE-2 with poly-[(dA·dT)-(dA·dT)], poly[(dI·dC)-(dI·dC)], and poly[(dG·dC)-(dG·dC)] (*25, 26*).

Microsome Preparation. Microsomes from cell culture and mouse epidermis samples were prepared as described by Otto *et al.* with minor modifications (*27*). The cells were homogenized in microsomal homogenization buffer (0.25 M KH_2PO_4, 0.15 M KCl, 10 mM EDTA, and 0.25 mM PMSF) and centrifuged at 15000*g* for 20 min at 4 °C. The supernatant was centrifuged at 105000*g* for 90 min at 4 °C, and the pellet was resuspended in microsome dilution buffer (0.1 M KH_2PO_4, 20% glycerol, 10 mM EDTA, 0.1 mM DTT, and 0.25 mM PMSF). Protein concentrations were determined by the bicinchoninic acid (BCA) protein assay (Pierce, Rockford, IL).

Western Immunoblotting. Microsomal proteins were separated by sodium dodecyl sulfate–polyacrylamide gel electrophoresis (SDS–PAGE) utilizing an 11-cm 8% acrylamide separating gel and a 2.5-cm 3% acrylamide stacking gel at a thickness of 0.75 mm according to Laemmli with the following modifications (*28*). The gels contained 1% by wt of *N,N'-bis*-methyleneacrylamide and were polymerized using 0.05% by vol of tetramethylethylenediamine (TEMED). All lanes were loaded with equal amounts of protein as measured by the BCA assay, and uniformity of loading was confirmed by staining gels with Ponceau S. The gels were run at 20 mA/gel for 3–4 h and transferred to nitrocellulose using a TE50 Transfor apparatus (Hoeffer Scientific, San Francisco, CA) at 250 mA for 2 h. The membranes were blocked with 5% Carnation nonfat dry milk in PBST (PBS with 0.3% (w/v) Tween-20) and 0.2% goat serum.

The rabbit polyclonal antibody utilized to detect human P4501A1 was previously elicited against rat hepatic P4501A1 and utilized at a 1:1000 dilution (*12*). Human P4501B1 was detected utilizing a rabbit polyclonal antibody prepared against a 15-mer peptide corresponding to a putative surface loop region epitope on the human P450 protein. The peptide consisted of 14 amino acids of P450 sequence plus an additional carboxy terminal cysteine for the conjugation reaction. The peptide was conjugated directly to KLH via the cysteine residue. Polyclonal antibodies were raised in a male New Zealand rabbit by standard protocols. Serum samples were screened for anti-CYP1B1 titer and specificity by Western blotting using a human CYP1B1-maltose binding protein fusion construct.[2] Mouse P4501A1 was detected utilizing the anti-mouse P4501A1 monoclonal antibody 1-36-1 (1:15000 dilution). Mouse P4501B1 was detected utilizing a 1:5000 dilution of a rabbit polyclonal P4501B1 antibody elicited against recombinant mouse P4501B1.[3] All primary and secondary antibodies were diluted in PBST with 0.2% goat serum. The immunoreactive proteins were detected with peroxidase-conjugated anti-rabbit or anti-mouse IgG (1:15000 dilution in PBST with 0.2% goat serum) using enhanced chemiluminescence detection (Amersham Life Science Inc., Arlington Heights, IL).

DMBA Metabolism Assays. The analysis of DMBA metabolism by microsomal preparations from cultured cells and mouse epidermis was carried out as previously described (*13*). Microsomal preparations (0.5 mg of protein) were incubated with an NADPH-regenerating system and DMBA (15 nmol/mL) for 15 min at 37 °C. The metabolites were extracted with acetone:ethyl acetate (*17, 29*) after adding 10 ng of 7-hydroxycoumarin (7OH-coumarin) to each reaction as an internal control. The organic solvent-soluble DMBA metabolites were analyzed by reverse-phase HPLC utilizing a 5-μm Ultrasphere C_{18} column (4.6 mm × 25 cm; Beckman Instruments Inc., St. Louis, MO) or a 5-μm Waters Radial Pak HPLC C_{18} column (10 cm; Millipore Corp., Milford, MA), with guard cartridges and an on-line Shimadzu RF-535 fluorescence HPLC monitor at the excitation wavelength of 269 nm and emission with a 375 nm cutoff filter. The metabolites were eluted at 0.75 mL/min with a gradient of 50–100% methanol over 50 min and isocratic elution at 100% methanol for 20 min; then the column was regenerated with 100–50% methanol over 5 min. The identity of DMBA-3,4-dihydrodiol was established by comparison of retention times with (±)-*trans*-DMBA-3,4-dihydrodiol purchased from the NCI Chemical Carcinogen Repository (Kansas City, MO). The identities of 7HOMMBA and 5,6- and 8,9-dihydrodiols were determined by the comparison of their retention times with those of DMBA metabolites from phenobarbital-induced rat liver microsomes (*30, 31*). DMBA metabolite quantitation by fluorescence was based upon comparison of peak integration values with microsomal incubation of [^{3}H]DMBA in which metabolites were measured by on-line radioisotope detection.

Results

Previous studies demonstrated that B[c]Ph treatment of the human mammary carcinoma cell line MCF-7 resulted in the formation of 10 pmol of B[c]Ph–DNA adducts/mg of DNA (*20*): To determine if increases of P450 enzyme levels in these cells could increase the binding of B[c]Ph to DNA, MCF-7 cells were treated with the potent Ah receptor agonist TCDD (10 nM) or 0.1% DMSO as a control for 24 h prior to treatment with 10 μM B[c]Ph for 24 h. The high dose of B[c]Ph ensured that it would allow maximal P450 enzyme induction and also that the B[c]Ph would not all be metabolized in 24 h to allow comparison of DNA binding in the TCDD and control groups at that time. The DNA was isolated and analyzed by ^{33}P-postlabeling and reverse-phase HPLC. DNA adduct values are the result of a single experiment, and all experiments have been repeated at least once with comparable effects of TCDD on relative adduct levels in each group. Replicate DNA adduct values typically varied by 20% or less. MCF-7 cells treated with TCDD, but not exposed to B[c]Ph, showed no formation of DNA adducts (Figure 1A). The treatment of MCF-7 cells with the vehicle control prior to treatment of 10 μM B[c]Ph for 24 h resulted in a total level of B[c]Ph–DNA adducts of 12 pmol/mg of DNA (Figure 1B). B[c]Ph–DNA adduct levels increased to 40 pmol/mg of DNA in cells treated with TCDD prior to B[c]Ph exposure (Figure 1C).

Adduct levels formed by the isomeric B[c]PhDEs were differentially affected by TCDD treatment in MCF-7 cells. The levels of the B[c]PhDE–DNA adducts/mg of DNA in cells exposed to B[c]Ph alone were 5.6 pmol of (+)-B[c]PhDE-1-dA_t, 2.6 pmol of (+)-B[c]PhDE-1-dA_c, and 1.4 pmol of (−)-B[c]PhDE-2-dA_t. The subscripts indicate either *cis* (c) or *trans* (t) opening of the epoxide at C1 by the exocyclic amino group of the purine. TCDD treatment resulted in a 10-fold increase in (−)-B[c]PhDE-2-dA_t, the adduct formed from the most carcinogenic diol epoxide of B[c]Ph. The level of (−)-B[c]PhDE-2-dA_t increased from 1.4 to 14.5 pmol/mg of DNA with TCDD treatment. The level of binding of the (+)-B[c]PhDE-1-dA_t and (+)-B[c]PhDE-1-dA_c adducts increased approximately 3-fold in TCDD-treated cells (16.1 and 7.3 pmol/mg of DNA, respectively).

[2] C. B. Marcus and W. F. Greenlee, manuscript in preparation.
[3] U. Savas, C. P. Carstens, and C. R. Jefcoate, submitted for publication.

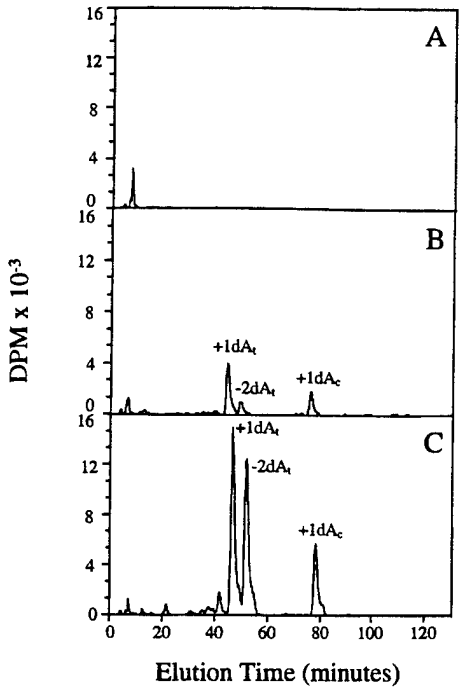

Figure 1. Effects of TCDD treatment on the binding of B[*c*]-Ph to DNA in human mammary MCF-7 cells. Reverse-phase HPLC profile of ^{33}P-postlabeled DNA adducts from MCF-7 cells treated with (A) 10 nM TCDD for 24 h prior to treatment with 0.1% DMSO for 24 h, (B) 0.1% DMSO for 24 h prior to treatment with 10 μM B[*c*]Ph for 24 h, and (C) 10 nM TCDD for 24 h prior to treatment with 10 μM B[*c*]Ph for 24 h.

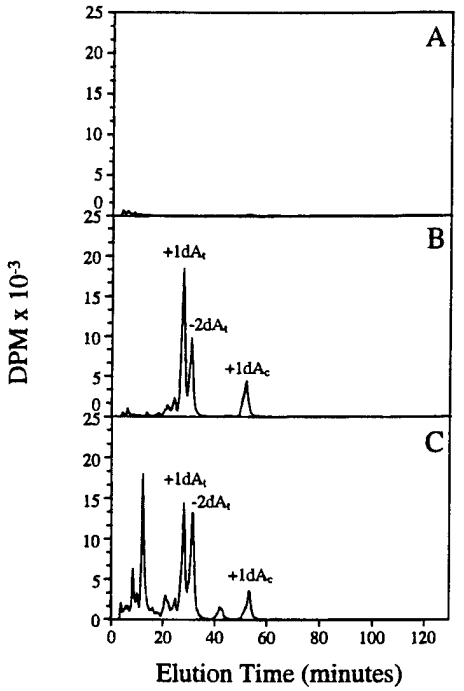

Figure 2. Effects of TCDD treatment on the binding of B[*c*]-Ph to DNA in human hepatoma HepG2 cells. Reverse-phase HPLC profile of ^{33}P-postlabeled DNA adducts from HepG2 cells treated with (A) 10 nM TCDD for 24 h prior to treatment with 0.1% DMSO for 24 h, (B) 0.1% DMSO for 24 h prior to treatment with 10 μM B[*c*]Ph for 24 h, and (C) 10 nM TCDD for 24 h prior to treatment with 10 μM B[*c*]Ph for 24 h.

HepG2 cells are a human hepatoma cell line which is known to express P4501A1 but not P4501B1 (*13*). To determine whether HepG2 cells could also metabolically activate B[*c*]Ph to DNA-binding metabolites and if the level of B[*c*]Ph–DNA adducts could be affected by the preinduction of P450-metabolizing enzymes, HepG2 cells were treated with 10 nM TCDD or 0.1% DMSO 24 h before adding 10 μM B[*c*]Ph and waiting for 24 h. HepG2 cells treated with TCDD but not exposed to B[*c*]Ph had no detectable DNA adducts (Figure 2A). Treatment of HepG2 cells with the vehicle control prior to treatment with 10 μM B[*c*]Ph resulted in a total level of B[*c*]Ph–DNA binding of 14.6 pmol/mg of DNA (Figure 2B). Treatment of HepG2 cells with TCDD before the addition of B[*c*]Ph resulted in B[*c*]Ph–DNA binding of 15.6 pmol/mg of DNA (Figure 2C). The level of binding of the (+)-B[*c*]PhDE-1-DNA adducts decreased in TCDD-treated cells compared to the vehicle control. The (+)-B[*c*]PhDE-1-dA$_t$ adduct decreased from 6.6 to 3.8 pmol/mg of DNA and (+)-B[*c*]PhDE-1-dA$_c$ decreased from 2.3 to 1.3 pmol/mg of DNA with TCDD treatment. The level of binding of the (−)-B[*c*]PhDE-2-dA$_t$ adduct remained constant with TCDD and DMSO treatment (4.3 and 4.0 pmol/mg of DNA, respectively).

Only low levels of B[*c*]Ph–DNA adducts were detected in epidermis of mice treated topically with B[*c*]Ph (*20*). To determine whether induction of P450 enzymes would alter B[*c*]Ph–DNA binding, female SENCAR mice received a topical application of 1 μg of TCDD or the vehicle control 73 h prior to treatment with 2 μmol of B[*c*]Ph for 24 h. TCDD treatment followed by application of the vehicle control did not produce DNA adducts (Figure 3A). Administration of the control vehicle to mouse epidermis prior to treatment with 2 μmol of B[*c*]Ph for 24 h resulted in a total level of binding of 2.2 pmol/mg of DNA (Figure 3B). This increased to 6.8 pmol/mg of DNA in TCDD-

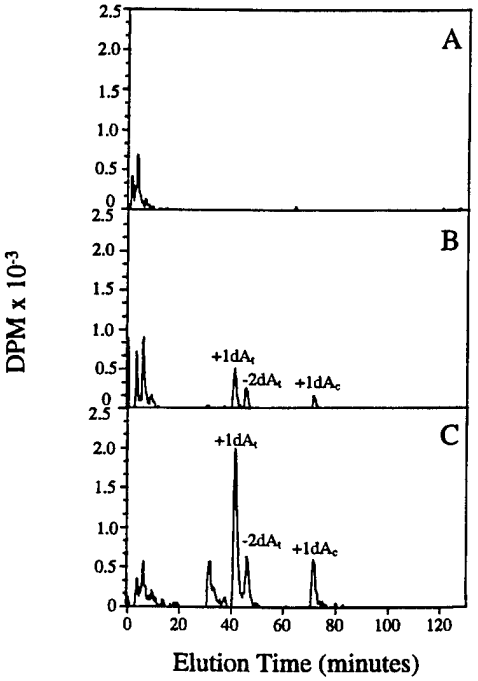

Figure 3. Effects of TCDD treatment on the binding of B[*c*]-Ph to DNA in mouse epidermis. Reverse-phase HPLC profiles of ^{33}P-postlabeled DNA adducts from mouse epidermis treated with (A) 1 μg of TCDD in 200 μL of acetone:DMSO (9:1, v/v) for 73 h prior to treatment with 200 μL of acetone for 24 h, (B) 200 μL of acetone:DMSO (9:1, v/v) for 73 h prior to treatment with 2 μmol of B[*c*]Ph for 24 h, and (C) 1 μg of TCDD in 200 μL of acetone:DMSO (9:1, v/v) for 73 h prior to treatment with 2 μmol of B[*c*]Ph for 24 h.

treated mice (Figure 3C). In contrast to human MCF-7 cells, however, the major increase in the total level of B[*c*]-PhDE–DNA binding was due to an increase in the binding of the less carcinogenic B[*c*]Ph-diol epoxide (+)-

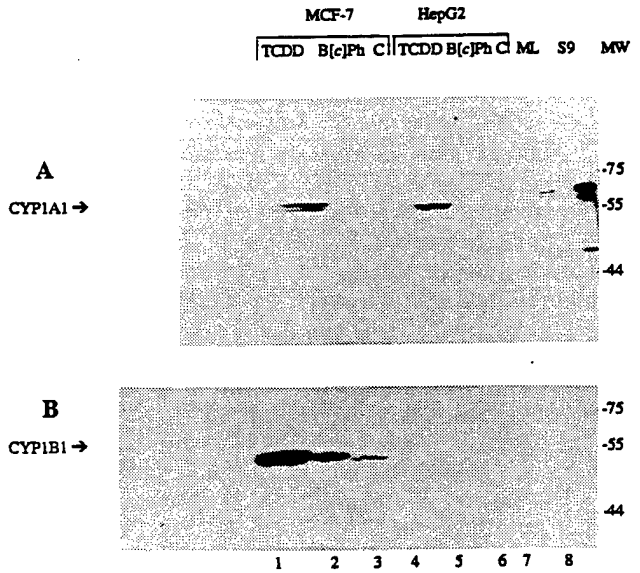

Figure 4. Immunoblot of cytochrome P450 protein in microsomes from control, B[c]Ph-treated, and TCDD-treated MCF-7 and HepG2 cells: (A) primary antibody against P4501A1 and (B) primary antibody against P4501B1. The amount of microsomal protein in each lane was as follows: lanes 1–3, 100 μg of microsomal protein from MCF-7 cells treated with 10 nM TCDD, 10 μM B[c]Ph, or 0.1% DMSO for 48 h; lanes 4–6, 50 μg of microsomal protein from HepG2 cells treated with 10 nM TCDD, 10 μM B[c]Ph, or 0.1% DMSO for 24 h; lane 7, 2 μg of BNF-induced mouse liver; lane 8, 2 μg of Aroclor-induced rat liver S9; lane 9 (labeled MW), molecular weight markers.

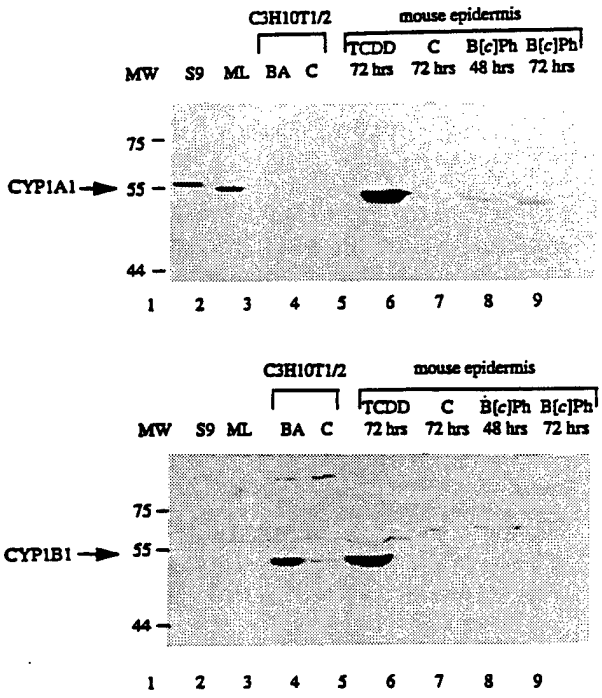

Figure 5. Immunoblot of cytochrome P450 protein in microsomes from solvent-, B[c]Ph-, and TCDD-treated mouse epidermis: (top) primary antibody against P4501A1 and (bottom) primary antibody against P4501B1. The amount of microsomal protein in each lane was as follows: lane 1, molecular weight markers; lane 2, 2 μg of Aroclor-induced rat liver S9; lane 3, 2 μg of BNF-induced mouse liver; lanes 4 and 5, microsomal protein from BA-induced or control mouse embryonic C3H10T1/2 cells; lanes 6–9, 75 μg of microsomal protein from mouse epidermis treated with 1 μg of TCDD or vehicle control for 72 h or with 2 μmol of B[c]Ph for 48 or 72 h.

B[c]PhDE-1. The level of binding per mg of DNA increased from 1.3 to 2.4 pmol of (+)-B[c]PhDE-1-dA_t and from 0.3 to 1.0 pmol of (+)-B[c]PhDE-1-dA_c after TCDD treatment. The (−)-B[c]PhDE-2-dA_t adduct increased from 0.6 to 1 pmol/mg of DNA with TCDD treatment.

To determine if P450 protein levels are increased in MCF-7 cells by B[c]Ph treatment, microsomal protein was isolated from MCF-7 cells treated with 10 μM B[c]Ph or 0.1% DMSO for 24 or 48 h and analyzed for P4501A1 or P4501B1 protein expression by Western immunoblot analysis. Microsomal proteins from MCF-7 and HepG2 cells treated with 10 nM TCDD for 24 h were used for Western blot analysis as positive controls for human P4501B1 and P4501A1 proteins, respectively (*13*). Aroclor-induced rat liver S9 and β-naphthoflavone (BNF)-induced mouse liver microsomes were used as positive controls for rodent P4501A1 protein, while microsomes from the BA-treated C3H10T1/2 mouse cell line were used as controls for P4501B1 expression (*13*). Figure 4A indicates that treatment of MCF-7 cells with 10 μM B[c]-Ph for 48 h led to, at most, a barely detectable increase in P4501A1 protein (Figure 4A): TCDD treatment caused a major increase in this protein as observed previously (*13*). Immunoblotting for P4501B1 protein demonstrated that MCF-7 cells treated with 10 μM B[c]Ph for 48 h contained high levels of this protein (Figure 4B). The level of P4501B1 protein from B[c]Ph-treated MCF-7 cells was lower than in cells treated with 10 nM TCDD (data not shown), indicating that B[c]Ph is not as potent as TCDD in increasing P450 protein levels. Similar results were observed in cells treated for 24 h (data not shown).

To determine whether the level of B[c]PhDE–DNA binding in HepG2 cells was related to P450 protein expression, HepG2 cells were treated with 10 μM B[c]-Ph, 10 nM TCDD, or 0.1% DMSO for 24 h and the level of P4501A1 protein in microsomal preparations was determined by Western immunoblot analysis (Figure 4).

P4501A1 protein was detected in TCDD-treated HepG2 cells; however, B[c]Ph treatment did not induce detectable levels of P4501A1 protein. No P4501B1 protein was detected in control or B[c]Ph- or TCDD-treated HepG2 cells (Figure 4B). TCDD-treated HepG2 cells had previously been reported to lack P4501B1 protein (*13*). Similar results were obtained in cells treated for 48 h (data not shown).

B[c]Ph bound to DNA only to a low extent in mouse epidermis (*20*). To determine if P450 protein levels increased in mouse epidermis in response to B[c]Ph treatment, female SENCAR mice received topically 1 μg of TCDD or the vehicle control for 72 h or 2 μmol of B[c]-Ph for 48 or 72 h. The levels of P4501A1 and P4501B1 in the microsomal proteins were determined by Western immunoblot analysis (Figure 5, top). Low, but detectable, constitutive levels of P4501A1 protein were present in mouse epidermis. P4501A1 protein levels were increased by B[c]Ph treatment as measured after 48 and 72 h. TCDD treatment resulted in a much greater increase in P4501A1 protein than B[c]Ph treatment (Figure 5, top). The western immunoblot indicated that P4501B1 protein was present in TCDD-treated mouse epidermis, but no P4501B1 protein was detected in solvent control or B[c]-Ph-treated mouse epidermis (Figure 5, bottom).

P4501A1 and P4501B1 enzymes have defined positional selectivities for the metabolism of DMBA. These differences in product distribution of DMBA metabolism by P4501A1 and P4501B1 have been utilized to determine the relative contributions of these P450 enzymes in hydrocarbon metabolism in numerous cells and tissues (*12, 13, 27, 31–35*). To determine the relative contribution of P4501A1 and P4501B1 to P450 enzyme activities

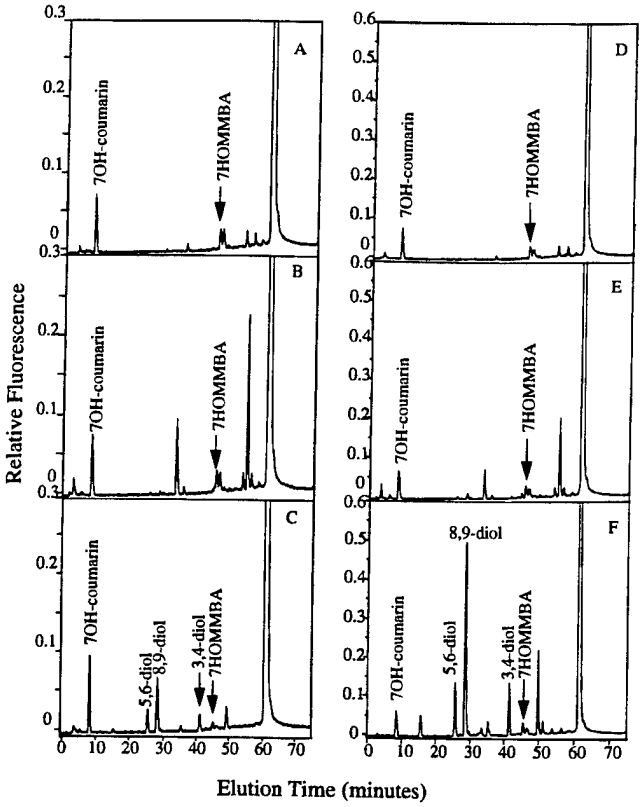

Figure 6. DMBA metabolites formed in microsomes from MCF-7 (A–C) and HepG2 (D–F) cells treated with DMSO, B[*c*]Ph, or TCDD and analyzed by reverse-phase HPLC and fluorescence detection: (A,D) DMBA metabolism profile of microsomes prepared from cells treated with 0.1% DMSO, (A) MCF-7 cells for 48 h and (D) HepG2 cells for 24 h; (B,E) DMBA metabolism profile of microsomes prepared from cells treated with 10 μM B[*c*]Ph, (B) MCF-7 cells for 48 h and (E) HepG2 cells for 24 h; and (C,F) DMBA metabolism profile of microsomes prepared from cells treated with 10 nM TCDD, (C) MCF-7 cells for 48 h and (F) HepG2 cells for 24 h.

present in B[*c*]Ph-treated MCF-7 and HepG2 cells and mouse epidermis, DMBA metabolites formed in microsomal preparations from these cells were examined by reverse-phase HPLC with fluorescence detection. The DMBA metabolism profiles from microsomal preparations of MCF-7 cells treated for 48 h and HepG2 cells treated for 24 h with 0.1% DMSO, 10 μM B[*c*]Ph, or 10 nM TCDD are shown in Figure 6. 7OH-coumarin was added to the reaction mixtures prior to extraction of the organic metabolites as an internal standard. Microsomes prepared from MCF-7 cells treated with DMSO or B[*c*]Ph had low DMBA-metabolizing activity (Figure 6A,B). TCDD treatment of MCF-7 cells increased the DMBA-metabolizing activity (Figure 6C): detectable amounts of the proximate carcinogenic 3,4-dihydrodiol were formed (Table 1). TCDD treatment increased DMBA metabolism almost 4-fold compared to microsomes from B[*c*]Ph-treated MCF-7 cells (Table 1). Microsomes prepared from HepG2 cells treated with DMSO had low DMBA-metabolizing activity comparable to that in DMSO-treated MCF-7 cells (Figure 6D, Table 1). B[*c*]Ph treatment increased the formation of 5,6- and 8,9-dihydrodiols to detectable levels in HepG2 cells (Figure 6E, Table 1). DMBA metabolism in microsomes from B[*c*]Ph-treated HepG2 cells was 2.8-fold higher than in microsomes from B[*c*]Ph-treated MCF-7 cells (Table 1). TCDD treatment increased the DMBA-metabolizing activity in HepG2 cells 7-fold (Figure 6F): the largest increase was in formation of DMBA dihydrodiols, including the 3,4-diol (Table 1).

Table 1. DMBA Metabolites Formed from Microsomal Preparations of Solvent-, B[c]Ph-, or TCDD-Treated MCF-7 Cells, HepG2 Cells, and Mouse Epidermis

	DMBA metabolites (pmol (mg of microsomal protein)$^{-1}$ h^{-1})[b]			
	dihydrodiols			
treatment[a]	5,6	8,9	3,4	7HOMMBA
	MCF-7 Cells			
control	nd[c]	nd	nd	131
B[c]Ph	nd	nd	nd	68
TCDD	58 (23)[d]	114 (45)	42 (16)	41 (16)
	HepG2 Cells			
control	nd	nd	nd	166
B[c]Ph	9 (5)	21 (11)	nd	158 (84)
TCDD	253 (18)	748 (55)	224 (16)	146 (11)
	Mouse Epidermis			
control	4 (22)	5 (28)	nd	9 (50)
B[c]Ph	4 (11)	7 (20)	nd	24 (69)
TCDD	99 (10)	216 (22)	15 (2)	670 (67)

[a] HepG2 and MCF-7 cells were treated with 0.1% DMSO (control), 10 μM B[*c*]Ph, or 10 nM TCDD for 24 and 48 h, respectively (Figure 6). Mouse epidermis was treated topically with 1 μg of TCDD or vehicle control for 72 h or with 2 μmol of B[*c*]Ph for 48 h (Figure 7). [b] The values represent the average of duplicate determinations. [c] Below detection limit. [d] Percentage of total identified DMBA metabolites.

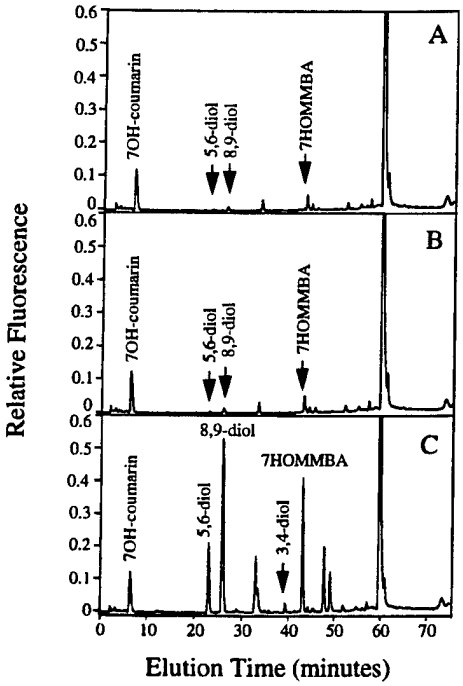

Figure 7. DMBA metabolites formed in microsomes from mouse epidermis treated with DMSO, B[*c*]Ph, or TCDD analyzed by reverse-phase HPLC and fluorescence detection. DMBA metabolism profile of microsomes prepared from mouse epidermis treated with (A) 200 μL of acetone:DMSO (9:1, v/v) for 72 h, (B) 2 μmol of B[*c*]Ph in 200 μL of acetone for 48 h, and (C) 1 μg of TCDD in 200 μL of acetone:DMSO (9:1, v/v) for 72 h.

Microsomes prepared from mouse epidermis treated with vehicle control or B[*c*]Ph for 48 h produced similar low levels of the 5,6- and 8,9-dihydrodiols (Figure 7A,B). Microsomes from the B[*c*]Ph-treated epidermis produced larger amounts of 7HOMMBA than control microsomes (Table 1). TCDD treatment increased the total DMBA-metabolizing activity 55- and 29-fold compared to microsomes from control and B[*c*]Ph-treated mouse epidermis, respectively (Figure 7C, Table 1). The microsomes from TCDD-treated mouse epidermis produced detectable levels of 3,4-dihydrodiol but much greater quantities of

the 5,6- and 8,9-dihydrodiols and especially 7HOMMBA (Table 1).

Discussion

The human mammary carcinoma cell line MCF-7 can metabolically activate B[c]Ph to B[c]Ph-3,4-diol 1,2-epoxides (*20*). Although mouse skin is also capable of activating B[c]Ph to B[c]PhDE, the level of B[c]PhDE–DNA adducts formed in mouse skin is very low. This low level of B[c]PhDE formation and the low DNA adduct level correlate with the weak tumorigenicity of B[c]Ph in mouse skin (*2, 20*). The formation of diol epoxide adducts may be limited by the ability of B[c]Ph to induce P450 enzymes which are involved in the activation of this PAH. The ability of P450 enzymes to be induced in these cells was examined with the Ah receptor agonist TCDD which is known to induce both P4501A1 and P4501B1 in human MCF-7 cells (*13*). TCDD induced P4501A1 and P4501B1 in mouse epidermis as shown in Figure 5. Rodent liver P4501A1 has been shown to metabolize B[c]-Ph effectively, although the formation of B[c]Ph-3,4-dihydrodiol and subsequent 1,2-epoxidation by P4501A1 are low (*16, 17*). Human P4501B1 has been shown to be more effective than human P4501A1 in the bioactivation of B[c]Ph-3,4-dihydrodiol (*18*).

TCDD treatment of MCF-7 cells and mouse epidermis increased the total level of B[c]PhDE–DNA binding to similar extents (3.5- and 3-fold, respectively). This supports the hypothesis that B[c]Ph–DNA binding may be limited by the ability of B[c]Ph to induce P450 enzymes. However, the activation of B[c]Ph to specific optical isomers of B[c]PhDE increased to different extents. In MCF-7 cells, the increase of B[c]Ph–DNA binding resulting from TCDD treatment was due to a 10-fold increase in the formation of the (−)-B[c]PhDE-2-dA_t adduct, whereas in mouse epidermis, most of the increase was due to enhanced formation of (+)-B[c]PhDE-1-dA adducts. The increased formation of the (−)-B[c]PhDE-2-dA_t adduct has important implications because of the higher carcinogenicity of (−)-B[c]PhDE-2 (*R,S,S,R*-configuration) in comparison to the other B[c]PhDE optical isomers on mouse skin or in newborn mice (*4, 36*) and higher mutagenicity in the mammalian V79 mutation assays (*37*). A high degree of formation of deoxyadenosine adducts has also been implicated in the high carcinogenic potency of other PAH diol epoxides, such as dibenzo[*a,l*]pyrene, DMBA, and benzo[*g*]chrysene (*20, 38–43*).

Previous studies by DiGiovanni, Slaga, and co-workers have demonstrated that treatment of mice with 1 μg of TCDD for 72 h prior to treatment with initiating doses of B[a]P or DMBA significantly decreased papilloma formation after 15–24 weeks of promotion (*44–46*). To determine whether TCDD could affect the levels of PAH–DNA adducts, they treated mouse skin with 1 μg of TCDD prior to treatment with DMBA or B[a]P and the PAH–DNA adducts were measured after 24 h (*44*). The levels of DMBA–DNA adducts were significantly decreased after TCDD treatment; this decrease correlated with the diminished carcinogenicity of DMBA after TCDD treatment. In contrast, the levels of B[a]P–DNA adducts increased 2.8-fold with TCDD treatment (*44*). In B[a]P-treated mouse epidermis the most abundant adduct was (+)-B[a]PDE-2-dG (from the diol epoxide with *R,S,S,R*-configuration, the most carcinogenic diol epoxide of B[a]P), but this adduct was absent when the skin was treated with TCDD before B[a]P treatment (*44*). These results indicated that the formation of specific adducts rather than the total level of PAH–DNA adducts is important for the carcinogenicity of the hydrocarbon (*44*). The increase in the level of B[c]PhDE–DNA adducts in mouse epidermal DNA after TCDD treatment (3-fold) correlated well with the greater extent of B[a]P–DNA binding in this tissue (*44*). In the present studies, the increased formation of (+)-B[c]PhDE-1-dA adducts and the lack of increase in the formation of the (−)-B[c]PhDE-2-dA_t adduct (*R,S,S,R*-configuration) in mouse epidermis after TCDD treatment demonstrated that the activation of B[c]Ph to the less carcinogenic B[c]PhDE-1 is responsible for the increase in DNA binding observed. The decrease in specific adducts in TCDD-treated mouse epidermis may be related to an increase in detoxification enzymes which selectively metabolize specific diol epoxide stereoisomers (*44–46*) or to differential induction of P450 enzymes that activate B[c]Ph.

TCDD increased the level of P4501A1 protein in the human hepatoma cell line HepG2; however, P4501B1 protein was not detected in these cells (Figure 4). The lack of increase in the levels of B[c]PhDE–DNA adducts in human HepG2 cells treated with TCDD suggests that the induction of P450 enzymes alone does not always increase B[c]Ph–DNA binding. It is possible that induction of high levels of P4501A1 may cause rapid oxidation of B[c]Ph and destroy potential DNA-binding metabolites before they are able to reach and bind to the DNA. Other factors that may limit the binding of B[c]Ph by TCDD-treated HepG2 cells could include limited availability of heme, P450-reductase or epoxide hydrase, or lack of induction of P4501B1. MCF-7 cells treated with TCDD exhibited a 3-fold increase in P4501B1 activity (*13*) and a 3.5-fold increase in the level of B[c]Ph–DNA binding. The increase in P4501B1 activity correlates positively with the increase in B[c]PhDE–DNA adduct formation in MCF-7 cells.

Western blot analysis indicated that B[c]Ph treatment caused, at most, a very small increase in P4501A1 in human cells but did cause formation of detectable levels of P4501A1 protein in mouse epidermis. In contrast, B[c]-Ph treatment resulted in an increase in P4501B1 protein in MCF-7 cells, but no detectable increase in P4501B1 in mouse epidermis. Due to the higher level of activation of B[c]Ph-3,4-dihydrodiol to the diol epoxide by P4501B1 than by P4501A1 (*18*), the ability of B[c]Ph to increase P4501B1 induction in MCF-7 cells and the failure to increase P4501B1 in mouse epidermis may be important factors in the different abilities of human cells and mouse epidermis to activate B[c]Ph to carcinogenic diol epoxides. Differences in the catalytic properties of human and mouse P4501B1 may also be important. Metabolism experiments to investigate this are in progress. Differences in the regioselectivity of DMBA metabolism by P4501A1 and P4501B1 enzymes have allowed measurements of DMBA metabolite formation to be used to characterize the relative contribution of these P450s to polycyclic aromatic hydrocarbon metabolism in a particular system. Christou *et al.* (*13*) characterized DMBA metabolism by P4501A1 and P4501B1 in microsomes from MCF-7 cells. Comparison of DMBA metabolism by untreated MCF-7 cells, which expressed P4501B1 and very little P4501A1, with TCDD-treated MCF-7 cells, which expressed high levels of P4501A1, indicated relatively higher formation of DMBA-3,4-dihydrodiol by P4501B1 (*13*). P4501B1 metabolism also resulted in a

greater proportion of DMBA-10,11-dihydrodiol relative to DMBA-8,9-dihydrodiol and a lack of 7-methyl hydroxylation of DMBA (*13*).

Analysis of DMBA metabolism in microsomal preparations of control and B[*c*]Ph-treated MCF-7 cells demonstrated low DMBA-metabolizing activity. Although control MCF-7 cells express some P4501B1, no DMBA-3,4-dihydrodiol was detected. The ratios of DMBA-8,9-dihydrodiol to DMBA-10,11-dihydrodiol also differ between P4501A1 and P4501B1 (*13*). The separation of these diols has been reported previously by reverse-phase C_{18} HPLC columns (*13, 34, 35*) and with normal-phase HPLC columns (*33*); however, the reverse-phase C_{18} columns used in the present study did not resolve the 8,9- and 10,11-dihydrodiols.

The DMBA metabolism profiles from microsomal preparations derived from TCDD-treated MCF-7 cells had similar ratios of DMBA metabolites as those from TCDD-treated HepG2 cells (Table 1). Most of the DMBA-metabolizing activity in TCDD-treated HepG2 cells and MCF-7 cells is due to P4501A1 (*13*). In microsomal preparations from mouse skin treated with B[*c*]Ph or TCDD, the ratios of DMBA metabolites were comparable to those in cells with high levels of P4501A1. Formation of a high proportion of 7HOMMBA (67–69%) and a low extent of formation of DMBA-3,4-dihydrodiol (0–2%) were observed in microsomes from mouse epidermis treated with TCDD. The higher level of P4501A1 in mice treated with TCDD than in those treated with B[*c*]Ph correlates with the higher DMBA metabolism in TCDD-treated mouse epidermis. The differences in the relative formation of DMBA-3,4-dihydrodiol and 7HOMMBA in TCDD-treated human cells and mouse epidermis may reflect differences in DMBA metabolism by human and mouse P4501A1 (*13*). Human P4501A1 has been found to form DMBA-3,4-dihydrodiol to a higher extent than mouse P4501A1 and to have lower activity for the formation of the 7HOMMBA than mouse P4501A1 (*13*). TCDD-treated human cells formed a higher proportion of the proximate carcinogenic metabolites of DMBA, DMBA-3,4-dihydrodiol (16% of total identified metabolites), than TCDD-treated mouse epidermis (2% of total identified metabolites).

The ability of B[*c*]Ph to induce P4501B1 in human cells but not in mouse epidermis may have important implications for the carcinogenicity of B[*c*]Ph in humans. Human P4501B1 has a higher capacity than P4501A1 for the formation of B[*c*]PhDE from B[*c*]Ph-3,4-dihydrodiol (*18*). TCDD pretreatment experiments suggest that in mouse epidermis P4501A1 activates a higher proportion of B[*c*]Ph to the less carcinogenic stereoisomer B[*c*]PhDE-1, whereas in human mammary MCF-7 cells P4501B1 activates B[*c*]Ph to both B[*c*]PhDE-2 and B[*c*]PhDE-1. There appear to be significant species and tissue specificities in the mechanisms by which various PAHs regulate expression of the P450 family. Thus, the ability of B[*c*]Ph to increase P450 activity in various tissues and species, the particular P450 enzyme induced, and their catalytic activities all may be important in determining the carcinogenic risk that B[*c*]Ph poses to a particular tissue and species.

Acknowledgment. The authors thank Marilyn Hines for her help in preparing the manuscript. This research was supported in part by USPHS Grants CA 40228 (W.M.B.), CA 28825 (W.M.B.), and CA 17613 (S.A.).

References

(1) Lunde, G., and Bjorseth, A. (1977) Polycyclic aromatic hydrocarbons in long-range transported aerosols. *Nature* **268**, 518–519.

(2) Levin, W., Wood, A. W., Chang, R. L., Ittah, Y., Croisy-Delcey, M., Yagi, H., Conney, A. H., and Jerina, D. M. (1980) Exceptionally high tumor-initiating activity of benzo(*c*)phenanthrene bay-region diol-epoxides on mouse skin. *Cancer Res.* **40**, 3910–3914.

(3) Wood, A. W., Chang, R. L., Levin, W., Ryan, D. E., Thomas, P. E., Croisy-Delcey, M., Ittah, Y., Yagi, H., Jerina, D. M., and Conney, A. H. (1980) Mutagenicity of the dihydrodiols and bay-region diol-epoxides of benzo(*c*)phenanthrene in bacterial and mammalian cells. *Cancer Res.* **40**, 2876–2883.

(4) Levin, W., Chang, R. L., Wood, A. W., Thakker, D. R., Yagi, H., Jerina, D. M., and Conney, A. H. (1986) Tumorigenicity of optical isomers of the diastereomeric bay-region 3,4-diol-1,2-epoxides of benzo(*c*)phenanthrene in murine tumor models. *Cancer Res.* **46**, 2257–2261.

(5) Amin, S., Desai, D., and Hecht, S. S. (1993) Tumor-initiating activity on mouse skin of bay region diol-epoxides of 5,6-dimethylchrysene and benzo[*c*]phenanthrene. *Carcinogenesis* **14**, 2033–2037.

(6) Amin, S., Krzeminski, J., Rivenson, A., Kurtzke, C., Hecht, S. S., and El-Bayoumy, K. (1995) Mammary carcinogenicity in female CD rats of fjord region diol epoxides of benzo[*c*]phenanthrene, benzo[*g*]chrysene and dibenzo[*a,l*]pyrene. *Carcinogenesis* **16**, 1971–1974.

(7) Hecht, S. S., El-Bayoumy, K., Rivenson, A., and Amin, S. (1994) Potent mammary carcinogenicity in female CD Rats of a fjord region diol-epoxide of benzo[*c*]phenanthrene compared to a bay region diol-epoxide of benzo[*a*]pyrene. *Cancer Res.* **54**, 21–24.

(8) Wood, A. W., Chang, R. L., Levin, W., Thakker, D. R., Yagi, H., Sayer, J. M., Jerina, D. M., and Conney, A. H. (1984) Mutagenicity of the enantiomers of the diastereomeric bay-region benzo(*c*)-phenanthrene 3,4-diol-1,2-epoxides in bacterial and mammalian cells. *Cancer Res.* **44**, 2320–2324.

(9) Glatt, H., Piée, A., Pauly, K., Steinbrecher, T., Schrode, R., Oesch, F., and Seidel, A. (1991) Fjord- and bay-region diol-epoxides investigated for stability, SOS induction in *Escherichia coli*, and mutagenicity in *Salmonella typhimurium* and mammalian cells. *Cancer Res.* **51**, 1659–1667.

(10) Phillips, D. H., Hewer, A., Seidel, A., Steinbrecher, T., Schrode, R., Oesch, F., and Glatt, H. (1991) Relationship between mutagenicity and DNA adduct formation in mammalian cells for fjord- and bay-region diol-epoxides of polycyclic aromatic hydrocarbons. *Chem.-Biol. Interact.* **80**, 177–186.

(11) Guengerich, F. P., and Shimada, T. (1991) Oxidation of toxic and carcinogenic chemicals by human cytochrome P450 enzymes. *Chem. Res. Toxicol.* **4**, 391–407.

(12) Pottenger, L. H., and Jefcoate, C. R. (1990) Characterization of a novel cytochrome P450 from the transformable cell line, C3H/10T1/2. *Carcinogenesis* **11**, 321–327.

(13) Christou, M., Savas, U., Spink, D. C., Gierthy, J. F., and Jefcoate, C. R. (1994) Co-expression of human P4501A1 and a human analog of cytochrome P450-EF in response to 2,3,7,8-tetrachlorodibenzo-*p*-dioxin in the human mammary carcinoma-derived MCF-7 cells. *Carcinogenesis* **15**, 725–732.

(14) Bhattacharyya, K. K., Brake, P. B., Eltom, S. E., Otto, S., and Jefcoate, C. R. (1995) Identification of a rat adrenal cytochrome P450 active in polycyclic hydrocarbon metabolism as rat P4501B1. *J. Biol. Chem.* **270**, 11595–11602.

(15) Bauer, E., Guo, Z., Ueng, Y.-F., Bell, L. C., Zeldin, D., and Guengerich, F. P. (1995). Oxidation of benzo[*a*]pyrene by recombinant human cytochrome P450 enzymes. *Chem. Res. Toxicol.* **8**, 136–142.

(16) Ittah, Y., Thakker, D. R., Levin, W., Croisy-Delcey, M., Ryan, D. E., Thomas, P. E., Conney, A. H., and Jerina, D. M. (1983) Metabolism of benzo[*c*]phenanthrene by rat liver microsomes and by a purified monooxygenase system reconstituted with different isozymes of cytochrome P450. *Chem.-Biol. Interact.* **45**, 15–28.

(17) Thakker, D. R., Levin, W., Yagi, H., Yeh, H. J. C., Ryan, D. E., Thomas, P. E., Conney, A. H., and Jerina, D. M. (1986) Stereoselective metabolism of the (+)-(*S,S*)- and (−)-(*R,R*)-enantiomers of *trans*-3,4-dihydroxy-3,4-dihydrobenzo[*c*]phenanthrene by rat and mouse liver microsomes and by a purified and reconstituted cytochrome P450 system. *J. Biol. Chem.* **261**, 5404–5413.

(18) Shimada, T., Hayes, C. L., Yamazaki, H., Amin, S., Hecht, S. S., Guengerich, F. P., and Sutter, T. R. (1996) Activation of chemically diverse procarcinogens by human cytochrome P4501B1. *Cancer Res.* **56**, 2979–2984.

(19) Jacob, J., Schmoldt, A., Raab, G., Hamann, M., and Grimmer, G. (1983) Induction of specific monooxygenases by isosteric heterocyclic compounds of benz[*a*]anthracene, benzo[*c*]phenanthrene and chrysene. *Cancer Lett.* **20**, 341–348.

(20) Einolf, H. J., Amin, S., Yagi, H., Jerina, D. M., and Baird, W. M. (1996) Benzo[c]phenanthrene is activated to DNA-binding diol epoxides more efficiently in the human mammary carcinoma cell line MCF-7 than in mouse skin. *Carcinogenesis* **17**, 2237–2244.
(21) Slaga, T. J., Das, S. B., Rice, J. M., and Thompson, S. (1974) Fractionation of mouse epidermal chromatin components. *J. Invest. Dermatol.* **63**, 343–349.
(22) Beach, A. C., and Gupta, R. (1992) Human biomonitoring and the ^{32}P-postlabeling assay. *Carcinogenesis* **13**, 1053–1074.
(23) Ralston, S. L., Seidel, A., Luch, A., Platt, K. L., and Baird, W. M. (1995) Stereochemical activation of dibenzo[*a,l*]pyrene to (−)-*anti*- and (+)-*syn*-11,12-diol-13,14-epoxides which bind extensively to deoxyadenosine residues of DNA in the human mammary carcinoma cell line MCF-7. *Carcinogenesis* **16**, 2899–2907.
(24) Lau, H. H. S., and Baird, W. M. (1994) Separation and characterization of post-labeled DNA adducts of stereoisomers of benzo[*a*]pyrene-7,8-diol-9,10-epoxide by immobilized boronate chromatography and HPLC analysis. *Carcinogenesis* **15**, 907–915.
(25) Butch, E. R., Lau, H. H. S., Shaw, K. L., Smolarek, T. A., Schmerold, I., Anderson, J. N., Baird, W. M., Yagi, H., and Jerina, D. M. (1992) High selectivity of polyclonal antibodies against DNA modified by diastereomeric benzo[c]phenanthrene-3,4-diol-1,2-epoxides. *Carcinogenesis* **13**, 895–899.
(26) Yagi, H., Thakker, D. R., Ittah, Y., Croisy-Delcey, M., and Jerina, D. M. (1983) Synthesis and assignment of absolute configuration to the trans 3,4-dihydrodiols and 3,4-diol-1,2-epoxides of benzo[*c*]phenanthrene. *Tetrahedron Lett.* **24**, 1349–1352.
(27) Otto, S., Marcus, C., Pidgeon, C., and Jefcoate, C. R. (1991) A novel adrenocorticotropin-inducible cytochrome P450 from rat adrenal microsomes catalyzes polycyclic aromatic hydrocarbon metabolism. *Endocrinology* **129**, 970–982.
(28) Laemmli, U. K. (1970) Cleavage of structural proteins during the assembly of the head of bacteriophage T4. *Nature* **227**, 680–685.
(29) Keller, G. M., Turner, C. R., and Jefcoate, C. R. (1982) Kinetic determinants of benzo[*a*]pyrene metabolism to dihydrodiol epoxides by 3-methylcholanthrene- induced rat liver microsomes. *Mol. Pharmacol.* **22**, 451–458.
(30) Christou, M., Wilson, N. M., and Jefcoate, C. R. (1984) The role of secondary metabolism in the metabolic activation of 7,12-dimethylbenz[*a*]anthracene by rat liver microsomes. *Carcinogenesis* **5**, 1239–1247.
(31) Christou, M., Wilson, N. M., and Jefcoate, C. R. (1987) Expression and function of three cytochrome P-450 isozymes in rat extrahepatic tissues. *Arch. Biochem. Biophys.* **258**, 519–534.
(32) Pottenger, L. H., Christou, M., and Jefcoate, C. R. (1991) Purification and immunological characterization of a novel cytochrome P450 from C3H/10T1/2 cells. *Arch. Biochem. Biophys.* **286**, 488–497.
(33) Morrison, V. M., Burnett, A. K., Forrester, L. M., Wolf, C. R., and Craft, J. A. (1991) The contribution of specific cytochrome P-450 in the metabolism of 7,12-dimethylbenz[*a*]anthracene in rat and human liver microsomal membranes. *Chem.-Biol. Interact.* **79**, 179–196.
(34) Otto, S., Bhattacharyya, K. K., and Jefcoate, C. R. (1992) Polycyclic aromatic hydrocarbon metabolism in rat adrenal, ovary and testis microsomes is catalyzed by the same novel cytochrome P450 (P450RAP). *Endocrinology* **131**, 3067–3076.
(35) Christou, M., Keith, I. M., Shen, X., Schroeder, M. E., and Jefcoate, C. R. (1993) Reversal of cytochrome P-4501A1 and P-450-EF expression in MCA-C3H/10T1/2 cell-derived tumors as compared to cultured cells. *Cancer Res.* **53**, 968–976.
(36) Jerina, D. M., Sayer, J. M., Yagi, H., Croisy-Delcey, M., Ittah, Y., Thakker, D. R., Wood, A. W., Chang, R. L., Levin, W., and Conney, A. H. (1982) Highly tumorigenic bay-region diol epoxides from the weak carcinogen bezno[c]phenanthrene. In *Adv. Exp. Med. Biol.: Biological Reactive Intermediates IIA* (Snyder, R., Parke, D. V., Kocsis, J. J., Jollow, D. J., Gibson, C. G., and Witmer, C. M., Eds.) pp 501–523, Plenum Publishing Co., New York.
(37) Wood, A. W., Chang, R. L., Levin, W., Thakker, D. R., Yagi, H., Sayer, J. M., Jerina, D. M., and Conney, A. H. (1984) Mutagenicity of the enantiomers of the diastereomeric bay-region benzo(*c*)-phenanthrene 3,4-diol-1,2-epoxides in bacterial and mammalian cells. *Cancer Res.* **44**, 2320–2324.
(38) Giles, A. S., Seidel, A., and Phillips, D. H. (1995) *In vitro* reaction with DNA of the fjord-region diol epoxides of benzo[*g*]chrysene and benzo[c]phenanthrene as studied by ^{32}P-postlabeling. *Chem. Res. Toxicol.* **8**, 591–599.
(39) Szeliga, J., Lee, H., Harvey, R. G., Page, J. E., Ross, H., Routledge, M. N., Hilton, B. D., and Dipple, A. (1994) Reaction with DNA and mutagenic specificity of *syn*-benzo[*g*]chrysene-11,12-diol 13,14-epoxide. *Chem. Res. Toxicol.* **7**, 420–427.
(40) Bigger, C. A. H., Sawicki, J. T., Blake, D. M., Raymond, L. G., and Dipple, A. (1983) Products of binding of DMBA to DNA in mouse skin. *Cancer Res.* **43**, 5647–5651.
(41) Dipple, A., Pigott, M., Moschel, R. C., and Costantino, N. (1983) Evidence that binding of 7,12-dimethylbenz[*a*]anthracene to DNA in mouse embryo cell cultures results in extensive substitution of both adenine and guanine residues. *Cancer Res.* **43**, 4132–4135.
(42) Dipple, A., Pigott, M. A., Agarwal, S. K., Yagi, H., Sayer, J. M., and Jerina, D. M. (1987) Optically active benzo[c]phenanthrene diol epoxides bind extensively to adenine in DNA. *Nature* **327**, 535–536.
(43) Jerina, D. M., Chadha, A., Cheh, A. M., Schurdak, M. E., Wood, A. W., and Sayer, J. M. (1991) Covalent bonding of bay-region diol epoxides to nucleic acids. In *Biological Reactive Intermediates IV. Molecular and cellular effects and their impact on human health (Adv. Expt. Med. Biol. 283)* (Witmer, C. M., Snyder, R., Jollow, D. J., Kalf, G. F., Kocsis, J. J., and Sipes, J. G., Eds.) pp 533–553, Plenum Press, New York.
(44) Cohen, G. M., Bracken, W. M., Iyer, R. P., Berry, D. L., Selkirk, J. K., and Slaga, T. J. (1979) Anticarcinogenic effects of 2,3,7,8-tetrachlorodibenzo-*p*-dioxin on benzo[*a*]pyrene and 7,12-dimethylbenz[*a*]anthracene tumor initiation and its relationship to DNA binding. *Cancer Res.* **39**, 4027–4033.
(45) DiGiovanni, J., Berry, D. L., Juchau, M. R., and Slaga, T. J. (1979) 2,3,7,8-Tetrachlorodibenzo-*p*-dioxin: potent anticarcinogenic activity in CD-1 mice. *Biochem. Biophys. Res. Commun.* **86**, 577–584.
(46) DiGiovanni, J. (1992) Multistage carcinogenesis in mouse skin. *Pharmacol. Ther.* **54**, 63–128.

TX960174N

[CANCER RESEARCH 58, 2366–2374, June 1, 1998]

Characterization of CYP1B1 and CYP1A1 Expression in Human Mammary Epithelial Cells: Role of the Aryl Hydrocarbon Receptor in Polycyclic Aromatic Hydrocarbon Metabolism[1]

Michele Campaigne Larsen, William G. R. Angus, Paul B. Brake, Sakina E. Eltom, Kristine A. Sukow, and Colin R. Jefcoate[2]

Environmental Toxicology Center [M. C. L., P. B. B., C. R. J.] and the Department of Pharmacology [W. G. R. A., S. E. E., K. A. S., C. R. J.], University of Wisconsin, Madison, Wisconsin 53706

ABSTRACT

CYP1B1 and CYP1A1 expression and metabolism of 7,12-dimethylbenz(*a*)anthracene (DMBA) have been characterized in early-passage human mammary epithelial cells (HMECs) isolated from reduction mammoplasty tissue of seven individual donors. The level of constitutive microsomal CYP1B1 protein expression was donor dependent (<0.01–1.4 pmol/mg microsomal protein). CYP1B1 expression was substantially induced by exposure of the cells to 2,3,7,8-tetrachlorodibenzo-*p*-dioxin (TCDD) to levels ranging from 2.3 to 16.6 pmol/mg among the seven donors. Extremely low, reproducible levels of constitutive CYP1A1 expression were detectable in three donors (0.03–0.16 pmol/mg microsomal protein). TCDD inductions were larger for CYP1A1, as compared to CYP1B1, demonstrating substantial variability in the induced levels among the donors (0.8–16.5 pmol/mg). Northern and reverse transcriptase PCR analyses corroborate the donor-dependent differences in protein expression, whereby CYP1B1 mRNA (5.2 kb) was constitutively expressed and was highly induced by TCDD (33-fold). The contributions of CYP1B1 and CYP1A1 to the metabolism of DMBA were analyzed using recombinant human CYP1B1 and CYP1A1, as references, in conjunction with antibody-specific inhibition analyses (anti-CYP1B1 and anti-CYP1A1). Constitutive microsomal activity exhibited a profile of regioselective DMBA metabolism that was characteristic of human CYP1B1 (increased proportions of 5,6- and 10,11-DMBA-dihydrodiols), which was inhibited by anti-CYP1B1 (84%) but not by anti-CYP1A1. TCDD-induced HMEC microsomal DMBA metabolism generated the 8,9-dihydrodiol of DMBA as the predominant metabolite, with a regioselectivity similar to that of recombinant human CYP1A1, which was subsequently inhibited by anti-CYP1A1 (79%). A CYP1B1 contribution was indicated by the regioselectivity of residual metabolism and by anti-CYP1B1 inhibition (25%). DMBA metabolism analyses of one of three donors expressing measurable basal expression of CYP1A1 confirmed DMBA metabolism levels equivalent to that from CYP1B1. The HMECs of all donors expressed similar, very high levels of the aryl hydrocarbon receptor and the aryl hydrocarbon nuclear translocator protein, suggesting that aryl hydrocarbon receptor and aryl hydrocarbon nuclear translocator protein expression are not responsible for differences in cytochrome P450 expression. This study indicates that CYP1B1 is an important activator of polycyclic aromatic hydrocarbons in the mammary gland when environmental chemical exposures minimally induce CYP1A1. Additionally, certain individuals express low levels of basal CYP1A1 in HMECs, representing a potential risk factor of mammary carcinogenesis through enhanced polycyclic aromatic hydrocarbon bioactivation.

INTRODUCTION

In the United States, breast cancer represents the second leading cause of cancer-related death in women (1). The etiology of breast cancer remains unknown, although developmental, genetic, endocrine, dietary, and environmental factors have been implicated as risk factors for mammary tumorigenesis. Environmental contaminants, including PAHs,[3] have been associated with chemical-mediated carcinogenesis in rodent models. In humans, mammary tissue is an important target site for PAH-mediated carcinogenesis, particularly because PAHs partition into mammary adipose tissue (2–8).

The cytochrome P450 superfamily of drug-metabolizing enzymes mediates the detoxication of environmental contaminants, including PAHs (9–11). However, PAHs often undergo bioactivation, thereby acquiring carcinogenic and mutagenic potential as a consequence of the oxidative metabolic process (12–14). Mutagenesis analyses have shown that rat mammary epithelial cells and HMECs preferentially activate DMBA and benzo(*a*)pyrene, respectively, to mutagenic dihydrodiol epoxides, which are the most potent cancer initiators produced by these compounds (15). The bioactivated PAHs have been implicated in the development of a variety of rodent tumors, including mammary cancer, by inducing mutations in genes that control cell proliferation (H-*ras*) or regulate cellular adaptation to chemical-mediated damage (*p53*; Refs. 16–19). In addition, cH-*ras* gene amplification has been demonstrated in primary HMECs following treatment with activated chemical carcinogens, and the immortalization and transformation of HMECs has been observed following treatment with PAHs (20–23).

This study focuses on the CYP1 superfamily of cytochrome P450 isozymes, which are largely responsible for both PAH activation and detoxication in many cells (24, 25). The CYP1A family of P450 cytochromes is composed of CYP1A1, which is broadly expressed after PAH induction but rarely observed constitutively, and CYP1A2, which is constitutively expressed and TCDD inducible almost exclusively in the liver (26). PAH-mediated induction of CYP1A1 and CYP1A2 is stimulated by ligand binding to AhR (24). TCDD, the most potent agonist of the AhR, mediates the transcriptional activation of CYP1A1 via a cellular cascade initiated by ligand binding, followed by dissociation of the M_r 90,000 heat shock protein hsp 90, nuclear translocation, and association with the Arnt protein and nuclear dioxin-responsive elements. The transcriptional activation of human CYP1A1 is highly cell line specific in mammary carcinoma-derived cell lines (27, 28).

This laboratory has recently purified and cloned an additional PAH-responsive cytochrome P450 of the *CYP1* gene family, CYP1B1, from C3H10T1/2 mouse embryo fibroblasts and rat adrenal

Received 8/4/97; accepted 4/1/98.

The costs of publication of this article were defrayed in part by the payment of page charges. This article must therefore be hereby marked *advertisement* in accordance with 18 U.S.C. Section 1734 solely to indicate this fact.

[1] This research was supported by National Institute of Environmental Health Sciences Grant 144EN46 and Department of Defense Breast Cancer Research Grant DAMD17-94-J-4054. This work was presented at the Society of Toxicology Annual Meeting, held March 9–13, 1997, in Cincinnati, OH, and at the Annual Meeting of the AACR, held April 12–16, 1997, in San Diego, CA.

[2] To whom requests for reprints should be addressed, at Department of Pharmacology, University of Wisconsin, 3770 Medical Sciences Center, 1300 University Avenue, Madison, WI 53706.

[3] The abbreviations used are: PAH, polycyclic aromatic hydrocarbon; HMEC, human mammary epithelial cell; DMBA, 7,12-dimethylbenz(*a*)anthracene; TCDD, 2,3,7,8-tetrachlorodibenzo-*p*-dioxin; AhR, aryl hydrocarbon receptor; Arnt, aryl hydrocarbon nuclear translocator; MEGM, mammary epithelial growth medium; ECL, enhanced chemiluminescence; BCA, bicinchoninie acid; HPLC, high-performance liquid chromatography; rt-PCR, reverse transcriptase-PCR; B[c]Ph, benzo(*c*)phenanthrene.

cells (29, 30). The human orthologue has been cloned from a human squamous carcinoma cell line, SCC-13 (31, 32). CYP1B1 appears to be preferentially localized in tissues of mesodermal origin, particularly those producing steroids (adrenal, testis, and ovary) or those responding to steroids (prostate, uterus, and mammary tissue; Refs. 29, 30, 33). Interestingly, a deficiency in human CYP1B1 protein expression has recently been shown to be responsible for the development of congenital glaucoma (34). CYP1B1 is expressed constitutively and is TCDD inducible in the human mammary carcinoma MCF-7 cell line (35). Human CYP1B1 has been associated with the hydroxylation of 17β-estradiol to form the 4-catecholestrogen in analyses using recombinantly expressed human CYP1B1, as well as in the MCF-7 cell line (36, 37). This activity has been shown to be enhanced in human mammary and uterine tumors relative to the surrounding tissue (38–40). Collectively, these findings clearly establish a developmental, as well as an endogenous, role for this P450 cytochrome in estrogen metabolism, in addition to a role in PAH bioactivation.

Mutagenesis analyses have recently demonstrated that human CYP1B1 activates numerous structurally diverse environmental contaminants, including PAHs and their dihydrodiol derivatives, heterocyclic and aryl amines, and nitroaromatic hydrocarbons, to genotoxic agents (33). The selectivity of these CYP1B1-specific responses differs substantially from those mediated by CYP1A1. Thus, the CYP1B1-mediated activation of many environmentally persistent xenobiotics likely plays a significant role in chemical-induced mammary carcinogenesis. Although previous studies have demonstrated species-related differences in PAH metabolism and bioactivation with respect to rat and human mammary epithelial cells, these studies subjected the cells to prolonged exposures of PAH (24–42 h) and, thus, are representative of inductive as well as activation processes (15, 41, 42). Subsequent analyses have shown that PAH metabolism in cultured rat mammary cells is mediated by both CYP1A1 and CYP1B1, in a cell-selective manner (43). In rat mammary fibroblasts, CYP1B1 was shown to be exclusively expressed both constitutively and following TCDD induction. However, in rat mammary epithelial cells, CYP1A1, absent constitutively, was highly inducible by TCDD, whereas CYP1B1 was scarcely detectable, even under conditions of TCDD exposure. Despite these differences in cell culture, immunohistochemical analyses have recently shown that CYP1B1 is extensively expressed in rat mammary ductal epithelia, demonstrating that CYP1B1 is, indeed, expressed in mammary epithelial cells *in vivo* (44). Although CYP1A1 and CYP1B1 are each expressed in human mammary tumor cell lines, little is known regarding CYP1B1 and CYP1A1 cell type-specific expression in cultured human mammary cells. This is of particular importance because many studies have emphasized the multiplicity of cell types existent in HMEC cultures and the dependence of culture conditions on cell-specific expression (45).

This study characterizes the expression of CYP1A1 and CYP1B1, the major PAH-metabolizing P450 cytochromes, in early-passage HMECs. The cells have been cultured under conditions used in previous PAH induction studies (15, 41, 42) and, thus, are composed of a heterogeneous population of basal and luminal epithelial cells. This study represents the first analysis of functional cytochrome P450 expression in cultured HMECs using conditions that measure basal levels of expression and activity, distinct from the induction response. HMECs isolated from seven women following reduction mammoplasty surgeries were used in this study. We have quantitated constitutive and TCDD-inducible expression of CYP1B1 and CYP1A1 with respect to the level of AhR and Arnt expression, two proteins that may influence the extent of PAH-inducible cytochrome P450 expression. DMBA metabolism was used as a biomarker for functional CYP1B1 and CYP1A1 expression. The regioselective profiles of recombinant human CYP1B1- and CYP1A1-mediated DMBA metabolism, in combination with antibody inhibition analyses, have been used to resolve the respective contributions of these P450 cytochromes to both cellular and microsomal metabolism. This study provides evidence that the relative contributions of CYP1B1 and CYP1A1 to cellular bioactivation are highly dependent upon the magnitude of the cellular exposure to environmental chemicals (*e.g.*, PAHs). We provide evidence that CYP1B1 is an important contributor to PAH bioactivation under conditions of low induction from environmental exposure. Additionally, we show that there are substantial differences in CYP1B1 and CYP1A1 expression that may represent a risk factor for chemical-mediated breast cancer.

MATERIALS AND METHODS

Materials. The MEGM-bullet kit was purchased from Clonetics (San Diego, CA). TRIzol reagent was obtained from Life Technologies, Inc. (Grand Island, NY). Random 9-mers and the random-primed DNA labeling kit were obtained from Stratagene (La Jolla, CA). The horseradish peroxidase-conjugated goat antirabbit IgG, Taq DNA polymerase, reverse transcriptase, dNTPs, and RNasin were purchased from Promega (Madison, WI). PCR primers were obtained from Integrated DNA Technologies (Iowa City, IA). The ECL detection system was purchased from Amersham (Arlington Heights, IL). The BCA protein assay reagent was obtained from Pierce (Rockford, IL). Nitrocellulose was supplied by Schleicher and Schuell (Kenne, NH), whereas all other materials used for SDS-PAGE were obtained from Bio-Rad (Richmond CA). DMBA was purchased from Aldrich Chemical Co. (Milwaukee, WI). HPLC-grade methanol was purchased from VWR Scientific (Detroit, MI). Human recombinant CYP1B1 and CYP1A1 microsomes and human epoxide hydratase were obtained from Gentest Corporation (Woburn, MA). All other chemicals and reagents were purchased from Sigma Chemical Co. and were of the highest quality available.

Primary Antibodies and Epoxide Hydratase. Polyclonal antiserum (IgG fraction) specifically recognizing CYP1A1 was generated in this laboratory, as described previously (46). Antipeptide antiserum specifically recognizing human CYP1B1 was provided by Dr. Craig Marcus (University of New Mexico, Albuquerque, NM) and Dr. William Greenlee (University of Massachusetts, Worcester, MA; Ref. 47). Monoclonal antibodies specific for AhR was provided by Dr. Gary Perdew (Penn State University, State College, PA), whereas polyclonal antiserum specifically recognizing Arnt was a gift from Dr. Richard Pollenz (University of South Carolina, Columbia, SC; Ref. 48). Polyclonal antibodies to mouse CYP1B1 (IgY) were prepared in this laboratory in female Leghorn chickens and purified from the eggs, as described previously (49).

Cells and Cell Culture. Human mammary organoid preparations isolated from seven individual donors (Table 1) were provided by Dr. Michael Gould and the University of Wisconsin Comprehensive Cancer Center Cell Bank. The mammary tissue was processed, and organoids were isolated in the Gould laboratory, according to previously published procedures (4, 15). Primary organoids were plated (2×10^4 cells/cm^2) on plastic and cultured in MEGM supplemented with penicillin-streptomycin (50 units/ml penicillin-0.05 mg/ml streptomycin). Cells were grown at 37°C in a humidified environment of 5% CO_2 and 95% air. Confluent cells (7–10 days postplating) were passaged by differential trypsinization, plated at 1.7×10^4 cells/cm^2, and subsequently analyzed at day 4, 6, or 13.

Cells either remained untreated or were treated with TCDD (10 nM) for a period of 24 h prior to analysis. Cells used for microsomal preparations were harvested by trypsinization and washed three times with ice-cold 1× PBS. Microsomal fractions were isolated by differential centrifugation, as described previously (46). Protein concentrations were determined according to the BCA procedure using the Pierce BCA protein assay kit, according to manufacturer's protocol, using BSA as the standard.

DMBA Metabolism Assay. Microsomal DMBA metabolism was analyzed as described previously (44). Briefly, microsomal incubations were composed of 0.2 and 1.0 mg/ml microsomal protein for induced and basal metabolism, respectively, 14.2 mM glucose-6-phosphate, 0.06 units glucose-6-phosphate dehydrogenase, 1.2 mM NADP, 6 mM $MgCl_2$, and 0.1 M potassium phosphate

Table 1 *Antibody inhibition of microsomal DMBA dihydrodiol formation in primary HMECs*

Treatment/IgG addition	Dihydrodiols 5,6	Dihydrodiols 8,9 + 10,11	Dihydrodiols 3,4	Total dihydrodiol formation (pmol/mg/h)	% inhibition
Primary HMECs					
Constitutive					
Donor D					
+ preimmune	0.29	0.34[a]	0.19	0.82	0
+ anti-CYP1A1[b]	0.29	0.35[a]	0.12	0.76	7
+ anti-CYP1B1[c]	0.07	0.05[a]	0.01	0.13	84
Donor E					
+ preimmune	0.21	1.96[a]	0.14	2.31	0
+ anti-CYP1A1[b]	0.32	1.25[a]	0.10	1.48	36
+ anti-CYP1B1[c]	0.13	1.01[a]	0.19	1.52	34

	Dihydrodiols 5,6	Dihydrodiols 8,9	Dihydrodiols 10,11	Dihydrodiols 3,4		
TCDD-induced[d]						
+ preimmune	17	68	12	7	104	0
+ anti-CYP1A1[b]	6	10	4	2	22	79
+ anti-CYP1B1[c]	10	55	8	5	78	25
+ anti-CYP1A1 + anti-CYP1B1[b,c]	2	5	2	1	10	90
Recombinant human cytochromes P450						
CYP1B1[e]	50	33	27	17	127	
CYP1A1[f]	189	870	73	80	1212	

[a] 8,9- + 10,11-DMBA-dihydrodiols; peaks were poorly resolved at this low level of activity.
[b] 10 mg IgG/mg microsomal protein.
[c] 5 mg IgG/mg microsomal protein.
[d] Metabolism demonstrated by donor D.
[e] Recombinant human CYP1B1 expressed in lymphoblast microsomes (Gentest Corp.), 74 pmol/mg.
[f] Recombinant human CYP1A1 expressed in lymphoblast microsomes (Gentest Corp.), 104 pmol/mg.

(pH 7.6) to a total reaction volume of 1 ml. The reaction was initiated by the addition of 1.5 μM DMBA (HPLC purified) and allowed to incubate for 15 min at 37°C, under conditions of subdued lighting. The analysis of the human recombinant CYP1B1 and CYP1A1 microsomal standards (0.075 and 0.050 mg microsomal protein/ml, respectively) were assayed, as above, with the addition of 0.5 mg/ml human epoxide hydratase. Metabolites were extracted, and the microsomal DMBA metabolic profiles were examined by reverse-phase HPLC analysis. All data were normalized relative to DMBA recovery following extraction procedures.

Cellular DMBA metabolism was examined in 12-well culture plates (3.8 cm^2 well) on actively growing cells. Each incubation was composed of 0.5 ml of culture medium supplemented with 10 μM DMBA. Basal and TCDD-induced cellular incubations were completed at 37°C for 60 and 30 min, respectively. The incubation medium was removed from the culture vessel and incubated with β-glucuronidase (1000 units in 0.5 M NaOAc, pH 5.2) for 4 h at 37°C to effect the release of all H_2O-soluble metabolites. DMBA metabolites were extracted, and HPLC metabolic profiles were examined, as described above.

Antibody Inhibition Analysis. Antibody inhibition of microsomal DMBA metabolism was analyzed by the addition of anti-CYP1B1 (chicken; IgY, 5 mg antibody/mg microsomal protein) and anti-CYP1A1 (rabbit; IgG, 10 mg antibody/mg microsomal protein), concentrations previously determined to optimally inhibit CYP1B1- and CYP1A1-specific activities in constitutive and TCDD-induced MCF-7 cells. The corresponding preimmune IgY or IgG was added at equivalent concentrations to serve as a control. All reaction mixtures were incubated for 45 min at room temperature prior to assaying DMBA metabolism (35).

Immunoblot Analysis. Microsomal proteins were subjected to SDS-PAGE (3% acrylamide stacking gel-7.5% acrylamide separating gel) followed by immunoblot analysis, as described previously (50, 51). Immunoreactive proteins were visualized using the ECL method of detection, according to the manufacturer's protocol. Cytochrome P450 expression was quantitated relative to human recombinant CYP1B1 (74 pmol P450/mg microsomal protein) and CYP1A1 (104 pmol P450/mg microsomal protein) microsomal standards. Quantitation was completed by soft laser scanning densitometry employing a Zeineh Model SL-504-XL soft laser scanning densitometer (Fullerton, CA).

Measurement of mRNA by rt-PCR. Total RNA was prepared from day 6 HMEC cultures that were either untreated or treated with 10 nM TCDD for 6 h prior to isolation. Cells were harvested with TRIzol reagent, and the RNA was isolated according to the manufacturer's protocol. cDNA templates for PCR were synthesized as follows: total RNA (2 μg) and the random 9-mer primer mix (1 μg), in a total volume of 31 μl, were heated to 60°C for 5 min. The samples were allowed to cool slowly to room temperature, and then the reverse transcription master mix, composed of 1.0 mM each dNTP, 40 units of RNasin, 10.0 mM DTT, and 200 units of Moloney murine leukemia virus reverse transcriptase, was added to total of 50 μl. The samples were incubated at 40°C for 1 h, followed by denaturation for 5 min at 100°C.

Primers specific to CYP1B1 (forward, 5′-CGTACCGGCCACTATCACTG-3′; reverse, 5′-GCAGGCTCATTTGGGTTGGC-3′) and CYP1A1 (forward, 5′-AAGCACGTTGCAGGAGCTGATG-3′; reverse, 5′-ACATTGGCGTTCTCATCCAGCTGCT-3′) were synthesized using an Applied Biosystems 380A synthesizer. All PCR amplifications were completed in a Perkin Elmer/Cetus model 480 DNA thermocycler. CYP1B1 amplifications were composed of 2 μg of cDNA template, 0.22 mM each dNTP, 0.625 units of Taq DNA polymerase, 0.56 μM each primer, and H_2O to a final volume of 22.5 μl. The reaction was initiated under "hot start" conditions, whereby the samples were heated to 94°C for 3 min, followed by the addition of 2.78 mM $MgCl_2$. The samples were cycled for 1 min at 94°C, 1.5 min at 60°C, and 2.0 min at 72°C, for a total of 30 cycles. CYP1A1 amplifications were composed of 2 μg of cDNA template, 0.6 mM each dNTP, 2.5 mM $MgCl_2$, 0.625 units of Taq DNA polymerase, 0.5 μM each PCR primer, and H_2O to a total volume of 25 μl. Cycle parameters were 1 min at 94°C, 1.5 min at 57°C, and 2.0 min at 72°C, for a total of 30 cycles. PCR products were analyzed by agarose gel (1.6% agarose) chromatography and visualized by staining in ethidium bromide.

Northern Analysis. cDNA probes specific for CYP1B1 and β-actin were labeled with [α-^{32}P]dCTP (400 Ci/mmol) using the random-primed DNA labeling kit, per manufacturer's protocol. The poly(A)$^+$ mRNA was isolated from day 6 HMEC cultures according to the method of Badley *et al.* (52). mRNA was fractionated in 1.2% agarose-37% formaldehyde gels, transferred to nitrocellulose, and probed as described previously (53).

RESULTS

HMECs Were Cultured from Seven Individual Donors. Organoid preparations, isolated from reduction mammoplasty procedures and cultured under serum-free conditions, generally demonstrated full attachment within 3–4 days followed by a period of rapid proliferative growth, reaching confluence within 7–10 days of initial plating. The proliferative efficiency varied among cultures of the

seven individual donors, with donors A and C demonstrating the slowest rate of growth.

Cellular DMBA Metabolism Analysis Demonstrated Optimal Enzymatic Activity at Day 6 of Culture. DMBA metabolism was examined in secondary HMEC cultures to evaluate the time dependence of functional cytochrome P450 expression. Cellular DMBA metabolism of three donors was analyzed at days 4, 6, and 13 of culture. Fig. 1 depicts the cellular metabolism of one donor, donor D, but the data are representative of all three individuals examined. HMECs were exposed to 10 nM TCDD for a period of 24 h prior to analysis. The level of TCDD-induced cellular metabolism increased until day 6 of culture, followed by a >60% decline in activity between days 6 and 13. Thus, all subsequent experiments were completed on cells harvested at day 6 of culture, representing optimal expression of functional P450 cytochromes.

TCDD-induced DMBA metabolism was examined in the intact cell (cellular assay), as well as in the isolated microsomal fraction. The rate of TCDD-induced metabolism in the intact cells was of a similar magnitude to that obtained in the microsomal assay (calculating 1 mg microsomal protein/10^7 cells). However, basal cellular metabolism was not measurable at these cell densities (10^5 cells/well) in assays that were of short enough duration to exclude induction by DMBA, an effective AhR agonist (Ref. 54; data not shown). Therefore, we focused all further analyses of DMBA metabolism and antibody inhibition in the isolated microsomal fraction of basal and TCDD-induced cells.

CYP1B1 Is Expressed Constitutively, whereas CYP1B1 and CYP1A1 Are TCDD inducible in Normal HMECs. Microsomal CYP1B1 and CYP1A1 expression was quantitated by immunoblot analysis in seven HMEC preparations at day 6 of culture, relative to recombinant human microsomal standards, as shown in Figs. 2 and 3. These values represent extremely low levels of expression (<0.3–16 pmol/mg) but were reproducibly quantifiable.

Each individual exhibited constitutive CYP1B1 expression that was substantially induced by TCDD (Fig. 2). The variability in TCDD-induced levels among the donors was similar to that observed for basal CYP1B1. The average levels of basal and induced CYP1B1

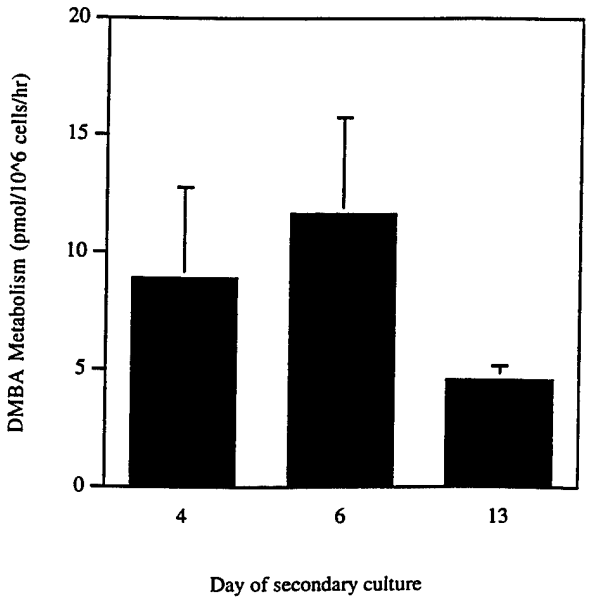

Fig. 1. Total cellular DMBA metabolism of TCDD-induced HMECs at days 4, 6, and 13 of culture. Secondary HMEC cultures of donor D were maintained in MEGM and were treated with 10 nM TCDD for 24 h prior to DMBA metabolism analysis, as described in "Materials and Methods."

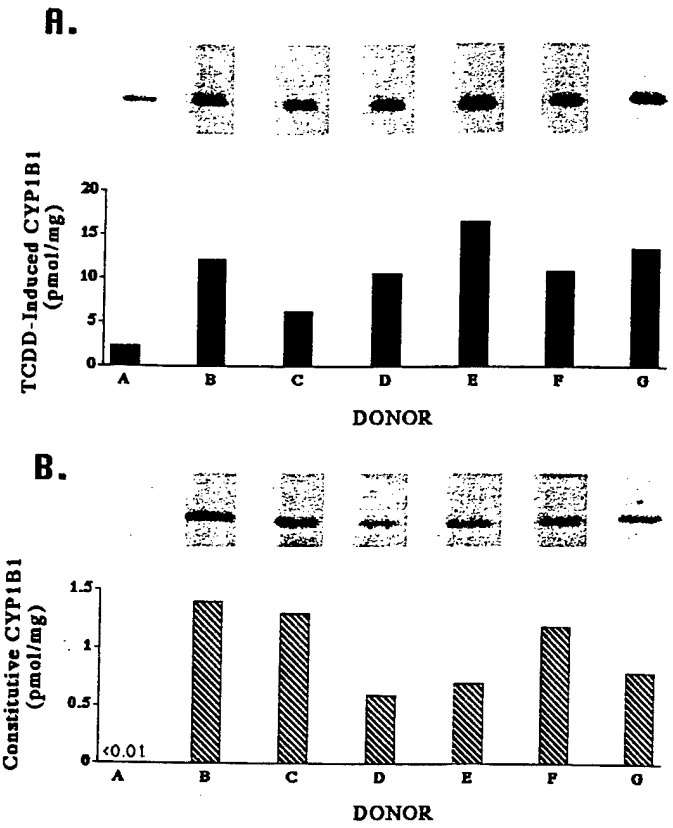

Fig. 2. Quantitative immunoblot analysis of TCDD-induced (*A*) and constitutive (*B*) CYP1B1 expression in secondary HMEC cultures of seven individual donors. Constitutive (30 μg/lane) and TCDD-induced (10 nM for 24 h; 5 μg/lane) microsomal proteins were analyzed by SDS-PAGE and the immunoreactive proteins were visualized using the ECL method, as described in "Materials and Methods." Membranes were exposed to film for a period of 1 min. Recombinant human CYP1B1 (74 pmol/mg), expressed in lymphocyte microsomes (Gentest Corp.), was used for the generation of standard curves for the quantitation of CYP expression by soft laser scanning densitometry using a Zeineh Soft Laser Scanning Densitometer (model SL-504-XL).

expression among six of the individuals (donors B–G) were 0.9 ± 0.5 and 10.4 ± 4.7 pmol/mg, respectively. Donor A demonstrated a 3–7-fold lower level of induced CYP1B1 expression, relative to the remaining six individuals. The level of constitutive expression of CYP1A1 was substantially lower than that of CYP1B1. Constitutive microsomal CYP1A1 expression was at the lower limit of detection (≤0.02 pmol/mg) in four of the donors (A, B, C, and D), whereas an extremely low level of expression (0.03–1.6 pmol CYP1A1/mg) was detectable in cultures of the donors E, F, and G (using exposure conditions that were 10 times longer than required for CYP1B1 detection; Fig. 3). However, the magnitude of TCDD-mediated induction was substantially greater for CYP1A1 (>100-fold) than for CYP1B1 (5–25-fold; excluding donor A), resulting in comparable TCDD-induced microsomal levels of the two P450 cytochromes. TCDD-induced CYP1A1 expression was more variable between the individual donors than was induced CYP1B1 expression (varying by 21- and 5-fold, respectively, between donors A and B, the donors demonstrating the highest and lowest levels of CYP1A1 expression).

Microsomal DMBA Metabolism Parallels Immunodetectable Cytochrome P450 Expression. The analysis of DMBA metabolism mediated by recombinant CYP1B1 and CYP1A1 expressed in lymphocyte microsomes demonstrated isoform-specific differences with respect to the pattern of regioselective product distribution (Table 1). However, the profiles were not as distinct as demonstrated previously with the rodent orthologues (44). Human CYP1A1-mediated DMBA metabolism demonstrated relatively low levels of 5,6- and 10,11-

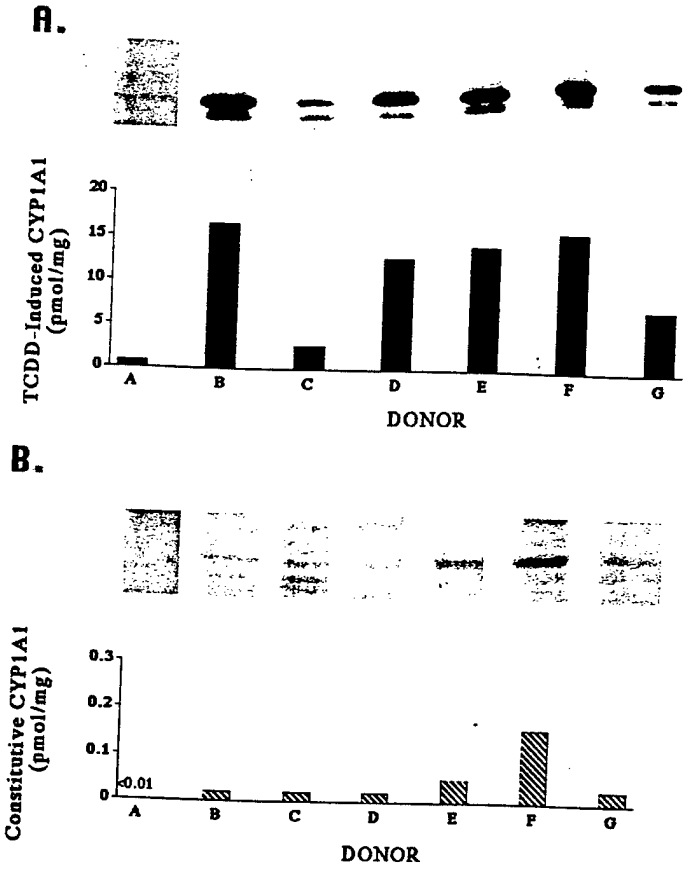

Fig. 3. Quantitative immunoblot analysis of TCDD-induced (*A*) and constitutive (*B*) CYP1A1 expression in secondary HMEC cultures of seven individual donors. Constitutive (30 μg/lane) and TCDD-induced (10 nM for 24 h; 30 μg/lane) microsomal proteins were analyzed by SDS-PAGE, and the immunoreactive proteins were visualized using the ECL method as described in "Materials and Methods." Membranes of constitutive and TCDD-induced expression were exposed to film for periods of 10 min and 2 min, respectively. Recombinant human CYP1A1 (104 pmol/mg), expressed in lymphocyte microsomes (Gentest Corp.), was used for the generation of standard curves for the quantitation of CYP expression by soft laser scanning densitometry using a Zeineh Soft Laser Scanning Densitometer (model SL-504-XL).

dihydrodiol formation relative to the 8,9-DMBA-dihydrodiol (ratios of 0.22 and 0.08, respectively). Conversely, human CYP1B1-directed metabolism generated equivalent levels of the 5,6- and 10,11-DMBA-dihydrodiols, relative to the 8,9-dihydrodiol of DMBA (ratios of 1.5 and 0.8, respectively). In addition, the rate of DMBA metabolism mediated by human CYP1A1 exceeded that of CYP1B1 by ~6-fold.

DMBA metabolism was analyzed as a biomarker of functional cytochrome P450 expression in HMECs at day 6 of culture, in parallel with the immunoblot analyses. Table 1 compares the regioselective profile of constitutive and TCDD-induced DMBA metabolism generated by donors D and E. These two donors represent the range of activities observed among all of the donors used in this study. The variability in the rate of constitutive metabolism exhibited by donors D and E is consistent with an ~2.5-fold difference in the level of constitutive CYP1A1 protein expression. The constitutive microsomal DMBA metabolism of donor D demonstrated equivalent proportions of 5,6- and 10,11-DMBA-dihydrodiol metabolites with low 8,9-dihydrodiol formation. This reproducible pattern of regioselective metabolism is similar but reproducibly different from the recombinant human CYP1B1. In contrast, the profile of constitutive metabolism generated by donor E clearly demonstrated a higher rate of metabolism reflective of an approximately equal component of CYP1A1-directed activity, as indicated by low ratios of 5,6:8,9 and 10,11:8,9 metabolite formation. This provides an important confirmation of the detection of constitutive CYP1A1 protein in cells from this donor.

The proportion of the 5,6- and 10,11-dihydrodiol metabolites, relative to the 8,9-dihydrodiols, generated by the TCDD-induced microsomes of donor D were consistent with the predominant involvement of CYP1A1. These profiles are typical of trends demonstrated by all donors following TCDD induction.

Antibody inhibition of DMBA metabolism further defined the contributions of CYP1B1 and CYP1A1 to DMBA metabolism in the HMECs (Table 1). The regioselective distribution of metabolism that is blocked by the specific antibody provides a characteristic profile of the inhibited enzyme. The addition of anti-CYP1A1 did not substantially effect basal activity (7% inhibition), whereas a parallel addition of anti-CYP1B1 inhibited DMBA-dihydrodiol formation by 84%. The addition of anti-CYP1A1 to TCDD-induced microsomal fractions reduced dihydrodiol formation by 79%, and left residual activity with a regioselective metabolite distribution consistent with CYP1B1-mediated metabolism. The initial TCDD-induced activity was inhibited by 25% by anti-CYP1B1, whereas the simultaneous addition of anti-CYP1A1 and anti-CYP1B1 to induced microsomes increased the extent of inhibition from 78 to 91%. This suggests a contribution of ~15–25% by CYP1B1 to these TCDD-induced activities. The observed equal expression of the proteins combined with a 6-fold higher specific activity for CYP1A1 predicts a 14% contribution from CYP1B1. This is fully consistent with the antibody inhibition data within the variability of these assays. Thus, when TCDD stimulates DMBA metabolism by 30–40-fold, the 5-fold increase in CYP1B1-mediated activity is overwhelmed by the contribution from the more than 100-fold induction of the more active CYP1A1.

As discussed above, HMECs from donor E consistently exhibited a DMBA product profile characteristic of a mixture of CYP1B1- and CYP1A1-mediated metabolism. This was confirmed by antibody inhibition, whereby CYP1B1 and CYP1A1 each inhibited this metabolism by ~35%, again consistent with equal contributions from each form (Table 1).

The analysis of DMBA metabolism with respect to the measurement of cytochrome P450 protein expression showed that CYP1B1 turnover in HMECs was 6 h^{-1} (constitutive microsomes; donors D and E), whereas CYP1A1 turnover was 90 h^{-1} in constitutive microsomes and 21 h^{-1} in TCDD-induced microsomes. The values for recombinant CYP1B1 and CYP1A1 in lymphoblast microsomes were 4 and 17 h^{-1}, respectively.

rt-PCR and Northern Blot analyses of RNA Expression of CYP1B1 and CYP1A1 in HMECs Support Immunoblot analyses. Constitutive and TCDD-inducible CYP1B1 expression was analyzed using total RNA isolated from cultured HMECs of donor D by rt-PCR methodologies (Table 2). Constitutive and TCDD-inducible CYP1B1

Table 2 *CYP1B1 steady-state mRNA and protein expression in primary HMECs*

Treatment	rt-PCR[a] (relative expression level)	Method of analysis: Northern hybridization[b] (relative expression level)	Method of analysis: Immunoblot[c] (pmol/mg)
Constitutive[d]	1.0	1.0	0.6
TCDD-induced[d]	11.7	32.9	10.7
Fold TCDD induction	12	33	18

[a] Expression was quantitated by soft laser scanning densitometry of ethidium bromide-stained PCR products. cDNA was synthesized from TCDD-induced MCF-7 cells and used for serial dilution in the analysis of the ethidium bromide detection response.

[b] Poly(A)$^+$ RNA (10 μg/lane) was probed for CYP1B1 using a rat CYP1B1 cDNA probe. Expression was quantitated by soft laser scanning densitometry following autoradiography. The relative expression level has been normalized relative to the level of β-actin expression.

[c] Recombinant human CYP1B1 (74 pmol/mg; Gentest Corp.) was used in constructing a standard curve for the quantitation of CYP1B1 protein expression. Immunoreactive proteins were visualized by ECL methodologies, and quantitation was completed by soft laser scanning densitometry.

[d] Metabolism demonstrated by donor D.

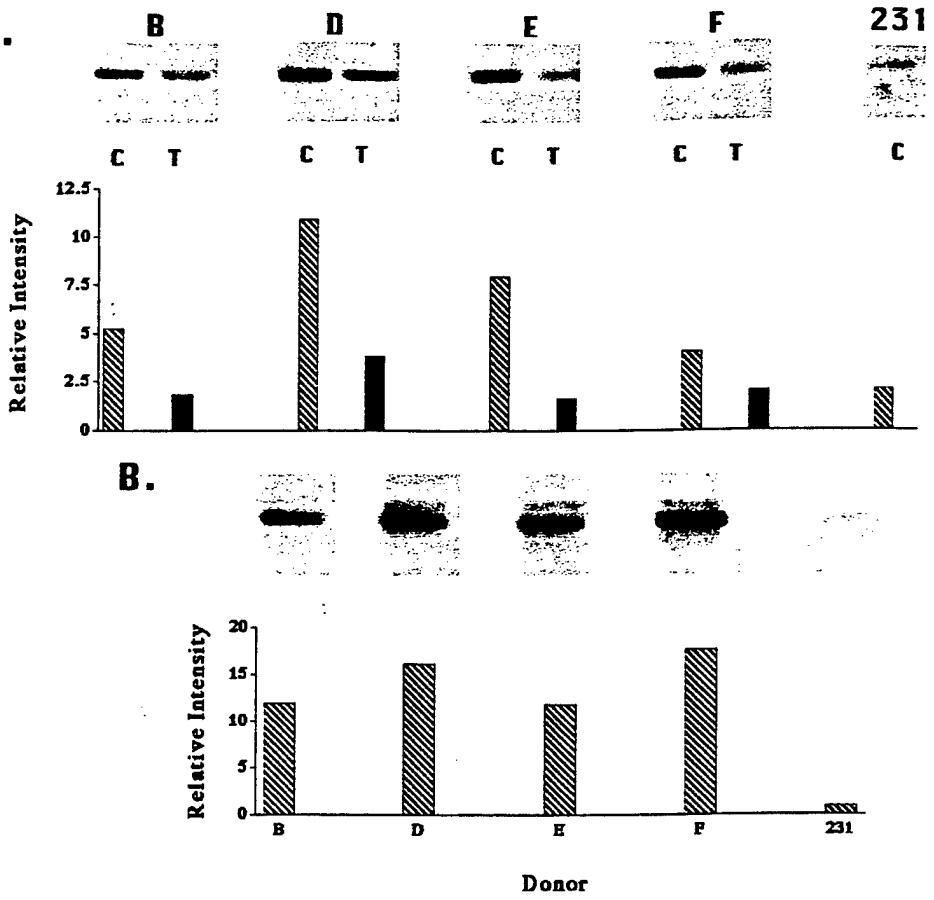

Fig. 4. Immunoblot analysis of constitutive and TCDD-induced AhR (*A*) and constitutive Arnt (*B*) expression in day 6 secondary HMEC cultures of four individual donors. Total proteins were isolated from constitutive (*Lanes C*) and TCDD-induced (*Lanes T*; 10 nM for 24 h) cells by TRIzol procedures and were analyzed by SDS-PAGE. Immunoreactive proteins were visualized by the ECL method, as described in "Materials and Methods." MDA-MB-231 and MCF-7 protein fractions were used as reference standards for comparison with expression levels in immortalized human mammary cell lines. Protein loadings were 20 μg/lane, and membranes were exposed to film for 5 min. Relative expression levels were analyzed by soft laser scanning densitometry using a Zeineh Soft Laser Scanning Densitometer (model SL-504-XL).

mRNA expression was detectable, demonstrating a >10-fold increase in TCDD-induced CYP1B1 mRNA, which was fully consistent with the induction of immunodetectable CYP1B1 protein following TCDD exposure. Similar results were observed in RNA isolated from donors A and B (data not shown). rt-PCR analysis of CYP1A1 expression has been completed for three donors (donors A, B, and D). Constitutive CYP1A1 expression was weakly yet reproducibly detectable in donor B, in parallel with the low magnitude of observed protein expression (data not shown).

Northern blot analysis of mRNA isolated from donor D confirmed the expression of constitutive CYP1B1 mRNA, which was highly inducible by TCDD (>30-fold; Table 2). These results corroborate the results obtained in the immunoblot and rt-PCR analyses.

Ah Receptor and Arnt Expression Are Elevated in Cultured HMECs. Cytosolic AhR expression was analyzed in the cultured HMECs of four donors (donors B, D, E, and F). Immunoblot analysis identified the expression of the M_r 104,000 protein in all individuals examined, the level of which varied by 3-fold (Fig. 4*A*). TCDD induction resulted in the down-regulation of the cytosolic receptor (~3-fold), which is mediated by nuclear translocation followed by proteolytic turnover (55). The level of receptor expression was many times higher in the cultured HMECs, as compared to MDA-MB-231 cell line, the human mammary carcinoma cell line shown to express the highest level of AhR expression among several mammary cell lines examined.[4]

The expression of Arnt was also much higher in the cultured HMECs, relative to the MDA-MB-231 human mammary carcinoma cell line (Fig. 4*B*). The level of Arnt expression varied by only 1.5-fold among the four donors.

[4] W. G. R. Angus and C. R. Jefcoate, unpublished observations.

DISCUSSION

This study has characterized functional CYP1B1 and CYP1A1 expression in early-passage HMECs isolated from tissues procured from seven women undergoing reduction mammoplasty surgeries. The roles of CYP1B1 and CYP1A1 in PAH metabolism have been quantitatively characterized under conditions that reflect the basal condition of the cultured HMECs. Thus, the potential for PAH-mediated induction of CYP1B1 and CYP1A1 has been eliminated by maintaining short PAH reaction periods in the intact cellular assay and by directly assaying microsomal metabolism. Cytochrome P450 induction has been studied using a nonmetabolizable AhR agonist, TCDD, which substantially induced both isoforms following a 24-h exposure. Through the immunoquantitation of each form, we can account for PAH metabolism in terms of the expressed level of these two P450 cytochromes under both constitutive and TCDD-induced conditions. Previous studies of PAH metabolism in cultured HMECs have used prolonged exposures of the hydrocarbons to the cells (24–42 h), thereby combining P450 induction with P450-mediated bioactivation events (15, 41, 42). In addition, these studies have not addressed which specific P450 isozyme(s) are responsible for PAH metabolism and bioactivation.

This study demonstrates that CYP1B1 is expressed constitutively, at quantifiable levels, in cultured HMECs. In contrast, constitutive CYP1A1 is expressed at extremely low levels (approaching the lower limit of detectability), although both P450 cytochromes are expressed at comparable levels (pmol P450/mg microsomal protein) in the HMECs following TCDD exposure. Northern hybridization and rt-PCR analyses demonstrate that mRNA expression parallels levels of the respective microsomal protein in these cells. The levels of immunodetectable constitutive and TCDD-inducible CYP1B1 expression

each varied by ~2.5-fold (excluding donor A), whereas induced levels of CYP1A1 varied by as much as 21-fold among the seven individuals.

The HMECs used in this study have been cultured under conditions similar to those applied in the previous studies of HMEC-mediated PAH metabolism, yielding a mixture of luminal and basal epithelial cell populations. Under these culture conditions, the proportion of basal HMECs progressively increased with increased passage and time in culture relative to the luminal subtype (45). In parallel with a predicted increase in the proportion of basal cells (45), we observed a marked decrease in TCDD-induced DMBA metabolism following day 6 of secondary culture. Recent preliminary studies have demonstrated the immunodetectable expression of CYP1A1 in an isolated luminal cell population, whereas CYP1B1 expression was observed in both the isolated basal and luminal epithelia.[5] Thus, the observed increased interdonor variability in CYP1A1 expression, relative to CYP1B1, may potentially arise from differing proportions of the luminal cells among the individual donors or may reflect donor-dependent differences in the magnitude of CYP1A1 expression. These issues are being addressed in ongoing studies.

Although DMBA is a highly discriminating substrate for the functional measurement of rodent CYP1A1 and CYP1B1 (44), elucidating the individual contributions of these forms to DMBA metabolism has been difficult in human cells. Although rodent CYP1B1 and CYP1A1 demonstrate highly distinct regioselective profiles of DMBA metabolite production, the corresponding profiles are less distinct for the human P450 cytochromes. For example, in rodents, CYP1A1-mediated metabolism is characterized by the preferential hydroxylation at the 7-methyl substituent of DMBA and the formation of the 8,9-DMBA-dihydrodiol, whereas CYP1B1 selectively metabolizes DMBA to produce high levels of the 10,11 and 3,4-dihydrodiol metabolites. However, by using recombinant human CYP1B1 and CYP1A1, we have shown that human CYP1A1-mediated metabolism is characterized by the preferential formation of the 8,9-DMBA-dihydrodiol with proportionally less 5,6-dihydrodiol and 7-hydroxy-DMBA than rodent CYP1A1-mediated metabolism. There is also clear production of the 3,4-dihydrodiol, which is absent with the rodent orthologue. Human CYP1B1-directed metabolism yielded relatively high proportions of the 5,6 and 10,11-DMBA-dihydrodiol metabolites, relative to human CYP1A1, but, unlike rodent CYP1B1, showed a similar proportion of the 3,4-dihydrodiol (5%). Human CYP1A1 is 6-fold more efficient in the metabolism of DMBA, as compared to CYP1B1, a much larger difference than observed in the rodent forms.

Secondary HMEC cultures demonstrated low levels of constitutive microsomal DMBA metabolism that was mediated by CYP1B1, consistent with the immunodetectable basal expression of this isoform. The regioselective profile of metabolite distribution generated from these HMECs was consistent with that produced by human recombinant CYP1B1, and this has been confirmed by the selective inhibitory effect of anti-CYP1B1 on DMBA metabolism, as compared to the lack of inhibition with anti-CYP1A1 antibodies. Small but significant differences in the regioselective profile of metabolite formation were observed between the HMECs and the recombinantly expressed protein (HMECs demonstrate a lower 5,6:10,11-dihydrodiol ratio). This may be due to differences in the configuration of CYP1B1 in HMECs and in lymphoblast endoplasmic reticulum. We have recently measured product distribution for DMBA metabolism by recombinant human CYP1B1 expressed in V79 cells, which more closely matches the HMEC product ratios (data not shown). Certainly, for each of these sources, the mobility of the CYP1B1 proteins in SDS-PAGE is indistinguishable. Donor E, one of a group of three individuals demonstrating low levels of basal CYP1A1 immunodetectable expression, yielded a profile of regioselective basal metabolism reflecting approximately equal contributions from both CYP1A1 and CYP1B1. Although the level of basal CYP1A1 expression in donor E is ~10 times lower than basal CYP1B1, the contribution of CYP1A1 to DMBA metabolism is consistent with the 6-fold higher turnover of the isoform. This provides a critical confirmation of the immunodetection of constitutive CYP1A1 in these cultures. The consistent finding of CYP1A1 in cells from these donors and not others cultured in the same medium indicates that this is not due to an inducer in the medium but, rather, results from a selective endogenous activation of CYP1A1 within these donors.

Exposure of the cultured HMEC to TCDD increased the overall rate of DMBA metabolism by 30–40-fold. Although TCDD-induced CYP1B1 and CYP1A1 were expressed at equivalent levels, the induced metabolism was predominantly mediated by CYP1A1. The profile of metabolite regiodistribution paralleled that of recombinant human CYP1A1. Because CYP1A1 is ~6-fold more efficient than CYP1B1 in metabolizing DMBA, we would predict, at equimolar levels of expression, CYP1A1 and CYP1B1 to mediate 86 and 14% of induced DMBA metabolism, respectively. Indeed, antibody inhibition analysis confirmed this activity distribution, within the sensitivity of the assay. We have shown that anti-CYP1A1 substantially inhibited metabolic activity, while yielding a regioselective profile of residual metabolism indicative of predominantly CYP1B1-mediated activity. Furthermore, much of the residual activity was removed by a further addition of anti-CYP1B1 antibodies.

We have estimated the turnover number for DMBA metabolism with the exceptionally low levels of the individual forms of cytochrome P450 calculated in this study. This involves comparison of expression levels with the proportion of the metabolism attributable to the individual form based on antibody inhibition. Constitutive activities from donors D and E indicate CYP1B1 turnover of 6 h^{-1}, in excellent agreement with the turnover of recombinant human CYP1B1 in lymphoblast microsomes (4 h^{-1}). CYP1A1 turnovers were estimated at 90 h^{-1} in constitutive microsomes from donor E and at 21 h^{-1} in TCDD-induced microsomes. Again, these rates compare remarkably well with the activity of recombinant human CYP1A1 in lymphoblast microsomes (17 h^{-1}).

Cellular DMBA metabolism was fully consistent with the microsomal activity. Both assays demonstrate TCDD-inducible metabolic activity, and the regioselective distribution of metabolites was consistent between the two methods of analysis. In cells, ~60% of dihydrodiols were released by β-glucuronidase, implicating their conjugation as glucuronides. This agrees with previous measurements of these conjugation ratios (42). The cellular and microsomal assays yielded an equivalent overall rate of metabolic activity, based upon a recovery of 1 mg of microsomal protein/10^7 cells. The cellular analysis of basal metabolism did not demonstrate measurable activity above nonenzymatic background of DMBA oxidation. However, based on the microsomal assays we would not expect to detect DMBA metabolism from these cellular assays, which typically contained only 10^5 cells.

Murray *et al.* (56) have recently demonstrated the immunohistochemical detection of CYP1B1 in tumor tissue but failed to detect CYP1B1 expression in the corresponding donor-matched normal breast tissue, raising questions regarding the magnitude of CYP1B1 expression in normal human breast tissue. We have completed rt-PCR analysis of seven normal and nine tumor-derived tissues in our laboratory and have observed comparable levels of CYP1B1 expression in

[5] M. C. Larsen and C. R. Jefcoate, unpublished results.

all of the samples examined.[6] Similar results have been reported by Huang *et al.* (57), who detected CYP1B1 mRNA in 22 of 23 samples examined, while demonstrating no discernible pattern in CYP1B1 expression between tumor and normal tissue from the same individuals (57). Although these studies have been limited to the analysis of CYP1B1 mRNA expression, Dr. Judith Weisz has shown that *in situ* hybridization analysis of CYP1B1 mRNA expression in breast tissue parallels immunohistochemical protein detection when using the same antibody preparation.[7] The rt-PCR determination of the magnitude of CYP1B1 mRNA expression in the cultured early-passage HMECs presented here fully corroborates our quantitation of low levels of functional microsomal protein expression. Although we have not completed a direct comparative analysis of CYP1B1 mRNA and protein expression in freshly isolated *versus* cultured HMECs, this study clearly demonstrates the expression of quantifiable levels of functionally active CYP1B1 in early-passage normal human breast epithelia.

AhR levels in the cultured HMECs were up to 5-fold higher than the highest level observed in an established human mammary cell line (MDA-MB-231 cells). TCDD-mediated down-regulation of the cytosolic receptor level clearly showed that the cells in culture were expressing a functional receptor, most of which translocated to the nucleus upon binding the ligand and was degraded, concomitant with nuclear activation (*i.e.*, enhanced transcription of CYP1A1 and CYP1B1). Because the levels are as much as 5 times higher than those in tumor cell lines, such as the MDA-MB-231 cells, in which TCDD is similarly effective in inducing these genes, apparently, AhR is not a limiting factor mediating cytochrome P450 expression in HMECs. This raises major questions regarding the functional significance of such high levels of AhR expression in these cells. Similarly, Arnt, the nuclear partner of the AhR, was elevated in the cultured HMECs, as compared to the human mammary cell lines. It appears that, when the AhR translocates to the nucleus, there is sufficient Arnt for heterodimerization of these proteins. Because an increased requirement for binding to gene enhancer binding elements is unlikely, this high level may function to complex and regulate additional nuclear factors.

Human CYP1B1 and CYP1A1 have previously been shown to discriminately mediate the bioactivation of numerous procarcinogenic chemicals to genotoxic agents (33). Although the bioactivation of carcinogenic PAHs has previously been attributed to CYP1A1, recent studies by Shimada *et al.* (33) demonstrate that CYP1B1 mediates the bioactivation of a wide range of procarcinogenic PAH dihydrodiols. However, they report that CYP1B1 was ineffective in activating the associated parent PAHs, which may be attributable to the omission of epoxide hydratase from the assay system. Interestingly, CYP1B1 and CYP1A1 were shown to be highly selective with respect to PAH dihydrodiol activation. CYP1B1 efficiently activated the bay- and fjord-region PAH dihydrodiols, DMBA-3,4-diol, and dibenzo-(*a,l*)pyrene-11,12-diol, respectively, whereas CYP1A1 was ineffective in the bioactivation of these potent mammary carcinogens. CYP1B1 and CYP1A1 have also been shown to exhibit tissue- and species-specific expression following exposure to B[c]Ph, a chemical with a fjord-region diol epoxide (B[c]Ph-3,4-diol 1,2-epoxide) that is among the most mutagenic and carcinogenic diol epoxides examined to date (58). For example, the treatment of MCF-7 cells with B[c]Ph resulted in increased CYP1B1 expression in the absence of immunodetectable CYP1A1, whereas exposure of murine epidermal cells to B[c]Ph resulted in elevated CYP1A1 levels and undetectable CYP1B1 expression. Our present studies indicate that human CYP1B1 should be active in generating dihydrodiol epoxides from DMBA and other PAHs, although the effectiveness, relative to CYP1A1, will certainly be dependent on additional metabolic factors. Clearly, interindividual and cellular specificity of cytochrome P450 expression, coupled with selectivity of CYP1B1- and CYP1A1-mediated bioactivation of procarcinogens, such as environmental PAHs, will largely determine a chemicals carcinogenic potency and an individuals associated risk of tumorigenesis.

This study has confirmed that human mammary epithelia express significant levels of basal CYP1B1 and that certain individuals constitutively express levels of CYP1A1 that are extremely low but, nevertheless, are functionally significant in PAH activation. Although the level of immunodetectable constitutive CYP1A1 expression is 7–70-fold lower than the level of CYP1B1 in these individuals and is only barely detectable by rt-PCR methodologies, the CYP1A1 expression has been demonstrated by the correlative expression of protein with metabolic activity analyses. This activity suggests that any individual expressing CYP1A1 in the mammary gland in this way is at an increased risk for PAH bioactivation, bearing in mind that the level of PAH exposure/bioaccumulation is maintained well below inducing levels due to constitutively active P450s, such as CYP1B1.

ACKNOWLEDGMENTS

We thank Dr. Michael Gould and Wendy Kennan (University of Wisconsin Clinical Cancer Center) for generously providing the HMEC organoid preparations used in this study. We also thank Leonardo Ganem for his assistance in the preparation of this manuscript.

REFERENCES

1. Cancer Facts and Figures: 1995. Atlanta, GA: American Cancer Society, Inc., 1995.
2. Dao, T. L. Studies on mechanism of carcinogenesis in the mammary gland. Prog. Exp. Tumor Res., *11:* 235–261, 1969.
3. Huggins, C. B. Induction of mammary cancer in rat. *In:* Experimental Leukemia and Mammary Cancer, pp. 73–79. Chicago: University of Chicago Press, 1979.
4. Gould, M. N., Cathers, L. E., and Moore, C. J. Human breast cell-mediated mutagenesis of mammalian cells by polycyclic aromatic hydrocarbons. Cancer Res., *42:* 4619–4624, 1982.
5. Eldridge, S., Gould, M. N., and Butterworth, B. E. Genotoxicity of environmental agents in human mammary epithelial cells. Cancer Res., *52:* 5617–5621, 1992.
6. Li, D., Wang, M., Dhingra, K., and Hittelman, W. N. Aromatic DNA adducts in adjacent tissues of breast cancer patients: clues to breast cancer etiology. Cancer Res., *56:* 287–293, 1996.
7. Obana, H., Hori, S., Kahimoto, L., and Kunita, N. Polycyclic aromatic hydrocarbons in human fat and liver. Bull. Environ. Contam. Toxicol., *27:* 23–27, 1981.
8. Martin, F. L., Carmichael, P. L., Crofton-Sleigh, C., Venitt, S., Phillips, D. H., and Grover, P. L. Genotoxicity of human mammary lipid. Cancer Res., *56:* 5342–5346, 1996.
9. Baron, J., Hildebrandt, A. G., Peterson, J. A., and Estabrook, R. W. The role of oxygenated cytochrome P-450 and of cytochrome b5 in hepatic microsomal drug oxidations. Drug Metab. Dispos., *1:* 129–138, 1973.
10. Conney, A. H. Induction of microsomal enzymes by foreign chemicals and carcinogenesis by polycyclic aromatic hydrocarbons: G. H. A. Clowes Memorial Lecture. Cancer Res., *42:* 4875–4917, 1982.
11. Jefcoate, C. R. Integration of xenobiotic metabolism in carcinogen activation and detoxication. *In:* J. Caldwell and W. Jakoby (eds.), Biological Basis of Detoxication, pp. 31–76. New York: Academic Press, 1983.
12. Guengerich, F. P. Roles of cytochrome P-450 enzymes in chemical carcinogenesis and cancer chemotherapy. Cancer Res., *48:* 2946–2954, 1988.
13. Shimada, T., Martin, M. V., Pruess-Schwartz, D., Marnett, L. J., and Guengerich, F. P. Roles of individual cytochrome P-450 enzymes in the bioactivation of benzo-(*a*)pyrene, 7,8-dihydroxy-7,8-dihydrobenzo(*a*)pyrene, and other dihydrodiol derivatives of polycyclic aromatic hydrocarbons. Cancer Res., *49:* 6304–6312, 1989.
14. Cavalieri, E., and Rogan, E. Mechanisms of tumor initiation by polycyclic aromatic hydrocarbons in mammals. *In:* A. H. Nelson (ed.), Handbook of Environmental chemistry: PAHs and Related Compounds, Vol. 3, pp. 10.1–10.11. Heidelberg, Germany: Springer-Verlag, 1997.
15. Moore, C. J., Tricomi, W. A., and Gould, M. N. Interspecies comparison of polycyclic aromatic hydrocarbon metabolism in human and rat mammary epithelial cells. Cancer Res., *46:* 4946–4952, 1986.
16. Balmain, A., and Brown, K. Oncogene activation in chemical carcinogenesis. *In:* O. Klein and S. Weinhouse (eds.), Advances in Cancer Research, Vol. 51, pp. 147–182. New York: Academic Press, 1988.
17. Hollstein, M., Sidransky, D., Vogelstein, B., and Harris, C. C. p53 mutations in human cancers. Science (Washington DC), *253:* 49–53, 1991.

[6] K. A. Sukow and C. R. Jefcoate, unpublished results.
[7] J. Weisz, personal communication.

18. Sukumar, S., Notario, V., Martin-Zanca, D., and Barbacid, M. Induction of mammary carcinomas in rats by nitroso-methylurea involves malignant activation of H-*ras*-1 locus by single point mutations. Nature (Lond.), *306:* 658–661, 1983.
19. Dandekar, S., Sukumar, S., Zarbl, H., Young, L. J. T., and Cardiff, R. D. Specific activation of the cellular Harvey-*ras* oncogene in dimethylbenzanthracene-induced mouse mammary tumors. Mol. Cell Biol., *6:* 4104–4108, 1986.
20. Lehman, T. A., Modali, R., Boukamp, P., Stanek, J., Bennett, W. P., Welsh, J. A., Metcalf, R. A., Stampfer, M. R., Fusenig, N., Rogan, E. M., and Harris, C. C. p53 mutations in human immortalized epithelial cell lines. Carcinogenesis (Lond.), *14:* 833–839, 1993.
21. Stampfer, M. R., and Bartley, J. C. Induction of transformation and continuous cell lines from normal human mammary epithelial cells after exposure to benzo(*a*)pyrene. Proc. Natl. Acad. Sci. USA, *82:* 2394–2398, 1985.
22. Russo, J., Calaf, G., and Russo, I. H. A critical approach to the malignant transformation of human breast epithelial cells with chemical carcinogens. Crit. Rev. Oncog., *4:* 403–417, 1993.
23. Russo, J., Calaf, G., Sohi, N., Tahin, Q., Zhang, P. L., Alvarado, M. E., Estrada, S., and Russo, I. H. Critical steps in breast carcinogenesis. Ann. N. Y. Acad. Sci., *698:* 1–20, 1993.
24. Whitlock, J. P. Genetic and molecular aspects of 2,3,7,8-tetrachlorodibenzo-*p*-dioxin action. Annu. Rev. Pharmacol. Toxicol, *30:* 251–277, 1990.
25. Whitlock, J. P., Okino, S. T., Dong, L., Ko, H. P., Clarke-Katzenberg, R., Ma, Q., and Li, H. Induction of cytochrome P4501A1: a model for analyzing mammalian gene transcription. FASEB J., *10:* 809–818, 1996.
26. Gonzalez, F. J. The molecular biology of cytochrome P450s. Pharmacol. Rev., *40:* 243–288, 1989.
27. Harris, M., Piskorska-Pliszczynska, J., Zacharewski, T., Romkes, M., and Safe, S. Structure-dependent induction of aryl hydrocarbon hydroxylase in human breast cancer cell lines and characterization of the Ah receptor. Cancer Res., *49:* 4531–4535, 1989.
28. Thomsen, J. S., Nissen, L., Stacey, S. N., Hines, R. N., and Autrup, H. Differences in 2,3,7,8-tetrachlorodibenzo-*p*-dioxin-inducible CYP1A1 expression in human breast carcinoma cell lines involve altered *trans*-acting factors. Eur. J. Biochem., *197:* 577–582, 1991.
29. Savas, U., Bhattacharayya, K. K., Christou, M., Alexander, D. L., and Jefcoate, C. R. Mouse cytochrome P-450-EF, representative of a new 1B subfamily of cytochrome P450s: cloning, sequence determination, and tissue expression. J. Biol. Chem., *269:* 14905–14911, 1994.
30. Bhattacharayya, K. K., Brake, P. B., Eltom, S. E., Otto, S. A., and Jefcoate, C. R. Identification of a rat adrenal cytochrome P450 active in polycyclic aromatic hydrocarbon metabolism as rat CYP1B1: demonstration of a unique tissue-specific pattern of hormonal and aryl hydrocarbon receptor-linked regulation. J. Biol. Chem., *270:* 11595–11602, 1995.
31. Sutter, T., Tang, Y. M., Hayes, C. L., Wo, Y. P., Jabs, E. W., Li, X., Yin, H., Cody, C. W., and Greenlee, W. F. Complete cDNA sequence of a human dioxin-inducible mRNA identifies a new gene subfamily of cytochrome P450 that maps to chromosome 2. J. Biol. Chem., *269:* 13092–13099, 1994.
32. Tang, Y. M., Wo, Y. P., Stewart, J., Hawkins, A. L., Griffin, C. A., Sutter, T. R., and Greenlee, W. F. Isolation and characterization of the human cytochrome P450 CYP1B1 gene. J. Biol. Chem., *271:* 28324–28330, 1996.
33. Shimada, T., Hayes, C. L., Yamazaki, H., Amin, S., Hecht, S. S., Guengerich, F. P., and Sutter, T. R. Activation of chemically diverse procarcinogens by human cytochrome P-450 1B1. Cancer Res., *56:* 2979–2984, 1996.
34. Stoilov, I., Akarsu, A. N., and Sarfarazi, M. Identification of three different truncating mutations in cytochrome P4501B1 (CYP1B1) as the principal cause of primary congenital glaucoma (Buphthalmos) in families linked to the *GLC3A* locus on chromosome 2p21. Hum. Mol. Genet., *6:* 641–647, 1997.
35. Christou, M., Savas, U., Spink, D. C., Gierthy, J. F., and Jefcoate, C. R. Co-expression of human CYP1A1 and a human analog of cytochrome P450-EF in response to 2,3,7,8-tetrachloro-dibenzo-*p*-dioxin in the human mammary carcinoma-derived MCF-7 cells. Carcinogenesis (Lond.), *15:* 725–732, 1994.
36. Spink, D. C., Hayes, C. L., Young, N. R., Christou, M., Sutter, T. R., Jefcoate, C. R., and Gierthy, J. F. The effects of 2,3,7,8-tetrachlorodibenzo-*p*-dioxin on estrogen metabolism in MCF-7 breast cancer cells: evidence for induction of a novel 17β-estradiol 4-hydroxylase. J. Steroid Biochem. Mol. Biol., *51:* 251–258, 1994.
37. Hayes, C. L., Spink, D. C., Spink, B. C., Cao, J. Q., and Walker, N. J. 17β-Estradiol hydroxylation catalyzed by human cytochrome P450 1B1. Proc. Natl. Acad. Sci. USA, *93:* 9776–9781, 1996.
38. Liehr, J. G., Ricci, M. J., Jefcoate, C. R., Hannigan, E. V., Hokanson, J. A., and Zhu, B. T. 4-Hydroxylation of estradiol by human uterine myometrium and myoma microsomes: implications for the mechanism of uterine tumorigenesis. Proc. Natl. Acad. Sci. USA, *92:* 9220–9224, 1995.
39. Abul-Hajj, Y. J., Thijssen, J. H. H., and Blakenstein, M. A. Metabolism of estradiol by human breast carcinoma. Eur. J. Cancer Clin. Oncol., *24:* 1171–1178, 1988.
40. Liehr, J. G., and Ricci, M. J. 4-Hydroxylation of estrogens as marker of human mammary tumors. Proc. Natl. Acad. Sci. USA, *93:* 3294–3296, 1996.
41. Bartley, J. C., and Stampfer, M. R. Factors influencing benzo(*a*)pyrene metabolism in human mammary epithelial cells in culture. Carcinogenesis (Lond.), *6:* 1017–1022, 1985.
42. Grover, P. L., MacNicoll, A. D., Sims, P., Easty, G. C., and Nelville, A. M. Polycyclic hydrocarbon activation and metabolism in epithelial cell aggregates prepared from human mammary tissue. Int. J. Cancer, *26:* 467–475, 1980.
43. Christou, M., Savas, U., Schroeder, S., Shen, X., Thompson, T., Gould, M. N., and Jefcoate, C. R. Cytochromes CYP1A1 and CYP1B1 in the rat mammary gland: cell-specific expression and regulation by polycyclic aromatic hydrocarbons and hormones. Mol. Cell. Endocrinol., *115:* 41–50, 1995.
44. Hushka, L., and Greenlee, W. F. Ah receptor activation impairs mammary gland development. Proc. Am. Assoc. Cancer Res., *38:* 555, 1997.
45. Taylor-Papadimitriou, J., Stampfer, M., Bartek, J., Lewis, A., Boshell, M., Lane, E. B., and Leigh, I. M. Keratin expression in human mammary epithelial cells cultured from normal and malignant tissue: relation to *in vivo* phenotypes and influence of medium. J. Cell Sci., *94:* 403–413, 1989.
46. Pottenger, L. H., and Jefcoate, C. R. Characterization of a novel cytochrome P450 from the transformable cell line, C3H/10T1/2. Carcinogenesis (Lond.), *11:* 321–327, 1990.
47. McKay, J. A., Melvin, W. T., Ah-See, A. K., Ewen, S. W. B., Greenlee, W. F., Marcus, C. B., Burke, M. D., and Murray, G. I. Expression of cytochrome P450 CYP1B1 in breast cancer. FEBS Lett., *374:* 270–272, 1995.
48. Pollenz, R. S., Sattler, C. A., and Poland, A. The aryl hydrocarbon receptor and aryl hydrocarbon receptor nuclear translocator protein show distinct subcellular localizations in Hepa1c1c7 cells by immunofluorescence microscopy. Mol. Pharmacol., *45:* 428–438, 1993.
49. Pottenger, L. H., Christou, M., and Jefcoate, C. R. Purification and immunological characterization of a novel cytochrome P450 from C3H/10T1/2 cells. Arch. Biochem. Biophys., *286:* 488–497, 1991.
50. Laemmli, U. K. Cleavage of structural proteins during the assembly of the head of bacteriophage T4. Nature (Lond.), *227:* 680–685, 1970.
51. Towbin, H., Staehlin, T., and Gordon, J. Electrophoretic transfer of proteins from polyacrylamide gels to nitrocellulose sheets: procedure and some applications. Proc. Natl. Acad. Sci. USA, *76:* 4350–4354, 1979.
52. Badley, J. E., Bishop, G. A., St. John, T., and Frelinger, J. A. A simple, rapid method for the purification of poly A^+ RNA. BioTechniques, *6:* 114–116, 1988.
53. Fritsch, E. F., and Sambrook, J. *In:* T. Maniatis (ed.), Molecular Cloning: A Laboratory Manual, pp. 7.19–7.22. Cold Spring Harbor, NY: Cold Spring Harbor Laboratory, 1982.
54. Piskorska-Pliszczynaska, J., Keys, B., Safe, S., and Newman, M. S. The cytosolic receptor binding affinities and AHH induction potencies of 29 polynuclear aromatic hydrocarbons. Toxicol. Lett., *34:* 67–74, 1986.
55. Pollenz, R. S. The aryl hydrocarbon receptor, but not the aryl hydrocarbon receptor nuclear transporter protein, is rapidly depleted in hepatic and non-hepatic cultured cells exposed to 2,3,7,8-tetrachlorodibenzo-*p*-dioxin. Mol. Pharmacol., *49:* 391–398, 1996.
56. Murray, G. I., Taylor, M. C., McFayden, M. C. E., McKay, J. A., Greenlee, W. F., Burke, M. D., and Melvin, W. T. Tumor-specific expression of cytochrome P450 CYP1B1. Cancer Res., *57:* 3026–3031, 1997.
57. Huang, Z., Fasco, M. J., Figge, H. L., Keyomarsi, K., and Kaminsky, L. S. Expression of cytochromes P450 in human breast tissue and tumors. Drug Metab. Dispos., *24:* 899–905, 1996.
58. Einolf, H. J., Story, W. T., Marcus, C. B., Larsen, M. C., Jefcoate, C. R., Greenlee, W. F., Yagi, H., Jerina, D. M., Amin, S., Park, S. S., Gelboin, H. V., and Baird, W. M. Role of cytochrome P450 enzyme induction in the metabolic activation of benzo [*c*]phenanthrene in human cell lines and mouse epidermis. Chem. Res. Toxicol., *10:* 609–617, 1997.

Carcinogenesis vol.19 no.8 pp.000–000, 1998

Expression of CYP1B1 but not CYP1A1 by primary cultured human mammary stromal fibroblasts constitutively and in response to dioxin exposure: Role of the Ah receptor

Sakina E.Eltom[1], Michele C.Larsen and Colin R.Jefcoate

Environmental Toxicology Center and The Department of Pharmacology, University of Wisconsin, Madison, WI 53706, USA

[1]To whom correspondence should be addressed

The expression of CYP1B1 in human mammary fibroblasts (HMFs) was characterized as a potential modulator of their individual function as well as effects on adjacent mammary epithelia. We have used these characteristics to explore the diversity of fibroblast cells isolated from reduction mammoplasty patients and from different breast locations in breast cancer patients (tumors, peripheral to tumor and skin). These parameters have also been used to examine differences between two donors. The results have shown that while none of these HMFs expressed a detectable CYP1A1 protein basally or in response to TCDD, they all expressed CYP1B1 constitutively at similar levels (0.5–0.9 pmol/mg microsomal proteins) and they were induced by TCDD (up to 5-fold) consistent with mediation by the Ah receptor (AhR). DMBA metabolism by HMFs exhibited high proportions of 5,6-, 10,11- and 3,4-dihydrodiols, a profile that is typical of human CYP1B1 regioselectivity. RT-PCR followed by Southern blot analyses demonstrated that CYP1B1 mRNA expression in HMFs parallels levels of respective microsomal proteins. The AhR is expressed in these HMFs as two cytosolic forms (~106 and 104 kDa) and a substantial proportion of the 104 kDa form was localized to the nucleus even prior to TCDD treatment. In all HMFs isolated directly from collagenase digested breast tissues the AhR is expressed at levels 10-fold lower than in breast epithelial cells. However, HMFs that were isolated after serial passaging of mammary epithelial cultures had shown much higher levels of the AhR expression and more dramatic TCDD-induced down-regulation (>80% in 24 h) associated with more efficient nuclear translocation. These differences suggested the presence of two functionally distinct subtypes of HMFs: interstitial stromal fibroblasts that are readily released by collagenase digestion of breast tissues, and lobular stromal fibroblasts which are more tightly associated with the breast epithelia.

Introduction

The stroma of the mammary gland accounts for >80% of the resting breast volume (1). This stroma consists of fibroblasts, blood vessels and a macromolecular network composed of glycoproteins and proteoglycans known collectively as extra cellular matrix (ECM*). There is accumulating evidence that stromal fibroblasts play a crucial role both in normal development and in carcinogenesis of the mammary gland. During the maturation of the mammary gland, the interaction between stroma and epithelia is critical for normal development (2). The matrix metalloproteinases, gelatinase A and stromalysin-1, and serine proteinase, a urokinase-type plasminogen activator, are expressed at low levels during lactation and are up-regulated during mammary gland involution to facilitate tissue remodeling. These enzymes are synthesized mainly in the fibroblast-like cells of the periductal stroma (3).

The estrogen sensitivity of mammary epithelia is mediated by stromal fibroblasts and only estrogen receptor (ER) expression in the mesenchyme is necessary for mammary development (4). This has been demonstrated by analysis of mammary development through the combination of epithelia and mesenchyme from wild-type and ER knock-out mice (5). On hormonal stimulation, stromal fibroblasts that express ER respond by expression and release of growth factors [tumor growth factor (TGF)α, TGFβ, human growth factor (HGF), growth factor (PDGF), fibroblast growth factor (FGF) I, FGFII, growth factor (KGF), vascular endothelial growth factor (VEGF), growth factor (IGF) I and IGFII] and ECM (6). Each of these stromal factors contribute to the regulation of epithelial growth in a paracrine fashion (7).

Breast tumors are a complex and heterogeneous mix of epithelia, stromal cells, matrix proteins and vascular elements. The growth and dissemination of breast cancer requires the complex interaction between these various tumor elements. Most human breast carcinomas are associated with aberrant stromal expression of ECM degrading proteinases and epithelial infiltration of the surrounding stroma (8). Stromal fibroblasts also contribute to the growth and progression of breast carcinomas by the secretion of angiogenic factors. Evidence for hypoxic-induced up-regulation of VEGF, a major angiogenic factor in human mammary fibroblasts was presented, which suggests a paracrine influence by fibroblasts on endothelia within hypoxic regions of the tumor (9).

Human breast is a target for many environmental chemicals including polycyclic and polyhalogenated aromatic hydrocarbons (PAHs). PAHs exert their pleotropic toxic responses, including carcinogenesis (10), by binding to the Ah receptor (AhR), which is a basic helix-loop-helix (b-HLH) protein (11). Ligand binding results in activation of AhR and subsequent nuclear translocation, where it heterodimerizes with another bHLH partner, the Ah receptor nuclear translocator protein (ARNT) (12). The AhR–ARNT dimer binds to specific regulatory elements, xenobiotic responsive elements (XREs), upstream of the responsive genes and enhances their transcrip-

*Abbreviations: AhR, aryl hydrocarbon receptor; ARNT, Ah receptor nuclear translocating protein; b-HLH, basic helix-loop-helix; CYP, cytochrome P450; DEPC, ??; DMBA, 7,12-dimethylbenz[*a*]anthracene; DMSO, dimethyl sulfoxide; DTT, ??; ECL, enhanced chemiluminescence; ECM, extra cellular matrix; ER, estrogen receptor; FBS, fetal bovine serum; FGF, fibroblast growth factor; FITC, fluorescein isothiocyanate; HGF, human growth factor; HMEC, human mammary epithelial cells; HMF, human mammary fibroblasts; IGF, ?? growth factor; KGF, ?? growth factor; M-LV, Maloney leukemia virus; PAH, polycyclic aromatic hydrocarbon; PDGF, ?? growth factor; PF, normal peripheral tissue surrounding a tumor; RT-PCR, reverse transcriptase-polymerase chain reaction; SKF, normal peripheral tissue from breast skin; TCDD, 2,3,7,8-tetrachlorodibenzo-*p*-dioxin; TF, fibroblasts derived from breast tumor; TGF, tumor growth factor; VEGF, vascular endothelial growth factor; XRE, xenobiotic responsive elements.

tion (13). In addition to induction of cytochrome P450s and some phase II drug metabolizing enzymes, 2,3,7,8-tetrachlorodibenzo-*p*-dioxin (TCDD), a prototype PAH, elicits multiple effects on growth factors, cytokines and plasminogen activator components through this Ah receptor-mediated signal transduction pathway (14–19).

This laboratory has cloned and characterized a novel form of rodent cytochrome P450, CYP1B1, which is preferentially expressed in fibroblasts under control of the AhR (20,21). In most mouse organs (liver, lung and kidney), activation of the AhR by TCDD results in increased expression of CYP1A1 mRNA, and there is only a minor induction of CYP1B1 mRNA (20). The human CYP1B1 cDNA was cloned from a human keratinocyte cell line as a dioxin-responsive gene (18,22). The gene characterization (23) and the functional analysis of its promoter has revealed the distinct regulation of CYP1B1 gene from the closely related CYP1A1 and CYP1A2 genes (24). The cell-specific expression of CYP1B1 has been identified in human cell lines and tissues (25) and, although CYP1A1 and CYP1B1 are expressed at similar levels in human breast epithelia after TCDD treatment, only CYP1B1 is present under basal conditions in these cells (26). Furthermore, fibroblasts from a wide range of species and tissue sources lack the expression of CYP1A1 and exclusively express CYP1B1 under the control of the AhR (20,27,28). The lack of CYP1A1 mRNA expression in human skin fibroblasts was attributed to the presence of a putative repressor that competes with AhR for binding to CYP1A1 regulatory elements (29). On the other hand, in mouse embryo fibroblasts, the AhR is required for the basal expression of CYP1B1 (30). Thus, CYP1B1 expression in fibroblasts provides a measure of AhR activity, even in the absence of an external chemical inducer.

Recent studies have shown that human CYP1B1 activates many structurally diverse chemicals, including PAHs and their dihydrodiol derivatives, heterocyclic and aryl amines, and nitroaromatic hydrocarbons to genotoxic metabolites (31). In addition to its metabolic activation of carcinogens, several lines of evidence suggest that CYP1B1 has a key physiological regulatory function. These factors are the unusual cell specificity of expression in cells of mesodermal origin including steroidogenic cells (adrenal, testis, ovary), expression in the embryo, and the most recent linkage of a genetic deficiency as the cause of human congenital glaucoma, which is a defect in mesodermal development (32). The physiological substrate remains to be identified; however, human CYP1B1 catalyzes the conversion of E_2 to 4-hydroxy E_2 (33). This high affinity but low turnover reaction, although not effectively conserved across species, may have pathophysiological consequences.

In the present study we characterize the mRNA and protein expression of human CYP1B1 in cultured primary mammary fibroblasts as a potential modulator of their function. In particular, we have examined the role of Ah receptor activation in regulating this expression. The study uses the criteria of activation of the Ah receptor by TCDD and the expression of CYP1B1 to explore the diversity of normal fibroblasts from different donors. The effect of the tissue source of fibroblasts on these parameters is also examined in matched sets of fibroblasts derived from breast tumor (TF), normal peripheral tissue surrounding the tumor (PF) or from breast skin (SKF) of two different breast cancer patients.

Materials and methods

Materials

All tissue culture media and supplements were purchased from Sigma (St Louis, MO). Fetal bovine serum (FBS) and Trizol® reagent were obtained from Gibco BRL (Grand Island, NY). The horseradish peroxidase conjugated goat anti-rabbit IgG was purchased from Promega (Madison, WI). The enhanced chemiluminescence (ECL) detection system was purchased from Amersham (Arlington Heights, IL). The BCA protein assay kit was purchased from Pierce Chemicals (Rockford, IL). All materials used for SDS–PAGE were obtained from Bio-Rad (Richmond, CA), and nitrocellulose membranes were purchased from Schleicher and Schull (Keene, NH). Purified human recombinant CYP1B1 and CYP1A1 proteins, expressed in human lymphoblasts, were obtained from Gentest (Woburn, MA).

Primary antibodies

Affinity-purified rabbit polyclonal antibodies raised to recombinant mouse CYP1B1 and purified mouse CYP1A1 proteins were generated in this laboratory as previously described (34,35). Rabbit polyclonal anti-CYP1A2 and anti-epoxide hydrolase antibodies were kind gifts from Dr James Hardwick (Northwestern Ohio University, Rootstown, OH) and Dr Charles Kasper (McArdle Laboratory for Cancer Research, WI), respectively. The anti-Ah receptor and anti-ARNT polyclonal antibodies were generously provided by Dr Richard Pollenz (University of South Carolina, Charleston, SC).

Cells and cell culture

Primary cultures of normal mammary fibroblasts were obtained through the University of Wisconsin Comprehensive Cancer Center (UW-CCC) where they were isolated from mammoplastic surgery specimens of three individuals (A488, A786, 5819) and cultured as described (36). These cells were cultured in 1:1 mixture of Dulbecco's minimum essential medium and Ham F12 (DMEM/F12) media, supplemented with 10% fetal bovine serum (FBS), 4.5 mg/ml glucose, 100 U/ml penicillin and 100 µg/ml streptomycin.

The matched fibroblast cultures were derived from three distinct locations: (i) tumor tissues (TF); (ii) normal (macroscopically and histopathologically confirmed) breast tissues in the periphery of a tumor (PF); and (iii) breast skin (SKF) from two breast cancer patients (G-163: age 59, lobular invasive carcinoma; and G-149: age 46, ductal infiltrating carcinoma). These two sets of matched fibroblasts were obtained from Dr Helene Smith's laboratory (Geraldine Brush Cancer Institute, UC/SF, San Francisco, CA) where they were established as described previously (37). These cells were maintained in DMEM/F12 media supplemented with 10% FBS, 10 µg/ml insulin, non-essential amino acids, penicillin and streptomycin. All cultures were maintained at 37°C in a humidified incubator that contained 5% CO_2 and 95% air.

Verification of fibroblast origin by immunofluorescence

To verify whether the cells being studied were indeed fibroblasts, all fibroblasts lines were cultured directly on glass cover slips and grown to ~80% confluency. Cells on the cover slips were fixed for 5 min in pre-chilled acetone/methanol mixture (1:1) at –20°C, and then incubated at 4°C for 20 min in a fresh change of these solvents. Cells were then dried completely before being rinsed in PBS. Cells were blocked in 3% BSA in PBS, including 0.03% Na Azide. Murine monoclonal antibodies against vimentin and cytokeratin 18 were used for primary staining and fluorescein isothiocyanate (FITC)-labeled goat anti-mouse as secondary antibody, as described previously (38). The fluorescence of the positive staining of the slides was captured and photographed by Nikon Optiphot equipped with an MRC Laser Sharp Confocal Imaging System (Bio-Rad).

Treatment

These primary fibroblasts were used for up to eight passages, and we had verified that they maintain their phenotypic characteristics for up to passage 15. Typically, cells were treated when they were ~80% confluent, with 10 nM TCDD or an equivalent volume of dimethyl sulfoxide (DMSO), to a final 0.1% concentration (vehicle control), for 24 h or as specified in the figure legends.

Treated cells were harvested by mechanical scraping in cold PBS, and cell pellets were washed in PBS and used to prepare microsomes that measured CYP1B1 and CYP1A1 proteins by immunoblotting analysis and DMBA metabolism. Microsomes were prepared as described (35), and protein concentration was determined by the BCA method (39).

Enzyme activity in microsomal preparations

DMBA metabolism was measured in microsomal preparation of control or TCDD-treated cells as described (35). The reaction mixtures contained 100 mM potassium phosphate buffer (pH 7.6), 6 mM $MgCl_2$, NADPH-generating system (14.2 mM glucose 6-phosphate, 1.2 mM NADP and 0.06 U/ml glucose-6-phosphate dehydrogenase). Samples (in duplicates) were pre-incubated 1 min at 37°C and the reaction was initiated by the addition of 1.5 µM 7,12-dimethylbenz[*a*]anthracene (DMBA) (HPLC purified) and allowed to incubate under conditions of subdued lighting. The analysis of the human recombinant CYP1B1 and CYP1A1 microsomal standards, 0.075 and 0.050 mg microsomal protein/ml, respectively, were assayed as above, with the addition of 0.5 mg/ml human epoxide hydratase. The reaction was terminated after 15 min by the addition of an ethyl acetate-acetone mixture (2:1 ratio) that contained

1 mM DTT, and the metabolites were extracted and prepared for analysis on HPLC as described earlier (40). Metabolites were separated and quantitated by reverse phase HPLC.

Analysis of the Ah receptor nuclear translocation in normal human fibroblasts

Primary cultures of normal fibroblasts were grown to ~80% confluency. The growing medium was removed and duplicate plates of each cell types were treated with either 1 nM TCDD or an equivalent volume of DMSO (0.1% final concentration) for 1 h at 37°C. Cells were harvested by trypsinization and washed three times with ice-cold PBS and counted. Cell pellets were resuspended and incubated on ice for 30 min in lysis buffer (150 mM NaCl, 1% NP-40 and 0.05% SDS in 25 mM MOPS buffer pH 7.4, 0.03% Na azide, 1 mM EDTA, 10% glycerol, 5 mM EGTA, 20 mM Na molybdate), supplemented with protease inhibitors (5 µg/ml leupeptin, 0.15 U/ml aprotinin, 10 µg/ml TLCK, 1 mM PMSF, 5 µg/ml soy bean trypsin inhibitor) and phosphatase inhibitors (1 mM Na orthovanadate and 1 mM Na fluoride). Cell lysates were centrifuged at 2000 r.p.m. for 5 min in a microcentrifuge to pellet nuclei. Supernatants were saved as 'cytosolic fractions', and nuclei were washed in lysis buffer four times to eliminate cytosolic contamination. Then nuclear pellets were lysed by sonication in lysis buffer that contained inhibitors. Samples were sonicated four times in an ice bath, at 15 s each with 15 s intervals, to eliminate sample heating. An equivalent protein to 0.5×10^6 cells of cytosolic fraction or nuclear extract of each cell type was subjected to SDS–PAGE and Western blot analysis.

Gel electrophoresis and immunoblotting analysis

Proteins were separated on 7.5% SDS–PAGE and electro-transferred to nitrocellulose membranes as described (41,42). Immuno-reactive proteins were visualized using the ECL detection system as instructed by the manufacturer. CYP1B1 and CYP1A1 were immunodetected in microsomal preparations using their specific antibodies. The specificity of these antibodies was confirmed by using the purified recombinant CYP1B1 and CYP1A1. The microsomal epoxide hydrolase, which is not affected with TCDD-treatment (40), was co-detected on the same blot as a loading control. The expression of CYP apoproteins in these cells were quantified relative to purified recombinant human CYP1B1 (specific activity of 74 pmol/mg protein) or CYP1A1 (specific activity of 104 pmol/mg protein) standards. To generate CYP1B1, immunoblotting quantitation standard curves of 0, 0.2, 0.4 and 0.8 µg of recombinant human CYP1B1 protein (equivalent to 0, 14.8, 29.6, 59.2 fmol P4501B1) were analyzed. Each of these protein points was spiked with 10 µg of microsomal proteins from cells that do not express CYP1B1 as a carrier to enhance their migration and resolution on SDS-gel. To avoid variability that results from gel running, blotting procedure, developing and exposure conditions, the samples to be quantified were analyzed on the same gel with the standard curve dilutions that were used for their respective quantitation. Images from blots were scanned by PDSI Scanning Densitometer (Molecular Dynamics, Sunnyvale, CA) and band intensities were quantified using the volume integration option of the ImageQuant® software (Molecular Dynamics). Regression lines of the curve that related the intensity of CYP1B1 band against amount of CYP1B1 (fmol) were calculated using linear regression analysis. The following two equations are representative of what was used for the calculations of values presented in Figures 1 and 4, respectively: ($y = 42.5 + 25.97x$, $R^2 = 0.997$), ($y = 28.5 + 10.7x$, $R^2 = 0.988$).

RNA isolation and RT-PCR analysis

RT-PCR was used to measure the level of expression of CYP1B1 mRNA. Total cellular RNA was prepared from control or treated cells by an improved Chomcynski (1993) method using Trizol® reagent (43). cDNA templates for PCR were synthesized from total RNA by reverse transcription as follows: 1 µg of total RNA in DEPC-treated water was annealed with 0.5 µg nanomer random primers at 65°C for 5 min, then cooled slowly to room temperature. Reverse transcription was carried out in a total volume of 25 µl of 50 mM Tris–HCl (pH 8.3), 75 mM KCl, 3 mM $MgCl_2$, 10 mM DTT, 1 mM each of dATP, dGTP, dCTP, dTTP, 25 U placental RNase inhibitor and 200 U murine Maloney leukemia virus (M-MLV) reverse transcriptase (Promega). Samples were then incubated at 40°C for 1 h and the reaction was terminated by heating the samples at 95°C for 5 min.

PCR primers for CYP1B1 were designed based on the human cDNA sequence (22) (forward primer: 5'-CGTACCGGCCACTATCACTG-3'; reverse primer: 5'- GCAGGCTCATTTGGGTTGGC-3'), and were synthesized with an Applied Biosystems 380A synthesizer. Reverse transcription products of 1 ng total RNA from fibroblasts were PCR-amplified along with serially diluted human CYP1B1 cDNA using the Perkin–Elmer thermal cycler according to standard conditions. Approximately 5% of the PCR products were electrophoresed on 1.5% agarose gels and transferred to nylon membranes. The DNA was UV-cross linked to nylon membranes, which were hybridized with ^{32}P-labeled cDNA probe for human CYP1B1 (full length cDNA 2×10^6 c.p.m./ml, 16 h at 42°C). Probed membranes were exposed to a Phosphoimager screen (Molecular Dynamics) and band intensities were quantified using the volume integration option of the ImageQuant data analysis package (Molecular Dynamics). Standard curves were generated with known amounts of CYP1B1 cDNA (in fmol), which were PCR amplified, and the signals that they generated (band intensity of the PCR products). Such standard curves (equation of the representative dilutions in Figure 2A was: $y = 174.5 + 0.876x$, $R^2 = 0.992$) were used to calculate the relative amounts of CYP1B1 cDNA present in the RT products of 1 µg total RNA from tested fibroblasts.

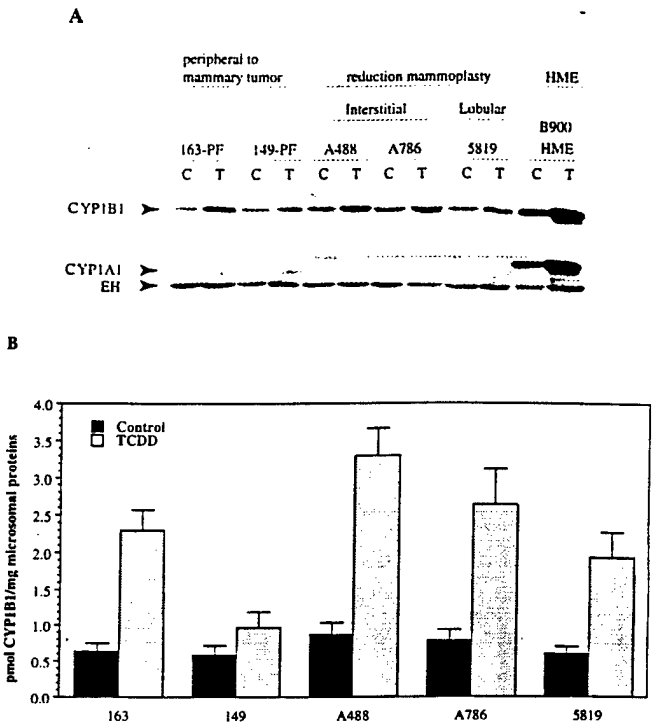

Fig. 1. Expression of basal and TCDD induced CYP1A1 and CYP1B1 in primary cultures of normal human mammary fibroblasts. Microsomes were prepared from control (C) or 24-h TCDD-treated cells at their seventh passage. Approximately 15 µg microsomal proteins were loaded per lane and subjected to electrophoresis and Western blotting as described in Materials and methods. (**A**) A representative immunoblot of CYP1B1 and CYP1A1 in HMFs. Microsomal proteins from human mammary epithelial cells (donor B900) were included as a positive control marker, and the microsomal epoxide hydrolase (EH) expression was probed with its specific antibody as a loading control within the individual fibroblast. (**B**) Quantitation of CYP1B1 expression in control and TCDD-treated HMFs. CYP1B1 proteins were quantified relative to standard curve generated using recombinant human CYP1B1 as described in Materials and methods. Both fibroblast samples and standard curve dilutions were analyzed on the same blot. Values in columns and bars are the means ± SD of the values obtained from two different cultures.

Results

Cellular characterization

Primary cultures of normal mammary fibroblasts were isolated from reduction mammoplastic surgery specimens of three individuals (A488, A786, 5819). A488 and A786 represent the fast sediment fibroblasts associated with the stromal components that were isolated during the separation from epithelial organoids, and following collagenase digestion of normal breast tissues. Further trypsinization of the epithelial organoids resulted in generation of 5819 fibroblasts. Therefore, fibroblasts A488 and A786 were of interstitial stromal origin, whereas 5819 represented lobular stromal fibroblasts (44). In addition, matched fibroblast sets from two breast cancer patients, G-163 and G-149, were derived from three distinct locations: breast tumor tissues (TF), normal breast tissues in the periphery

Table I. Summary of the tissue source and the growth conditions of the human fibroblasts used in the study

Designated name	Tissue source	Location	Specific growth media requirement
A488	Reduction mammoplasty	Interstitial stroma	High glucose
A786	Reduction mammoplasty	Interstitial stroma	High glucose
5819	Reduction mammoplasty	Lobular stroma	High glucose
PF[a]	Normal tissues peripheral to breast tumor	Tumor periphery stroma	High insulin
TF[a]	Breast tumor	Tumor stroma	High insulin
SKF[a]	Skin overlying breast tissues	Subcutaneous stroma	High insulin

[a]Isolated from either G163 or G149 breast cancer patients.

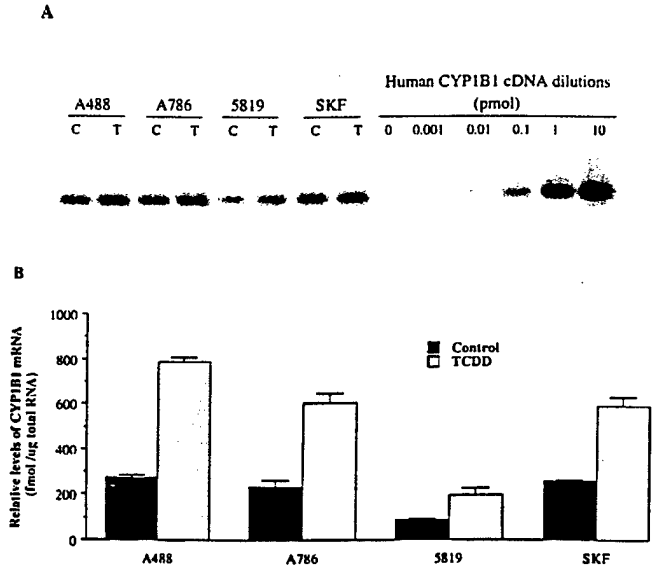

Fig. 2. RT-PCR analysis of CYP1B1 mRNA expression in constitutive and TCDD-induced normal mammary, and skin fibroblasts. Total RNA from constitutive (C) or TCDD-treated, [10 nM for 24 h (T)] fibroblasts was isolated by Trizol procedure, and cDNA was synthesized and subjected to PCR amplification as described in Materials and methods. Serial dilutions of full length human CYP1B1 cDNA were included in the PCR amplification and used to calculate the amounts of cDNA (hence mRNA) present in each fibroblast sample. The PCR products were visualized by Southern blotting using ^{32}P-labeled human CYP1B1 cDNA as a probe, and quantified by the phosphoimager as described in Materials and methods. **(A)** A representative Southern blot of PCR amplified CYP1B1 products in selected HMF. **(B)** Quantitation of CYP1B1 mRNA in HMF. Columns and bars are the means ± SD of duplicate PCRs from two different cultures.

of the tumor (PF) and overlying breast skin (SKF). Morphologically, there were no significant differences among these fibroblasts, although the SKFs from both individuals were more rapidly growing than the rest of the fibroblasts. Both PF and TF of G-163 proliferated faster than those of G-149. Table I summarizes the source and growth conditions of the different fibroblasts used in the study. All fibroblasts showed strong vimentin expression, whereas none stained with antibodies against keratin-18 (data not shown). This is the expected phenotype for cells of mesenchymal origin.

Effect of media and passage number on CYP1B1 expression in a single individual donor (A488) and comparison to epithelia

The expression of microsomal CYP1A1 and CYP1B1 was examined in five normal human mammary fibroblasts (HMFs) primary cultures. In addition to the three normal fibroblasts from mammoplasty procedures (A488, A786 and 5819), we included in the comparison the two peripheral normal fibroblasts from the two matched sets (163-PF and 149-PF) from tumor patients. We cultured these fibroblasts in the exact culture conditions recommended by the manufacturers (matched sets in 10 μg/ml insulin; mammoplasty fibroblasts in high glucose). For A488 mammoplasty cells and 163-PF cells no significant difference in expression of basal or TCDD-induced levels of CYP1B1 was observed between the two growth conditions (data not shown). A488 fibroblasts were examined at an early (fifth) and a late (15th) passage. No significant difference was observed in constitutive or TCDD-induced expression of CYP1B1 protein between early and late passages. Examining the expression of CYP1B1 in primary mammary fibroblasts and epithelial cells from a single donor (A488), revealed that both the basal and induced levels were ~10 times lower in fibroblasts than in the epithelial cells (data not shown).

Expression of constitutive and TCDD-induced CYPs protein and mRNA in normal HMFs

The CYP1A1 protein expression was not detected in HMFs as compared with a normal human mammary epithelial sample, which was included as a positive control, at a detection level of 1 fmol (Figure 1A). CYP1A2 protein expression was also examined in these cells by immunoblotting with the use of polyclonal antibodies specific for CYP1A2. No CYP1A2 protein was detectable in these HMFs, whereas microsomal samples from control rat liver stained positive (data not shown). Western blot analysis of microsomal preparations of basal or TCDD-induced fibroblasts from five individual donors showed substantial levels of constitutive microsomal CYP1B1 protein expression, which was induced ~4-fold by TCDD. The quantitation of these levels, relative to purified recombinant human CYP1B1 standards, showed that the constitutive expression in these individuals ranged from 0.5 to 0.9 pmol of CYP1B1/mg microsomal proteins, with low variability among the different individuals (Figure 1B). Treatment of these cells with TCDD for 24 h induced the expression of CYP1B1 protein to levels ranging between 1.2 and 3.7 pmol of CYP1B1/mg microsomal proteins (Figure 1B).

Examining the mRNA expression of some selected fibroblasts (Figure 2A and B) revealed a similar picture to the protein expression. Cells from each donor showed similar induction but there were substantial parallel variations of basal and induced CYP1B1 mRNA for these cells (A488 > A786 > 5819). This was similar to the pattern seen for microsomal protein expression for these three donors.

DMBA metabolism by normal HMFs

The regioselective profile for DMBA metabolism by microsomes from basal and TCDD-treated normal HMFs in comparison to human mammary epithelial cells (HMEC) and recombinant human CYP1B1 and CYP1A1 is summarized in Table II. Based on the DMBA metabolite profile generated by recombinant human CYP1B1 and CYP1A1, the HMF basal

Table II. Microsomal DMBA metabolism in human mammary fibroblasts and epithelial cells

Sample	Dihydrodiols				Phenols		Total DMBA Metabolism (pmol/mg/h)
	5,6-	8,9-	10,11-	3,4-	A	B	
Primary HMF[a]							
Constitutive	0.36 (19)[d]	<0.50[b,c] (<27)		0.27 (14)	<0.50[b] (<27)	0.24 (13)	1.87
TCDD-induced	1.79 (29)	1.47[c] (24)		1.05 (17)	1.19 (19)	0.64 (10)	6.14
Primary HMEC[e]							
Constitutive	0.29 (10)	0.34[c] (10)		0.19 (7)	1.55[b] (53)	0.63 (20)	3.00
TCDD-Induced	17 (11)	68 (45)	12 (8)	7 (5)	38 (25)	8 (5)	150
Recombinant human cytochromes P450							
CYP1B1[f]	50 (17)	33 (11)	27 (9)	17 (6)	154 (54)	2 (<1)	287
CYP1A1[g]	189 (11)	870 (51)	73 (4)	79 (5)	450 (26)	45 (3)	1716

[a]Microsomes were isolated from primary human mammary fibroblasts of donor A488, 0.620 mg microsomal proteins of control or TCDD-treated fibroblasts were used per reaction.
[b]Quantitative metabolite detection is not possible because of the presence of a contaminating background peak.
[c]8,9- and 10,11-DMBA dihydrodiols, peaks were poorly resolved at this low level of activity.
[d]Percentage metabolite distribution.
[e]Microsomes were isolated from primary human mammary epithelial cells of donor B402.
[f]Recombinant human CYP1B1 (Gentest); 74 pmol/mg.
[g]Recombinant human CYP1A1 (Gentest); 104 pmol/mg.

microsomal DMBA metabolism exhibited a profile resembling that of CYP1B1, where it produced similar proportions of 5,6-, 10,11- and 3,4-dihydrodiols. TCDD treatment induced this activity by 3- to 5-fold without changing the ratio of these metabolites, which is in agreement with results obtained by immunoblotting. This is consistent with the exclusive expression of CYP1B1 and the complete lack of CYP1A1 expression. HMEC basal microsomes exhibited a CYP1B1-specific DMBA metabolites profile, but unlike fibroblasts, TCDD preferentially induced the production of a predominant proportion of 8,9-dihydrodiols, which characterized CYP1A1-mediated DMBA metabolism.

Expression of the Ah receptor signaling components in HMFs

The expression of the AhR and its partner ARNT proteins in normal HMF cells was examined in the context of their regulation of TCDD induction of CYP1B1. ARNT expression was consistently high in all cells. The AhR levels were also similar among the different sources of fibroblasts but exhibited distinguishing characteristics according to their source. TCDD induced complete down-regulation of the AhR within 24 h in fibroblasts isolated from epithelial cultures (5819) and fibroblasts peripheral to tumors (163-PF and 149-PF). However, the A488 and A786 fibroblasts, which were isolated from the initial collagenase digestion of breast tissues, responded to TCDD by down-regulating AhR by only 50% in 24 h. No effect for TCDD was observed on ARNT levels in all fibroblasts (Figure 3A).

There was very little inter-individual or tissue source differences in the receptor levels, and TCDD treatment for 24 h resulted in a similar down-regulation of the AhR in each set of fibroblasts (Figure 4A). Although consistent among the two individuals (G163 and G-149), ARNT showed a 10-fold lower level of expression in peripheral fibroblasts compared with skin- and tumor-derived fibroblasts (Figure 3B).

Since AhR down-regulation is preceded by receptor nuclear translocation, nuclear translocation of AhR in response to TCDD was examined in the two categories of isolated HMFs. A period of only 1 h after TCDD treatment was allowed before cellular fractionation and isolation of nuclei so as to allow a reasonable partitioning, but there was no depletion of the receptor. This time period was sufficient for maximal TCDD-induced nuclear accumulation of AhR in rodent cell lines (45). Even in the absence of TCDD, there was a substantial fraction of the cellular Ah receptor in the nuclei of HMFs. One hour of TCDD treatment resulted in a slight increase in this level in A488 fibroblasts (interstitial stromal-origin) and more than doubled the receptor level in 5819 fibroblasts (lobular stromal-origin) (Figure 3B). Probing these blots for cytosolic proteins marker (GAPDH) confirmed that the constitutive nuclear AhR was not an artifact from cytosolic contamination (Figure 3B). Moreover, the AhR in these preparations resolved in a doublet (~106 and 104 kDa) in the non-nuclear fractions (cytosolic), and only the 104 kDa species of the doublet prevailed in the nuclei. The pattern of nuclear translocation in these fibroblasts correlates with their ability to down-regulate the Ah receptor in response to TCDD treatment. Paradoxically, the A488 fibroblasts expressed higher levels of basal and induced CYP1B1 than 5819 cells, which suggests that these AhR nuclear translocation and down-regulation differences may not correlate with transcriptional regulation.

Comparison of CYP expression in matched fibroblast cultures from three distinct tissue locations

Matched sets of fibroblasts derived from breast tumor, normal peripheral tissues surrounding the tumor or from breast skin

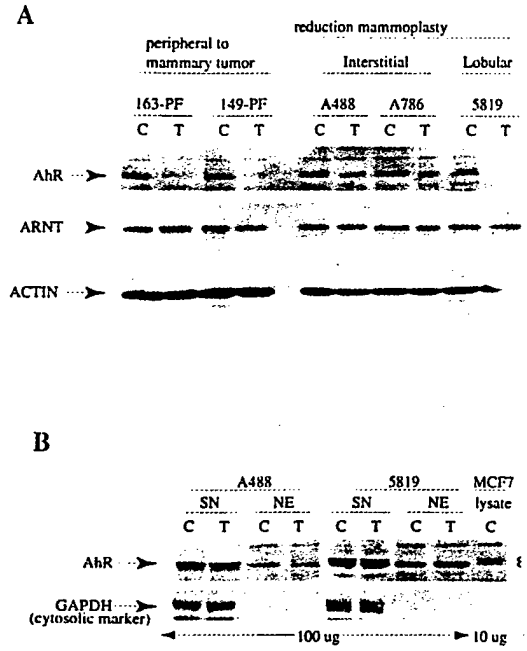

Fig. 3. Analysis of the AhR and ARNT expression and the TCDD-induced nuclear translocation and down-regulation of the AhR in normal HMF. **(A)** Detection of AhR and ARNT in total cellular protein extracts of control or 24-h TCDD-treated HMF. Proteins were isolated from Trizol lysate following RNA isolation as described in Materials and methods. Protein (40 μg) was loaded on each lane and subjected to SDS–PAGE and immunoblotting. Membranes were probed with anti-actin antibody for loading control. **(B)** Nuclear translocation of AhR following 1 h of treatment with 10 nM TCDD. Treated cells were lysed and fractionated into cytosolic (SN) or nuclear (NE) fractions as described in Materials and methods. Approximately 100 μg of SN or NE of each cell type was analyzed by SDS–PAGE and Western blot analysis. Trizol protein extract from MCF-7 cell line was co-analyzed as a positive control.

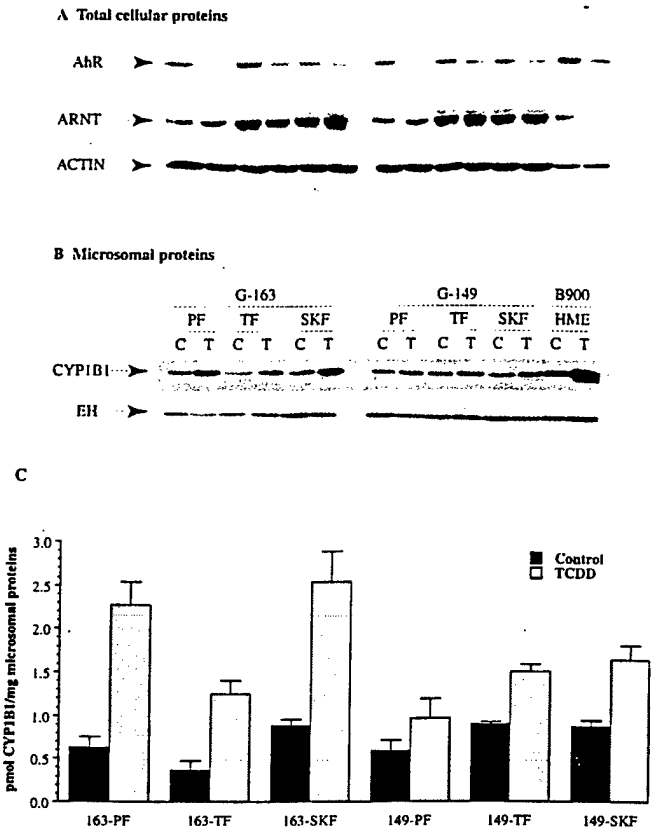

Fig. 4. Immunoblot analysis of expression of CYP1B1, AhR and ARNT in primary cultures of peripheral, tumor- and skin-derived human fibroblasts from two breast cancer patients (G163 and G149). **(A)** A representative immunoblot of CYP1B1 and CYP1A1 in matched fibroblast sets. Microsomes were prepared from control (C) or 24 h TCDD-treated cells (T) at their seventh passage. Approximately 15 μg microsomal proteins were analyzed by SDS–PAGE and immunoblotted with anti-CYP1B1 antibodies as described in Materials and methods. Microsomes from human mammary epithelial cells (donor B900) were used as a positive control, and the blots were re-probed for EH as a loading control within the same individual. **(B)** Immunoblot analysis of AhR and ARNT in the matched fibroblast sets. Total cellular proteins were isolated and analyzed as described in Materials and methods and Figure 3A. Approximately 40 μg of protein from each fibroblast type was analyzed, and 10 μg of total cellular proteins of donor B900 was included in the analysis as a reference standard. **(C)** Quantitation of microsomal CYP1B1 expression in control or TCDD-induced matched fibroblasts. CYP1B1 protein expression was quantitatively relative to a standard curve generated using recombinant human CYP1B1 as described in Materials and methods. Columns and bars are the means ± SD of the values obtained from two different cultures.

of two patients were examined for their basal and TCDD-induced expression of CYP1A1 and CYP1B1. Similar to the reduction mammoplasty HMFs examined earlier, fibroblasts from the three different tissue sources completely lacked detectable CYP1A1 protein (data not shown). All fibroblasts from the three different tissue sources of each donor expressed basal levels of CYP1B1 and similar TCDD-induction. The expression patterns varied substantially between the fibroblasts from the two individuals (Figure 4B). Although basal CYP1B1 expression in the fibroblasts from different tissue source of individual G163 showed a substantial variability, these levels were quite consistent in patient G149. Overall, G149 was less inducible than G163, and averaged a 1.5-fold induction factor compared with 3.5-fold (Figure 4C).

Discussion

Previous work from this laboratory has shown that rodent embryo, mammary and uterine fibroblasts express basal and TCDD-inducible CYP1B1 under the control of the Ah receptor, whereas CYP1A1 is scarcely detectable (20,21,28,30,46). Here we show that these same characteristics are conserved in fibroblasts from the human breast. In this respect, human mammary fibroblasts (HMF) differ from human mammary epithelial cells (HMEC), which also express basal and inducible CYP1B1, but additionally express CYP1A1 (26). The levels of basal and TCDD-induced CYP1B1 in HMF are each ~10-fold lower than in epithelial cells. The level of CYP1B1 mRNA expression showed a similar variation to that of microsomal CYP1B1 protein for the same cell source. This level of expression is also ~10 times lower than in rat mammary fibroblasts (46).

Based on the regioselectivity in metabolizing DMBA, rodents produce a highly characteristic DMBA metabolite profile for each of CYP1A1 and CYP1B1, which is unlike humans whose profile for the two CYPs is not as distinct (26,34). Whereas rodent CYP1A1-mediated DMBA metabolism was characterized by the production of high ratios of 8,9-dihydrodiols, and CYP1B1 selectively produced high levels of 10,11- and 3,4-dihydrodiols (34), human CYP1B1-mediated DMBA metabolism produced relatively higher proportions of the 5,6- and 10,11-dihydrodiols, relative to CYP1A1, but unlike rodents, humans showed similar ratios of 3,4-dihydrodiols (5%) for both CYP1A1 and CYP1B1 (26). HMF differs from HMEC with respect to its DMBA metabolism. Under both basal and TCDD-treatment conditions, HMF produced a CYP1B1-

specific profile; in contrast, HMEC exhibited a CYP1B1-specific profile under basal conditions, whereas TCDD treatment switched the selectivity to a CYP1A1-specific profile. The much greater stimulation of this activity in HMEC is caused by the induction of the much more active CYP1A1. These differences in DMBA metabolism were fully consistent with results obtained by immunoblotting, which showed that HMF exclusively expresses CYP1B1 under both basal and induced conditions. It further supports the significant role of HMF in estrogen-mediated breast cancer, since human CYP1B1 also metabolizes estrodiol to the potentially reactive 4-hydroxy metabolite (33).

We have attempted to determine whether CYP1B1 expression is dependent on the location of fibroblasts in the breast and whether they differ between the tumor-bearing and normal healthy breast. We also tested whether CYP1B1 expression would distinguish fibroblasts that are readily released by collagenase from breast tissue (interstitial stroma) versus fibroblasts generated during culture of the associated mammary epithelia (lobular stroma) (44). The levels of basal and TCDD-induced expression showed only subtle variations according to tissue or location sources. Even though they can be substantially distinguished by the release of specific growth factors released (37,47), the peripheral, tumor and subcutaneous HMF from two donors exhibited larger differences between the donors than between the tissue sources. For one donor, peripheral tumor and subcutaneous HMF each showed 3- to 5-fold induction, whereas for a second donor, the increases were only ~50%.

AhR in the HMF generally showed TCDD-induced down-regulation, which is consistent with previous results in rodent cells (48). AhR and ARNT, the two key regulators of CYP1B1 expression, exhibited some reproducible differences in their functional characteristics according to the source of HMF. First, peripheral HMF showed five times lower levels of ARNT than tumor or subcutaneous HMF, secondly, the lobular stromal HMFs showed very effective TCDD-induced AhR down-regulation. Although ligand binding is required for activation of AhR, subsequent nuclear translocation and DNA binding, a substantial proportion of the receptor was detected in HMFs tightly bound to the nuclear fractions in the absence of ligand treatment. This finding may parallel other data from human cells in culture. Significant levels of AhR in the nuclear fraction of untreated HeLa cells were detected by immunofluorescence localization (49). We also distinguished two cytosolic AhR species (106 and 104 kDa) of which only the 104 kDa protein translocated preferentially to the nucleus. This is consistent with a report of two functionally distinct forms of AhR in human cell lines (50). We have seen a similar preferentially nuclear translocation of allelic variants of mouse AhR in mouse BMS2 bone stromal fibroblasts (?.Heidel and C.R.Jefcoate, unpublished data).

A previous study has reported an absence of TCDD-induced CYP1A1 in human dermal fibroblasts, which was attributed to inhibition of AhR activity by a putative repressor (29). Our previous reports (20,21,27,28,30) and the data presented here indicate that TCDD induction in fibroblasts cannot be readily evaluated by CYP1A1 expression, since this form is not typically expressed in these cells. We observed induction of CYP1B1 in all human fibroblasts examined. However, we found that the extent of inducibility is linked to the human genotype rather than to the tissue source of the fibroblasts. The lack of correlation with AhR or ARNT is certainly compatible with the presence of an AhR-suppression mechanism. The apparent heterogeneity in HMFs with respect to AhR transfer to the nucleus indicates the presence of other modulatory mechanisms, although in this case, slow nuclear translocation was not correlated with a deficiency in CYP1B1 induction.

Acknowledgements

The authors appreciated the generous donation of the human mammary fibroblasts by Dr Michael Gould, obtained from the University of Wisconsin Medical School Comprehensive Center (Madison, WI) and the late Dr Helene Smith (Geraldine Brush Cancer Institute, University of California, San Francisco, CA). We are also thankful for the generous gift of the anti-AhR and anti-ARNT polyclonal antibodies from Dr Richard Pollenz (University of South Carolina, Charlestone, NC). This research was supported by NIEHS grant 144EN46 and US Department of Defense Breast Cancer Research grant DAMD17-94-J4054.

References

1. Drife,J.O. (1986) Breast development in puberty. In Ageli,A., Bradlow,H.L. and Dogliotti L. (eds) *Annals of the New York Academy of Sciences. Endocrinology of the Breast: Basic and Clinical Aspects*. New York Academy of Sciences, New York, pp. 58–65.
2. Sakakura,T. (1991) New aspects of stromal–parenchyma relations in mammary gland differentiation. *Int. Rev. Cytol.*, **125**, 165–202.
3. Lund,L.R., Romer,J., Thomasset,N., Solberg,H., Pyke,C., Bissell,M.J., Dano,K. and Werb,Z. (1996) Two distinct phases of apoptosis in mammary gland involution: proteinase-independent and -dependent pathways. *Development*, **122**, 181–193.
4. Haslam,S.Z. (1986) Mammary fibroblast influence on the normal mouse mammary epithelial cell responses to estrogen *in vitro*. *Cancer Res.*, **46**, 310–316.
5. Cooke,P.S., Buchanan,D.L., Young,P., Setiawan,T., Brody,J., Korach,K.S., Taylor,J., Lubahn,D.B. and Cunha,G.R. (1997) Stromal estrogen receptors mediate mitogenic effects of estradiol on uterine epithelium. *Proc. Natl Acad. Sci., USA*, **94**, 6535–6540.
6. Cunha,G.R. (1994) Role of mesenchymal-epithelial interactions in normal and abnormal development of the mammary gland and prostate. *Cancer*, **74**(suppl.), 1030–1044.
7. Dickson,R.B. and Lippman,M.E. (1995) Growth factors in breast cancer. *Endocrine Rev.* **16**, 559–589.
8. Stetler-Stevenson,W.G. (1990) Type IV collagenase in tumor invasion and metastasis. *Cancer Metastas. Rev.*, **9**, 289–303.
9. Hlatky,L., Tsionou,C., Hahnfeldt,P. and Coleman,C.N. (1994) Mammary fibroblasts may influence tumor angiogenesis via hypoxia-induced vascular endothelial growth factor up-regulation and protein expression. *Cancer Res.*, **54**, 6083–6086.
10. Poland,A.P. and Knutson,J.C. (1982) 2,3,7,8-Tetrachlorodibenzo-*p*-dioxin and related aromatic hydrocarbons: examination of the mechanism of toxicity. *Annu. Rev. Pharmacol. Toxicol.*, **22**, 517–554.
11. Burback,K.M., Poland,A.P. and Bradfield,C.A. (1992) Cloning of the Ah receptor cDNA reveals a distinctive ligand-activated transcription factor. *Proc. Natl Acad. Sci. USA*, **89**, 8185–8989.
12. Hoffman,E.C., Reyes,H., Chu,F.F., Sander,F., Conley,L.H., Brooks,B.A. and Hankinson,O. (1991) Cloning of a factor required for activity of the Ah (dioxin) receptor. *Science*, **252**, 954–958.
13. Jones,P.B.C., Durrin,L.K., Galeazzi,D.R. and Whitlock,J.P.Jr (1986) Control of cytochrome P_1-450 gene expression: analysis of a dioxin-responsive enhancer system. *Proc. Natl Acad. Sci. USA*, **83**, 2802–2806.
14. Madhukar,B.V., Brewster,D.W. and Matsumura,F. (1984) Effects of *in vitro*-administered 2,3,7,8-tetrachlorodibenzo-*p*-dioxin on receptor binding of epidermal growth factor in the hepatic plasma membrane of rat, guinea-pig mouse and hamster. *Proc. Natl Acad. Sci. USA*, **83**, 7407–7411.
15. Choi,E.J., Toscano,D.G., Ryan,J.A., Riedel,N. and Tuscano,W.A. (1991) Dioxin induces transforming growth factor-α in human keratinocytes. *J. Biol. Chem.*, **266**, 9591–9597.
16. Gaido,K.W., Maness,S.C., Leonard,L.S. and Greenlee,W.F. (1992) 2,3,7,8-tetrachlorodibenzo-*p*-dioxin-dependent regulation of transforming growth factors-α and β2 expression in a human keratinocyte cell line involve both transcription and post-transcriptional control. *J. Biol. Chem.*, **267**, 24591–24595.

June 1st Cancer Res June 1st

17. Vogel,C. and Abel,J. (1995) Effect of 2,3,7,8-tetrachlorodibenzo-*p*-dioxin on growth factor expression in human breast cancer cell line MCF-7. *Arch. Toxicol.*, **69**, 259–265.
18. Sutter,T.R., Guzman,K., Dold,K.M. and Greenlee,W.F. (1991) Targets for dioxin-genes for plasminogen activator inhibitor-2 and interleukin-1β. *Science*, **254**, 415–518.
19. Gaido,K.W. and Maness,S.C. (1995) Post-transcriptional stabilization of urokinase-plasminogen activator mRNA by 2,3,7,8-tetrachlorodibenzo-*p*-dioxin in human keratinocyte cell line. *Toxicol. Appl. Pharmacol.*, **133**, 34–42.
20. Savas,U., Bhattacharyya,K., Christou,M., Alexander,D. and Jefcoate,C.R. (1994) Mouse cytochrome p450EF representative of a new 1B subfamily of cytochrome P450s. Cloning, sequence determination and tissue expression *J. Biol Chem.*, **269**, 14905–14911.
21. Savas,U. and Jefcoate,C.R. (1994) Dual regulation of cytochrome P450EF expression via the aryl hydrocarbon receptor and protein stabilization in C3H/10T1/2 cells. *Mol. Pharmacol.*, **45**, 1153–1159.
22. Sutter,T.R., Tang,Y.M., Hayes,C.L., Wo,Y.Y.P., Jabs,E.W., Li,X., Yin,H., Cody,C.W. and Greenlee,W.F. (1994) Complete cDNA sequence of a human dioxin-inducible mRNA identifies a new gene subfamily of cytochrome P450 that maps to chromosome 2. *J. Biol. Chem.*, **269**, 13092–13099.
23. Tang,Y.M., Wo,Y.Y.P., Stewart,J., Hawkins,A.L., Griffin,C.A., Sutter,T.R. and Greenlee,W.F. (1996) Isolation and characterization of the human cytochrome P450 CYP1B1 gene. *J. Biol Chem.*, **271**, 28324–28330.
24. Wo,Y.Y.P., Stewart,J. and Greenlee,W.F. (1997) Functional analysis of the promoter for the human CYP1B1 gene. *J. Biol Chem.*, **272**, 26702–26707.
25. Kress,S. and Greenlee,W.F. (1997) Cell-specific regulation of human CYP1A1 and CYP1B1 genes. *Cancer Res.*, **57**, 1264–1269.
26. Larsen,M.C., Angus,W.G., Brake,P.B., Eltom,S.E., Sukow,K.A. and Jefcoate,C.R. (1998) Characterization of CYP1B1 and CYP1A1 expression in human mammary epithelial cells: role of the Ah receptor in polycyclic aromatic hydrocarbon metabolism. *Cancer Res.* (in press).
27 Bhattacharyya,K., Brake, P., Eltom,S.E., Otto,S. and Jefcoate,C.R. (1995) Identification of a rat adrenal cytochrome P450 active in polycyclic hydrocarbon metabolism as rat CYP1B1. Demonstration of a unique tissue-specific pattern of hormonal and aryl hydrocarbon receptor-linked regulation. *J. Biol Chem.*, **270**, 11595–11602.
28. Savas,U., Christou,M. and Jefcoate,C.R. (1993) Mouse endometrium stromal cells express a polycyclic aromatic hydrocarbon-inducible cytochrome P450 that closely resembles the novel P450 in mouse embryo fibroblasts (P450EF). *Carcinogenesis*, **14**, 2013–2018.
29. Gardin,K., Wilhelmsson,A., Poellinger,L. and Gerghard,A. (1993) Non-responsiveness of normal human fibroblasts to dioxin correlates with the presence of a constitutive xenobiotic response element-binding factor. *J. Biol. Chem.*, **268**, 4061–4068.
30. Zhang,L., Savas,U., Alexander,D. and Jefcoate,C.R. (1998) Characterization of the mouse CYP1B1 gene: identification of an enhancer region that directs aryl hydrocarbon receptor-mediated constitutive and induced expression. *J. Biol. Chem.*, **273**, 5174–5183.
31. Shimada,T., Hayes,C.L., Yamazaki,H., Amin,S., Hecht,S.S., Guengerich,F.P. and Sutter,T.R . (1996) Activation of chemically diverse pro-carcinogens by human cytochrome P4501B1. *Cancer Res.*, **56**, 2979–2984.
32. Stoilov,I., Akarsu,A.N. and Sarfarazi,M. (1997) Identification of three truncation mutations in cytochrome P4501B1 (CYP1B1) as the primary congenital glaucoma (Buphthalmos) in families linked to GLC3A locus on chromosome 2p21. *Hum. Mol. Genet.*, **6**, 641–647.
33. Hayes,C.L., Spink,D.C., Spink,B.C., Cao,J.Q., Walker,N.J. and Sutter,T.R. (1996) 17 Beta-estradiol hydroxylation catalyzed by human CYP1B1. *Proc. Natl Acad. Sci. USA*, **93**, 9776–9781.
34. Savas,U., Carstens,C.P. and Jefcoate,C.R. (1997) Biological oxidations and p450 reactions- recombinant mouse CYP1B1 expressed in *E.coli* exhibits selective binding by polycyclic hydrocarbons and metabolism which parallels C3H10T1/2 cell microsomes but differs from human recombinant CYP1B1. *Arch. Biochem. Biophys.*, **347**, 181–192.
35. Pottenger,L.H. and Jefcoate,C.R. (1990) Characterization of a novel cytochrome P450 from the transformable cell line, C3H/10T1/2. *Carcinogenesis*, **11**, 321–327.
36. Wolman,S.R., Smith,H.S., Stampfer,M. and Hackett,A.J. (1985) Growth of diploid cells from breast cancers. *Cancer Genet.Cytogenet.*, **16**, 49–64.
37. Yee,D., Paik,S., Lebovis,G.S., Marais,R.R., Favoni,R.E., Cullen,K.J., Lippman,M.E. and Rosen,N. (1989) Analysis of insulin-like growth factor I gene expression in malignancy: evidence for a paracrine role in human breast cancer. *Mol. Endocrinol.*, **3**, 509–517.
38. Sommers,C.L., Walker-Jones,D., Heckford,S.E. *et al.* (1989) Vimentin rather than keratin expression in some hormone-independent breast cancer cell lines and in oncogene-transformed mammary epithelial cells. *Cancer Res.*, **49**, 4258–4263.
39. Smith,P.K., Krohn,R.I., Hermanson,G.T. *et al.* (1985) Measurement of protein using bicinchoninic acid. *Anal. Biochem.*, **150**, 76–85 [published erratum appears in *Anal. Biochem.* 1987, **163**, 279].
40. Christou,M., Jovanovich,M.C. and Jefcoate,C.R. (1989) Epoxide hydratase: sex specific expression and rate limiting role in DMBA metabolism. *Carcinogenesis*, **10**, 1883–90.
41. Laemmli,U.K. (1970) Cleavage of structural proteins during the assembly of the head of bateriophage T4. *Nature*, **227**, 680–685.
42. Towbin,H., Staehlin,T. and Gordon,J., (1979) Electrophoretic transfer of proteins from polyacrylamide gels to nitrocellulose sheets: procedure and some applications. *Proc. Natl Acad. Sci. USA*, **76**, 4350–4354.
43. Chomcynski,P. (1993) A reagent for the single step simultaneous isolation of RNA, DNA and proteins from cells and tissue samples. *BioTechniques*, **15**, 532–537.
44. Ronnov-Jessen,L., Petersen,O.W. and Bissell,M.J. (1996) Cellular changes involved in conversion of normal to malignant breast: importance of the stromal reaction. *Physiol. Rev.*, **76**, 69–125.
45. Reik,M., Robertson,R.W., Pasco,D.S. and Fagan,J.B. (1994) Down-regulation of nuclear aryl hydrocarbon receptor DNA-binding and transcription functions: requirement for a labile factor. *Mol. Cell. Biol.*, **14**, 5653–5660.
46. Christou,M., SavasU., Schroeder,S., Shen,X., Thompson,T., Gould,M.N. and Jefcoate,C.R. (1995) Cytochrome CYP1A1 and CYP1B1 in the rat mammary gland: Cell-specific expression and regulation by polycyclic aromatic hydrocarbons and hormones. *Mol. Cell. Endocrinol.*, **115**, 41–50.
47. Cullen,K.J. *et al.* (1991) Growth factor messenger RNA expression by human breast fibroblasts from benign and malignant lesions. *Cancer Res.*, **51**, 4978–4985.
48. Pollenz,R.S. (1996) The arylhydrocarbon receptor, but not the arylhydrocarbon receptor nuclear translocator protein is rapidly depleted in hepatic and nonhepatic culture cells exposed to 2,3,7,8-tetrachlorodibenzo-*p*-dioxin. *Mol. Pharmacol.*, **49**, 391–398.
49. Singh,S.S., Hord,N.G. and Perdew,G.H. (1996) Characterization of the activated form of the aryl hydrocarbon receptor in the nucleus of HeLa cells in the absence of exogenous ligand. *Arch. Biochem. Biophys.*, **329**, 47–55.
50. Perdew,G.H. and Hollenback,C.E. (1995) Evidence for two functionally distinct forms of the human Ah receptor. *J. Biochem Toxicol.*, **10**, 95–102.

Received on January 30, 1998; revised on April 22, 1998; accepted on April 28, 1998

Expression of CYP1A1 and CYP1B1 Depends on Cell-Specific Factors in Human Breast Cancer Cell Lines: Role of Estrogen Receptor Status

William G.R. Angus[a], Michele C. Larsen[b], and Colin R. Jefcoate[a,b,III]
Department of Pharmacology[a] and Environmental Toxicology Center[b], University of Wisconsin, Madison, WI 53706

Running Title:
Estrogen Receptor Influence on CYP1A1 and CYP1B1

Key Words:
Mammary cancer, cytochromes P450, ICI 182,780

Footnotes:

[I]This work was presented at the Society of Toxicology Annual Meeting, Cincinnati, OH, 1997.

[II]This research was supported by NIEHS Grant 144EN46, DOD Breast Cancer Research Grant DAMD17-94-J-4054 (CRJ) and NRSA 1-F32-ES05733-01(WA).

[III]Author to whom correspondence should be addressed, at the University of Wisconsin, Department of Pharmacology, 3770 Medical Sciences Center, 1300 University Avenue, Madison, WI 53706.

[IV]Abbreviations: CYP, cytochrome P450; PAH, polycyclic aromatic hydrocarbon; TCDD, 2,3,7,8-tetrachlorodibenzo-p-dioxin; ER, estrogen receptor; DMBA, 7,12-dimethylbenz(a)anthracene; AhR, aryl hydrocarbon receptor; ARNT, aryl hydrocarbon receptor nuclear translocator protein; AHH, aryl hydrocarbon hydroxylase; ICI, ICI 182,780; ECL, enhanced chemiluminescence; $T47D^+$, T47D:A18 cells; $T47D^-$, T47D:C4:2W cells; MDA^+, S30 cells; MDA^-, MDA-MB-231 cells; HMEC, human mammary epithelial cells.

[V] Estrogen receptor α

Abstract

The impact of estrogen receptor (ER) was examined on expression and activity of CYP1B1 and CYP1A1 in two pairs of ER^+/ER^- human breast epithelial cell lines derived from single lineages, and representing earlier (T47D) or later (MDA-MB-231) stages of tumorigenesis. Acute loss of ER was evaluated using the antiestrogen ICI 182,780 (ICI). In all lines, CYP1B1 was expressed constitutively, and was induced by TCDD, whereas CYP1A1 was expressed only following induction. Expression of each CYP (with or without TCDD) was greater in T47D cells than MDA cells. The ER impacted expression of these genes in opposite directions. The ER^- phenotype was associated with less TCDD-induced CYP1A1 expression, but greater basal and induced CYP1B1 expression. A 48-hour treatment of ER^+ cells with ICI did not revert the P450 expression pattern to that of ER^- cells. Based on activities of recombinant enzyme and expression levels, differences in DMBA metabolism between the cell lines were consistent with differences in CYP1A1 and CYP1B1 expression. In T47D lines, basal microsomal DMBA metabolism was primarily due to CYP1B1, based on regioselective metabolite distribution and inhibition by anti-CYP1B1 antibodies (>80%). Metabolism in TCDD-induced microsomes was mostly due to CYP1A1, and was inhibited by anti-CYP1A1 antibody (>50%). TCDD-induced MDA^+ cells demonstrated CYP1A1 activity, whereas TCDD-induced MDA^- cells displayed CYP1B1 activity. Aryl hydrocarbon receptor (AhR) levels, but not ARNT levels were highly dependant on cell type; AhR was high and ER-independent in MDA, low and ER-linked in T47D. AhR levels were insensitive to ICI. ER does not directly modulate the expression of CYP1A1, CYP1B1 or AhR. Indeed, factors that have replaced ER in growth regulation during clonal selection predominate in this regulation. Characteristics unique to each cell line, including ER status, determine CYP1A1 and CYP1B1 expression.

Introduction

Cytochrome P4501B1 (CYP1B1)[IV] is found in steroid-responsive mesodermal tissues, such as the breast, uterus and prostate (1,2). Like its familial relative, cytochrome P4501A1 (CYP1A1), CYP1B1 can be induced by polycyclic aromatic hydrocarbons (PAHs) through a mechanism involving the aryl hydrocarbon receptor (AhR) (3,4). 2,3,7,8-Tetrachlorodibenzo-p-dioxin (TCDD), the archetypal agonist for AhR-mediated gene induction, induces the expression of CYP1B1 and CYP1A1 in human breast epithelial MCF7 cells, although CYP1B1 alone is expressed constitutively (3). CYP1B1 is also present basally in normal human breast epithelial cells, while CYP1A1 is below the lower limit of detectability or present at very low levels (<0.03 to 0.16 pmol/mg microsomal protein) (5).

The functional involvement of CYP1B1 in PAH metabolism has been demonstrated in MCF7 cells (3). Metabolism of the potent rodent mammary carcinogen 7,12-dimethylbenz (a) anthracene (DMBA; 6-9) by microsomes from uninduced MCF7 cells resulted in a different metabolite distribution from that observed for CYP1A1, which, further, is inhibited by anti-CYP1B1 antibodies, but not anti-CYP1A1 antibodies (3). By contrast, microsomes from TCDD-induced MCF7 cells display a CYP1A1 pattern of DMBA metabolites, which is completely inhibited by anti-CYP1A1 antibodies. DMBA, like other PAHs, requires metabolic activation through P450 cytochromes to a dihydrodiolepoxide to initiate carcinogenesis (10-12). Hence, activation of PAHs by CYP1A1 and CYP1B1 could be an important pathway for breast cancer initiation.

A natural substrate for CYP1B1 could mediate important physiological functions, since 1) the expression of CYP1B1 is under hormonal control in many steroidogenic tissues, 2) CYP1B1 displays selective expression in the mouse embryo cells [D. L. Alexander et al. Submitted, Cancer Research], and 3) there is a reported linkage between CYP1B1 mutations and congenital glaucoma in humans (13). Importantly, human CYP1B1 has been linked to the conversion of 17ß-estradiol to 4-hydroxyestradiol (14, 15) in addition to the bioactivation of many PAHs. Elevations of estradiol 4-hydroxylation activity in breast and uterine tumors, relative to surrounding tissues, indicates that there may be an elevation of functional CYP1B1 in these tumors, suggesting a possible role for CYP1B1 in tumorigenesis, in addition to mutagen activation (16).

Some commonly used human mammary cell lines, including MCF7 and T47D cells express the estrogen receptor (ER^+)[V] (17,18), while others, such as MDA-MB-231, lack the receptor completely (ER^-) (19). The ER has been implicated in the induced expression and activity of CYP1A1 through a deficiency in aryl hydrocarbon hydroxylase (AHH) activity (a measure of CYP1A1 activity) in ER-negative MDA-MB-231 cells, which was restored by transient transfection of ER into these cells (20). Another report has demonstrated a lack of TCDD-inducible AHH (CYP1A1) activity in several additional ER^- breast tumor cell lines,

regardless of their capacity to bind TCDD (21). It was concluded that ER status plays an important role in the TCDD-induction of CYP1A1 in human breast epithelial cells. In contrast to these findings, however, we have recently observed TCDD-induction of CYP1A1 and CYP1B1 mRNA in primary human breast epithelial cells, which are ER^- (5), suggesting that the ER is probably not directly connected to TCDD-induction in human breast cells. Further, recent studies suggest that unusually low levels of Ah receptor nuclear translocator protein (ARNT) in some cell lines may also contribute to low CYP1A1 induction (22). Hence, the AhR and ARNT status of the cell, in addition to the ER status, may influence CYP1A1 and CYP1B1 expression.

There are multiple factors linked to ER status and therefore we have paired cell lines which derive from the same background, but differ in ER status. An ER^- clone T47D:C4:2W ($T47D^-$) was derived from normally ER^+ T47D cells by long-term culture in estrogen-free medium (23). MDA-MB-231 (MDA^-) cells, which normally lack ER, have been paired with a clone resulting from stable transfection of the ER into these cells, S30 (MDA^+) (24). These cell lineages were widely different and therefore introduce differences in many additional regulatory factors. T47D cell lines depict a classic epithelial cell morphology, while the MDA cells are morphologically fibroblast-like, representative of a more advanced malignant and metastatic nature. The effect of a rapid loss of ER activity was examined through treatment of the ER^+ lines with the "pure" antiestrogen ICI 182,780 (ICI). ICI inhibits ER dimer formation and prevents shuttling of the ER into the nucleus, thereby eliminating interaction with DNA and decreases levels of the protein (25, 26). These combinations of cells and treatments have been used to evaluate whether ER status or other aspects of the cell phenotype are important in determining CYP expression. Since changes in CYP expression may be mediated by differences in levels of AhR and ARNT proteins, we have also examined the expression of these proteins under the same conditions.

Materials and Methods

MDA-MD-231 cells (19) were purchased from ATCC. The cell lines T47D:A18, T47D:C4:2W, and S30 were generous gifts from Drs. V. Craig Jordan and John Pink (Northwestern University, University of Wisconsin Comprehensive Cancer Center)(23, 24). ICI 182,780 was obtained from Dr. Alan Wakling (Zenica Pharmaceuticals, Manchester, England). The human CYP1B1 antibody used in these studies was a generous gift from Dr. Craig Marcus (University of New Mexico) and Dr. William Greenlee (University of Massachusetts); the Ah receptor monoclonal antibody was obtained from Dr. Gary Perdew (Penn State University). Polyclonal antibody to ARNT was a gift from Dr. Rick Pollenz. Antibody to estrogen receptor was purchased from Santa Cruz Biologicals (HC-20; Santa Cruz, CA). The antibodies for CYP1A1, and inhibitory antibodies for CYP1A1 and CYP1B1 were generated in this laboratory (3). TCDD was purchased from Accustandard, Inc. (New Haven, CT). [α-^{32}P] dCTP was

purchased from NEN DuPont (Boston, MA). Reagents purchased from GIBCO (Grand Island, NY) included Dulbecco's Modified Eagle Medium/Ham's F12 (DMEM/F12), RPMI 1640, and agarose. Cell culture was carried out using Falcon flasks and Corning plates. Fetal bovine serum (FBS) was obtained from Gemini (Calabasas, CA) or HyClone (Logan, UT) and dextran charcoal stripped FBS was purchased from HyClone (Logan, UT). Reagents purchased from the Sigma Chemical Co. (St. Louis, MO) included glucose-6-phosphate, 7,12-dimethylbenz(a)anthracene, nicotinamide dinucleotide phosphate (NADP), HEPES, insulin, ammonium persulfate, TEMED, dimethylsulfoxide (DMSO), phenylmethylsulfonyl fluoride (PMSF), leupeptin, aprotinin, soybean trypsin inhibitor, aurin tricarboxylic acid (ATA), salmon sperm DNA, diethyl pyrocarbonate (DEPC), penicillin/streptomycin solution and phenol red-free DMEM/F12. Sodium dodecyl sulfate (SDS) was purchased from BioRad, Inc. (Hercules, CA). Proteinase K was obtained from Fisher Chemical (LaJolla, CA). Formamide was purchased from Ambion (Austin, TX). Oligo dT was obtained from Calbiochem (LaJolla, CA). The PRIME IT II kit was purchased from Stratagene (LaJolla, CA). Nylon (Hybond N+) and nitrocellulose membranes (Hybond ECL), Hyperfilm ECL film, and ECL reagents were obtained from Amersham (Arlington Heights, IL). BCA protein determination kit was purchased from Pierce (Rockford, IL). Recombinant human CYP1A1 and CYP1B1 protein were obtained from Gentest Corp. (Worburg, MA) Other reagents used for these studies were of the highest grade possible.

Cell Culture

All cells were maintained in monolayer culture in 75 cm^2 or 175 cm^2 flasks in a humidified 5% CO_2 atmosphere. MDA^- cells were grown in DMEM/F12 with 10 mM HEPES, 5% FBS, and penicillin/streptomycin. The MDA^+ cells, which are growth inhibited by estrogens (24), were grown in phenol red-free DMEM/F12 containing 15 mM HEPES and 5% dextran charcoal stripped FBS. $T47D^+$ and $T47D^-$ cells were cultured in phenol red-free RPMI 1640 with 10% FBS, 6 ng/ml insulin and penicillin /streptomycin. All cells were passaged using 0.5% trypsin at 80-90% confluence.

Hybridization analysis of mRNA

Cells cultured in 150 mm plates were treated or not for 24 hours with 10^{-7} M ICI 182,780, then for an additional 24 hours with or without 10^{-8} M TCDD in the continued presence or absence of ICI. Controls were treated for 24 hours with DMSO (0.1%). Cells were harvested and poly A^+ RNA isolated according to the technique of Badley et al., 1988 (27). Briefly, cells were washed with PBS (0.01 M phosphate buffer in 2.7 mM KCl and 137 mM NaCl, pH 7.4) containing 20 µM ATA and lysed in a buffer consisting of 0.2 M NaCl, 0.2 M Tris-HCl, pH 7.5, 0.15 mM $MgCl_2$ 2% SDS, 200 µg/ml Proteinase K, and 20 µM ATA. Lysates were sheared with a 23 gauge needle and incubated for 2 hours at 45 C°, then agitated with oligo dT, eluted in DEPC-treated water and precipitated with ethanol. The RNA was resuspended in sterile DEPC-treated

H_2O and quantitated by reading absorbance at 260 nm.

Poly A^+ RNA was electrophoresed through a formaldehyde-containing 1% agarose gel. Capillary action was used to transfer the RNA to nylon membrane, and RNA was crosslinked to the membrane by UV. Membranes were prehybridized in a buffer of 6X SSC, 5X Denhardt's reagent, 0.1% SDS, 10 µg/ml salmon sperm DNA, and 50% formamide at 42 C° for at least 2 hours. Membranes were then incubated with probes for ß-actin, human CYP1A1, and human CYP1B1 as described below. Probes were randomly labeled using [α-^{32}P] dCTP (50 µCi) following the manufacturer's instructions for the Prime-It II kit. Specific activity was 10^6 cpm or greater per ml of probe. Nonspecific hybridization was removed by sequential washing with 2X SSPE + 0.5% SDS, 1X SSPE + 0.5% SDS, 0.5X SSPE + 0.5% SDS, and 0.25X SSPE + 0.25% SDS at hybridization temperature for 15 min. Signals were visualized by autoradiography and quantitated by densitometry on a laser scanner.

A 1.4 Kb cDNA probe from the 3' end of the human CYP1A1 was obtained from Dr. Lynne Allen-Hoffman (University of Wisconsin). The CYP1B1 cDNA probe was a 3.1 Kb fragment encoding the open reading frame of human CYP1B1, and was obtained from Dr. William Greenlee (University of Massachusetts).

Microsomal metabolism of DMBA

Microsomes were generated by differential centrifugation as previously described (28) from $T47D^+$, $T47D^-$, MDA^-, and MDA^+ cells treated with or without 10^{-7} M ICI for 24 hours, then with or without TCDD for an additional 24 hours in the presence/absence of ICI. Microsomal metabolism was performed using 0.2 or 1 mg of TCDD-induced and basal microsomal protein, respectively, as described by Christou, et al., 1991 (3). Incubations were 15 min at 37 C°, and 1.5 µM DMBA was used in a 1 ml volume reaction. Inhibition studies were carried out using chicken anti-CYP1B1 (IgY) at 5 mg/mg microsomal protein or rabbit anti-CYP1A1 (IgG) antibodies (3) at 10 mg/mg microsomal protein. The reaction mixtures containing the antibodies and preimmune serum were incubated at room temperature for 40 min prior to the 15 min incubations with DMBA at 37 C°.

Cell lysates and Western Immunoblots

Confluent cells in 60 mm plates, treated as previously described for ICI and TCDD, were harvested by scraping in PBS and pelleted. A lysis buffer consisting of 20 mM Tris-HCl, pH 7.4, 1% Triton X-100, 0.1% SDS, 0.5% sodium deoxycholate, 1 mM EDTA, 1 mM sodium orthovanadate, 5 µg/ml aprotinin, 5 µg/ml leupeptin, 5 µg/ml soy bean trypsin inhibitor, and 1 mM PMSF was added to each pellet. Following 10 min on ice, samples were sheared using a pipette tip and centrifuged at 10,000 g for 30 min at 4 C°. Supernatants were transferred to new tubes, an aliquot removed for protein determination, and frozen at -80 C°.

Cellular proteins were separated on SDS-PAGE containing 7.5% acrylamide as per Laemmli

(1970) (29), and transferred to nitrocellulose membrane. Membranes were probed for CYP1A1, CYP1B1, AhR, ER, and ARNT. Reactive proteins were visualized using the ECL procedure according to manufacturer's instructions.

Protein levels in cellular extracts and microsomal preparations were determined using the BCA method as per manufacturer's instructions using bovine serum albumin as a standard.

Results

These studies were undertaken to examine the direct involvement of the ER in the expression and activity of CYP1A1 and CYP1B1 in human mammary epithelial cells. The expression of CYP1A1 and CYP1B1 mRNA and protein and the associated metabolism of DMBA has been examined in two pair of human mammary cell lines, each pair providing a comparison between ER^+ and ER^- status ($T47D^+$, $T47D^-$, MDA^+, MDA^-). Additionally the antiestrogen ICI 182,780 was used to determine if CYP expression patterns in ER^+ cells could be shifted to those observed in ER^- cells. Cells were examined under basal conditions, and following a 24 hour treatment with 10^{-8} M TCDD.

We have measured expression in confluent cells with and without a 24 hour exposure to TCDD (10^{-8} M). Quantitation was made from three separate culture experiments for each line. The levels of CYP mRNA and protein were measured by, respectively, Northern hybridization (Figure 1) and Western immunoblots (Figure 2), each with fully selective probes. We found that the changes in ER status in both types of breast cell resulted in systematic effects on CYP1B1 and CYP1A1 expression, but in opposite directions. Similar results were obtained for both mRNA and protein. The basal expression of CYP1B1 mRNA, which was very apparent in each line, was 4-5 times lower in the ER^+ line than the ER^- counterpart ($T47D\ ER^+/ER^- = 0.28 \pm 0.07$; $MDA\ ER^+/ER^- = 0.2 \pm 0.1$). Similar differences were seen in basal CYP1B1 protein expression, although the levels in MDA cells were much lower and difficult to quantitate (Figure 2). Following a 24 hour TCDD treatment, CYP1B1 expression increased substantially in each cell line, but by a larger factor in ER^+ cells. In T47D cells, the larger stimulus in ER^+ cells as measured by either protein or by mRNA (mRNA ER^+ 21 ± 5 versus ER^- 4 ± 1.5; protein ER^+ 23 ± 15 versus ER^- 3 ± 0.2) completely removed the sensitivity to ER status for both mRNA and protein. In MDA cells, the deviation in the induction factors in ER^+ cells was less marked (mRNA 10 ± 4 versus 6 ± 2) leaving levels of CYP1B1 mRNA and protein about 2-fold higher in ER^- cells. CYP1A1 was only observable after induction by TCDD, but here the opposite effect of ER status was seen. TCDD-induced levels of both CYP1A1 mRNA and protein were each 2-3 fold greater in ER^+ cells. It can also be seen (Figure 1, 2) that by either measurement expression of both of these CYPs is much greater for the equivalent ER status in T47D than in MDA cells (threefold for mRNA, fourfold for protein). This indicates a strong influence of lineage-dependant, ER-independent factors that act

similarly on transcription of either basal or induced CYP1B1 and induced CYP1A1. The close parallels between mRNA and protein indicate that each of these regulatory differences largely arises at the level of transcription.

Functional Activity

The functional activity of CYP1A1 and CYP1B1 from cellular microsomal protein has been calculated relative to recombinant CYP1A1 and CYP1B1 protein standards (M. L. Larsen, in preparation) as shown in Table I. Dihydrodiol ratios (5,6/8,9 or 10,11/8,9) was used as reference parameters to determine if the metabolism pattern was CYP1A1-like or CYP1B1-like. Based on metabolism by the recombinant human cytochromes, a 5,6/8,9 ratio of 0.6 - 0.7 indicated a pure CYP1B1 activity, while a ratio of 0.1 - 0.2 was typical for CYP1A1. A higher 10,11/8,9 ratio also typified CYP1B1 rather than CYP1A1 activity (1.0 versus 0.1). The DMBA metabolizing activity of CYP1A1 was demonstrated to be about six times that for an equivalent amount of CYP1B1 protein (5).

Consistent with the measurement of cytochrome P450 protein expression, the T47D lines had a much greater DMBA-metabolizing activity than the equivalent MDA cells (6-13 fold). Basal T47D cells, irrespective of ER status, and TCDD-induced MDA^- cells provided indistinguishable ratios typical of CYP1B1 metabolism (5,6/8,9 ratio = 0.5; 10,11/8,9 ratio = 0.2). Basal MDA^+ products were essentially background, being similar in pattern of distribution and picomolar amount per mg protein to what is observed in cell-free blanks (M. L. Larsen, unpublished results). Meanwhile, the elevated activity observed in MDA^- cells was consistent with CYP1B1 participation. Under basal conditions, the $T47D^-$ cells had 50% greater activity than $T47D^+$ cells or TCDD-induced MDA^- cells, which, in turn, were 4-8 fold more active than basal MDA^- cells. These findings were consistent with levels of protein expression.

TCDD treatment shifted the metabolite pattern in T47D cells and MDA^+ cells, in contrast to MDA^- cells, to a CYP1A1 distribution (5,6/8,9 = 0.25; 10,11/8,9 = 0.1). The TCDD-induced metabolic activity of the $T47D^+$ cells was equivalent to that of $T47D^-$ cells, while TCDD-induced MDA^+ cells exhibited 10 times less activity. The differences in TCDD-induced activity between T47D cells and MDA cells parallels the relative expression of the much more active CYP1A1.

Inhibition Studies

Inhibitory antibodies were used to determine the contribution of CYP1A1 and CYP1B1 to the DMBA-metabolism profile in $T47D^+$ cells (Table II). Under basal conditions, the anti-CYP1B1 antibody inhibited overall metabolism by 84%, while the anti-CYP1A1 antibody had no effect. In contrast, the anti-CYP1A1 antibody inhibited greater than 50% of the TCDD-induced DMBA metabolism (Table II). The distribution of metabolites removed from the reaction by the anti-CYP1B1 treatment was evaluated by subtraction of anti-CYP1B1 metabolite values from preimmune metabolite values. This indicated that ratios of dihydrodiols were very similar to those

found for recombinant hCYP1B1 (5,6-/8,9 = 0.9; 10,11/8,9 = 0.4). A similar subtraction was used to demonstrate the activity of CYP1A1 (5,6/8,9 = 0.15; 10,11/8,9 = 0.07). The residual activity from these TCDD-induced microsomes after removal of the CYP1A1 contribution with this antibody treatment was consistent with induced CYP1B1 activity (5,6/8,9 = 0.4; 10,11/8,9 = 0.14). The remaining metabolites that are unaffected by either antibody indicate a residual basal metabolic activity that may be due to other P450s present in breast epithelial cells (30) or to a peroxidative mechanism. This activity seems to contribute to the very low basal activity in MDA^+ cells.

Specific Enzyme Content and Specific Activity

To be able to compare the relative rates of DMBA-metabolizing activity in cell lines to primary cells (5), a turnover value (P450/hr) was calculated for CYP1A1 and CYP1B1 in each line based on the specific enzyme content, the total DMBA metabolizing activity, and the fractions of total activity inhibited by specific antibodies under both basal and induced conditions (Table III). The products of distribution of residual activity after 50 percent inhibition of TCDD-induced microsomes with anti-CYP1A1 antibodies indicates approximately equal contributions of residual CYP1A1 and CYP1B1 activity. This indicates a CYP1A1 turnover of 24 pmoles/mg/hr (363 pmoles/mg/hr; 15 pmole CYP1A1) and a CYP1B1 activity of 3 pmoles/mg/hr (121 pmoles/mg/hr; 43 pmols CYP1B1). For uninduced microsomes the CYP1B1 turnover was higher at about 18 pmoles/mg/hr (35 pmoles/mg/hr; 2 pmoles CYP1B1). CYP1B1 activities for uninduced microsomes for other cells were somewhat lower (4-6 pmoles/mg/hr). Taken together, these CYP1B1 activities are close to the basal activity reported for primary breast epithelial cells (6.0 pmoles/mg/hr) (5). TCDD-induced $T47D^-$ contained about as much CYP1B1 as CYP1A1, thus, the product distribution was indistinguishable from equivalent $T47D^+$ microsomes. Based on the P450 content, this same product distribution is obtained with specific activities of about 40 pmoles/mg/hr for CYP1A1 and 4 pmoles/mg/hr for CYP1B1. Taken together, this indicates turnover number for CYP1A1 that are 8-10 times larger than for CYP1B1, but reasonably consistent with those in primary human breast epithelial cells. Specific activities following TCDD-induction in MDA^+ and MDA^- cells were 2-4 times lower than in T47D cells.

Effects of Antiestrogen and Expression of Estrogen Receptor

Levels of ER protein in the 4 lines were verified by immunoblotting (Figure 3). As expected, MDA^- and $T47D^-$ cells expressed no ER protein. Treatment with ICI 182,780 for 48 hours decreased the amount of ER protein in both the $T47D^+$ and MDA^+ cells by 70%. This treatment of the ER^+ cell lines with 10^{-7} M ICI had little effect on CYP1A1 message or protein (Table IV). Treatment with ICI also had minimal effects on CYP1B1 mRNA and protein. Thus, this 48-hour treatment with ICI failed to reproduce the differences in CYP expression observed between ER^+ and ER^- lines.

Ah Receptor and ARNT Expression

AhR, which mediates the induction of CYP1A1 and CYP1B1 by TCDD, was present in all 4 lines (Figure 4). The AhR levels in the MDA lines was about 7-fold greater than in the T47D lines. The presence or absence of the ER did not affect the level of AhR, even though cell lineage was a factor in AhR expression. The 24-hour TCDD treatment decreased the amount of AhR in each cell line, which was consistent with previous observations in mouse hepatoma cell lines that TCDD induces a translocation of the receptor to the nucleus followed by downregulation (31).

Levels of ARNT protein, which forms a heterodimer with AhR, and is necessary for binding to xenobiotic response elements, were similar in both T47D and MDA cell lines. No apparent effect of the ER on ARNT protein expression was observed. Further, TCDD treatment had no effect on levels of ARNT protein in any of these cell lines (Figure 4).

Discussion

These studies have characterized the expression of CYP1A1 and CYP1B1 in two pairs of ER^+ and ER^- cell lines which were derived from T47D and MDA-MB-231, and which represent earlier and later stage tumor cells, respectively. As in other cell lines (3), we show that CYP1B1 is expressed in the absence of an external stimulus, whereas CYP1A1 is only expressed after treatment with the AhR agonist, TCDD. CYP1B1 is also stimulated by TCDD, but by a smaller factor than CYP1A1. The current studies indicate that stable loss of the ER is associated with differential effects on the expression and activity of CYP1A1 and CYP1B1. CYP1A1 expression (TCDD-induced) was greater, and CYP1B1 expression (basal) was lower, in the ER^+ clones of both cell types compared to the ER^- clones. This pattern was observed both at the mRNA and protein levels, and was reflected in the DMBA metabolic activity profiles. TCDD induction of CYP1B1 largely removed the ER-linked constraints on CYP1B1 expression. These ER-associated effects on the expression and activity were superimposed on the generally lower expression of CYP1A1 and CYP1B1 in the MDA lines as compared to the T47D lines. This difference was observed with both the basal and TCDD-induced expression of these genes, and suggests a strong effect of ER-independent factors which may emerge as cells progress to later stage tumors.

The contributions of CYP1A1 and CYP1B1 to the metabolism of the prototypical PAH, DMBA, was resolved by determining differences in regioselectivity of DMBA metabolites and selective antibody inhibition. Consistent with the expression profiles, CYP1B1-like metabolic activity predominated under basal conditions, as previously reported for MCF7 cells (3) and as reported elsewhere for normal human mammary epithelial cells (5). The strong suppression of CYP1A1 expression in MDA^- cells resulted in TCDD-induced activity which was almost entirely attributable to CYP1B1. In the other cell lines most of the TCDD-induced activity was due to CYP1A1, even though CYP1B1 protein levels were comparable to those of CYP1A1. This

incongruity can be rationalized based on the 6-fold greater metabolic activity of CYP1A1 (5). Additionally, a recent report describes the relative contributions of TCDD-induced CYP1A1 and CYP1B1 to estradiol metabolism in a number of human mammary cell lines, including T47D and MDA-MB-231 (32). Our data on DMBA metabolism is consistent with this report that 83% of estrogen metabolism in TCDD-induced T47D cells is mediated by CYP1A1, and 17% by CYP1B1. For MDA-MB-231 cells, the numbers are 16% for CYP1A1 and 84% for CYP1B1. Contributions of CYP1A1 and CYP1B1 to basal metabolism were not reported (32).

An acute loss of the ER from ER^+ clones of both lineages by 48 hours of treatment with 10^{-7} M ICI (25, 26) did not convert the expression patterns of CYP1A1 and CYP1B1 over to the different expression patterns observed in ER^- clones. Thus, while the presence or absence of the ER may influence the expression of CYP1A1 and CYP1B1, the regulatory pattern is not a direct result of transcriptional regulation of these genes by ER. These pairs of cell lines have been derived by clonal growth selection procedures. Through this process, ER^- cells have acquired ER-independent mechanisms to sustain growth that probably include the generation of ER-independent autocrine stimulatory factors and additional ER-independent signaling processes. The insensitivity to ICI indicates that these differences are due to this type of change in regulation. Previous work has shown that transient transfection of ER into MDA- cells enhances CYP1A1 promoter activity in and estrogen-dependent manner (20). Apparently integration of the ER produces a similar result , but without the incorporation of the ER into the eventual signaling process.

It might be expected that levels of the AhR might affect PAH induction of CYP1A1 (33) and CYP1B1 (3, 4). The very low AhR levels in $T47D^-$ cells were not linked to lower AhR activity, as evidenced by CYP1B1 induction in these cells. The lower AhR content in $T47D^-$ cells compared to $T47D^+$ appears not to be related to ER status, since in the MDA lines, there is no significant difference in AhR expression between the ER^+ and ER^- clones. Interestingly, the approximately 7-fold differences in AhR protein expression between T47D lines and MDA lines were inversely related to mRNA and protein expression of CYP1A1 or CYP1B1. Thus, a cell's lineage appears to have a greater impact on AhR expression than its ER status. The excess AhR expression in the MDA lines, therefore, may be involved in alternate pathways and may be heterodimerizing with other PAS domain containing proteins (34). Amounts of ARNT protein were not different between T47D and MDA cells, regardless of ER status.

Aside from ER status and AhR/ARNT expression, the backgrounds of T47D and MDA cells differ significantly (18, 19). These additional factors may be important for expression of CYP1A1 and CYP1B1. The ER^+, hormone-dependent T47D line displaying epithelial cell morphology was used as a model of an early stage tumor. These cells express keratins and casein proteins (18,35,36) similarly to normal mammary luminal epithelial cells. We used the ER^-, hormone-independent, fibroblast-shaped MDA^- cells as a model of an aggressive, later stage tumor. These

cells express vimentin and CD44 (36) -- markers for fibroblasts, and suggestive of dedifferentiation. The estrogen-independent growth of MDA^- cells suggests that another mitogenic ligand/receptor pathway has taken over the mitogenic functions previously filled by estrogen and the ER. The heregulin/ErbB receptor pathway could possibly fulfill this role, since MDA^- cells produce heregulin and contain ErbB receptors (37). Such mitogenic reprogramming may be just one of many systematic alterations occurring in cells stably lacking ER. For instance, $T47D^-$ cells, which were derived from $T47D^+$ by long term growth in estrogen-free medium over a period of greater than 8 months, have had the time to reprogram their mitogenic pathways to respond to ER-independent growth stimuli in a manner similar to the MDA^- cells. MDA^+ cells, which are stably ER transfected, are growth inhibited by estrogens. This phenomenon has also been observed in other ER^- lines stably transfected with ER (38, 39). Thus it appears that following the reintroduction of the ER, the cell's mitogenic machinery remains under the influence of the reprogrammed, compensatory mitogenic pathway(s). The reintroduced ER is not only mitogenically ineffective, but even growth inhibitory.

One of the implications that emerge from these studies is that ER^- mammary epithelial cell lines (like most normal primary mammary epithelial cells; (5)) demonstrate induction of AhR-linked genes in response to AhR agonists. Many PAHs can stimulate AhR-mediated metabolism (CYPs) which can lead to the formation of additional metabolites which can form adducts with DNA and initiate tumor formation. Under basal conditions, these data demonstrate that CYP1B1 would be the cytochrome P450 responsible for the initial metabolism of such xenobiotics. A further implication from these studies is that levels of cytochromes P450 decrease as cells tumorigenically progress (e.g. from T47D to MDA-MB-231). The levels and activities of CYP1A1 and CYP1B1 in T47D and MDA cells are representative of the range of expression seen in primary human mammary epithelial cells (HMEC; 5). However, the diversity in HMEC may reflect differing properties of luminal and basal cells . The latter in some respect show expression patterns similar to MDA^- cells.

From the current studies, we conclude that, while ER status plays an influential role in the expression of CYP1A1 and CYP1B1, the ER itself does not directly modulate this expression, as demonstrated by treatment of ER^+ cells with ICI. Other aspects of cellular phenotype appear to play a more prominent role in CYP expression. We are currently determining whether this CYP expression pattern holds across a spectrum of human mammary cell lines of differing ER status and state of progression. These studies are currently underway in this laboratory.

(1) Savas, U., Bhattacharyya, K.K., Christou, M., Alexander, D.L., and Jefcoate, C.R. (1994) Mouse cytochrome P-450ER, representative of a new 1B subfamily of cytochrome P450s. Cloning, sequence determination, and tissue expression. J. Biol. Chem., **269**, 14905-14911.

(2) Tang, Y.M., Wo, Y-Y.P., Stewart, J., Hawkins, A.L., Griffin, C.A., Sutter, T.R., and Greenlee, W.F. (1996) Isolation and characterization of the human cytochrome P450 CYP1B1 gene. J. Biol. Chem., **271**, 28324-28330.

(3) Christou, M., Savas, U., Spink, D., Gierthy, J.F., and Jefcoate, C.R. (1994) Co-expression of human CYP1A1 and a human analog of cytochrome P450-EF in response to 2,3,7,8-tetrachloro-dibenzo-p-dioxin in the human mammary carcinoma-derived MCF-7 cells. Carcinogenesis **15**, 725-732.

(4) Sutter, T.R., Tang, M.Y., Hayes, C.L., Wo, Y-Y.P., Jabs, E.W., Li, X., Yin, H., Cody, C.W. and Greenlee, W.F. (1994) Complete cDNA sequence of a human dioxin-inducible cytochrome P450 that maps to chromosome 2. J. Biol. Chem., **269**, 13092-13099.

(5) Larsen, M.C., Angus, W.G.R., Brake, P.B., Eltom, S.E., Sukow, K.A., and Jefcoate, C.R. (1998) Characterization of CYP1B1 and CYP1A1 expression in human mammary epithelial cells: Role of the aryl hydrocarbon receptor in polycyclic aromatic hydrocarbon metabolism. Cancer Res., **58**, 2366-2374.

(6) Huggins, C., Grand, L.C., and Brillantes, F.K. (1961) Mammary cancer induced by a single feeding of polynuclear hydrocarbons, and its suppression. Nature, **189**, 204-207.

(7) Murad, T.M. and Von Haam, E. (1972) Studies of mammary carcinoma induced by 7,12-dimethylbenz-(a)-anthracene administration. Cancer Res., **32**, 1404-1415.

(8) Sinha, D. and Dao, T.L. (1975) Site of origin of mammary tumors induced by 7,12-dimethylbenz(a)anthracene in the rat. J. Natl. Cancer Inst., **54**, 1007-1009.

(9) Terada, S., Uchide, K., Suzuki, N., Akasofu, K., and Nishida, E. (1995) Induction of ductal carcinomas by intraductal administration of 7,12-dimethylbenz(a)anthracene in Wistar rats. Breast Cancer Res. Treatment, **34**, 35-43.

(10) Slaga, T.J., Gleason G.L., DiGiovanni, J., Sukumaran, K.B., and Harvey, R.G. (1979)

Potent tumor-initiating activity of the 3,4-dihydrodiol of 7,12-dimethylbenz (a) anthracene in mouse skin. Cancer Res., **39**, 1721-1723.

(11) Sims, P. and Grover, P.L. (1981) Involvement of dihydrodiols and diol epoxides in the metabolic activation of polycyclic hydrocarbons other than benzo (a) pyrene. In: Gelboin HV Ts'o POP (eds) Polycyclic Hydrocarbons and Cancer, Academic Press, New York, Vol. 3, pp. 117-181.

(12) Dipple, A., Moschel, R.C., and Bigger, C.A.H. (1984) Polynuclear aromatic carcinogens. In: Searle CE (ed) Chemical Carcinogens, 2nd Edn., American Chemical Society, Washington, Vol. 1, pp. 245-314.

(13) Stoilov, I., Akarsu, A.N., and Sarfarazi, M. (1997) Identification of three different truncating mutations in cytochrome P4501B1 (CYP1B1) as the principle cause of primary congenital glaucoma (Buphthalmos) in families linked to the GLC3A locus on chromosome 2p21. Human Molec. Genet., **6**, 641-647.

(14) Hayes, C.L., Spink, D.C., Spink, B.C., Cao, J.Q., Walker, N.J., and Sutter, T.R. (1996) 17ß-estradiol hydroxylation catalyzed by human cytochrome P450 1B1. Proc. Natl. Acad. Sci., U.S.A., **93**, 9776-9781.

(15) Spink, D.C., Hayes, C.L., Young, N.R., Christou, M., Sutter, T.R., Jefcoate, C.R., and Gierthy, J.F. (1994) The effects of 2,3,7,8-tetrachlorodibenzo-p-dioxin on estrogen metabolism in MCF7 breast cancer cells: Evidence for induction of a novel 17ß-estradiol 4-hydroxylase. J. Steroid Biochem. Molec. Biol., **51**, 251-258.

(16) Liehr, J.G., Ricci, M.J., Jefcoate, C.R., Hannigas, E.V., Hokanson, J.A., and Zhu, B.T. (1995) 4-Hydroxylation of estradiol by human uterine myometrium and myoma microsomes: Implications for the mechanism of uterine tumorigenesis. Proc. Natl. Acad. Sci., U.S.A., **92,** 9220-9224.

(17) Soule, H.D., Vazquez, J., Long, A., Albert, S., and Brennan, M. (1973) A human cell line from a pleural effusion derived from a breast carcinoma. J. Natl. Cancer Inst., **51,** 1409-1416.

(18) Keydar, I., Chen, L., Karby, S., Weiss, F.R., Delarea, J., Radu, M., Chaitcik, S., and Brenner, H.J. (1979) Establishment and characterization of a cell line of human breast carcinoma

origin. Europ. J. Cancer, **15,** 659-670.

(19) Cailleau, R., Young, R., Olive, M., and Reeves, Jr., W.J. (1974) Breast tumor cell lines from pleural effusions. J. Natl. Cancer Inst., **53**,661-674.

(20) Thompson, J.S., Wang, X., Hines, R.N., and Safe, S. (1994) Restoration of aryl hydrocarbon (Ah) responsiveness by transient transfection of the estrogen receptor. Carcinogenesis, **15,** 933-937.

(21) Vickers, P.J., Dufresne, M.J. and Cowan, K.H. (1989) Relation between cytochrome P4501A1 expression and estrogen receptor content in human breast cancer cells. Mol. Endocrinol., **3**, 157-164.

(22) Wilson, C., Hoivik, D., Holtzapple, C., Stanker, L., and Safe, S. (1997) Variable aryl hydrocarbon-responsiveness in MDA-MB-231 human breast cancer cells is associated with ARNT expression. *Fund. Appl. Toxicol.*, **36**, 130.

(23) Pink, J.J., Bilimoria, M.M., Assikis, J., and Jordan, V.C. (1996) Irreversible loss of the oestrogen receptor in T47D breast cancer cell following prolonged oestrogen deprivation. Br. J. Cancer, **74**, 1227-1236.

(24) Jiang, S-Y. and Jordan, V.C. (1992) Growth regulation of estrogen receptor-negative breast cancer cells transfected with complementary DNAs for estrogen receptor. J. Natl. Cancer Inst., **84,** 580-591.

(25) Fawell, S.E., White, R., Hoare, S., Sydenham, M., Page, M., and Parker, M.G. (1990) Inhibition of estrogen receptor-DNA binding by the "pure" antiestrogen ICI 164,384 appears to be mediated by impaired receptor dimerization. Proc. Natl. Acad. Sci., USA, **87,** 6883-6887.

(26) Dauvois, S., White, R., and Parker, M.G. (1993) The antiestrogen ICI 182,780 disrupts estrogen receptor nucleocytoplasmic shuttling. J. Cell Sci., **106,** 1377-1388.

(27) Badley, J.E., Bishop, G.A., St. John, T., and Frelinger, J.A. (1988) A simple, rapid method for the purification of poly A+ RNA. Biotechniques, **6**, 114-116.

(28) Pottenger, L.H., Christou, M. and Jefcoate, C.R. (1991) Purification and immunological

characterization of a novel cytochrome P450 from C3H/10T1/2 cells. Arch. Biochem. Biophys. **286,** 488-497.

(29) Laemmli, U.K. (1970) Cleavage of structural proteins during the assembly of the head of bacteriophage T4. Nature, **227,** 680-685.

(30) Huang, Z., Fasco, M.J., Figgi, H.L., Keyomarsi, K., and Kaminski, L.S. (1996) Expression of cytochrome P450 in human breast tissues and tumors. Drug Metab. Disposit., **24,** 899.

(31) Pollenz, R.S. (1996) The aryl-hydrocarbon receptor, but not the aryl-hydrocarbon receptor nuclear transporter protein, is rapidly depleted in hepatic and nonhepatic culture cells exposed to 2,3,7,8-tetrachlorodibenzo-p-dioxin. Molec. Pharmacol., **49**, 391-398.

(32) Spink, D.C., Spink, B.C., Cao, J.Q., DePasquale, J.A., Pentecost, B.T., Fasco, M.J., Li, Y., and Sutter, T.R. (1998) Differential expression of CYP1A1 and CYP1B1 in human breast epithelial cells and breast tumor cells. Carcinogenesis, **19**, 291-298.

(33) Hines, R.N., Mathis, J.M., and Jacob, C.S. (1988) Identification of multiple regulatory elements on the human cytochrome P4501A1 gene. Carcinogenesis, **9**, 1599-1605.

(34) Hogenesch, J.B., Chan, W.K., Jackiw, V.H., Brown, R.C., Gu, Y-Z., Pray-Grant, M., Perdew, G.H., and Bradfield, C.A. (1997) Characterization of a subset of the basic-helix-loop-helix-PAS superfamily that interacts with components of the dioxin signaling pathway. J. Biol. Chem., **272**, 8581-8593.

(35) Chalbos, D., Vignon, F., Keydar, I., and Rochefort, H. (1982) Estrogens stimulate cell proliferation and induce secretory proteins in a human breast cancer cell line (T47D). J. Clin. Endocronol. Metab., **55,** 276-283.

(36) Culty, M., Shizari, M., Thompson, E.W., and Underhill, C.B. (1994) Binding and degradation of hyluronan by human breast cancer cell lines expression different forms of CD44: Correlation with invasive potential. J. Cell. Physiol., **160**, 275-286.

(37) Holmes, W.E., Sliwkowski, M.X., Akita, R.W., Henzel, W.J., Lee, J., Park, J.W., Yansura, D., Abadi, N., Raab, H., Lewis, G.D., Shepard, H.M., Juang, W-J., Wood, W.I., Goeddel, D.V., and Vandlen, R.L. (1992) Identification of Heregulin, a specific activator of

p185erbB2. Science, **256**, 1205-1210.

(38) Levenson, A.S. and Jordan, V.C. (1994) Transfection of human estrogen receptor (ER) cDNA into ER-negative mammalian cell lines. J. Steroid Biochem. Molec. Biol., **51,** 229-239.

(39) Pilat, M.J., Christman, J.K., and Brooks, S.C. (1996) Characterization of the estrogen receptor transfected MCF10A breast cell line 139B6. Breast Cancer Res. Treat., **37,** 253-266.

Acknowledgments

We thank Dr. V. Craig Jordan and Dr. John Pink for kindly providing the two T47D cell lines and the S30 cell line used in these studies. We also thank Paul Hanlon for assistance in the isolation of mRNA, and Leonardo Ganem for assistance in preparation of this manuscript.

Table I. Generation of DMBA Metabolites from Microsomal Proteins

Sample	Dihydrodiols 5,6-	8,9-	10,11-	3,4-	Total [a]	Ratio 5,6/8,9	10,11/8,9	3,4/8,9
T47D+								
DMSO	6.7	9.0	2.6	2.3	41.6	0.74	0.29	0.26
TCDD	87.0	344.0	30.0	31.0	512.4	0.25	0.09	0.09
T47D-								
DMSO	9.6	16.0	3.7	3.6	65.9	0.60	0.23	0.23
TCDD	89.0	322.0	34.0	31.0	499.9	0.28	0.11	0.09
MDA+								
DMSO	BKG	BKG	BKG	BKG	BKG	n.d.	n.d.	n.d.
TCDD	4.1	15.0	2.4	2.1	34.9	0.27	0.16	0.14
MDA-								
DMSO	0.6	2.0	0.2	0.5	6.8	0.30	0.10	0.25
TCDD	6.3	10.8	3.1	2.6	43.5	0.58	0.29	0.24
Recombinant Proteins								
CYP1A1	21.0	184.0	30.0	3.9	338.9	0.11	0.16	0.02
CYP1B1	2.8	4.3	4.2	0.4	36.2	0.65	0.29	0.09
Background	0.2	3.0	0.0	0.0				

Microsomes (0.2 mg (TCDD) or 1.0 mg (DMSO)), isolated from cells treated for 24 hours with or without 10^{-8} M TCDD, were incubated with 1.5 μM DMBA for 15 min at 37°C, extracted, and analyzed by HPLC for metabolites as described in Methods. Results were calculated as pmol/mg protein/hr.

[a] Total of dihydrodiols and phenols, which are alternate metabolic products.

n.d. Not Determined.

BKG Background

Table II. Antibody Inhibition of DMBA Metabolism

Sample	Dihydrodiols				Total	Ratios		
	5,6-	8,9-	10,11-	3,4-		5,6/8,9	10,11/8,9	3,4/8,9
T47D+								
DMSO								
preimmune	6.7	9.0	2.6	2.3	41.6	0.74	0.29	0.26
anti-CYP1A1	7.7	10.0	3.1	2.7	48.5	0.77	0.31	0.27
anti-CYP1B1	0.7	1.5	0.5	0.3	6.5	0.47	0.33	0.20
CYP1B1	6.0	7.5	1.9	2.0	34.9	0.80	0.25	0.27
TCDD								
preimmune	87.0	344.0	30.0	31.0	512.4	0.25	0.09	0.09
anti-CYP1A1	41.0	99.0	12.0	14.0	254.8	0.43	0.13	0.14

Microsomes (0.2 mg (TCDD) or 1.0 mg (DMSO)), isolated from T47D+ cells treated for 24 hours with or without 10^{-8} M TCDD, were preincubated for 40 minutes at room temperature with or without anti-CYP antibodies, then incubated with 1.5 μM DMBA for 15 min at 37°C, extracted, and analyzed by HPLC for metabolites as described in Methods. Results were calculated as pmol/mg protein/hr. metabolites.

Table III. Specific Content and Turnover of CYP1A1 and CYP1B1 in T47D and MDA Cells

	CYP1A1 Specific Content (pmol/mg protein)	CYP1B1 Specific Content (pmol/mg protein)	CYP1A1 Turnover (P450/hour)	CYP1B1 Turnover (P450/hour)
T47D+				
DMSO	n.d.	1.9	n.d.	18.4
TCDD	15.1	42.8	24.1	2.8
T47D-				
DMSO	n.d.	11.6	n.d.	4.8
TCDD	9.5	35.2	39.5	3.6
MDA+				
DMSO[a]	n.d.	n.d.	n.d.	n.d.
TCDD	4.8	7.8	5.5	1.1
MDA-				
DMSO	n.d.	1.1	n.d.	5.2
TCDD	1.9	18.4	17.2	0.6
HMEC[b]				
DMSO	$\leq$ 0.02	0.9	n.d.	6.0
TCDD	10.3	10.4	21.0	n.d.[c]

The pmoles of CYP1A1 and CYP1B1 for determination of specific contents were determined by regression analysis against a standard curve of recombinant protein values as described in Methods, and divided by the mg protein in the sample. Specific activity was determined by dividing the total DMBA metabolizing activity (Table 1) adjusted by the percent contribution of the enzyme as determined by antibody inhibition (Table 2) by the specific content.

[a] Levels of CYP1A1 protein so low that turnover values could not be calculated.

[b] Data on HMEC from reference 5, Larsen et al., 1998.

[c] Value could not be determined due to a lack of specific CYP1B1-only inducer

n.d. Not Determined

Table IV. Comparison of Treatments Without/With 100 nM ICI 182,780

	-ICI/+ICI	+TCDD -ICI/+ICI
T47D+		
CYP1A1		
mRNA	nd	0.51 ± 0.01
Protein	nd	0.74 ± 0.21
CYP1B1		
mRNA	0.56 ± 0.23	1.09 ± 0.26
Protein	0.79 ± 0.07	1.03 ± 0.30
MDA+		
CYP1A1		
mRNA	nd	0.90 ± 0.11
Protein	nd	1.08 ± 0.44
CYP1B1		
mRNA	1.00 ± 0.01	1.00 ± 0.01
Protein	1.42 ± 0.65	0.97 ± 0.28

nd Not Detected
Values represent mean ± SEM for at least 3 separate experiments

Figure 1. Expression of CYP1A1 and CYP1B1 mRNA in T47D and MDA cells treated with or without TCDD.

a) Five μg mRNA from T47D or MDA cells treated with or without 10^{-8} M TCDD for 24 hours was Northern blotted and probed for CYP1A1 or CYP1B1 as described in Methods. Image is representative of 3 separate measurements. b) Bar graphs represent relative levels of CYP1A1 or CYP1B1 message found in 5 μg mRNA as determined by densitometry, mean ± SEM. In the top graph, bars represent only TCDD-induced CYP1A1 mRNA levels; in the bottom graph, solid bars represent basal CYP1B1 mRNA and hatched bars depict TCDD-induced CYP1B1 mRNA levels. Levels of mRNA were normalized to TCDD-induced $T47D^+$ cells for CYP1A1, and to basal $T47D^+$ cells for CYP1B1, which were each assigned a value of 1. Inset: Basal levels of CYP1B1 mRNA shown in enlarged scale. Ordinate measured in arbitrary units. Actin standardization was consistent (< 10% variation) within a cell type, however, MDA cells contained only 70% of T47D actin levels (data not shown).

Figure 2. Relative CYP1A1 and CYP1B1 protein levels in T47D and MDA cells treated with or without TCDD.

a) Protein (30 μg) from solubilized T47D or MDA cells treated with or without 10^{-8} M TCDD for 24 hours was immunoblotted for CYP1A1 or CYP1B1 as described in Methods. Image is representative of at least 2 separate experiments. b) Bar graphs represent relative levels of CYP1A1 or CYP1B1 protein found in 30 μg total cellular protein as determined by densitometry, mean ± SEM. In the top graph, bars represent only TCDD-induced CYP1A1 protein levels; in the bottom graph, solid bars represent basal CYP1B1 protein and hatched bars depict TCDD-induced CYP1B1 protein levels. Protein levels were normalized to TCDD-induced $T47D^+$ cell levels (CYP1A1) or basal $T47D^+$ cell levels (CYP1B1), each assigned a value of 1. Inset: Basal levels of CYP1B1 protein shown in enlarged scale. Ordinate measured in arbitrary units.

Figure 3. Estrogen receptor content in T47D and MDA cell clones.

ER^+ cells were treated with or without 10^{-7} M ICI for 24 hours, followed by treatment with or without 10^{-8} M TCDD for an additional 24 hours in the continued presence/absence of ICI. ER^- cells were treated for TCDD only. 30 μg protein from whole-cell solubilizations was immunoblotted for ER as described in Methods.

Figure 4. Ah receptor and ARNT content in T47D and MDA cell clones.

Cells were treated with or without 10^{-8} M TCDD for 24 hours and 30 μg protein from whole cell solubilizations was immunoblotted for AhR or ARNT as described in Methods.

A

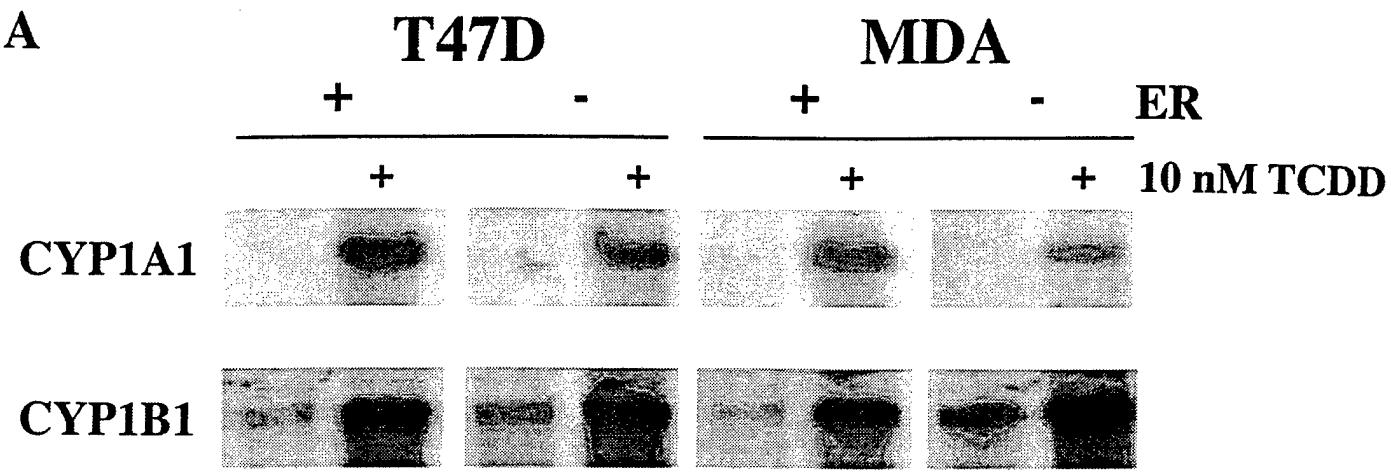
T47D
MDA
+
-
+
-
ER
+
+
+
+
10 nM TCDD
CYP1A1
CYP1B1

B

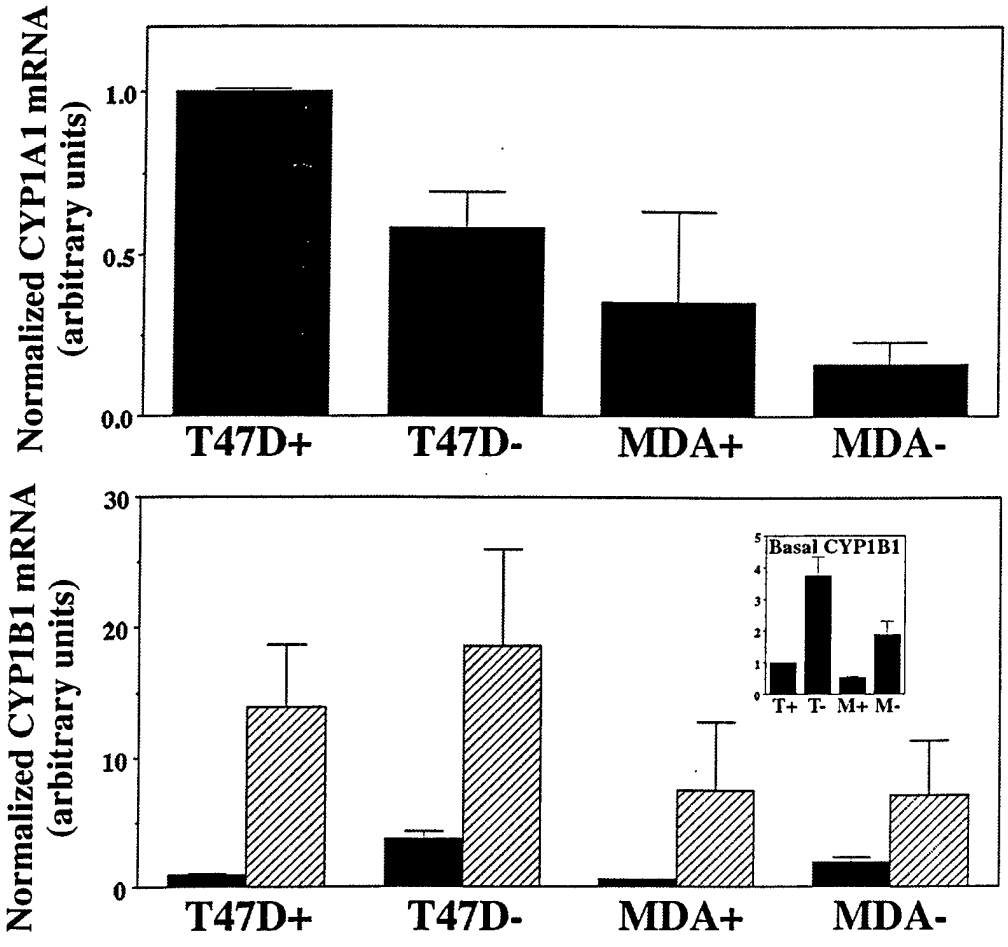
Normalized CYP1A1 mRNA (arbitrary units)
1.0
0.5
0.0
T47D+
T47D-
MDA+
MDA-
Normalized CYP1B1 mRNA (arbitrary units)
30
20
10
0
Basal CYP1B1
5
4
3
2
1
0
T+
T-
M+
M-
T47D+
T47D-
MDA+
MDA-

Figure 1

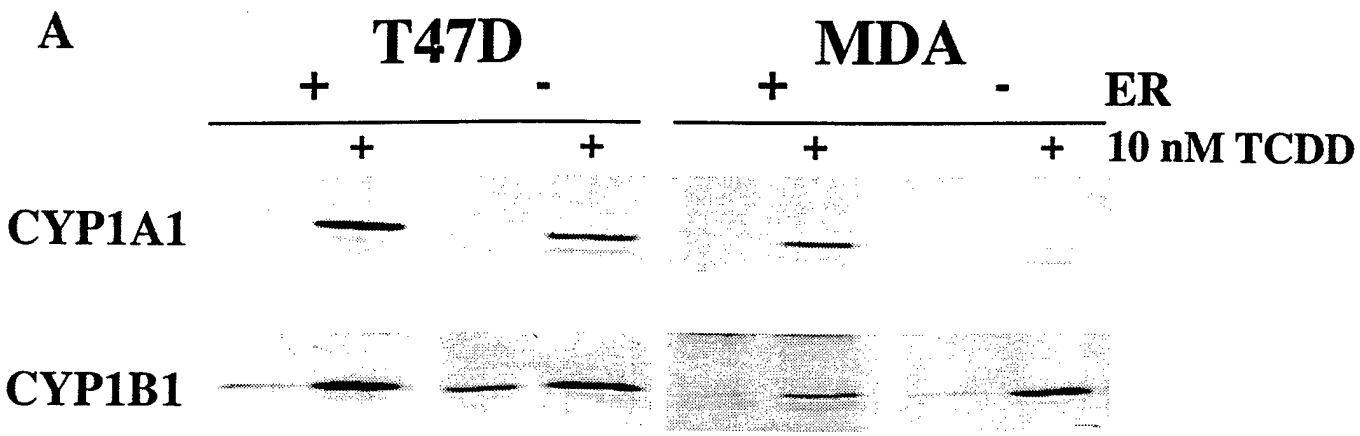
A
T47D
MDA
+
-
+
-
ER
+
+
+
+
10 nM TCDD
CYP1A1
CYP1B1

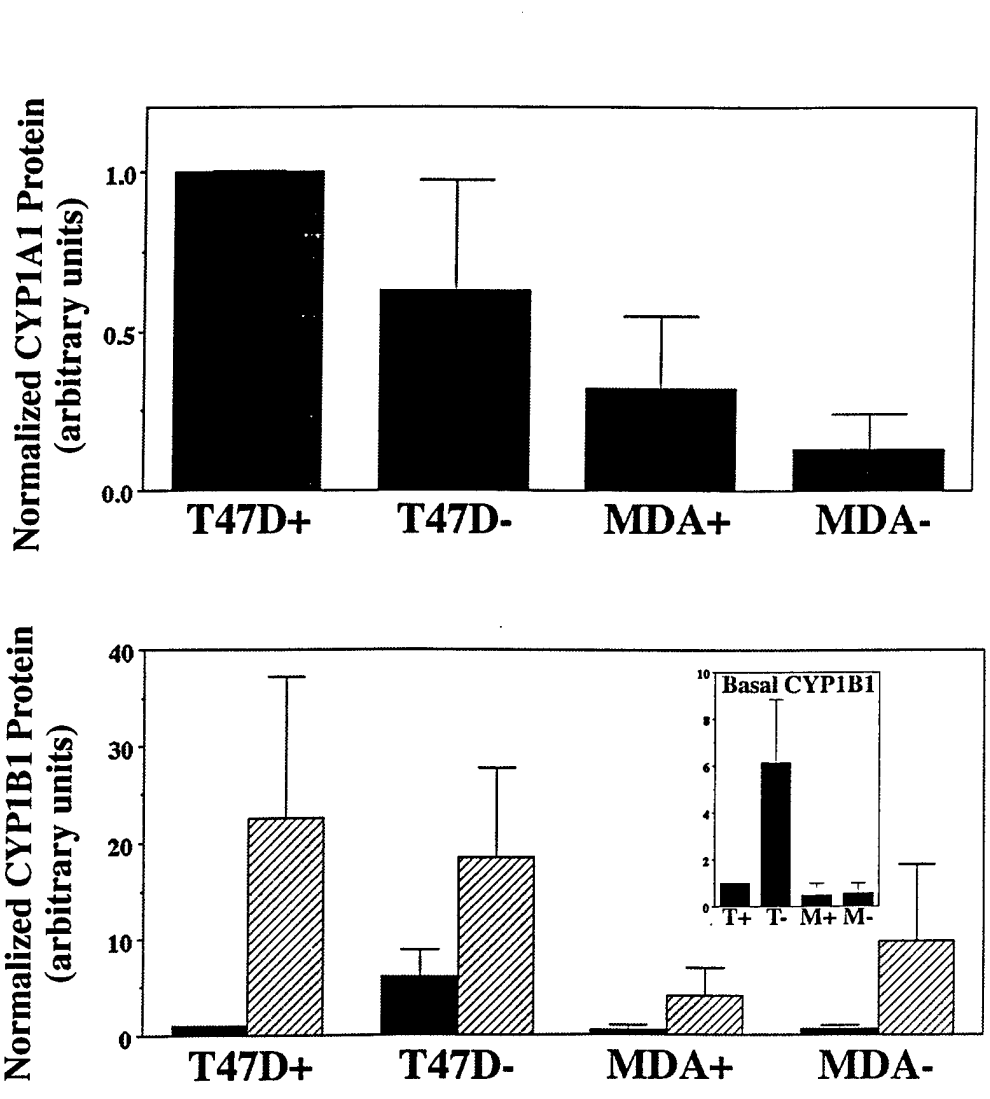
B
Normalized CYP1A1 Protein (arbitrary units)
1.0
0.5
0.0
T47D+
T47D-
MDA+
MDA-
Normalized CYP1B1 Protein (arbitrary units)
40
30
20
10
0
Basal CYP1B1
10
8
6
4
2
0
T+
T-
M+
M-
T47D+
T47D-
MDA+
MDA-

Figure 2

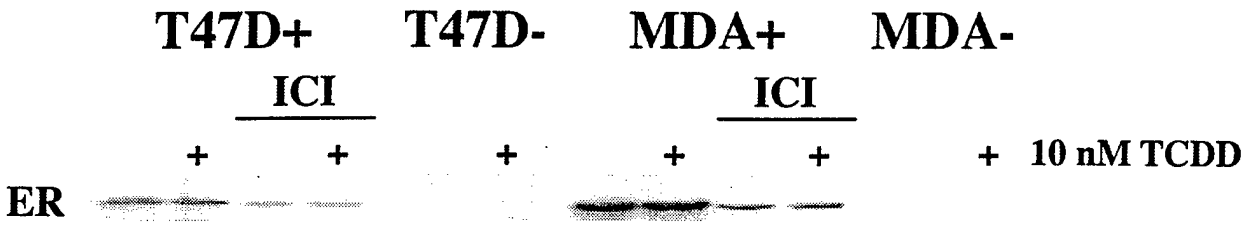

Figure 3

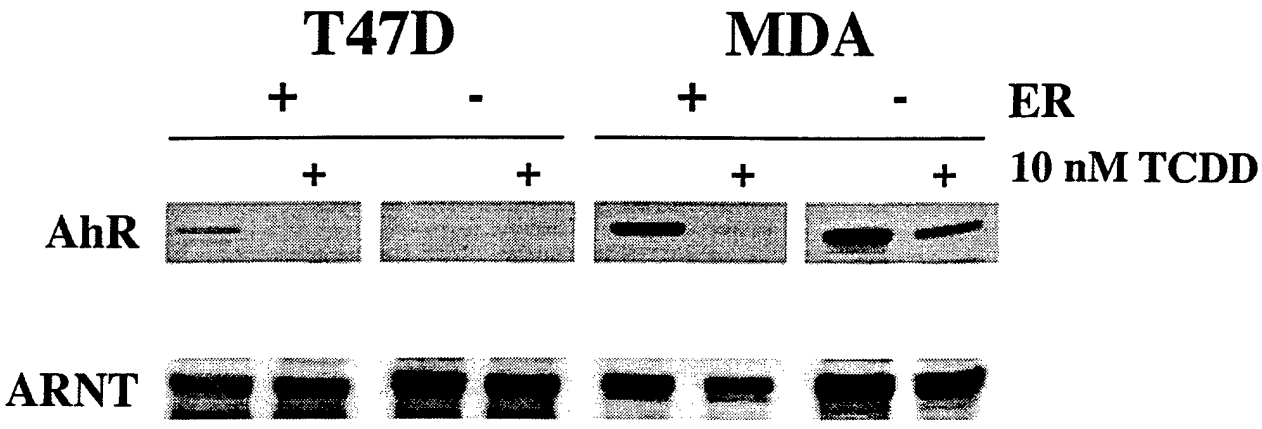

Figure 4

TCDD Elevates ErbB2, ErbB3, and Heregulin Signaling in T47D Human Mammary Epithelial Cells

William G. R. Angus, Department of Pharmacology, University of Wisconsin, Madison, 53706, U.S.A.

Paul R. Hanlon, Department of Pharmacology, University of Wisconsin, Madison, 53706, U.S.A.

Colin R. Jefcoate, Department of Pharmacology and Environmental Toxicology Center, University of Wisconsin, Madison, 53706, U.S.A.

Proofs should be sent to:

William G. R. Angus

3770 MSC

1300 University Avenue

Madison, WI 53706

Telephone: (608) 263-3128

Fax: (608) 262-1257

Running Title: Increase in ErbB2 and ErbB3 by TCDD

Key Words: Breast cancer, TCDD, ErbB2, ErbB3, T47D cells, Heregulin

Abstract

Expression of membrane tyrosine kinase c-erbB2 is elevated in estrogen receptor-positive (ER^+) cells exposed to antiestrogens. The environmental contaminant 2,3,7,8-tetrachlorodibenzo-p-dioxin (TCDD) has reported antiestrogenic activity. The effects of TCDD on expression of c-erbB2 and c-erbB3 receptors was investigated in ER^+ and ER^- T47D cells. Exposure of T47D/ER^+ cells to 10^{-8} M TCDD increased c-erbB2 and c-erbB3 mRNA fourfold at 24 hours; c-erbB2 and c-erbB3 protein expression increased by nine- and two-fold, respectively, at 48 hours. No effect was observed in T47D/ER^- cells. Tyrosine phosphorylation of c-erbB2 and c-erbB3 in T47D/ER^+ cells increased in proportion to the overall increase in the receptor proteins, suggesting that TCDD does not directly activate these receptors. Heregulinß$1_{177-244}$ increased levels of activated mitogen activated protein kinases (ERK 1 and ERK 2), and tyrosine phosphorylation of the p85 subunit of phosphatidylinositol 3-kinase (PI3-K) following a 48-hour TCDD exposure. These results indicate that TCDD increases c-erbB2 and c-erbB3 expression and cellular signaling in response to a given concentration of heregulinß$1_{177-244}$.

Introduction

The 185 kDa membrane tyrosine kinase c-erbB2/neu/HER2 (**1**) is one of four members of the EGF receptor or erbB receptor family, the others being the EGF receptor (c-erbB1) (**2**), c-erbB3/HER3 (**3,4**) and c-erbB4/HER4 (**5**). ErbB2 is overexpressed in a number of different types of cancer, including breast cancer, and it is a negative prognostic indicator for survival (**6-8**). Additionally, overexpression of c-erbB2 is most often associated with hormone non-responsive, ER^- tumors (**8,9**). ErbB3 is also overexpressed in about 20% of human breast cancers (**10,11**). Members of the erbB receptor family initiate signaling cascades following homo- or heterodimer formation of liganded receptors (**12-18**). Ligands for the EGF receptor include EGF and TGFa (**19**), while c-erbB3 and c-erbB4 bind heregulins, members of the neu differentiation factors (NDFs) (**20-22**), which comprise at least 12 differentially spliced proteins generated from a single gene (**23,24**). Exposure of breast cancer epithelial cell lines to heregulins results in enhanced proliferation at low concentrations (5 ng/ml), or differentiation at higher concentrations (50 ng/ml) (**25**). Signaling can be mediated through phosphatidylinositol 3-kinase (PI3-K) (**26-29,31**), p70 ribosomal S6 kinase ($p70^{S6K}$) (**30**), mitogen activated kinases (ERK 1, 2) (**30,31**), SHC (**31**), Csk-homologous kinase (CHK) (**32**) and stress activated protein kinase/c-Jun N-terminal kinases (SAPK/JNK) in cancer cells (**33**). However, the exact signaling cascades evoked are highly dependent on cell type, NDF isoform, and components of the dimer formed.

The regulation of c-erbB2 or c-erbB3 has been studied, and the promoters of both c-erbB2 and c-erbB3 have been identified (**34-36**). The gene expression of c-erbB2 responds to EGF, TPA, dibutryl cAMP, and retinoic acid (**35**); while c-erbB3 appears to be strongly influenced by the OB2-1 DNA binding transcription factor (**36**). Response elements for the aryl hydrocarbon receptor (AhR) were not reported. Recent reports indicate that c-erbB2 and c-erbB3 are downregulated by estrogen (E_2), and, conversely, cell stimulation by NDFs causes decreased ER levels (**37-41**). Furthermore, in cell lines, estrogen withdrawal or treatment with antiestrogens such as tamoxifen or ICI compounds increase c-erbB2 expression (**37,38,40,42,43**). Recent

reports (**37,38**) indicate that the E_2 responsiveness of c-erbB2 is related to a DNaseI hypersensitive site in the first intron. Interestingly, the negative regulatory site is only observed in the ER^+ cell lines examined, and not in ER-negative MDA-MB-231 cells.

The well known environmental contaminant TCDD has reported antiestrogenic activity (**44-50**). Exposure to this contaminant could, therefore, lead to an elevated expression of c-erbB2 in breast epithelial cells by altering the E_2-mediated suppression of this gene. The expression of c-erbB3 may also be affected. Overexpression of these two receptors could significantly alter cellular signaling.

In these studies, two lines of T47D human mammary carcinoma cells (**51-53**) were used -- standard, ER^+ T47D cells ($T47D^+$) and an ER^- clone ($T47D^-$). Cells were exposed to 10^{-8} M TCDD for 24-72 hours and levels of c-erbB2 and c-erbB3 message and protein were determined. The phosphorylation of these proteins, as well as MAPK and PI3-K p85 subunit was also determined.

Results

c-erbB2 and c-erbB3 messages are increased by 10^{-8} M TCDD

To determine whether exposure to TCDD resulted in an increase of c-erbB2 or c-erbB3 message, mRNA from $T47D^+$ and $T47D^-$ cells was Northern blotted and probed for c-erbB2 and c-erbB3. The expression of c-erbB2 message was increased in $T47D^+$ cells by 4-fold following a 24 hour exposure to 10^{-8} M TCDD, as measured by Northern blot, while TCDD had no effect on c-erbB2 message levels in $T47D^-$ cells (Figure 1, top). The expression of c-erbB3 message was increased 3-fold in the $T47D^+$ cells following TCDD exposure, but was again unaffected in $T47D^-$ cells (Figure 1, bottom). The increase in c-erbB2 and c-erbB3 message caused by TCDD in $T47D^+$ cells was compared to an increase following exposure to the antiestrogen ICI 182,780 (10^{-7} M, 24 h). ICI-treatment, with or without concomitant TCDD exposure, increased message levels of both kinases beyond those observed following TCDD exposure alone, but this was more apparent for c-erbB2 than c-erbB3. Interestingly, the levels of c-erbB2 message in the ICI-treated

T47D$^+$ cells was similar to levels of message observed in T47D$^-$ cells, however, the levels of c-erbB3 mRNA in the T47D$^-$ cells was closer to basal levels in T47D$^+$ cells. These data indicate that TCDD exposure increases the messages for these two receptors in ER$^+$ T47D cells, but not in ER$^-$T47D cells, and the increase of TCDD-stimulated message is less than that observed following antiestrogen treatment. The mechanism by which the TCDD-stimulated increase is affected is under investigation.

c-erbB2 and c-erbB3 proteins are increased by 10^{-8} M TCDD

To determine whether the increase in c-erbB2 and c-erbB3 message translated into an increase in protein, immunoblots were prepared from total cellular extracts. DMSO itself did not induce or inhibit the levels of c-erbB2 or c-erbB3 proteins. The expression of c-erbB2 and c-erbB3 proteins were slightly elevated in T47D$^+$ cells within 12 hours following exposure to 10^{-8} M TCDD (data not shown). By 24 hours of exposure, c-erbB2 protein in the cells was elevated by 3-fold, compared to DMSO vehicle treated cells, which increased to 13-fold by 72 hours (Figure 2A). c-erbB3 protein showed a different timecourse. Levels were elevated about 3-fold at 24 hours compared to controls, but were not elevated at 48 and 72 hours. As time increased (48 and 72 hours), the signal for c-erbB3 progressively split into a doublet, with the lower band becoming increasingly intense and the upper band less intense with time (Figure 2A). This phenomenon was observed in multiple experiments, and the reason for it is unclear; there may be some effect of TCDD on the processing of the protein or maintenance in culture medium for 72 hours may result in some metabolic alterations affecting c-erbB3 protein stability. Possibly the receptor may be processed or deglycosylated to produce the smaller molecular weight form.

Expression of c-erbB2 protein was compared in T47D$^+$ and T47D$^-$ cells at 24 hours of exposure to TCDD or DMSO. T47D$^-$ cells contained 10-fold greater protein than T47D$^+$ cells, regardless of treatment (Figure 2B). These levels of protein expression agree well with message expression in these two cell lines.

c-erbB2 and c-erbB3 receptor tyrosine phosphorylation is increased by 10^{-8} M TCDD

Following dimerization-associated tyrosine phosphorylation, c-erbB2 and c-erbB3 can activate several cellular signaling pathways. We tested whether TCDD exposure increased the extent of tyrosine phosphorylation of these proteins in $T47D^+$ cells. The tyrosine phosphorylation levels of c-erbB2 and c-erbB3 were examined under basal, TCDD-stimulated, or 10^{-9} M heregulinß$1_{177-244}$ (HRG)-stimulated conditions. Exposure of $T47D^+$ cells to 10^{-8} M TCDD for 48 hours resulted in an increased tyrosine phosphorylation signal from immunoprecipitated c-erbB2 and c-erbB3 proteins (Figure 3). Tyrosine phosphorylation from immunoprecipitated c-erbB2 was increased 5-fold, and from immunoprecipitated c-erbB3 was elevated 2-fold, which was proportional to the increase in overall levels of the receptors. This indicates that TCDD increases the amount of each erbB protein, but does not affect the activation of either. A 5 min challenge with 10^{-9} M HRG, used to elicit a maximal phosphorylation response, produced a signal greater than that for TCDD-stimulated cells for both c-erbB2 and c-erbB3 tyrosine phosphoprotein in control cells. Thus exposure of $T47D^+$ cells to TCDD resulted in enhanced tyrosine phosphorylation of the receptors, but not activation of the receptors.

Cellular estrogen receptor levels are not altered by TCDD

One of the proposed mechanisms of antiestrogenicity by TCDD is by decrease of ER **(54)**. To determine if this occurred in the current studies, total cell proteins from $T47D^+$ and $T47D^-$ cells exposed to TCDD for 24 hours were immunoblotted for ER. Lysates from cells treated with 10^{-7} M ICI served as a positive control for the effects of an antiestrogen on ER levels (Figure 4). ICI treatment decreased levels of ER by at least 70%, either in the presence or absence of TCDD. However, TCDD alone failed to alter cellular ER levels, suggesting that ER did not decrease in response to TCDD at 24 hours.

Heregulinß$1_{177-244}$-stimulated intracellular signaling is increased by 10^{-8} M TCDD

Stimulation of c-erbB receptors and the ensuing tyrosine phosphorylation leads to the recruitment of signaling proteins, such as Grb2 and p85, and results in elevated signaling through cellular cascades such as the MAPK and PI3-K. To assess the effect of 48 hours of exposure to

10^{-8} M TCDD on one of the downstream c-erbB receptor signaling cascades, $T47D^+$ cells, treated with or without TCDD, were challenged for 5 min with 10^{-9} M HRG, then immunoblotted ERK 1/2 or for activated MAPKs. Levels of total ERK 1 and 2 were unaffected by TCDD or HRG treatment (Figure 5A). The activated forms of p44 ERK 1 and p42 ERK 2 were observed only in HRG-stimulated samples (Figure 5B). TCDD exposure resulted in a 6-fold enhancement of activated ERK 1 and a 4-fold increase in ERK 2, compared to control, indicating that the MAPK branch of c-erbB receptor signaling is enhanced in response to ligand challenge following exposure to TCDD.

The effect of this exposure to TCDD was also assessed on PI3-K. Total cell lysates from $T47D^+$ cells treated with or without TCDD for 48 hours, then stimulated or not with 10^{-9} M HRG for 5 min, were immunoblotted for p85 (Figure 6A). A single band was observed in the correct molecular weight range, with minor band at a smaller size. Tyrosine-phosphorylated proteins were immunoprecipitated from total cell lysates of $T47D^+$ cells which were treated with or without TCDD for 48 hours, followed by stimulation with HRG for 5 min. Activation of PI3-K was indicated by an increase in tyrosine phosphorylation of the p85 subunit (Figure 6B). Tyrosine phosphorylation of the p85 subunit of PI3-K was only observed following HRG treatment, and exposure of the cells to TCDD greatly increased (15-fold) the levels of phosphorylation compared to the vehicle treated cells. Hence, signaling through both the MAPK and PI3-K pathways are enhanced in $T47D^+$ cells in response to a given concentration of heregulin (10^{-9} M) following exposure to 10^{-8} M TCDD.

Discussion

These studies have demonstrated that exposure of $T47D^+$ cells to TCDD results in an increased expression of c-erbB2 and c-erbB3 receptor tyrosine kinases at both the message and protein levels. Although these increases in expression were less than those produced by the antiestrogen ICI 182,780, this effect is consistent with antiestrogenic activity reported for TCDD. The $T47D^-$ cells demonstrated a c-erbB2 expression level similar to that of ICI-treated $T47D^+$

cells, suggesting that in these cells, c-erbB2 is expressed at a maximal level. The levels of non-HRG-stimulated tyrosine phosphorylation of c-erbB2 and c-erbB3 was increased in proportion to the increase in protein levels following TCDD treatment. Thus, TCDD did not appear to directly activate these kinases. Further, key mediators of downstream signaling cascades for the c-erbB receptors, MAPK and PI3-K, demonstrated enhanced stimulation to a given concentration of HRG (10^{-9} M), following exposure to 10^{-8} M TCDD.

Although TCDD is considered to be an antiestrogen, how it mediates this effect is not clear. TCDD and E_2 do not bind each other's cognate receptors, and the AhR, through which TCDD acts at the transcriptional level, does not appear to interact with the estrogen response element (ERE) (**49**). Nonetheless, TCDD has documented antiestrogenic effects in both in vivo and in vitro systems. Exposure female rats to a single dose of TCDD significantly reduced uterine and hepatic ER levels, either in the presence or absence of E_2 (**46**), indicating that the antiestrogenic effect is not a competition with E_2. In mouse Hepa 1c1c7 cells, pretreatment with, but not co-treatment with 10^{-9} M TCDD decreased the accumulation of ER complex in the nucleus. These effects were not observed, however, in 2 mutants of the Hepa cells, class 1 (decreased AhR levels) or class 2 (decreased AhR nuclear transport protein (arnt) levels), indicating a role for the AhR in the process. Additionally, actinomycin D and cycloheximide inhibited the effects of TCDD on the ER nuclear complex, indicating that TCDD may be inducing gene products responsible for altering ER nuclear complex formation (**47**). Exposure of human mammary MCF 7 cells to 10^{-9} M TCDD has been reported to result in decreased levels of nuclear ER, with a concomitant decrease in binding of ER to the ERE. RNA and nuclear run-on analyses indicated that message levels and rate of ER transcription were unaffected by TCDD (**49**), suggesting a direct effect of TCDD at the translational or post-translational level. However, another report indicated that 10^{-8} M TCDD was without effect on ER mRNA levels, E_2 binding, or the accumulation of ER in the nucleus. The investigators suggested that the antiestrogenic effects of TCDD were mediated by TCDD-inducible gene products, and not by a direct action of

TCDD on the ER (**50**). Together, these data indicate that the antiestrogenic effect of TCDD may involve an interaction of at least two interdependent processes, altered ER production and altered E_2 availability. Numerous reports indicate that c-erbB2 mRNA and protein levels are elevated in cultured ER^+ human mammary cancer cell lines following antiestrogen treatment (**38,40,55**). Since TCDD is able to act antiestrogenically by either a direct or indirect mechanism, it is reasonable to postulate that TCDD may also act to attenuate the E_2/ER-mediated suppression of c-erbB2 and c-erbB3 expression.

Since the presence of AhR DNA-binding elements (XREs) have not been reported for c-erbB2 or c-erbB3, it is possible that there is a direct induction of these genes by TCDD. However, most genes induced by TCDD, such as cytochrome P450 1A1 (CYP1A1) have large factors of induction (e.g. 50-fold), and the induction of these two erbB genes was only 4-fold, suggesting that direct TCDD induction is likely not the case. However, this possibility is being investigated. Another possible scenario for the increase in c-erbB2 and c-erbB3 in $T47D^+$ cells following TCDD exposure involves induction of the E_2-hydroxylases --cytochromes P450 1A1 and 1B1 (CYP1A1 and CYP1B1).

Environmental contaminants such as TCDD can induce CYP1A1 and CYP1B1 in numerous mammary cell lines (**56-58, unpublished observations**). These enzymes can metabolize estrogen at the C-2, C-6a, and C-15a positions (CYP1A1) or C-4 (CYP1B1)(**58**). The human form of CYP1B1 is one of the more efficient E_2 hydroxylases known (**59,60**). Hydroxyestrogens are further capable of participating in peroxidative mechanisms and forming DNA adducts, leading to cancer initiation (**61**). It is possible to speculate that removal of E_2 via metabolism may thus attenuate the negative regulation on c-erbB2 and c-erbB3, and that this is indeed a possible explanation for why TCDD increases the protein expression of these receptors to an increasing extent over time, e.g. 3-fold at 24 h to 13-fold at 72 h for c-erbB2. This lab is exploring this possibility. Another possible explanation for the increase in c-erbB2 and c-erbB3 proteins over time is that post-transcriptional modification is occurring, in addition to the increase

in levels of message following exposure of the cells to TCDD. Such possible alterations require further investigation. In addition to increasing the levels of c-erbB2 and c-erbB3 receptors, TCDD may also induce the production of heregulins by these cells, leading to an autocrine growth stimulatory loop, which is also currently being investigated.

Early in vivo investigations of the interactions of TCDD with the EGF receptor (c-erbB1), were performed in various animal strains with differing susceptibilities to TCDD **(62,63)**. In the earliest studies **(64)**, TCDD was found to increase the phosphorylation of p170 EGF receptor in rat liver plasma membranes. Meanwhile, the binding of ^{125}I-EGF to its receptor has been shown to be decreased 80-90% in the absence of any changes in plasma EGF levels **(62,63)**. The effects of TCDD on EGF binding have been attributed to a decreased receptor number, and not to changes in affinity or levels of EGF receptor mRNA or levels of mRNA for the ligand TGFa **(63,65)**. One of findings suggested by these studies is that the AhR mediates the effects of TCDD on the EGF receptor, however, the mechanism is unclear. Since c-erbB2 and c-erbB3 are members of the EGF receptor family, TCDD could have been expected to decrease levels of these receptors, and the resulting signaling through them in response to ligand challenge. Apparently this is not the case, and TCDD can differentially affect members of the c-erbB receptor family.

The role of organochlorine environmental contaminants (OCs), such as TCDD, 1,1,1-dichloro-2,2-bis(p-chlorophenyl)-ethane (DDT), and hexachlorohexanes (HCHs), in the etiology of breast cancer has been the subject of intense debate for a number of years **(66-69)**. DDT and γ-HCH (lindane) demonstrate estrogenic effects in a number of in vivo and in vitro systems **(70-74)**, and TCDD is reported to have antiestrogenic effects **(44-50)**. While it is clear that human mammary and adipose tissue contains significant quantities of OCs **(67,75)**, what is less evident is the effects that they have on breast cancer initiation, promotion, and cell signaling.

Recently, the effects of DDT congeners (o,p'- and p,p'-) have been investigated in MCF 10A human breast cancer cells **(76)**, and it was determined that 10^{-4} M p,p'-DDT, but not o,p'-DDT, increased tyrosine phosphorylation of c-erbB2, increased association of Grb2-SOS,

increased MAPK phosphorylation, and enhanced ^{3}H-thymidine incorporation. Interestingly, the p,p'- congener did not induce or repress protein levels of c-erbB2 in MCF 10A cells. The p,p'-DDT congener is weakly estrogenic, while o,p'-DDT is considered a strongly estrogenic environmental contaminant (**77**). Since MCF 10A cells are reported to be ER-negative (**62,76**), it is not surprising that the ER-binding o,p'-DDT has no repressive effects on c-erbB2 (**37**). However, the effectiveness of p,p'-DDT to cause phosphorylation of c-erbB2 and to stimulate downstream signaling cascades indicates that organochlorine compounds need to be carefully investigated as potential epigenetic mammary cancer stimulants. Other environmental contaminants having estrogenic or antiestrogenic properties may also act on the c-erbB receptors to stimulate their signaling.

These studies demonstrate that exposure of human mammary epithelial cells to TCDD results in a time-dependent increase in c-erbB2 and c-erbB3 protein levels, with a pursuant increase in downstream signaling cascades in response to a given concentration of heregulin. There is therefore a further need to investigate the role of organochlorine environmental contaminants in breast cancer.

Materials

T47D:A18 ($T47D^{+}$) and T47D:C4:2W ($T47D^{-}$) cells (**53**) were obtained from Dr. John Pink (University of Wisconsin) and Dr. V. C. Jordan (Northwestern University). TCDD was purchased from AccuStandard, Inc. (New Haven, CT), and dissolved in dimethylsulfoxide (DMSO) (Sigma, St. Louis, MO) at 1000-fold concentrations. Monoclonal antibodies for c-erbB2 and c-erbB3 were obtained from NeoMarkers (Fremont, CA). Antibodies for PI3-K were purchased from Upstate Biologicals (Lake Placid, NY). The antibodies for ERK 1/2 were obtained from Transduction Laboratories (Lexington, KY). Polyclonal antibodies for activated MAPK were obtained from Promega (Madison, WI). Monoclonal antibody to phosphotyrosine and polyclonal antibody for estrogen receptor were purchased from Santa Cruz Biologicals (Santa Cruz, CA). Heregulin $\beta1_{177-244}$ and the cDNA for c-erbB2 were generous gifts from Dr. Mark

Sliwkowski (Genentech, South San Francisco, CA). A cDNA probe for c-erbB2 was obtained from Oncogene Research Products (HP-125; Cambridge, MA). A plasmid containing the cDNA for c-erbB3 was a generous gift form Dr. Greg Plowman (Sugen, Inc., Redwood City, CA). ICI 182,780 was a generous gift from Dr. Alan Wakling (Zenica Pharmaceuticals, Manchester, England). Protein levels were determined with the BCA protein reagents (Pierce, Rockford, IL). RPMI 1640 cell culture medium was obtained from GIBCO (Grand Island, NY), and fetal calf serum was purchased from Hyclone (Logan, UT). ECL reagents, ECL hyperfilm, nylon and nitrocellulose and PVDF membrane were obtained from Amersham (Arlington Heights, IL). Ready-to-Go DNA labeling beads and G-50 spin columns were purchased from Pharmacia Biotech, Inc. (Piscataway, NJ). Protease inhibitor cocktail, phenylmethylsulfonyl fluoride (PMSF), insulin, ammonium persulfate, TEMED, aurin tricarboxylic acid (ATA), penicillin/streptomycin solution, phosphate buffered saline (PBS) tablets and diethylpyrocarbamate (DEPC) were purchased from Sigma. Sodium dodecyl sulfate and bis-acrylamide were obtained from BioRad, Inc. (LaJolla, CA), and acrylamide was obtained from ICN Biomedicals, Inc. (Auora, OH). Formaldehyde solution and Proteinase K were purchased from Fisher Chemical (LaJolla, CA), formamide and oligo dT cellulose was purchased from Ambion (Austin, TX). [α^{32}P]-dCTP was obtained from New England Nuclear-DuPont (Boston, MA). All other reagents were of the highest grade possible.

Cell Culture

T47D cells were cultured in monolayers in 75 cm^2 flasks in RPMI 1640 medium containing 10% FBS, 6 ng/ml insulin, and 10 ml/L penicillin/streptomycin solution. The cultures were maintained in a humidified atmosphere containing 5% CO_2.

For experimental procedures involving protein analysis, confluent cultures in 60 mm plates were treated with 10^{-8} M TCDD or 0.1% DMSO for 24 to 72h. Following ice cold PBS wash, ice cold lysis buffer (150 mM NaCl, 50 mM TRIS-HCl, pH 7.4, 1 mM EDTA, 1% NP-40, 0.25% deoxycholate, 0.05% SDS, 1 mM Na_3VO_4, 1 mM PMSF, 1 mM molybdate, 40 mM

NaF, and 10 µl/ml protease inhibitor cocktail) was added, cells were scraped, sheared through a 27 gauge needle, and centrifuged at 4 C°. Supernatants were transferred to clean tubes and stored at -80 C° until use. An aliquot was saved out for protein determination. For experiments involving heregulinß1$_{177-244}$ treatment, cells were exposed to TCDD, starved in serum free medium for 6 hours, then heregulinß1$_{177-244}$ in PBS was added to the medium at 1000-fold concentration for 5 minutes, media was removed, and the aforementioned method of harvesting cellular proteins was then utilized. For experiments involving ICI, cells were treated in fresh medium with 10^{-7} M for 24 hours prior to exposure to TCDD. ICI treatment was maintained during TCDD exposure.

Nucleic Acid Hybridization

Cells were grown to confluence in 150 mm plates, then treated with or without 10^{-8} M TCDD for 24 hours. Control cells were treated with 0.1% DMSO. Poly A$^+$ RNA (mRNA) was isolated according to the method of Badley et al. **(78)**. Briefly, cells were washed in PBS containing 20 µM ATA and lysed in a buffer consisting of 0.2 M NaCl, 0.2 M TRIS-HCl, pH 7.5, 0.15 mM $MgCl_2$, 2% SDS, 200 µg/ml proteinase K, and 20 µM ATA. Lysates were sheared through a 23 gauge needle and incubated for 2 hours at 45 C°, then incubated with oligo dT cellulose for 1 hour. Poly A$^+$ RNA was eluted with four 750 µl aliquots of DEPC-treated water. Eluted RNA was precipitated with 2 volumes of ethanol and chilling at -80 C° for at least 2 hours, then washed with 70% ethanol and air dried. RNA was resuspended in loading buffer (per sample; 2.25 µl DEPC H_2O, 2.00 µl 5X running buffer, 1.75 µl formaldehyde solution, and 5.00 µl formamide) and quantitated by reading absorbance at 260 nm.

The mRNA was electrophoresed through a formaldehyde-containing 1% agarose gel at 5 V/cm, then transferred by capillary action to nylon membrane and crosslinked to the membrane using UV. Probes for c-erbB2, c-erbB3 and ß-actin were labeled with [α ^{32}P]-dCTP using Ready-To-Go labeling beads, and purified through G-50 columns. Membranes were prehybridized with QuikHyb (Stratagene) for 15 min. at 65 C°, then probed with 10^6 cpm/ml of specific probe for 90 min. Membranes were washed for 20 min with 1X SSC, 1% SDS at room

temperature, then twice for 10 min with 0.1X SSC, 0.5% SDS at 65 C°. Autoradiographs of the probed membranes were quantitated by densitometry.

The probes used for c-erbB2 were a 50:50 mixture of a 1.4 Kb neu fragment (HP-125) from Oncogene Research Products, and an 882 bp fragment of the c-erbB2 cDNA obtained from Dr. Sliwkowski cut using Hind III and EcoR I. The c-erbB3 probe was excised from the cDNA obtained from Dr. Plowman using Xba I and Bgl II, and was 1.3 Kb long.

Immunoprecipitation

Immunoprecipitation of c-erbB2 and c-erbB3 was accomplished from 1 mg total cellular protein. Proteins were cleared with protein A/G$^+$ agarose (Santa Cruz Biologicals), then incubated with 2 µg monoclonal anti-c-erbB2 or anti-c-erbB3 antibody for 1 hour at 4 C°. Protein A/G$^+$ agarose was added and incubated for 2 hour at 4 C°. Pellets were washed 3 times with lysis buffer, then 40 µl Lammeli buffer was added, and the samples boiled for 5 min. The samples were then stored at -20 C° until use.

Immunoprecipitation of phosphotyroproteins utilized 500 µg cellular protein and 5 µg monoclonal PY20 (Santa Cruz). Proteins were cleared with protein A/G$^+$ agarose then incubated with 5 µg antibody for 6 hours at 4 C°. Protein A/G$^+$ agarose was added and samples were incubated overnight at 4 C°. Pellets were washed twice with lysis buffer and twice with PBS. Laemmli buffer (50 µl) was added, and samples boiled for 5 min. Samples were aliquoted and stored at -20 C° until use. Immunoprecipitates were separated on 7.5% acrylamide gels and transferred to nitrocellulose and probed as described below.

Immunoblotting

Cellular proteins were resolved on 7.5% acrylamide gels and transferred to nitrocellulose or PVDF membranes according to the method of Laemmli (**79**). Proteins for activated MAPK were resolved on 12% acrylamide gels. Membranes were probed for phosphotyrosine, PI3-K, c-erbB2 or c-erbB3. For phosphotyrosine, membranes were blocked in Tris-buffered saline with Tween 20 (TBST) containing 0.25% gelatin (TBST-G), and primary and secondary antibodies were

incubated in TBST-G. Other antibodies were blocked utilizing 5% milk in TBST.

Abbreviations

TCDD, 2,3,7,8-tetrachlorodibenzo-p-dioxin; AhR, aryl hydrocarbon receptor; arnt, AhR nuclear translocator protein; EGF, epidermal growth factor; TGFa, transforming growth factor a; ECL, enhanced chemoluninescence; Grb2, an adaptor protein; SOS, son of sevenless - an adaptor protein; CYP1A1, cytochrome P450 1A1; CYP1B1, cytochrome P450 1B1; ERE, estrogen response element; DDT, 1,1,1-dichloro-2,2-bis(p-chlorophenyl)-ethane; HCH, hexachlorohexane; MAPK, mitogen activated protein kinase; PI3-K, phosphatidylinositol 3-kinase; ER, estrogen receptor; E_2, estrogen; DMSO, dimethylsulfoxide.

Acknowledgements

We wish to thank Dr. Paul Bertics and Dr. Atul Tandon for advice on these studies. A special note of thanks to Dr. Mark Sliwkowski and Dr. Greg Plowman for cDNAs and heregulin. This work was supported by NRSA 1-F32-ES05733-01(WGRA) and NIEHS Grant 144EN46, DOD Breast Cancer Research Grant DAMD17-94-J-4054 (CRJ).

References:

1 Yamamoto T, Ikawa S, Akiyama T, Semba K, Nomura N, Miyajima N, Saito T, and Toyoshima K. (1986). Nature, 319, 230-234.

2 Ullrich A, Coussens L, Hayflick JS, Dull TJ, Gray A, Tam AW, Lee J, Yarden Y, Libermann TA, Schlessinger J, Downward J, Mayes ELV, Whittle N, Waterfield MD, and Seeburg PH. (1984). Nature, 309, 418-425.

3 Kraus MH, Issing W, Miki T, Popescu NC, and Aaronson AA. (1989). Proc. Natl. Acad. Sci., U.S.A., 86, 9193-9197.

4 Plowman GD, Whitney GS, Neubauer MG, Green JM, McDonald VL, Todaro GJ, and Shoyab M. (1990). Proc. Natl. Acad. Sci., U.S.A., 87, 4905-4909.

5 Plowman GD, Culouscou J-M, Whitney GS, Green JM, Carlton GW, Foy L, Neubauer MG, and Shoyab M. (1993). Proc. Natl. Acad. Sci., U.S.A., 90, 1746-1750.

6 Slamon DJ, Clark GM, Wond SG, Levin WJ, Ullrich A, and McGuire WL. (1987). Science, 235, 177-182.

7 Gullick WJ. (1990). Int. J. Cancer, Suppl. 5, 55-61.

8 Keshgegian AA. (1995). Breast Canc. Res. Treatment, 35, 201-210.

9 Press MF, Pike MC, Chazin VR, Hung G, Udove JA, Markowicz M, Danyluk J, Godolphin W, Sliwkowski M, Akita R, Paterson MC, and Slamon DJ. (1993). Cancer Res., 53,

4960-4970.

10 Kraus MH, Fedi P, Starks V, Muraro R, and Aaronson SA. (1993). Proc. Natl. Acad. Sci., U.S.A., 90, 2900-2904.

11 Lemoine NR, Barnes DM, Hollywood DP, Hughes CM, Smith P, Dublin E, Prignet SA, Gullick WJ, and Hurst HC. (1992). Br. J. Cancer, 66, 1116-1121.

12 Tzahar E, Waterman H, Chen X, Levkowitz G, Karunagaran D, Lavi S, Ratzkin BJ, and Yarden Y. (1996). Mol. Cell. Biol., 16, 5276-5287.

13 Graus-Porta D, Beerli RR, Daly JM, and Hynes NE. (1997). EMBO J., 16, 1647-1655.

14 Alimandi M, Romano A, Curia MC, Muraro R, Fedi P, Aaronson SA, DiFiore PP, and Kraus MH. (1995). Oncogene, 10, 1813-1821.

15 Earp HS, Dawson TL, Li X, and Yu H. (1995). Breast Canc. Res. Treatment, 35, 115-132.

16 Karunagaran D, Tzahar E, Beerli RR, Chen X, Graus-Porta D, Ratzkin BJ, Seger R, Hynes NE, and Yarden Y. (1996). EMBO J., 15, 254-264.

17 Caraway III KL, and Cantley LC. (1994). Cell, 78, 5-8.

18 Weiß FU, Wallasch C, Campiglio M, Issing W, and Ullrich A. (1997). J. Cell. Physiol., 173, 187-195.

19 Beerli RR and Hynes NE. (1996). J. Biol. Chem., 271, 6071-6076.

20 Tzahar E, Levkowitz G, Karunagaran D, Peles E, Lavi S, Chang D, Liu N, Yayon A, Wen D, and Yarden Y. (1994). J. Biol. Chem., 269, 25226-25233.

21 Pinkas-Kramarski R, Shelly M, Glathe S, Ratzkin BJ, and Yarden Y. (1996). J. Biol. Chem., 271, 19029-19032.

22 Plowman GD, Green JM, Culouscou J-M, Carlton GW, Rothwell VM, and Buckley S. (1993). Nature, 366, 473-475.

23 Wen D, Suggs SV, Karunagaran D, Liu N, Cupples RL, Luo Y, Janssen AM, Ben-Baruch N, Trollinger DN, jacobsen VL Meng S-Y, Lu HS, Hu S, Chang D, Yang W, Yanigahara D, Koski RA, and Yarden Y. (1994). Molec. Cell. Biol., 14, 1909-1919.

24 Wen D, Peles E, Cupples R, Suggs SV, Bacus SS, Luo Y, Trail G, Hu S, Silbiger SM, Ben Levy R, Koski RA, Lu HS, and Yarden Y. (1992). Cell, 69, 559-572.

25 Bacus SS, Yarden Y, Oren M, Chin DM, Lyass L, Zelnick CR, Kazarov A, Toyofuku W, Gray-Bablin J, Beerli RR, Hynes NE, Nikiforov M, Haffner R, Gudkov A, and Keyomarsi K. (1995). Oncogene, 12, 2535-2547.

26 Soltoff SP, Carraway III KL, Prignet SA, Gullick WG, and Cantley LC. (1994). Molec. Cell. Biol., 14, 3550-3558.

27 Kim H-H, Sierke SL, and Koland JG. (1994). J. Biol. Chem., 269, 24747-24755.

28 Carraway III KL, Soltoff SP, Diamonti J, and Cantley LC. (1995). J. Biol. Chem., 270, 7111-7116.

29 Hamburger AW and Yoo J-Y. (1997). Anticancer Res., 17, 2197-2200.

30 Marte BM, Graus-Porta D, Jeschke M, Fabbro D, Hynes NE, and Taverna D. (1995). Oncogene, 10, 167-175.

31 Sepp-Lorenzino L, Eberhard I, Ma Z, Cho C, Serve H, Liu F, Rosen N, and Lupu R. (1996). Oncogene, 12, 1679-1687.

32 Zrihan-Licht S, Lim J, Keydar I, Sliwkowski MX, Groopman JE, and Avraham H. (1997). J. Biol. Chem., 272, 1856-1863.

33 Grasso AW, Wen D, Miller CM, Rhim JS, Pretlow TG, and Kung H-J. (1997). Oncogene, 15, 2705-2716.

34 Tal M, King CR, Kraus MH, Ullrich A, Schlessinger J, and Givol D. (1987). Molec. Cell. Biol., 7, 2597-2601.

35 Hudson LG, Ertl AP, and Gill GN. (1990). J. Biol. Chem., 265, 4389-4393.

36 Skinner A and Hurst HC. (1993). Oncogene, 8, 3393-3401.

37 Bates NP and Hurst HC. (1997). Oncogene, 15, 473-481.

38 Russell KS and Hung M-C. (1992). Cancer Res., 6624-6629.

39 Grunt TW, Saceda M, Martin MB, Lupu R, Dittrich E, Krupiza G, Harant H, Huber H, Dittrich C. (1995). Int. J. Cancer, 63, 560-567.

40 Dati C, Antoniotti S, Taverna D, Perroteau I, and De Bortoli M. (1990). Oncogene, 5, 1001-1006.

41 Saceda M, Grunt TW, Colomer R, Lippman ME, Lupu R, and Martin MB. (1996). Endocrinology, 137, 4322-4330.

42 Pietras RJ, Arboleda J, Reese DM, Wongvipat N, Pegram MD, Ramos L, Gorman CM, Parker MG, Sliwkowski MX, and Slamon DL. (1995). Oncogene, 10, 2435-2446.

43 Liu Y, El-Ashry D, Chen D, Ding IYF, and Kern FG. (1995). Breast Canc. Res. Treatment, 34, 97-117.

44 Fernandez P and Safe S. (1992). Toxicol. Lett., 61, 185-197.

45 Fernandez P, Burghardt R, Smith R, Nodland K, and Safe S. (1994). Eur. J. Pharmacol., 270, 53-66.

46 Romkes M, Piskorska-Pliszczynska J, and Safe S. (1987). Toxicol. Appl. Pharmacol., 87, 306-314.

47 Zacharewski T, Harris M, and Safe S. (1991). Biochem. Pharmacol., 1931-1939.

48 DeVito MJ, Thomas T, Martin E, Umbreit TH, and Gallo MA. (1992). Toxicol. Appl. Pharmacol., 113, 284-292.

49 Wang X, Porter W, Krishnan V, Narasimhan TR, and Safe S. (1993). Mol. Cell. Endocrinol., 96, 159-166.

50 Gierthy JF, Spink BC, Figge HL, Pentecost BT, and Spink DC. (1996). J. Cell. Biochem., 60, 173-184.

51 Kedar I, Chen L, Karby S, Weiss FR, Delarea J, Radu M, Chaitcik S, and Brenner HJ. (1979). Eur. J. Cancer, 15, 659-670.

52 Chalbos D, Vignon F, Keydar I, and Rochefort H. (1982). J. Clin. Endochrinol. Metab., 55, 276-283.

53 Pink JJ, Bilimoria MM, Assikis J, and Jordan VC. (1996) Br. J. Cancer, 74, 1227-1236.

54 Harris M, Zacharewski T, and Safe S. (1991) Cancer Res. 50, 3579-3584.

55 Sewall CH, Clark GC, and Lucier GW. (1995). Toxicol. Appl. Pharmacol., 132, 263-272.

56 Warri AM, Laine AM, Majasuo KE, Alitalo KK, and Harkonen PL. (1991). Int. J. Caner, 49, 2087-2090.

57 Christou M, Savas U, Spink D, Gierthy JF, and Jefcoate CR. (1994). Carcinogenesis, 15, 725-732.

58 Spink DC, Spink BC, Cao JQ, DePasquale JA, Pentecost BT, Fasco MJ, Li Y, and Sutter TR. (1998). Carcinogenesis, 19, 291-298.

59 Spink DC, Eugster H-P, Lincoln II DW, Schuetz JD, Schuetz EG, Johnson JA, Kaminsky LS, and Gierthy JF. (1992). Arch. Biochem. Biophys., 293, 342-348.

60 Hayes CL, Spink DC, Spink BC, Cao JQ, Walker NJ, and Sutter TR. (1996). Proc. Natl. Acad. Sci., U.S.A., 93, 9776-9781.

61 Zhu BT and Conney AH. (1998). Carcinogenesis, 19, 1-27.

62 Miller FR, Soule HD, Tait L, Pauley RJ, Wolman SR, Dawson PJ, and Heppner GH. (1993). J. Natl. Cancer Inst., 85, 1725-1732.

63 Madhukar BV, Ebner K, Matsumura F, Bombick DW, Brewster DW, and Kawamoto TK. (1988). J. Biochem. Toxicol., 3, 261-272.

64 Lin EH, Clark G, Birnbaum LS, Lucier GW, and Goldstein JA. (1991). Molec. Pharmacol., 39, 307-313.

65 Bombick DW, Madhukar BV, Brewster DW, and Matsumura F. (1985). Biochem. Biophys. Res. Comm., 127, 296-302.

66 Wolff MS, Toniolo PG, Lee EW, Rivera M, and Dublin N. (1993). J. Natl. Cancer Inst., 85, 648-652.

67 Ahlborg UG, Lipworth L, Titus-Ernstoff L, Hsieh C-C, Hanberg A, Baron J, Trichopoulos D, and Adami H-O. (1995). Crit. Rev. Toxicol., 25, 463-531.

68 Wolff MS and Toniolo PG. (1995). Environ. Health Perspect., Suppl 7, 141-145.

69 Hunter DJ, Hankinson SE, Laden F, Colditz GA, Manson JE, Willett WC, Speizer FE and Wolff MS. (1997). N. Engl. J. Med., 337, 1253-1258.

70 Dees C, Askari M, Foster JS, Ahamed S, and Wimalasena J. (1997). Molec. Carcinogen., 18, 107-114.

71 Soto AM, Chung KL, and Sonnenschein C. (1994). Environ. Health Perspect., 102, 380-383.

72 vom Saal FS, Nagel SC, Palanza P, Boechler M, Parmigiani S, Welshons WV. (1995). Toxicol. Lett., 77, 343-350.

73 Steinmetz R, Young PCM, Caperell-Grant A, Gize EA, Madhukar BV, Ben-Jonathan N, and Bigsby RM. (1996). Cancer Res., 56, 5403-5409.

74 Bigsby RM, Caperell-Grant A, and Madhukar BV. (1997). Cancer Res., 57, 865-869.

75 Mes J. (1992). Bull. Environ. Contam. Toxicol., 48, 815-820.

76 Shen K and Novak RF. (1997). Biochem. Biophys. Res. Comm., 231, 17-21.

77 Kelce WR, Stone CR, Laws SC, Gray LE, Kemppainen JA, and Wilson EM. (1995). Nature, 375, 581-585.

78 Badley JE, Bishop GA, St. John T, and Frelinger JA. (1988). Biotechniques, 286, 488-497.

79 Laemmli UK. (1970). Nature, 227, 680-685.

Figure 1 TCDD increases c-erbB2 and c-erbB3 mRNA in T47D$^+$ but not T47D$^-$ cells.

Membranes containing 5 µg of mRNA from T47D$^-$ cells treated with or without 10^{-8} M TCDD, and T47D$^+$ cells treated with or without 10^{-7} M ICI 182,780 for 24 hours, followed by exposure to TCDD for 24 hours in the continued presence or absence of ICI, were probed for c-erbB2, c-erbB3 and ß-actin, as described in Methods. An increase in both c-erbB2 message (4-fold) and c-erbB3 message (3-fold) was observed in T47D$^+$ cells in response to TCDD. ICI further increased mRNA levels for both kinases. TCDD was without effect on c-erbB2 or c-erbB3 levels in T47D$^-$ cells. The figure depicts a representative blot, n≥3.

Figure 2 TCDD increases c-erbB2 and c-erbB3 protein in T47D$^+$ cells, but not in T47D$^-$ cells.

A) Total cellular proteins were isolated from T47D$^+$ cells treated with or without 10^{-8} M TCDD for 24 to 72 hours. 30 µg total cellular protein was immunoblotted for c-erbB2 or c-erbB3, as described in Methods. The doublet observed in c-erbB3 protein expression beginning at 48 hours was repeatable in 3 total trials, and may be the result of cellular processing of the receptor or altered phosphorylation status. B) Total cell lysates from T47D$^+$ and T47D$^-$ cells treated with or without TCDD for 24 hours were immunoblotted for c-erbB2. Protein levels in T47D$^-$ cells, unaffected by TCDD, were much greater than levels observed in T47D$^+$ cells, with or without TCDD treatment. The figure depicts representative blots, n≥3.

Figure 3 Tyrosine phosphorylation of c-erbB2 and c-erbB3 is elevated in T47D$^+$ cells following TCDD treatment.

Total cellular proteins were isolated from T47D$^+$ cells treated with or without 10^{-8} M TCDD for 48 hours. Proteins for c-erbB2 and c-erbB3 were immunoprecipitated from 1 mg total

protein and immunoblotted for phosphotyrosine, as described in Methods. Tyrosine phosphorylation of c-erbB2 and c-erbB3 increased following TCDD exposure (5- and 2-fold, respectively) to an extent reflective of the TCDD-induced increase in the total c-erbB2 or c-erbB3 receptor levels (9- and 2-fold, respectively). Heregulin stimulation further elevated tyrosine phosphorylation levels for both receptors above TCDD-stimulated levels. This suggests that TCDD is not activating c-erbB2 or c-erbB3 directly, as heregulin does.

Figure 4 TCDD does not affect ER levels in $T47D^+$ cells after 24 hours.

Total cell lysates (30 μg) from $T47D^+$ cells treated with or without 10^{-7} M ICI for 24 hours, followed by exposure to 10^{-8} M TCDD for 24 hours in the continued presence or absence of ICI, along with 30 μg of total cell lysates from $T47D^-$ cells treated with or without TCDD, were immunoblotted for ER. TCDD alone had no effect on cellular ER protein levels. ICI treatment decreased cellular ER protein by 70%, either in the presence or absence of TCDD. $T47D^-$ cells did not express ER protein.

Figure 5 Signaling through MAP kinase is increased in TCDD-treated $T47D^+$ cells in response to 10^{-9} M heregulinß$1_{177-244}$.

$T47D^+$ cells, treated for 48 h with 10^{-8} M TCDD, were starved in serum free medium for 6 hours then stimulated with 10^{-9} M HRG for 5 min. Total cellular proteins (30 μg) were immunoblotted for ERK1/2 (A) or activated MAP kinase (B), as described in Methods. Levels of total cellular ERK 1 and ERK 2 were not changed by exposure to TCDD or HRG. Signal for activated MAPKs was not visible for non-heregulin-stimulated samples. Following exposure to TCDD, activated MAP kinase levels were 6-fold or 4-fold greater than in DMSO-treated cells for ERK 2 and ERK 1, respectively. The figure depicts a representative blot, $n \geq 3$.

Figure 6 Amounts of tyrosine phosphorylated p85 subunit of PI3 kinase are increased in

TCDD-treated cells in response to 10^{-9} M heregulinß1$_{177-244}$.

T47D^{+} cells, treated for 48 h with or without 10^{-8} M TCDD, were starved in serum free medium for 6 hours then stimulated with 10^{-9} M heregulin for 5 min. A) Total cell lysates (30 µg) were immunoblotted for p85 as described in Methods. Neither TCDD or HRG effected levels of total cellular p85. B) Total cellular proteins (500 µg) were immunoprecipitated with anti-phosphotyrosine antibody as described in Methods. Membranes were immunoblotted for p85. Non-heregulin stimulated samples displayed no signal. Immunoprecipitates from heregulin-challenged cells treated with TCDD had 15-fold greater tyrosine phosphorylation of p85 than heregulin-challenged cells treated with DMSO.

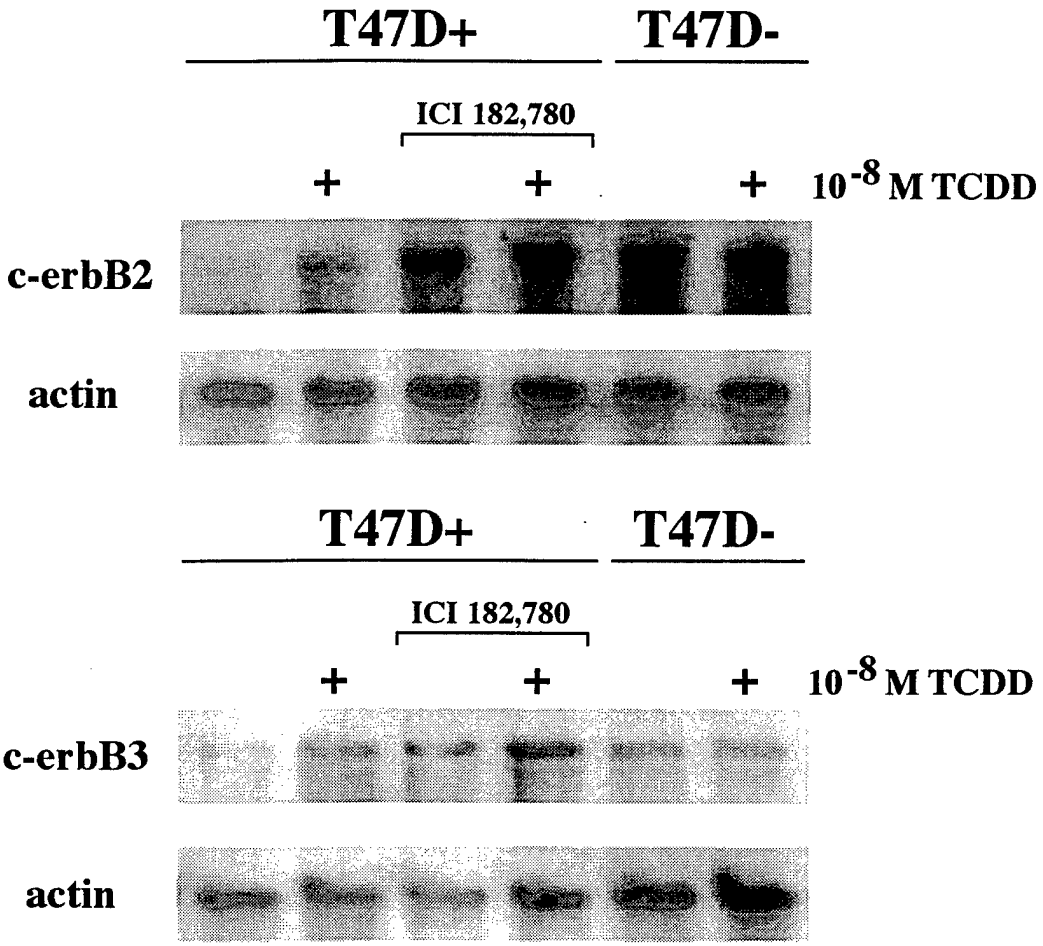
T47D+
T47D-
ICI 182,780
+
+
+
10-8 M TCDD
c-erbB2
actin
T47D+
T47D-
ICI 182,780
+
+
+
10-8 M TCDD
c-erbB3
actin

A

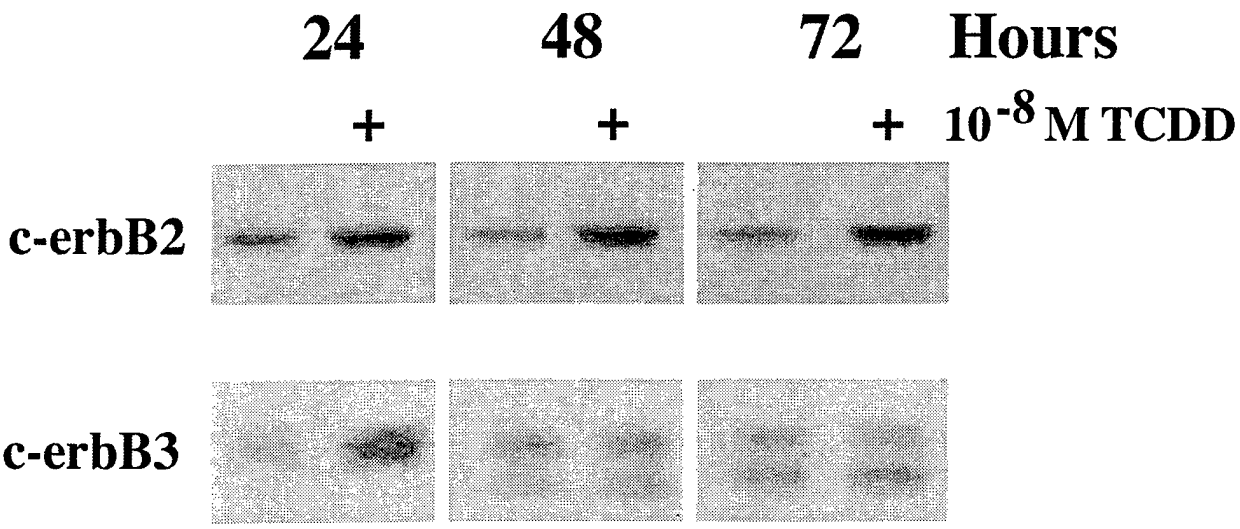
24
48
72
Hours
+
+
+
10-8 M TCDD
c-erbB2
c-erbB3

B

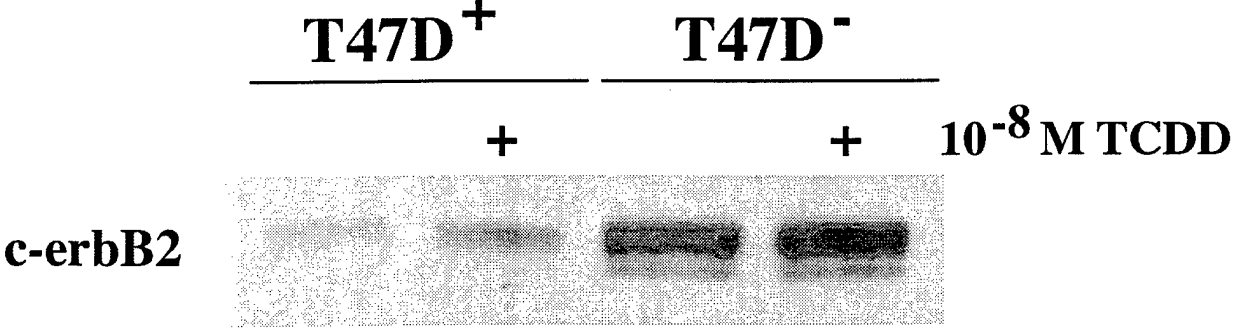
T47D+
T47D-
+
+
10-8 M TCDD
c-erbB2

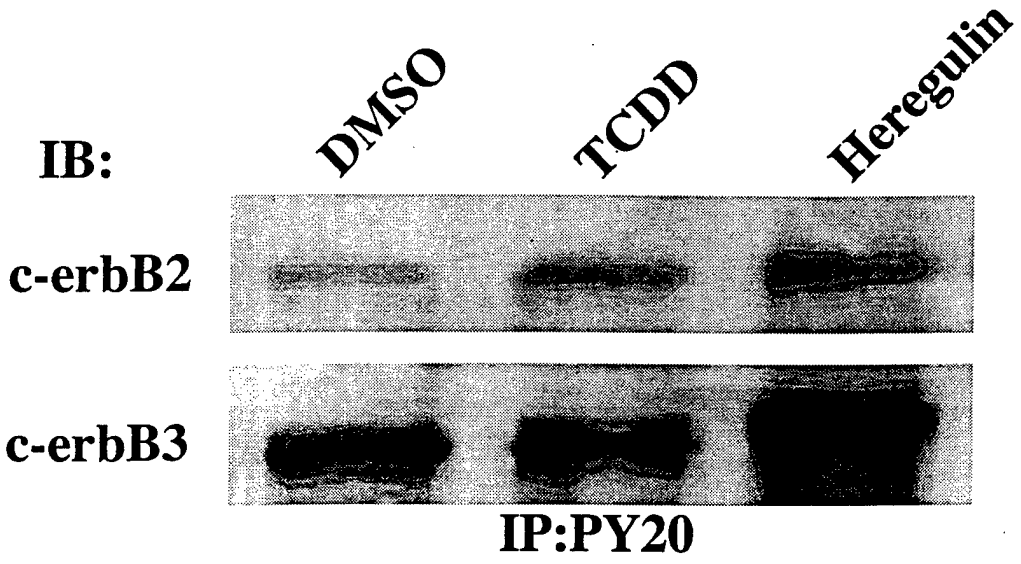
DMSO
TCDD
Heregulin
IB:
c-erbB2
c-erbB3
IP:PY20

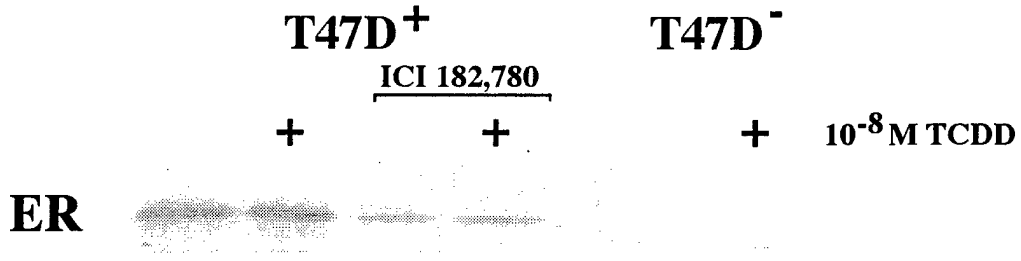
T47D+
T47D-
ICI 182,780
+
+
+
10-8 M TCDD
ER

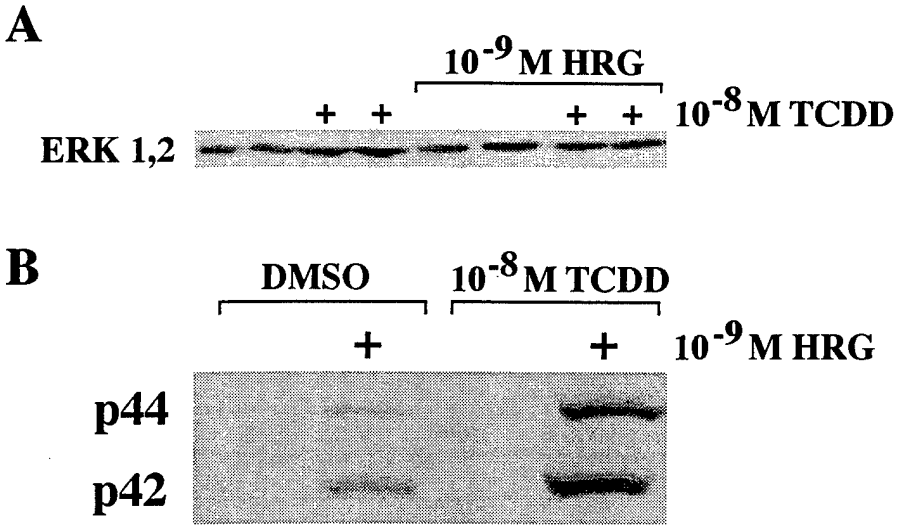
A
10-9 M HRG
+ +
+ +
10-8 M TCDD
ERK 1,2
B
DMSO
10-8 M TCDD
+
+
10-9 M HRG
p44
p42

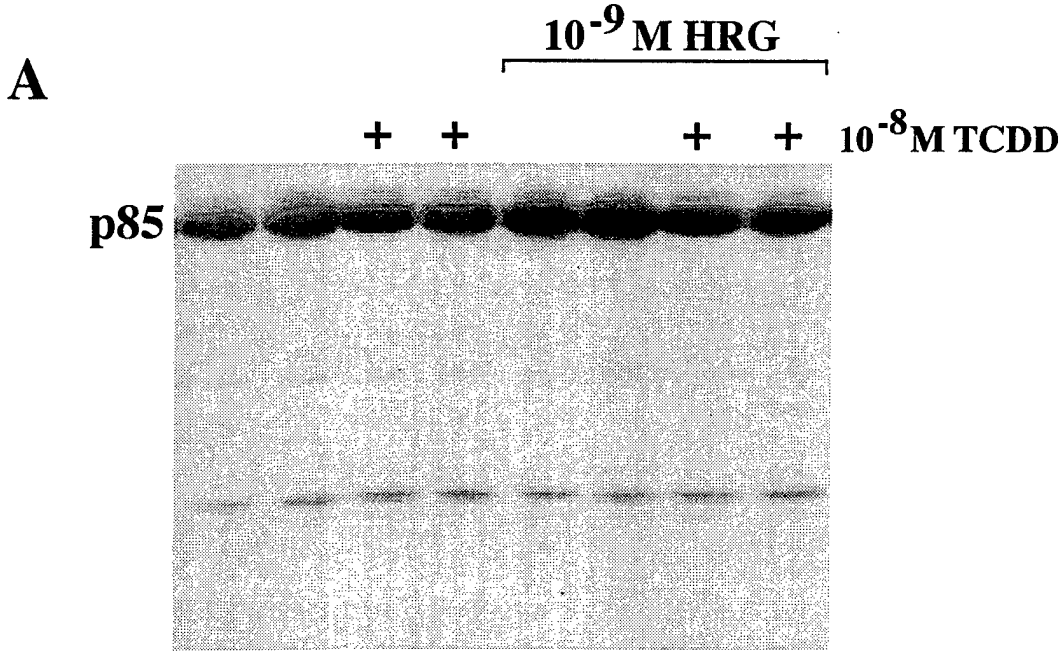
A
10-9 M HRG
+ + + +
10-8 M TCDD
p85

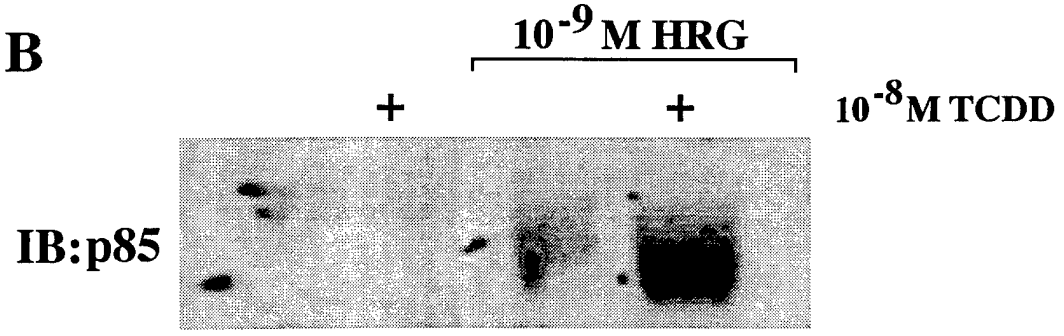
B
10-9 M HRG
+ +
10-8 M TCDD
IB:p85
IP: Phosphotyrosine

(Submitted to Carcinogenesis)

Cell- and Developmental Stage-specific Expression of Cytochrome P4501B1 in the Rat Mammary Gland.

Paul B. Brake[1], Michele Campaigne Larsen[1], Paul R. Hanlon[2], and Colin R. Jefcoate[1,2,3]

[1]Environmental Toxicology Center and [2]Department of Pharmacology, University of Wisconsin Medical School, 1300 University Avenue, Madison, WI 53706.

[3] Author to whom correspondence should be addressed.

Abbreviations: Cytochrome P450, CYP; polycyclic aromatic hydrocarbon, PAH; aryl hydrocarbon receptor, AhR; β–napthoflavone, β–NF; Wistar Furth, WF; Wistar Kyoto, WK; rat mammary epithelial cells, RMEC; 2,3,7,8-tetrachlorodibenzo-p-dioxin, TCDD; rat mammary fibroblasts, RMF; reconstituted basement membrane, Matrigel; 7,12-dimethylbenz[a]anthracene, DMBA; fetal bovine serum, FBS.

Abstract

Cytochrome P4501B1 (CYP1B1) is the major constitutive polycyclic aromatic hydrocarbon (PAH)-metabolizing CYP expressed in the rat mammary gland. In this tissue, both CYP1B1 and the related CYP1A1 protein are induced by the aryl hydrocarbon receptor (AhR) agonist, ß-naphthoflavone (ß-NF). Induction occurs to 3- and 5-fold higher levels, respectively, in pregnant as compared to virgin animals. Immunohistochemical analysis indicates extensive expression of CYP1B1 in ductal epithelia, notably at the proliferating terminal end buds. Two strains of rats, Wistar Furth (WF) and Wistar Kyoto (WK), that are, respectively, highly susceptible and resistant to chemically-induced mammary carcinogenesis, display differences in ß-NF-induced mammary gland expression of these CYPs. WF rats express 5-fold higher levels of ß-NF-induced CYP1B1 compared to similarly-treated WK rats; conversely, WK rats express 3-fold higher induced levels of CYP1A1 than WF rats. Although CYP1B1 is expressed in the mammary epithelia *in vivo* following AhR activation, its expression is nearly undetectable in isolated rat mammary epithelial cells (RMECs) cultured on plastic and stimulated with 2,3,7,8-tetrachlorodibenzo-*p*-dioxin (TCDD) which then preferentially express CYP1A1. CYP1B1 is, however, constitutively expressed and stimulated by TCDD in isolated rat mammary fibroblasts (RMF). When RMEC are cultured on reconstituted basement membrane (Matrigel) for 2 days, this promotes ductal morphogenesis and increases the levels of TCDD-induced CYP1B1 and CYP1A1 expression 2- to 3-fold relative to levels seen in RMEC cultured on plastic. We also observed increases in 7, 12-dimethylbenz[*a*]anthracene (DMBA) metabolism for RMEC cultured on matrigel compared to plastic, consistent with similar increases in functional CYP1B1 and CYP1A1.

Introduction

The formation of mammary cancer depends upon the interplay of, in part, various developmental, hormonal, and environmental factors with the multiple stages of the cancer process. Growth and differentiation of the mammary gland is dependent upon tightly controlled mesenchymal-epithelial interactions occurring in the developing gland (1). Stromal fibroblasts, of mesenchymal origin, probably play a key role in regulating growth and differentiation of epithelia and myoepithelia which form the ductal structures of the mammary gland (2). The demonstration of interactions between these cell types *in vitro* and the observation that fibroblasts mediate some of the estrogenic control of mammary development (3) lends credence to this hypothesis. These interactions may also be important in determining the regulatory activity of stromal cells on epithelial cells, which almost certainly involves the release of multiple growth factors (4,5). This growth promotion may be a key part of the cancer process.

In rats, polycyclic aromatic hydrocarbons (PAHs) such as 7,12-dimethylbenz[*a*]anthracene (DMBA) are proven mammary carcinogens (6), presumably through metabolic activation to a mutagenic dihydrodiol epoxide (7) catalyzed by cytochrome P4501A1 (CYP1A1) (8) and the recently described rodent CYP1B1 (9,10). The 2,3,7,8-tetrachlorodibenzo-*p*-dioxin (TCDD)-inducible human ortholog of CYP1B1 has also recently been described (11). Each is regulated through the aryl hydrocarbon receptor (AhR) and induced by PAHs and halogenated aromatic hydrocarbons. This laboratory has previously shown that DMBA is metabolized in cultured rat mammary epithelial cells (RMEC), principally by CYP1A1 (12). Conversely, PAH metabolism within rat mammary fibroblasts (RMF), which selectively express CYP1B1 (13), is constitutively high.

A 52 kDa TCDD-inducible protein was previously recognized with antibodies raised against purified mouse and a rat CYP1B1 in human squamous carcinoma cells and a mammary carcinoma cell line, MCF-7 (14). Constitutive metabolism of DMBA in these MCF-7 cells has been attributed to CYP1B1 by antibody inhibition studies using antibodies generated against CYP1B1. TCDD has also been shown to increase the C-4 hydroxylation of estradiol in MCF-7 cells, an activity that was similarly inhibited with antibodies to CYP1B1 (15) and is catalyzed by recombinant human CYP1B1 (16).

We are interested in further characterizing expression of the PAH-metabolizing CYPs, CYP1B1 and CYP1A1, in the rat mammary gland. CYP1B1 metabolizes PAHs such as DMBA and benzo[*a*]pyrene with only slightly lower specific activities than CYP1A1, but more effectively catalyzes the formation of the DMBA-3,4-dihydrodiol (17). This is the precursor to the bay region

diol epoxide believed to be the ultimate carcinogenic form of DMBA (18,19). However, its constitutive expression and hormonal regulation in steroidogenic and steroid-responsive tissues (9,17,20,21) leads us to believe that CYP1B1 has a physiological function.

In this manuscript we have analyzed the expression of CYP1B1 in the rat mammary gland *in vivo*, and compared this expression to that seen *in vitro*, using isolated RMEC. We hypothesize that the apparent discrepancy between the *in vivo* and *in vitro* expression of CYP1B1 results from culturing RMEC on plastic (13), and that CYP1B1 expression in rat mammary epithelia is dependent on the cellular environment. To this end, RMEC have been cultured on reconstituted basement membrane (matrigel), which stimulates ductal morphogenesis of RMEC, to investigate the effect of ECM on expression and regulation of CYP1B1 by the AhR. We have also compared the expression of CYP1B1 in two strains of rats that show differing susceptibilities to chemically-induced mammary cancer.

Materials and Methods

Chemicals

DMBA, benz[*a*]anthracene, ß-NF, cortisone, DNase II, and dimethylsulfoxide (DMSO) were purchased from Sigma Chemical Company (St. Louis, MO). TCDD was purchased from Chemsyn Science Laboratories (Lenexa, KS). Collagenase (type III) for rat mammary cell preparations was purchased from Worthington Biochemical Corp. (Freehold, NJ). Dulbecco's modified Eagle's medium/F12 (DME:F12, 1:1) for cell culture work was purchased from Gibco (Grand Island, NY). Fetal bovine and dextran/charcoal-stripped fetal bovine serums were purchased from Gemini Bioproducts, Inc. (Calabasas, CA). Solvents for HPLC analyses were purchased from Fisher Scientific (Itasca, IL). Tissue culture plates (Falcon) were purchased from Fisher Scientific (Itasca, IL). Reconstituted basement membrane (manufactured and distributed under the trademark name, matrigel) and low zinc insulin were purchased from Collaborative Biomedical Products. (Bedford, MA). All other chemicals were purchased from Sigma Chemical Company (St. Louis, MO).

Animals and tissues

All animals and animal tissues used in these studies were purchased from Harlan Sprague-Dawley and Harlan Bioproducts for Science, Inc. (Madison, WI). Virgin female Sprague-Dawley rats, 7-8 weeks old, and timed-pregnant Sprague-Dawley rats, were used for comparison of CYP

expression in mammary glands in response to AhR agonists. Virgin female WF and WK rats, 7-8 weeks old, were used for the comparison of CYP expression in mammary gland studies. Fresh mammary glands from virgin female Sprague-Dawley rats, 50-55 days old, were used for all rat mammary cell preparations.

Animal treatments

In the studies measuring the effect of ß-NF on CYP1B1 expression in the mammary glands of virgin and pregnant animals, adult female Sprague-Dawley rats, virgin or pregnant, were injected intraperitoneally with vehicle control (canola oil) or 60 mg/kg body weight of ß-NF for three consecutive days. Twenty-four hr after a final injection, rats were sacrificed by cervical dislocation and mammary glands removed, weighed, and processed for isolation of microsomal protein. In the studies measuring the effect of ß-NF on CYP1B1 expression in the mammary glands of Wistar animals, adult female WF and WK rats, virgin, were injected intraperitoneally with vehicle control (canola oil) or 60 mg/kg body weight of ß-NF for three consecutive days. Twenty-four hr after a final injection, rats were sacrificed by cervical dislocation and mammary glands removed, weighed, and processed for isolation of microsomal protein.

Preparation of rat mammary cells and cell culture

Rat mammary fibroblast (RMF) and epithelial cells (RMEC) were prepared following the protocols of Hahm and Ip (22,23), except for a few modifications. Briefly, the lower 4 to 6 abdominal/anogenital mammary glands were excised from virgin female Sprague-Dawley rats and placed in PBS buffer on ice. In a sterile hood, the glands were finely minced with a scalpel and resuspended in a digestion solution [DME/F12 (1:1), pH 7.2, supplemented with 0.2% (w/v) collagenase (type III), 0.2% (w/v) dispase (grade II), 5% FBS, 50 µg/ml gentamycin]. This mixture was incubated in a shaking incubator (200 rpm) at 37°C for 3 hr. At the end of this incubation, 100 µg/ml DNase (type III) was added and the mixture incubated another 10 min. Undigested tissue was allowed to settle for 2-3 minutes and the cells aspirated off, removed to another sterile 50 ml tube, and centrifuged at 500 x *g* for 5 min to pellet the cells. Fat was aspirated off and discarded and the cell/organoid pellet was resuspended in fresh medium [DME/F12, pH 7.2, supplemented with 5% FBS and 50 µg/ml gentamycin] and centrifuged at 500 x *g* for 5 min. The pellet was resuspended in 10 ml fresh medium and organoids were filtered through a sterile nylon mesh (Nytex membrane) and the organoid clumps rinsed with fresh medium. The flow through, which is comprised of single cells and small cell clumps, was collected and centrifuged at 500 x *g* for 5 min, and the resulting cell pellet was resuspended in

fresh fibroblast medium [DME/F12 (1:1), pH 7.2, supplemented with 10% FBS], and plated in 175 cm^2 flasks. The RMEC were washed from the membrane and collected in a sterile 50 ml tube and centrifuged at 500 x *g* for 5 min. The RMEC were resuspended in fresh medium and plated onto 175 cm^2 dishes and incubated in a humidified atmosphere of 5% $C0_2$/95% air at 37°C for 1 hr to allow for fibroblast attachment. RMF were reseeded 3-4 times to remove any contaminating epithelial cells before experiments were performed on these cells. The organoids were then collected from the dish, pelleted, and resuspended in complete mammary epithelial cell medium [DME/F12 (1:1), pH 7.2, supplemented with 5% FBS, 10 µg/ml insulin (low zinc), 1 µg/ml progesterone, 1 µg/ml cortisol, 5 µg/ml transferrin, 10 ng/ml epidermal growth factor, 1 µg/ml prolactin, 5 µM vitamin C, 50 µg/ml gentamycin, 1 mg/ml fatty acid-free bovine serum albumin (BSA)], plated onto 30 cm^2 plates, and incubated overnight in a humidified atmosphere of 5% $C0_2$/95% air at 37°C. In certain cases organoids were plated onto matrigel-coated 30 cm^2 plates. These plates were thin-coated with matrigel solution (500 µl/10 cm^2) according to manufacturer's instructions and kept at 4°C under sterile conditions until use, at which time the plates were incubated at 37°C for at least 1 hr to solidify the matrigel. Following the overnight incubation fresh medium was added to the attached organoids, this medium being a serum-free complete mammary epithelial cell medium. Experiments were usually performed on these cells within 2 days of the original plating.

Preparation of microsomal protein from tissue and cell sources

Microsomal protein was prepared from tissue samples as follows, with all steps being performed on ice or at 4°C. Tissues were washed once with homogenization buffer [0.1 M $KHPO_4$, pH 7.25, 150 mM KCl, 10 mM EDTA, 0.25 mM phenylmethylsulfonylfluoride (PMSF), 0.1 mM dithiothreitol (DTT)] and resuspended in 2-3 volumes of homogenization buffer. Samples were then homogenized twice with a tissuemizer (Tekmar Tissuemizer) at 6000 rpm for 10 sec. The homogenate was centrifuged at 15,000 x *g* for 20 min and the post-mitochondrial/nuclear supernate collected. This supernate was then centrifuged at 105,000 x *g* for 90 min. The resulting cytosolic fraction (supernatant) was collected for later use, and the microsomal pellet was resuspended in wash buffer (0.1 M K PO_4, 10 mM EDTA, 0.25 mM PMSF, 0.1 mM DTT) and centrifuged at 105,000 x *g* for 60 min. Following washing, which lyses heme-containing contaminating red blood cells, the microsomal pellet was resuspended in 2-3 volumes of dilution buffer [0.1 M KH PO_4, pH 7.25, 10 mM EDTA, 0.25 mM PMSF, 0.1 mM DTT, 20% glycerol] and kept at -70°C until further use.

For microsomal preparations from monolayers of cultured cells, cells were washed once with PBS buffer and collected by scraping. In the case of mammary epithelial cells cultured on Matrigel, the cells were collected by scraping, centrifuged, and the solidified Matrigel removed from the cell pellet. Cells were resuspended in 2 volumes of hypotonic buffer and swelled on ice for 10 minutes then 2 volumes of homogenization buffer [0.1 M KH PO_4, pH 7.25, 150 mM KCl, 10 mM EDTA, 0.25 mM PMSF, 0.1 mM DTT] were added and the cells lysed by sonication using a sonicator cell disruptor (Heat Systems-Ultrasonics, Inc., model W185F, Plainview, NY) at 10 sec pulses. The lysate was centrifuged at 15,000 x *g* for 20 min to remove the mitochondrial/nuclear fraction. The post-mitochondrial/nuclear fraction was then centrifuged at 105,000 x *g* for 90 min to pellet the microsomal fraction. The resulting cytosolic fraction was collected and the microsomal pellet was resuspended in 2 volumes of dilution buffer [0.1 M $KHPO_4$, pH 7.25, 10 mM EDTA, 0.25 mM PMSF, 0.1 mM DTT, 20% glycerol] and kept at -70°C until further use. Both cytosolic and microsomal protein concentrations determined by the BCA protocol (Pierce, Rockford, IL).

In vitro PAH metabolism assay

RMECs grown in 30 cm^2 plates and treated with indicated compounds or 0.1% DMSO (control) for 24 hr were incubated with medium containing 5 µM DMBA for 1 hr. At the end of the incubation period the medium was removed and placed into individual 10 ml glass borosilicate tubes and treated with ß-glucuronidase solution [2000 IU ß-glucuronidase/ml, 0.5 M sodium acetate, pH 5.0, 0.5 mg/ml ascorbate] for 5 hr at 37°C to recover the polar glucuronidated DMBA metabolites. Cell number was determined for each sample by brief trypsinization of remaining cells at 37°C and counting on a hemocytometer. Cortisone, which is not produced by RMECs, was added as an internal standard before DMBA metabolites were extracted with ethyl acetate/acetone containing DTT (2:1:0.003). The solvent phases containing the DMBA metabolites and cortisone were removed and dried down under nitrogen gas and resuspended in 100 µl of methanol for HPLC analysis. Separation of DMBA metabolites by C18-reverse phase HPLC and quantitation relative to cortisone was carried out as previously described (12,24).

Western immunoblot analysis

Microsomal proteins were prepared for immunoblot analysis by suspension in sample loading buffer, heated at 100°C for 5 min, and separated by SDS-PAGE (8% acrylamide). Following separation, the proteins were transferred to nitrocellulose membranes (Shleicher & Schuell) and blocked in 1X TBST containing 5% milk overnight at 4°C (or for 1 hr at room

temperature). The membranes were washed in 1X TBST for 20 min before addition of the primary antibodies. Primary antibodies used in these studies include affinity purified antibodies to recombinant mouse CYP1B1 (25) and rat CYP1A1 (L. Shore and C. Jefcoate, unpublished). Following incubation with primary antibodies, the membranes were washed with 1X TBST for 20 min, then incubated with secondary antibody, anti-rabbit horse radish peroxidase (Promega, Madison, WI). Immunoreactive proteins were visualized by the enhanced chemiluminescence method (Amersham Corp., San Diego, CA) according to manufacturer's instructions.

RNA isolation and Northen hybridization analysis

Total RNA was isolated from cells using TRIzol reagent (Molecular Research Center, Inc., Cincinnati, OH) according to manufacturer's instructions. RNA was dissolved in diethylpyrocarbonate-treated, double-distilled H_20 (RNase-free) and kept at -70°C until use. Total RNA for each sample was separated on a 1% agarose-formaldehyde-formamide denaturing gel as previously described (26) and transferred by capillary action to a Nytran nylon membrane (Schleicher & Schuell) in 20X SSC for 18 hr. RNA was immobilized by UV-induced covalent linkage to the membrane using a UV Stratalinker 1800 (Fisher Scientific) (1900 joule x 100 for 30 sec). Hybridization was carried out with an EcoRI-HindIII fragment of the C-terminal of rat CYP1B1 cDNA (700 bp) (9). A ß-actin probe was used to quantitate the levels of RNA in each lane. Each probe was labeled with [a-^{32}P]dCTP (3000 Ci/mmol) by the random-primed labeling method of Stratagene (San Diego, CA) according to manufacturer's instructions. Signals were detected by phosphoimager analysis.

Analytical methods

Quantitation and densitometry of the immunoblot and Northern blots was performed using a Zeineh soft laser scanning densitometer (model SL-504-XL, Biomed Instruments, Inc., Fullerton, CA) and by analysis of electronically scanned images on a Power Macintosh 6100/60 using the public domain NIH Image (version 1.56) program (written by Wayne Rasband at the U.S. National Institutes of Health and available from the Internet by anonymous FTP from zippy.nimh.nih.gov). Quantitation of phosphoimages and electronically scanned images (saved as TIFF files) was also performed with the software Imagequant (version 1.0).

Statistics

Statistical analysis of results was carried out using a Student's *t*-test. Values for DMBA metabolism are reported as cell variance. Significance was set at $p < 0.05$.

Results

Expression of CYP1B1 in control and ß-NF-induced rat mammary glands

Virgin and pregnant female Sprague-Dawley rats were treated with vehicle control or ß-NF to assess the expression and regulation of CYP1B1 in the rat mammary gland and compare this expression in the glands of functionally developed animals (pregnant) to immature animals (virgin). CYP1B1 is only weakly expressed basally but induced following ß-NF induction in virgin rats. The induced levels were 3-fold higher in the mammary glands of pregnant animals (Figure 1A). CYP1A1 is similarly highly induced in the mammary gland, with again 3-fold higher levels in the pregnant animals (Figure 1B). The increase in induced CYP1B1 and CYP1A1 in the mammary glands of pregnant animals could be attributable to an increase in the epithelial population associated with the extensive ductal proliferation in the gland and also to the more extensive differentiation (27). The relative levels of expression for CYP1B1 are about 10-fold lower than CYP1A1. AhR was expressed at lower than detectable levels in these tissues (not shown).

Expression of CYP1B1 in the mammary glands of two Wistar rat strains

WF and WK rat strains exhibit differing susceptibilities to the mammary carcinogen, DMBA, with WF being highly susceptible and WK being very resistant (28). We, therefore, assessed the levels of expression of the PAH-metabolizing CYPs, CYP1B1 and CYP1A1, in response to AhR activation, in the mammary glands of virgin female WF and WK rats. The highly sensitive WF rats expressed 5-fold higher levels of ß-NF-induced CYP1B1 protein levels in the mammary gland compared to similarly treated WK rats (Figure 2A). Conversely, WK rats express 3-fold higher levels of CYP1A1 in the mammary gland (Figure 2B). Interestingly, CYP1B1 is also expressed at 3-fold higher levels in the livers of WF rats, while CYP1A1 did not display strain-specific expression in the livers (Figures 2A and 2B). Levels of induced CYP1B1 protein in WF mammary glands are about 2-fold higher than induced CYP1A1, while induced CYP1A1 levels are estimated to be about 8-fold higher than induced CYP1B1 in WK mammary glands.

Expression of CYP1B1 in isolated rat mammary epithelial cells

There seems to be a discrepancy between this expression of CYP1B1 in the rat mammary gland *in vivo* and in isolated RMEC *in vitro* (13). The epithelia clearly provide the major location for this expression based on immunohistochemical analysis with anti-CYP1B1 antibodies (J.

Weisz, Penn State Medical Center, personal communication). However, when cultured on plastic substratum, expression of CYP1B1 was primarily localized to rat mammary fibroblasts (RMF), with very low expression in RMEC. We have attempted to characterize the basis for this difference in CYP1B1 expression in RMEC. Isolated rat mammary cells were characterized for expression of CYP1B1. As seen previously (13), CYP1B1 and CYP1A1 demonstrated cell-specific expression in cultured rat mammary cells, with constitutive and AhR-regulated CYP1B1 expressed in the RMF, and induced CYP1A1 preferentially expressed in RMEC (Figures 3A and 3B). RMEC cultured on plastic express only very low levels of induced CYP1B1, which is probably attributable to fibroblast contamination, which grow in between the RMECs (see below).

Effect of matrigel on CYP1B1 expression in RMEC

RMEC were cultured on plastic and on thin-layer matrigel for 2 days, and photographed to visualize the effects of Matrigel on morphology of RMEC (Figure 4). RMEC cultured on a plastic substratum display less organized structures, with a lawn of tightly-growing, fibroblast-like cells spread out between the RMECs, and minimal growth projections. RMEC cultured on matrigel, however, exhibit ductal projections and three-dimensional web units composed of ducts and lobular-like budding clusters. Fibroblast-like cells were not detectable in the presence of matrigel. RMEC morphologies seen here are consistent to those characterized elsewhere, where RMEC cultured on matrigel proliferate and develop structures such as ductules and lobular-like clusters (29,30).

We assessed the expression of CYP1B1 and CYP1A1 from RMEC grown on matrigel. RMEC cultured on matrigel displayed readily detectable levels of TCDD-induced 5.2 kilobase (kb) CYP1B1 mRNA and protein (Figures 5A and 5B). TCDD-induced CYP1A1 protein was also strongly expressed in RMEC on matrigel (Figure 5B). In several experiments in which RMEC were grown on plastic, CYP1B1 was detectable but this was in proportion to the level of contaminating RMF (13).

Effect of matrigel on in vitro PAH metabolism in RMEC

RMEC cultured on plastic or thin-layer matrigel were assessed for DMBA metabolism in response to TCDD stimulation. Although metabolic activities were highly induced in RMEC cultured on matrigel, induced activities of cells cultured on plastic were substantial as well at 60% of the total activity seen in RMEC cultured on matrigel (Table I). The profile of regioselective DMBA metabolites is indicative of a mixture of both CYP1B1 and CYP1A1 catalyzed activity, based on the fact that CYP1B1 selectively metabolizes DMBA at the 10,11- and 3,4-dihydrodiol

positions (25), while CYP1A1 is mainly responsible for 5,6- and 8,9-dihydrodiol and 7-OH-methyl positions (8). Again, this high level of activity in RMEC cultured on plastic is probably attributable to contaminating fibroblasts (13), that express high basal and inducible levels of CYP1B1.

Discussion

We provide evidence here that CYP1B1 expression in RMEC is controlled by the culture conditions of the cells. RMEC cultured on matrigel exhibit clearly defined ductal morphologies that are not seen on plastic and also show evidence of a more differentiated state. We now find that RMEC grown on matrigel express much higher levels of induced CYP1B1 than cells cultured on plastic substratum. Matrigel contains several extracellular matrix proteins, but is predominantly laminin, and may also contain several growth factors. It is not known at this point what effect these factors have on expression of CYP1B1 or CYP1A1. Expression of specific CYPs in cultured hepatocytes has also been demonstrated to be dependent upon matrigel (31,32). We also present evidence here for strain differences in mammary cancer susceptible WF and resistant WK rats in expression of the major PAH-metabolizing CYPs in the rodent mammary, CYP1B1 and CYP1A1. CYP1B1 is induced to high levels by PAHs in the mammary glands of susceptible WF rats, which also display significantly higher levels of induced CYP1B1 in their livers as well. This has not been observed before, and may link expression of this CYP to development of mammary cancer in this strain. A possible reason for this difference could be linked to differences in the developmental stage of the mammary gland between these two strains. The glands of the WK rats show more ductal proliferation and express more differentiated functions (i.e. casein production) than the mammary glands of WF rats (33).

We have also confirmed that isolated RMF selectively express CYP1B1, and not CYP1A1 (13). A constitutively expressed CYP1B1 is induced through the AhR to high levels. There is strong evidence that stromal fibroblasts modulate hormonal responses in endocrine tissues such as the mammary gland (5,27), uterus (34), and prostate (35). Upon hormonal stimulation, fibroblasts respond by releasing growth factors and extracellular matrix proteins that positively and negatively regulate epithelial cell growth and differentiation.

It has previously been determined in this laboratory that RMEC express PAH-metabolizing forms (12). Selective antibody-inhibition studies demonstrated that CYP1A1 contributed to half of the induced total DMBA metabolism. DMBA-induced mammary carcinomas arise predominantly

from parenchymal cells, but cultures of both stromal fibroblasts and epithelial cells are able to metabolize DMBA to a number of toxic metabolites, including the 3,4-dihydrodiol, precursor to the bay region diol epoxide believed to be the ultimate carcinogenic form of DMBA (18,19). It is now known that CYP1B1 is responsible for metabolism of DMBA to the 3,4-dihydrodiol (25). Of interest is that RMEC and human MEC differ in their metabolism of PAH in culture. RMEC metabolize DMBA with high specific activity, resulting in increased rates of mutagenesis in cocultured V-79 cells (36). Human MEC, on the other hand, specifically metabolize benzo[*a*]pyrene to mutagenic by-products, and are less efficient at catalyzing the formation of the DMBA 3,4-dihydrodiol.

Expression of CYPs in the rat mammary gland has received little attention. Levels of CYP in the rat mammary gland have been determined by carbon monoxide difference spectra as ~5 pmol/mg in virgin animals and ~18 pmol/mg for pregnant animals (37). The authors did not speculate on the reason for this increase in CYP content in the mammary gland of pregnant animals, whether it is due to proliferation of epithelial cells, or an increase in the expression of specific CYP isoforms. Immunohistochemical analysis of rat mammary glands reveals that CYP1B1 is localized to the epithelial cells of the ducts and terminal end buds (J. Weisz, Penn State Medical Center, personal communication). Culturing of RMEC on matrigel, which promotes ductal morphogenesis and differentiated functions such as casein production (38,39), leads to increased AhR induction of CYP1B1. Several isoforms of P450 cytochromes, including CYP1A1, CYP2E1, CYP2D1, CYP2D3, CYP2D4, and CYP4A3, were shown to be substantially higher in the mammary glands of pregnant animals compared to lactating animals (37). These authors also observed constitutive levels of CYP1A1 in the glands of pregnant and lactating animals, which is absent in virgin animals and animals undergoing mammary gland involution. Thus, it appears that multiple forms of CYPs display a developmental- or differentiation-state specific expression profile in the rat mammary gland. We confirm here that ß-NF-induced levels of CYP1B1 and CYP1A1 are much higher in the glands of pregnant rats.

Thus, CYP1B1 expression and regulation in the rat mammary gland is cell- and developmental stage-dependent. The role of extracellular matrix in mediating CYP1B1 expression in RMEC explains the loss of this form in previous studies that used RMEC cultured on plastic. CYP1B1 also displays strain-specific expression in mammary glands, with PAH-induced CYP1B1 expressed at higher levels in the glands of mammary cancer susceptible WF rats. However, differences in strain susceptibility are not exclusive to DMBA, as direct-acting carcinogens like nitrosomethylurea display strain susceptibilities (40). The significance of these strain differences remains unknown at this point. However, they suggest that the ratio of CYP1B1/CYP1A1 may be

regulated in the rat mammary gland and is susceptible to genetic differences between these otherwise genetically similar strains. It is an intriquing possibility that there may be a relationship to cancer susceptibility genes.

Acknowledgments

We would like to thank Rene McCray of Harlan Bioproducts for Science (Madison, WI) for isolation of the rat mammary glands used in these studies. We would also like to thank Dr. Margaret Benton and Dr. Todd Thompson for advice in culturing rat mammary cells. This research was supported by NIEHS grant 144EN46 and DOD Breast Cancer Research grant DAMD17-94-J-4054.

References

1. Cunha, G. R. (1994) Role of mesenchymal-epithelial interactions in normal and abnormal development of the mammary gland and prostate. *Cancer*, **74**, 1030-1044.

2. Lazard, D., Sastre, X., Frid, M. G., Glukhova, M. A., Thiery, J. P., and Koteliansky, V. E. (1993) Expression of smooth muscle-specific proteins in myoepithelium and stromal myofibroblasts of normal and malignant human breast tissue. *Proc. Natl. Acad. Sci. U.S.A.*, **90**, 999-1003.

3. McGrath, C. M. (1983) Augmentation of the response of normal mammary epithelial cells to estradiol by mammary stroma. *Cancer Res.*, **43**, 1355-1360.

4. Seslar, S., Nakamura, T., and Byers, S. (1995) Tumor-stroma interactions and stromal cell density regulate hepatocyte growth factor protein levels: a role for transforming growth factor-beta activation. *Endocrinol..*, **136**, 1945-1953.

5. Seslar, S. P., Nakamura, T., and Byers, S. W. (1993) Regulation of fibroblast hepatocyte growth factor/scatter factor expression by human breast carcinoma cell lines and peptide growth factors. *Cancer Res.*, **53**, 1233-1238.

6. Huggins, C., and Fukunishi, R. (1963) Mammary and peritoneal tumors induced by intraperitoneal administration of 7,12-dimethylbenz[a]anthracene in newborn and adult rats. *Cancer Res.*, **23**, 785-789.

7. Cooper, C. S., Pal, K., Hewer, A., Grover, P. L., and Sims, P. (1982) The metabolism and activation of polycyclic aromatic hydrocarbons in epithelial cell aggregates and fibroblasts prepared from rat mammary tissue. *Carcinogenesis*, *3*, 203-210.

8. Wilson, N. M., Christou, M., Turner, C. R., Wrighton, S. A., and Jefcoate, C. R. (1984) Binding and metabolism of benzo[a]pyrene and 7,12-dimethylbenz[a]anthracene by seven purified forms of cytochrome P-450. *Carcinogenesis*, **5**, 1475-1483.

9. Bhattacharyya, K. K., Brake, P. B., Eltom, S. E., Otto, S. A., and Jefcoate, C. R. (1995) Identification of a rat adrenal cytochrome P450 active in polycyclic hydrocarbon metabolism as rat CYP1B1. Demonstration of a unique tissue-specific pattern of hormonal and aryl hydrocarbon receptor-linked regulation. *J. Biol. Chem..*, **270**, 11595-11602.

10. Savas, Ü., and Jefcoate, C. R. (1994) Dual regulation of cytochrome P450EF expression via the aryl hydrocarbon receptor and protein stabilization in C3H/10T1/2 cells. *Mol. Pharmacol..*, **45**, 1153-1159.

11. Sutter, T. R., Tang, Y. M., Hayes, C. L., Wo, Y. Y., Jabs, E. W., Li, X., Yin, H., Cody, C. W., and Greenlee, W. F. (1994) Complete cDNA sequence of a human dioxin-inducible mRNA identifies a new gene subfamily of cytochrome P450 that maps to chromosome 2. *J. Biol. Chem..*, **269**, 13092-13099.

12. Christou, M., Moore, C. J., Gould, M. N., and Jefcoate, C. R. (1987) Induction of mammary cytochromes P-450: an essential first step in the metabolism of 7,12-dimethylbenz[a]anthracene by rat mammary epithelial cells. *Carcinogenesis*, **8**, 73-80.

13. Christou, M., Savas, Ü., Schroeder, S., Shen, X., Thompson, T., Gould, M. N., and Jefcoate, C. R. (1995) Cytochromes CYP1A1 and CYP1B1 in the rat mammary gland: cell-specific expression and regulation by polycyclic aromatic hydrocarbons and hormones. *Mol. Cell. Endocrinol..*, **115**, 41-50.

14. Christou, M., Savas, Ü., Spink, D. C., Gierthy, J. F., and Jefcoate, C. R. (1994) Co-expression of human CYP1A1 and a human analog of cytochrome P450-EF in response to 2,3,7,8-tetrachlorodibenzo-p-dioxin in the human mammary carcinoma-derived MCF-7 cells. *Carcinogenesis*, **15**, 725-732.

15. Spink, D. C., Hayes, C. L., Young, N. R., Christou, M., Sutter, T. R., Jefcoate, C. R., and Gierthy, J. F. (1994) The effects of 2,3,7,8-tetrachlorodibenzo-p-dioxin on estrogen metabolism in MCF-7 breast cancer cells: evidence for induction of a novel 17 beta-estradiol 4-hydroxylase. *J. Steroid Biochem. Molec. Biol..*, **51**, 251-258.

16. Shimada, T., Hayes, C. L., Yamazaki, H., Amin, S., Hecht, S. S., Guengerich, F. P., and Sutter, T. R. (1996) Activation of chemically diverse procarcinogens by human cytochrome P-450 1B1. *Cancer Res.*, **56**, 2979-2984.

17. Otto, S., Bhattacharyya, K. K., and Jefcoate, C. R. (1992) Polycyclic aromatic hydrocarbon metabolism in rat adrenal, ovary, and testis microsomes is catalyzed by the same novel cytochrome P450 (P450RAP). *Endocrinol.*, **131**, 3067-3076.

18. Slaga, T. J., Gleason, G. L., DiGiovanni, J., Sukumaran, K. B., and Harvey, R. G. (1979) Potent tumor-initiating activity of the 3,4-dihydrodiol of 7,12-dimethylbenz(a)anthracene in mouse skin. *Cancer Res.*, **39**, 1934-1936.

19. Slaga, T. J., Gleason, G. L., Mills, G., Ewald, L., Fu, P. P., Lee, H. M., and Harvey, R. G. (1980) Comparison of the skin tumor-initiating activities of dihydrodiols and diol-epoxides of various polycyclic aromatic hydrocarbons. *Cancer Res.*, **40**, 1981-1984.

20. Otto, S., Marcus, C., Pidgeon, C., and Jefcoate, C. (1991) A novel adrenocorticotropin-inducible cytochrome P450 from rat adrenal microsomes catalyzes polycyclic aromatic hydrocarbon metabolism. *Endocrinol.*, **129**, 970-982.

21. Savas, Ü., Bhattacharyya, K. K., Christou, M., Alexander, D. L., and Jefcoate, C. R. (1994) Mouse cytochrome P-450EF, representative of a new 1B subfamily of cytochrome P-450s. Cloning, sequence determination, and tissue expression. *J. Biol. Chem.*,. **269**, 14905-14911.

22. Hahm, H. A., and Ip, M. M. (1990) Primary culture of normal rat mammary epithelial cells within a basement membrane matrix. I. Regulation of proliferation by hormones and growth factors. *In Vitro Cell. Develop. Biol.*., **26**, 791-802.

23. Hahm, H. A., Ip, M. M., Darcy, K., Black, J. D., Shea, W. K., Forczek, S., Yoshimura, M., and Oka, T. (1990) Primary culture of normal rat mammary epithelial cells within a basement membrane matrix. II. Functional differentiation under serum-free conditions. *In Vitro Cell. Develop. Biol.*., **26**, 803-814.

24. Christou, M., Marcus, C., and Jefcoate, C. R. (1986) Selective interactions of cytochromes P450 with the hydroxymethyl derivatives of 7,12-dimethylbenz[a]anthracene. *Carcinogenesis*, **7**, 871-877.

25. Savas, Ü., Carstens, C-P., and Jefcoate, C. R. (1997) Biological oxidations and P450 reactions. Recombinant mouse CYP1B1 expressed in *Escherichia coli* exhibits selective binding by polycyclic aromatic hydrocarbons and metabolism which parallels C3H10T1/2 cell microsomes, but differs from human recombinant CYP1B1. *Arch. Biochem. Biophys.*, **347**, 181-192.

26. Sambrook, J., Fritsch, E. F., and Maniatis, T. (1989) Molecular cloning, a laboratory manual. Cold Springs Harbor Laboratory Press, Cold Spring Harbor, NY.

27. Imagawa, W., Bandyopadhyay, G. K., and Nandi, S. (1990) Regulation of mammary epithelial cell growth in mice and rats. *Endocrine Rev.*, **11**, 494-523.

28. Haag, J. D., Newton, M. A., and Gould, M. N. (1992) Mammary carcinoma suppressor and susceptibility genes in the Wistar-Kyoto rat. *Carcinogenesis*, **13**, 1933-1935.

29. Kim, N. D., and Clifton, K. H. (1993) Characterization of rat mammary epithelial cell subpopulations by peanut lectin and anti-Thy-1.1 antibody and study of flow-sorted cells in vivo. *Exp. Cell Res.*, **207**, 74-85.

30. Kim, N. D., Oberley, T. D., and Clifton, K. H. (1993) Primary culture of flow cytometry-sorted rat mammary epithelial cell (RMEC) subpopulations in a reconstituted basement membrane, Matrigel. *Exp. Cell Res.*, **209**, 6-20.

31. Brown, S. E. S., Guzelian, C. P., Schuetz, E., Quattrochi, L. C., Kleinman, H. K., and Guzelian, P. S. (1995) Critical role of extracellular matrix on induction by phenobarbital of cytochrome P450 2B1/2 in primary cultures of adult rat hepatocytes. *Laboratory Investigations*, **73**, 818-827.

32. Guzelian, P. S., Li, D., Schuetz, E. G., Thomas, P., Levin, W., Mode, A., and Gustafsson, J. A. (1988) Sex change in cytochrome P450 phenotype by growth hormone

treatment of adult rat hepatocytes maintained in a culture system on matrigel. *Proc. Natl. Acad. Sci. U.S.A.*, **85**, 9783-9787.

33. Hsu, L. C., and Gould, M. N. (1993) Cloning and characterization of overexpressed genes in the mammary gland of rat strains carrying the mammary carcinoma suppressor (Mcs) gene. *Cancer Res.*, **53**, 5766-5774.

34. Wegner, C. C. and Carson, D. D. (1992) Mouse uterine stromal cells secrete a 30-kilodalton protein in response to coculture with uterine epithelial cells. *Endocrinol..*, **131**, 2565-2572.

35. Chung, L. W., Gleave, M. E., Hsieh, J. T., Hong, S. J., and Zhau, H. E. (1991) Reciprocal mesenchymal-epithelial interaction affecting prostate tumour growth and hormonal responsiveness. *Cancer Surveys* ,**11**, 91-121.

36. Moore, C. J., Tricomi, W. A., and Gould, M. N. (1986) Interspecies comparison of polycyclic aromatic hydrocarbon metabolism in human and rat mammary epithelial cells. *Cancer Res.*, **46**, 4946-4952.

37. Hellmold, H., Lamb, J. G., Wyss, A., Gustafsson, J. Å., and Warner, M. (1995) Developmental and endocrine regulation of P450 isoforms in rat breast. *Mol. Pharmacol..*, **48**, 630-638.

38. Darcy, K. M., Black, J. D., Hahm, H. A., and Ip, M. M. (1991) Mammary organoids from immature virgin rats undergo ductal and alveolar morphogenesis when grown within a reconstituted basement membrane. *Exp. Cell Res.*, **196**, 49-65.

39. Darcy, K. M., Shoemaker, S. F., Lee, P. P., Ganis, B. A., and Ip, M. M. (1995) Hydrocortisone and progesterone regulation of the proliferation, morphogenesis, and functional differentiation of normal rat mammary epithelial cells in three dimensional primary culture. *J. Cell. Physiol..*, **163**, 365-379.

40. Chan, P. C., Head, J. F., Cohen, L. A., and Wynder, E. L. (1977) Influence of dietary fat on the induction of mammary tumors by N-nitrosomethylurea: associated hormone

changes and differences between Sprague-Dawley and F344 rats. *J. Natl. Cancer Inst..*, **59**, 1279-83.

Fig. 1. Expression of ß-NF-induced CYP1B1 in the rat mammary gland. Virgin and pregnant female Sprague-Dawley rats were injected with vehicle control or 60 mg/kg ß-NF, as described in materials and methods. Animals were sacrificed and mammary glands removed and microsomal proteins prepared and analyzed by Western immunoblot for CYP1B1 (A) or CYP1A1 (B), as described in materials and methods. Protein loadings: for both CYP1B1 and CYP1A1 blots, 10 µg. Shown is an immunoblot representative of findings from two experiments.

Fig. 2. Expression of ß-NF-induced CYP1B1 in the mammary glands of WF and WK rats. Female Wistar/Furth (WF) and Wistar/Kyoto (WK) rats were injected with vehicle control or 60 mg/kg ß-NF, as described in materials and methods. Animals were sacrificed and mammary glands and livers removed and microsomal proteins prepared and analyzed by Western immunoblot for CYP1B1 (A) or CYP1A1 (B), as described in materials and methods. Protein loadings: mammary gland, 5 µg; liver, 2 µg. This experiment has been performed once.

Fig. 3. Cell-specific expression of CYP1B1 in isolated rat mammary cells. Rat mammary fibroblasts (RMF) and epithelial cells (RMEC) were isolated and cultured, as described in materials and methods. RMF (passage 3-4) or RMEC were treated with 0.1% DMSO (Con), 10^{-9} M TCDD, or 10^{-5} M benz[*a*]anthracene (BA) for the times (hr) indicated and the cells isolated and microsomal protein isolated and analyzed by Western immunoblot, as described in materials and methods, for CYP1B1 (A) or CYP1A1 (B). Loadings: for RMF (both CYP1B1 and CYP1A1 blots), 5 µg; for RMEC (both CYP1B1 and CYP1A1 blots), 10 µg. A CYP1A1 standard (1A1 Std), 10 ng, was included for control. Shown is a representative blot from two experiments.

Fig. 4. Effect of Matrigel on morphology of RMEC. Rat mammary epithelial cells (RMEC) were isolated and cultured as described in materials and methods on plastic dishes (A) or dishes prepared with thin layer Matrigel (B). Cells were grown for 2 days before being photographed. Ductal branching is indicated by arrows.

Fig. 5. Effect of matrigel on expression of CYP1B1 in RMEC. RMEC were isolated and cultured on dishes prepared with thin-layer matrigel. Cells were grown for 2 days before being treated with 0.1% DMSO (Co) or 10^{-9} M TCDD for 6 hr. Total RNA was isolated and analyzed by Northern hybridization (25 µg/lane) for CYP1B1 and ß-actin (A), as described in materials and methods. This experiment has been performed once. In panel (B), RMEC were grown for 2 days before being treated with 0.1% DMSO (C) or 10^{-9} M TCDD for 24 hr.

Microsomal protein was isolated and analyzed by Western immunoblot for CYP1B1 or CYP1A1 (B), as described in materials and methods. Protein loadings for (B): CYP1B1 blot, 10 μg; CYP1A1 blot, 10 μg. Standards for CYP1B1, 100 ng, and CYP1A1, 10 ng, were included as markers. This experiment has been performed once.

Submitted to Mol. Pharmacol
2/23/98

Ah-Receptor Regulation of Cytochrome P4501B1 in Rat Mammary Fibroblasts: Evidence for Transcriptional Repression by Glucocorticoids.

Paul B. Brake, Leying Zhang, and Colin R. Jefcoate

Environmental Toxicology Center (P.B., C.R.J.) and Department of Pharmacology (L.Z., C.R.J.), University of Wisconsin Medical School, 1300 University Avenue, Madison, WI 53706.

Running Title: Glucocorticoid Regulation of CYP1B1 in Rat Mammary Fibroblasts.

Corresponding Author: Colin R. Jefcoate
University of Wisconsin
Department of Pharmacology
3770 Medical Sciences Center
1300 University Avenue
Madison, WI 53706

Text: 27 pages
Figures: 6 figures
References: 39 references
Abstract: 244 words
Introduction: 756 words
Discussion: 923 words

Abbreviations: Cytochrome P450, CYP; polycyclic aromatic hydrocarbon, PAH; aryl hydrocarbon receptor, AhR; rat mammary fibroblasts, RMF; rat embryo fibroblasts, REF; 2,3,7,8-tetrachlorodibenzo-p-dioxin, TCDD; glucocorticoid, GC; dexamethasone, DEX; glucocorticoid receptor, GR; aryl hydrocarbon nuclear translocator, Arnt; glucorticoid response element, GRE; xenobiotic response element, XRE; fetal bovine serum, FBS.

Abstract

Cytochrome P4501B1 (CYP1B1), which actively metabolizes polycyclic aromatic hydrocarbons (PAH), is regulated by the aryl hydrocarbon receptor (AhR) in primary cultures of rat mammary fibroblasts (RMF) and embryo fibroblasts (REF). 2,3,7,8-tetrachlorodibenzo-*p*-dioxin (TCDD), induced the 5.2 kb CYP1B1 mRNA in RMF (12-fold) and REF (14-fold) following a 6 hr treatment, with comparable increases in the microsomal protein. The glucocorticoid, dexamethasone (DEX), suppresses TCDD-induced expression of CYP1B1 in RMF and REF. Suppression of CYP1B1 mRNA in RMF (maximal suppression, 70%) was observed when DEX was added 2 hr prior to TCDD, but not with co-administration. The concentration dependence ($EC_{50} \approx 10$ nM) and reversal by the antagonist, RU486, implicates the glucocorticoid receptor (GR). DEX inhibition of TCDD-induced CYP1B1 protein needed more extensive preincubation (>6 hr). TCDD-induction of CYP1B1-luciferase constructs in RMF was mediated by a 265 bp upstream region (-810 to -1075) which was similarly suppressed (50-70%) by a 2 hr preincubation with 10^{-7} M DEX via this enhancer region. Expression of the AhR is suppressed by DEX (70% after 12 hr), but not after the 2 hr period that is sufficient for suppression of transcription. The AhR nuclear translocator (Arnt) is not affected by this treatment. We conclude that GR rapidly suppresses activity of the AhR/Arnt complex in the CYP1B1 enhancer region, even though lacking GC responsive element(s). DEX inhibits proliferation of RMF in this same concentration range (35%, $EC_{50} \approx 5$ nM), indicating additional effects on intracellular signalling that may link to this suppression.

Introduction

This laboratory has established expression of cytochrome P4501B1 (CYP1B1) in the rat mammary gland. In culture, rat mammary epithelial cells express CYP1A1 but very little CYP1B1 when induced by aryl hydrocarbon receptor (AhR) agonists, while rat mammary fibroblasts (RMF) express both constitutive and AhR-inducible CYP1B1 (Christou, 1995). In RMF, CYP1B1 expression is suppressed by a complete hormonal mixture containing, in part, progesterone and glucocorticoids (GCs).

Systemic hormones, as well as locally acting growth factors combine to control the proliferation and differentiation of the mammary gland (Imagawa, 1990). Lactogenic hormones, such as GCs and prolactin, are examples of systemically-derived molecules that play a role in maintenance of mammary gland development (Dembinski and Shiu, 1987; Haslam, 1987). For example, the stage-specific regulation of milk protein gene expression is controlled by GC and prolactin. Multiple GC receptor (GR)-binding sites are present in the promoters of the ß-casein and whey acidic protein genes, and appear to work in synergy with prolactin-stimulated signal transduction pathways to activate transcription (Lechner, 1997) or to maintain the lactogenic state by downregulating remodeling proteases (Andreasen, 1990; Lund, 1996).

Previous work in this laboratory has reported that a complete hormonal mixture, which includes GCs, suppressed constitutive and PAH-induced levels of cytochrome P4501B1 (CYP1B1) in isolated rat mammary fibroblasts (RMF) (Christou, 1995). GCs have been shown to regulate a number of other drug metabolizing genes (Prough, 1996). In cultured adult rat hepatocytes, GCs potentiated the PAH-induction of CYP1A1, as well as a number of other phase II enzymes (glutathione S-transferase-Ya and UDP-glucuronyltransferase), while suppressing PAH-induction of NADPH:quinone oxidoreductase (Xiao, 1995). The CYP1A1 gene contains a functional GC response element in the first intron that mediates this potentiation (Mathis, 1989). GC suppression of CYP1A1 is developmentally specific, with neonatal rats being responsive to exogenously applied dexamethasone (DEX), while adolescent rats are relatively unaffected possibly because of much higher endogenous levels of GCs in adult rats (Linder, 1993).

TCDD activates transcription of CYP1A1 by stimulating AhR complex formation with the AhR nuclear translocator (Arnt) protein which then targets a cluster of xenobiotic response elements (XREs) approximately 1 kb upstream of the transcriptional start site (Denison, 1988; Denison, 1989; Whitlock, 1996). CYP1B1 is also regulated by the AhR in stromal fibroblasts from a number of sources, including the mammary gland, uterus, and embryo (Christou, 1995; Pottenger and Jefcoate, 1990; Savas, 1993). Basal levels of the 5.2 kilobase (kb) CYP1B1 mRNA are elevated several fold following TCDD treatment of these cells. Recently, a 265 base pair enhancer region of the CYP1B1 gene promoter, containing 5 XREs, has been shown to be essential for both basal and TCDD-induced expression (Zhang, 1998).

The AhR also controls a number of genes whose products may be involved in a number of cellular proliferation and differentiation processes (Okey, 1994). Recently, AhR-deficient mice were generated, and their phenotypes suggest a role for this receptor in hepatic growth and development (Fernandez-Salguero, 1995; Schmidt, 1996). AhR-deficient cells exhibit a decreased rate of cell proliferation due to a prolongation of cells in G_1 (Ma and Whitlock, 1996; Weiss, 1996) and TCDD has been demonstrated to exert a delay in G_1-S progression in hepatoma cells (Wiebel, 1991).

The glucocorticoid receptor (GR), regulates transcription in multiple ways which may affect AhR activity. GR homodimers bind to cognate DNA sequences known as GR responsive elements (GREs) then interact with the initiation complex on the promoter and enhance transcription (Bamberger, 1996, and references therein). In some cases, activated GR binds to so-called negative GREs (nGRE), causing inhibition, rather than enhancement of transcription. In other cases, genes regulated by activating protein-1, involving dimers of the Jun and Fos family of proteins, are negatively regulated when activated GR interacts directly with c-jun. GCs may also act indirectly and more slowly to inhibit transcriptional regulation of certain genes. For example, GCs may suppress a number of genes involved in the inflammatory response, such as cyclooxygenase-2, inducible nitric oxide synthase, and cytosolic phospholipase A, through induction of the transcriptional repressor, adenovirus E4 promoter binding protein (Wallace, 1997).

In this paper, we establish a similar regulation of CYP1B1 in RMF and in primary rat embryo fibroblasts (REF). We present a first analysis of promoter regulation of the AhR in these primary cells and link this to suppression of CYP1B1 expression by GCs (Christou, 1995). Notably, this study addresses whether steroid regulation is mediated through the TCDD enhancer region in the CYP1B1 gene through use of CYP1B1 promoter constructs. We also address whether GC affects TCDD induction of CYP1B1 by an indirect mechanism, such as through changes in AhR expression.

Materials and Methods

Chemicals

7,12-Dimethylbenz[*a*]anthracene (DMBA), dexamethasone (DEX), DNase II, and dimethylsulfoxide (DMSO) were purchased from Sigma Chemical Company (St. Louis, MO). TCDD was purchased from Chemsyn Science Laboratories (Lenexa, KS). RU486 was a kind gift from Dr. Terence Berry (University of

Wisconsin). Proteinase K was purchased from Boehringer Mannheim (Indianapolis, IN). Collagenase A for rat adrenocortical cell preparations was purchased from Boehringer Mannheim (Indianapolis, IN) and collagenase (type III) for rat mammary cell preparations was purchased from Worthington Biochemical Corp. (Freehold, NJ). Dulbecco's modified Eagle's medium/F12 (DME:F12, 1:1) for cell culture work was purchased from Gibco (Grand Island, NY). Donor horse, fetal bovine and dextran/charcoal-stripped fetal bovine serums were purchased from Gemini Bioproducts, Inc. (Calabasas, CA). Tissue culture plates (Falcon) were purchased from Fisher Scientific (Itasca, IL). Oligo(dT)-cellulose was purchased from Collaborative Biomedical Products. (Bedford, MA). All other chemicals were purchased from Sigma Chemical Company (St. Louis, MO).

Animals and tissues

All animals and animal tissues used in these studies were purchased from Harlan Bioproducts for Science, Inc. (Madison, WI). Fresh mammary glands from virgin female Sprague-Dawley rats, 50-55 days old, were used to isolate RMF. REF were isolated from 15 day old fetuses isolated from timed-pregnant Sprague-Dawley rats.

Preparation of rat mammary fibroblasts and cell culture

RMF were isolated as follows. Briefly, the lower 4 to 6 abdominal/anogenital mammary glands were excised from virgin female Sprague-Dawley rats and placed in PBS buffer on ice. In a sterile hood, the glands were finely minced with a scalpel and resuspended in a digestion solution [DME/F12 (1:1), pH 7.2, supplemented with 0.2% (w/v) collagenase (type III), 0.2% (w/v) dispase (grade II), 5% FBS, 50 μg/ml gentamycin]. This mixture was incubated in a shaking incubator (200 rpm) at 37°C for 3 hr. At the end of this incubation, 100 μg/ml DNase (type III) was added and the mixture incubated another 10 min. Undigested tissue was allowed to settle for 2-3 min and the cells aspirated off, removed to another sterile 50 ml tube, and centrifuged at 500 x *g* for 5 min to pellet the cells. Fat was aspirated off and discarded and the cell/organoid pellet was resuspended in fresh medium [DME/F12, pH 7.2, supplemented with 5% FBS and 50 μg/ml gentamycin] and centrifuged at 500 x *g* for 5 min. The pellet was resuspended in 10 ml fresh medium and cells were filtered through a sterile nylon mesh (Nytex; 0.22 μm). The flow through, which is comprised of single cells and small cell clumps, was collected and centrifuged at 500 x *g* for 5 min, and the resulting cell pellet was resuspended in fresh fibroblast medium [DME/F12 (1:1), pH 7.2, supplemented with 10% FBS] and plated in 175 cm^2 flasks. RMF were grown in a humidified atmosphere of 5% CO_2/95% air at 37°C, and reseeded 3-4 times to remove any contaminating epithelial cells before experiments were begun on these cells.

Preparation of rat embryo fibroblasts and cell culture

REF were prepared as follows. Fifteen day old rat embryos were removed from a freshly killed pregnant Sprague-Dawley rat, decapitated, and eviscerated. The resulting tissue was minced and placed in a sterile 50 ml polypropylene tube containing trypsin solution [0.05% trypsin, 5 mM EDTA] at room temperature for 1 hr with constant mixing. The resulting tissue fragments were gently pipetted to loosen adherent cells and the cell solution centrifuged at 500 x *g* for 5 min to pellet the cells. The cells were washed twice by resuspension in fresh cell medium [DME:F12, pH 7.2, supplemented with 10% FBS] and pelleting at 500 x *g* for 5 min. The final suspension of cells were plated onto 175 cm^2 dishes and allowed to attach and grow overnight in a humidified atmosphere of 5% CO_2/95% air at 37°C. At confluency, rat embryo fibroblasts were collected by trypsinization and split 1:3 for reseeding. All experiments on REF were performed on passages 3 to 5.

Preparation of microsomal protein from cells

For microsomal preparations from monolayers of cultured cells, cells were washed once with PBS buffer and collected by scraping. Cells were resuspended in 2 volumes of hypotonic buffer and swelled on ice for 10 min then 2 volumes of homogenization buffer [0.1 M $KHP0_4$, pH 7.25, 150 mM KCl, 10 mM EDTA, 0.25 mM PMSF, 0.1 mM DTT] were added and the cells lysed by sonication using a sonicator cell disruptor (Heat Systems-Ultrasonics, Inc., model W185F, Plainview, NY) at 10 sec pulses. The lysate was centrifuged at 15,000 x *g* for 20 min to remove the nuclear/mitochondrial fraction. The post-mitochondrial/nuclear fraction was then centrifuged at 105,000 x *g* for 90 min to pellet the microsomal fraction. The resulting cytosolic fraction was collected and the microsomal pellet was resuspended in 2 volumes of dilution buffer [0.1 M $KHP0_4$, pH 7.25, 10 mM EDTA, 0.25 mM PMSF, 0.1 mM DTT, 20% glycerol] and kept at -70°C until further use. Both cytosolic and microsomal protein concentrations determined by the BCA protocol (Pierce, Rockford, IL).

Preparation of cytosolic and nuclear protein for AhR and Arnt studies

To determine the effects of GCs on expression of AhR and Arnt, cytosolic and nuclear protein was isolated as follows. Briefly, cells were preincubated with DEX, diluted in DMSO, for various times before addition of the AhR ligand, TCDD. Cells were collected by scraping at the time of TCDD addition (0 hr) and 1 hr later, pelleted, and resuspended (100 µl/1 x 10^6 cells) in lysis buffer [25 mM MOPS, pH 7.4, 5 mM EGTA, 1 mM EDTA, 10% glycerol, 0.02% sodium azide] containing protease inhibitors [5 µg/ml leupeptin, 100 U/ml aprotinin, 5 µg/ml soy bean trypsin inhibitor, 50 µg/ml PMSF] and phosphatase inhibitors [2 mM sodium orthovanadate, 1 mM sodium fluoride, 20 mM sodium molybdate]. The cells were incubated for 30 min at 4°C to facilitate lysis, and centrifuged at 100 x *g* for 5 min to isolate the nuclear fraction. The cytosolic fraction was

collected and kept at -20°C until further use, and the nuclear pellet was carefully washed three times in lysis buffer to remove contaminating cytosolic proteins. After the final wash, the nuclear pellet was resuspended in lysis buffer and disrupted 2-3 times by sonication using a sonicator cell disruptor (Heat Systems-Ultrasonics, Inc., model W185F, Plainview, NY) at 10 sec pulses. This nuclear lysate was centrifuged at 15,000 x *g* for 2 min to remove debris and the nuclear protein collected and kept at -20°C until further use.

Western immunoblot analysis

Proteins were prepared for immunoblot analysis by suspension in sample loading buffer, heated at 100°C for 5 min, and separated by SDS-PAGE (8% acrylamide). Following separation, the proteins were transferred to nitrocellulose membranes (Shleicher & Schuell) and blocked in 1X TBST containing 5% milk overnight at 4°C (or for 1 hr at room temperature). The membranes were washed in 1X TBST for 20 min before addition of the primary antibodies. Primary antibodies used in these studies include affinity-purified polyclonal antibodies to recombinant mouse CYP1B1 (Savas, 1997), mouse AhR, and mouse Arnt (gifts from Dr. Richard Pollenz, Medical College of South Carolina). Following incubation with primary antibodies, the membranes were washed with 1X TBST for 20 min, then incubated with secondary antibody, either anti-rabbit horse radish peroxidase (Promega, Madison, WI). After washing the membranes immunoreactive proteins were visualized by the enhanced chemiluminescence method (Amersham Corporation) according to manufacturer's instructions.

Poly(A)$^+$ RNA isolation

Isolation of poly(A)$^+$ RNA from cultured cells was carried out as described previously (Badley, 1988) with modifications. Following treatment of the cells, the media was removed and the cells washed once with sterile PBS containing 25 μM aurin tricarboxylic acid, an RNase inhibitor. Cell lysis buffer [0.2 M Tris-HCl, pH 7.5, 0.2 M NaCl, 0.15 mM $MgCl_2$, 2% SDS, 200 μg/ml proteinase K, and 20 μM aurin tricarboxylic acid] was added and the cell lysate collected and placed in sterile polypropylene tubes. DNA was sheared by passing the lysate through a sterile plastic syringe fitted with a 23 gauge needle 4-5 times, and the lysate incubated at 45°C for 2 hr in a shaker waterbath to digest proteins, including ribonucleases. At the end of the incubation period the salt content of the lysate was adjusted to a final concentration of 0.5 M NaCl to facilitate binding of the poly(A)$^+$ RNA to oligo(dT)-cellulose. Binding, washing, and elution of mRNA was carried out in sterile Eppendorf tubes according to standard protocols (Sambrook, 1989).

Northen hybridization analysis

Poly(A)$^+$ RNA for each sample was separated on a 1% agarose-formaldehyde-formamide denaturing gel as previously described (Sambrook, 1989) and transferred by capillary action to a Nytran nylon membrane

(Schleicher & Schuell) in 20X SSC for 18 hr. RNA was immobilized by UV-induced covalent linkage to the membrane using a UV Stratalinker 1800 (Fisher Scientific) (1900 joule x 100 for 30 sec). Hybridization was carried out with either an EcoRI-HindIII fragment of the C-terminal of rat CYP1B1 cDNA (700 base pairs) (Bhattacharyya, 1995). A ß-actin probe was used to quantitate the levels of RNA in each lane. Each probe was labeled with [α-^{32}P]dCTP (3000 Ci/mmol) by the random-primed labeling method of Stratagene (San Diego, CA) according to manufacturer's instructions. RNA signals were visualized either by autoradiography or by phosphoimager analysis.

Transient transfection of primary cells

Primary cultures of RMF were transiently transfected with various CYP1B1 promoter-luciferase reporter gene constructs (Zhang, 1998) using a modified calcium phosphate method (Ausubel, 1996). Briefly, reseeded cells were grown to 50% confluency at which time the medium was changed to low serum [DME/F12, pH 7.2, supplemented with 4% FBS, without antibiotics] for 2-3 hr. Meanwhile, the transfection buffer was prepared [0.125 M $CaCl_2$, 25 mM *N,N*-bis(2-hydroxyethyl)-2-aminoethanesulfonic acid, 140 mM NaCl, 0.75 mM Na_2HPO_4, pH 6.95] containing the DNA construct of interest [6.5 µg luciferase + 1.5 µg ß-galactosidase DNA/30 cm^2 well]. The transfection buffer containing the DNA constructs of interest were added directly to the cells (100 µl/30 cm^2 well) and the DNA allowed to precipitate and attach to the cells for 5-6 hr in a humidified atmosphere of 5% CO_2/95% air at 37°C. The medium was removed and the cells shocked at room temperature for 5 min with warmed medium [DME/F12, pH 7.2, no serum] containing 10% glycerol to facilitate uptake of the precipitated DNA by the cells. The cells were then rinsed with fresh warmed medium (no glycerol) once, placed in regular culture medium [DME/F12, pH 7.2, supplemented with 10% FBS and antibiotics], and incubated overnight in a humidified atmosphere of 5% CO_2/95% air at 37°C. The next day, the cells were treated as described in the figure legends. For the luciferase assay, the cells were collected in lysis buffer (Promega) by scraping and lysed according to manufacturer's instructions. Protein concentrations were determined and the luciferase assay carried out according to manufacturer's instructions and determined in a luminometer. Transfection efficiency and normalization of activities of different constructs was carried out with a co-transfection with a ß-galactosidase-expressing vector (gift from Dr. John Fagan, Maharishi University) and measurement of ß-galactosidase activity.

Cell proliferation assay

The effect of GCs on proliferation of RMF was carried out with a CellTiter 96 Aqueous non-radioactive cell proliferation assay (Promega, Madison, WI). The assay is based on a novel tetrazolium compound which is bioreduced by metabolically active cells to a water soluble formazan product that can be determined by absorbance at 490 nm in a 96-well assay plate. The quantity of formazan product is directly proportional to the number of actively rowing cells in culture. Briefly, cells were plated into 96-well plates at 20,000 cells/well

and allowed to attach for 2 hr. At this time the cells were treated with various concentrations of DEX, 0.1% DMSO, or 10^{-9} M TCDD for 24 hr and the assay performed according to manufacturer's instructions.

Analytical methods

Quantitation and densitometry of the immunoblot and Northern blots was performed using a Zeineh soft laser scanning densitometer (model SL-504-XL, Biomed Instruments, Inc., Fullerton, CA) and by analysis of electronically scanned images on a Power Macintosh 6100/60 using the public domain NIH Image (version 1.56) program (written by Wayne Rasband at the U.S. National Institutes of Health and available from the Internet by anonymous FTP from zippy.nimh.nih.gov). Quantitation of phosphoimages and electronically scanned images (saved as TIFF files) was also performed with the software Imagequant (version 1.0).

Statistics

For comparison among several groups statistical analysis of results was carried out using one-way analysis of variance, followed by a two-tailed Student's t-test. Values reported for DMBA metabolism are reported as cell variance. Significance was set at $p < 0.05$.

Results

Effect of preincubation with DEX on constitutive and induced CYP1B1 mRNA

RMF and REF were treated with 10^{-9} M TCDD, either with or without pretreatment with DEX. The 5.2 kb CYP1B1 mRNA was constitutively expressed in primary cultures of RMF and levels were elevated 12-fold following 6 hr of TCDD treatment (Fig. 1A). Constitutive CYP1B1 mRNA and TCDD induction were similarly seen for REF (not shown). RMF were pretreated with 10^{-7} M DEX for 2 hr before addition of either 0.1% DMSO (Con) or 10^{-9} M TCDD for 6 hr. DEX preincubated for 2 hr only marginally lowered constitutive levels of CYP1B1 (20%) but significantly suppressed TCDD induction of CYP1B1 mRNA by 65% ($p < 0.05$) (Fig. 1B). This suppression was almost fully relieved with 1 μM of the strong GR antagonist, RU486, establishing a role for the GR in mediating this suppression. Co-administration of DEX with TCDD had no measurable effect on transcriptional stimulation of CYP1B1 by TCDD (not shown). DEX suppression of TCDD-induced CYP1B1 mRNA was duplicated in REF (Fig. 1C and 1D). For both cell types, inhibition of TCDD-induced CYP1B1 by DEX exhibited a concentration-dependence typical of GR binding ($EC_{50} \approx 10$ nM, $p < 0.05$) (Fig. 2A and 2B). Interestingly, the suppressive effects of GCs on CYP1B1 were not confined to fibroblasts or AhR regulation, since in primary rat adrenocortical cells, GCs suppress cAMP stimulation of CYP1B1 by 70% (not shown).

Effect of DEX on TCDD induction of CYP1B1 protein

The level of TCDD-induced CYP1B1 protein in RMF was also quantitated. Primary cultures of RMF were pretreated with 10^{-7} M DEX for various times to assess the time-dependency of GC suppression on TCDD-induced CYP1B1 protein. Again a preincubation with DEX was required for inhibition as co-administration with TCDD did not result in inhibition of CYP1B1 protein expression (Fig. 3A). However, in contrast to the rapid effects on CYP1B1 mRNA, a 6 hr preincubation produced only a marginal suppression while this effect increased rapidly between 6 and 12 hr (Fig. 3A and 3B). The levels of TCDD-induced CYP1B1 protein were inhibited 65% following 12 and 24 hr of DEX pretreatment.

Analysis of CYP1B1 promoter-luciferase activities

In order to further define the mechanism of GC/GR activity on the regulation of CYP1B1 we examined the effects of GCs on CYP1B1 promoter activity. Several 5'-flanking sequences have been isolated from mouse genomic CYP1B1 clones and have been characterized for responsiveness to TCDD in mouse embryo fibroblasts (Zhang, 1998). These studies identified a 265 base pair enhancer region that is essential for TCDD induction located approximately 1 kb upstream (-810 to -1075). A minimal promoter of 210 base pairs was also characterized immediately upstream of the transcriptional start site that is active in the absence of TCDD. An additional sequence in exon 1 was also inhibitory. These constructs were utilized here to determine the effect of GCs on CYP1B1 promoter activities and regulatory effects of exon 1 (Fig. 4A).

A 1.4 kilobase construct (p1075/+371) that contains the TCDD enhancer region, and a complete exon 1, was transiently transfected into RMF and assessed for responsiveness to DEX. This construct expressed constitutive activity and responded to TCDD with a 10-fold increase in activity (Fig. 4B). A second construct, p1075/+150, in which a previously identified inhibitory sequence in exon 1 was deleted, exhibited a much higher basal activity consistent with observations seen in mouse embryo fibroblasts, and was highly responsive to TCDD (17-fold increase) (Fig. 4B). A third construct, p210N265, that contains the TCDD enhancer region fused directly to the proximal promoter and which lacked a second identified suppressive region, was highly responsive to TCDD (Fig. 4B). Preincubation with 10^{-7} M DEX for 2 hr suppressed activity of each of these TCDD-induced constructs (50-70%, $p < 0.05$), with suppression partially relieved ($p < 0.05$) by co-treatment with the GC antagonist, RU486 [10^{-6} M] (Fig. 4C). A fourth construct, p210/+124, which contains only the proximal promoter of CYP1B1 was unresponsive to both TCDD and to DEX (Fig. 4B and 4C). Therefore, we conclude that GCs directly inhibit CYP1B1 at the transcriptional level and that this inhibition is mediated through the enhancer region.

Effect of DEX on AhR expression

We reasoned that DEX could be inhibiting CYP1B1 induction by decreasing AhR expression. When TCDD binds to the cytosolic AhR protein this complex translocates to the nucleus, briefly accumulates, along with its heterodimerization partner, the AhR nuclear translocator (Arnt) protein, and then is downregulated (Pendurthi, 1993; Pollenz, 1994). In RMF, TCDD translocates about 60% of the receptor to the nucleus in a 1 hr treatment (Fig. 5A), consistent with previous observations in mouse cells (Pollenz, 1994). Co-administration of TCDD and DEX had no effect on AhR levels or accumulation of the receptor in the nucleus. RMF that were pretreated with DEX for 2 hr exhibited marginal effects on initial levels of cytosolic AhR or TCDD-induced translocation (Fig. 5A and 5B). When RMF were preincubated with DEX for 12 hr before TCDD stimulation, expression of the AhR was significantly ($p < 0.05$) suppressed by 70% (Fig. 5A and 5B). The same proportion of AhR was translocated after 1 hr TCDD treatment. Levels of Arnt protein were not affected by DEX treatment (Fig. 5C). Some Arnt is found in the cytosol and decreases with TCDD treatment. This probably reflects leakage from the nucleus during preparation of the cytosol and nuclear extracts.

Effect of DEX on cellular proliferation of RMF

GCs can give rise to multiple effects that may impact on AhR activity, including inhibition of fibroblast growth (Durant, 1986). We treated actively proliferating RMF with various concentrations of DEX to quantitate this effect of GCs. A 24 hr treatment of RMF with DEX resulted in a dose-dependent ($EC_{50} \approx 5$ nM) inhibition of cell proliferation, with maximal suppression of 35% at 10^{-6} M DEX (Fig. 6). This level of growth inhibition is consistent with DEX's effects in other cells, including rat hepatoma and mammary tumor cell lines (Cook, 1988; Webster, 1990). TCDD alone had no effect on cell growth.

Discussion

Studies presented here document the expression of CYP1B1 in primary cultures of RMF and REF. We show that basal and TCDD-induced expression of the 5.2 kb CYP1B1 mRNA is comparable in both cell types, paralleling previous findings in C3H10T1/2 cells (Pottenger, 1991) and mouse embryo fibroblasts (Alexander, 1997). We have established suppression of this AhR regulation by GCs that is similar in RMF and REF. We have determined that transcription of the CYP1B1 gene is enhanced by TCDD through a 265 bp enhancer region that is located 1 kb upstream of the transcriptional start site, and provide evidence that the transcriptional control by GCs acts through the GR. The suppression by GCs occurs in this same region, even though there is no GRE. These effects of GCs on TCDD-induced transcription require addition of DEX 2 hr prior to

TCDD. DEX suppresses AhR expression in RMF, but this effect is not at preincubation times that suppress CYP1B1 mRNA.

These results suggest a different pattern of regulation to what was reported for previous investigations where PAH induction of CYP1A1 was potentiated by GCs in cultured hepatocytes (Mathis, 1986; Mathis, 1986; Xiao, 1995). These effects were at the transcriptional level and produced comparable effects at the activity, protein, and mRNA levels. Work presented here demonstrates that TCDD enhances CYP1B1 expression at the transcriptional level to a comparable extent to promoter activity as measured with CYP1B1-luciferase reporter constructs. DEX also suppressed CYP1B1 mRNA levels and promoter activity to comparable extents (70%). Both TCDD induction and DEX suppresion were mediated via the 265 bp enhancer region. A functional GRE, that binds GR, has been identified in the first intron of the rat CYP1A1 gene and is linked to the effects of GR (Mathis, 1989). No consensus GRE has been identified in the first 1.08 kilobases of the 5'-flanking sequences or the first intron of mouse CYP1B1 gene structures, notably in the active 265 base pair enhancer (Zhang, 1998).

We have shown that DEX inhibits CYP1B1 upregulation following TCDD treatment with an apparent $EC_{50} \approx 10$ nM. This value is comparable to those seen for other DEX-mediated up- or downregulation of gene transcription (Guller, 1994; Schoffelmeer, 1995; Yang, 1994). Involvement of the GR was evident by effects of the antagonist, RU486 (1 μM), which almost fully relieved suppression. Another group has reported that 10 μM of RU38486, another strong glucocoticoid antagonist, was required to fully reverse DEX's effect on potentiation of PAH-induction of CYP1A1 (Xiao, 1995). DEX inhibits CYP1B1 expression at the transcriptional and protein levels to a comparable extent (70%). However, there was no effect on protein expression with preincubations that effectively lowered RNA levels, and substantially longer DEX pretreatment was needed for a comparable effect (12 vs. 2 hr). However, this may reflect longer TCDD treatment used for protein determination (6 vs. 12 hr), and/or that the steady-state mRNA level is not the only determinant of AhR induction of CYP1B1 protein.

The 2 hr preincubation with GCs is crucial, even for a subsequent 6 hr incubation of DEX and TCDD, as co-administration of DEX and TCDD together had no effect on transcription of CYP1B1. This suggests one of two mechanisms for the suppression. First, there is an ordered process in which DEX changes initiating events immediately after translocation of AhR to the nucleus. AhR activity is then less critical for the subsequent maintenance of transcription. This is consistent with the idea that AhR activity at the enhancer opens up proximal promoter sequences by relaxing nucleosomes (Whitlock, 1996), for example by an increase in histone acetylation. A second possibility is that once present, TCDD activation of the AhR overrides the activity of GR.

Evidence presented here suggests that GCs suppress expression of the AhR, the major regulatory factor for constitutive and inducible CYP1B1 in fibroblasts (Zhang, 1998). However, since short preincubations (2

hr) with DEX, which suppress CYP1B1 mRNA, do not affect AhR levels, we conclude that the primary affect of GCs on transcription of CYP1B1 does not involve expression or translocation of the AhR. Levels of the heterodimer partner, Arnt, were not affected by DEX. Downregulation of AhR expression has only been demonstrated to this point in response to exogenous ligand binding (Prokipcak and Okey, 1991; Swanson and Perdew, 1993). Sadek and Hoffmann (1994a; 1994b) have reported upregulation of AhR activity in the absence of exogenous ligand, by suspension of human keratinocytes. This suspension prohibits adhesion and promotes differentiation. Other researchers have reported similar upregulation of the AhR during the differentiation of cells (Hayashi, 1995; Wanner, 1995), while the GC, hydrocortisone, completely antagonized TCDD-mediated growth inhibition of a human keratinocyte cell line (Rice and Cline, 1984). Here, GCs effects on CYP1B1 protein expression occur several hours after the effects on transcription and in parallel to changes in AhR levels.

In summary, it is presented here that DEX inhibits CYP1B1 regulation by TCDD, effects that are mediated through the enhancer region of the CYP1B1 gene, in a dose-dependent manner. These effects are mediated through the GR as evidenced by the potent GR antagonist, RU486, being effective at relieving this suppression. The inhibition of CYP1B1 transcription by GCs could be a direct effect mediated by competition for trans-acting factors or effects on histone acetylation, or secondary to changes in early response genes that affect AhR activity. This may reflect the slower synthesis or degradation of CYP1B1 protein and possibly also the longer observation period for protein expression (24 vs. 6 hr). In addition, the AhR may possibly play a role in determining the translation of CYP1B1 protein.

Acknowledgments

We would like thank Dr. Sakina Eltom for her technical advice in the isolation of cytosolic and nuclear protein for the AhR studies. We also thank Dr. Richard Pollenz (Medical University of South Carolina) for generously donating the AhR and Arnt antibodies used in these studies.

References

Alexander, DL, Eltom, SE, and Jefcoate, CR (1997) Ah receptor regulation of CYP1B1 expression in primary mouse embryo-derived cells. *Cancer Res* **57**:4498-4506.

Andreasen, PA., Georg, B, Lund, LR, Riccio, A, and Stacey, SN (1990) Plasminogen activator inhibitors: hormonally regulated serpins. *Mol Cell Endocrinol.* **68**:1-19.

Badley, JE, Bishop, GA, St. John, T, and Frehlinger, JA (1988). Rapid method for the purification of poly(A)+ RNA. *Biotechniques* **6**:114-116.

Bamberger, CM, Schulte, HM, and Chrousos, GP (1996) Molecular determinants of glucocorticoid receptor function and tissue sensitivity to glucocorticoids. *Endocrine Rev* **17**:245-261.

Christou, M, Savas, Ü, Schroeder, S, Shen, X, Thompson, T, Gould, MN, and Jefcoate, CR (1995) Cytochromes CYP1A1 and CYP1B1 in the rat mammary gland: cell-specific expression and regulation by polycyclic aromatic hydrocarbons and hormones. *Mol Cell Endocrinol* **115**:41-50.

Dembinski, TC, and Shiu, RPC (1987) Growth factors in mammary gland development and function. In The Mammary Gland: Development, Regulation, and Function, (MC Neville and CW Daniel, eds.) pp. 355-381, Plenum Press, New York.

Denison, MS, Fisher, JM, and Whitlock, JP, Jr. (1988). The DNA recognition site for the dioxin-Ah receptor complex. Nucleotide sequence and functional analysis. *J Biol Chem* **263**:17221-17224.

Denison, MS, Fisher, JM, and Whitlock, JP, Jr. (1989). Protein-DNA interactions at recognition sites for the dioxin-Ah receptor complex. *J Biol Chem* **264**:16478-16482.

Fernandez-Salguero, P, Pineau, T, Hilbert, DM, McPhail, T, Lee, SS, Kimura, S, Nebert, DW, Rudikoff, S, Ward, JM, and Gonzalez, FJ (1995). Immune system impairment and hepatic fibrosis in mice lacking the dioxin-binding Ah receptor. *Science* **268**:722-726.

Haslam, SZ (1987). Role os sex steroid hormones in normal mammary gland function. In The Mammary Gland: Development, Regulation, and Function (MC Neville and CW Daniel, eds) pp. 499-533, Plenum Press, New York.

Hayashi, S, Okabe-Kado, J, Honma, Y, and Kawajiri, K (1995). Expression of Ah receptor (TCDD receptor) during human monocytic differentiation. *Carcinogenesis* **16**:1403-1409.

Lechner, J, Welte, T, Tomasi, JK, Bruno, P, Cairns, C, Gustafsson, JÅ, and Doppler, W (1997) Promoter-dependent synergy between glucocorticoid receptor and Stat5 in the activation of ß-casein gene transcription. *J Biol Chem* **272:**20954-20960.

Lund, LR, Rømer, J, Thomasset, N, Solberg, H, Pyke, C, Bissell, MJ, Danø, K, and Werb, Z (1996) Two distinst phases of apoptosis in mammary gland involution: proteinase-independent and -dependent pathways. *Development* **122**:181-193.

Ma, Q, and Whitlock, JP., Jr. (1996). The aromatic hydrocarbon receptor modulates the Hepa 1c1c7 cell cycle and differentiated state independently of dioxin. *Mol Cell Biol* **16**:2144-2150.

Mathis, JM, Houser, WH, Bresnick, E, Cidlowski, JA, Hines, RN, Prough, RA, and Simpson, ER (1989). Glucocorticoid regulation of the rat cytochrome P450c (P450IA1) gene: receptor binding within intron I. *Arch Biochem Biophys* **269**:93-105.

Mathis, JM, Prough, RA, Hines, RN, Bresnick, E, and Simpson, ER (1986). Regulation of cytochrome P-450c by glucocorticoids and polycyclic aromatic hydrocarbons in cultured fetal rat hepatocytes. *Arch Biochem Biophys* **246**:439-448.

Okey, AB, Riddick, DS, and Harper, PA (1994) The Ah receptor: mediator of the toxicity of 2,3,7,8-tetrachlorodibenzo-p-dioxin (TCDD) and related compounds. *Tox Lett* **70**:1-22.

Pendurthi, UR, Okino, ST, and Tukey, RH (1993) Accumulation of the nuclear dioxin (Ah) receptor and transcriptional activation of the mouse Cyp1a-1 and Cyp1a-2 genes. *Arch Biochem Biophys* **306**, 65-69.

Pollenz, RS, Sattler, CA, and Poland, A (1994) The aryl hydrocarbon receptor and aryl hydrocarbon receptor nuclear translocator protein show distinct subcellular localizations in Hepa 1c1c7 cells by immunofluorescence microscopy. *Mol Pharmacol* **45**:428-438.

Pottenger, LH, Christou, M, and Jefcoate, CR (1991) Purification and immunological characterization of a novel cytochrome P450 from C3H/10T1/2 cells. *Arch Biochem Biophys* **286**:488-497.

Prokipcak, RD, and Okey, AB (1991) Downregulation of the Ah receptor in mouse hepatoma cells treated in culture with 2,3,7,8-tetrachlorodibenzo-p-dioxin. *Can J Physiol Pharmacol* **69**:1204-1210.

Prough, RA, Linder, MW, Pinaire, JA, Xiao, GH, and Falkner, KC (1996) Hormonal regulation of hepatic enzymes involved in foreign compound metabolism. *FASEB J* **10**:1369-1377.

Rice, RH, and Cline, PR (1984) Opposing effects of 2,3,7,8-tetrachlorodibenzo-p-dioxin and hydrocortisone on growth and differentiation of cultured malignant human keratinocytes. *Carcinogenesis* **5**:367-371.

Sadek, CM, and Allen-Hoffmann, BL (1994a) Cytochrome P450IA1 is rapidly induced in normal human keratinocytes in the absence of xenobiotics. *J. Biol. Chem.* **269**:16067-16074.

Sadek, CM, and Allen-Hoffmann, BL (1994b) Suspension-mediated induction of Hepa 1c1c7 Cyp1a-1 expression is dependent on the Ah receptor signal transduction pathway. *J Biol Chem* **269**:31505-31509.

Sambrook, J, Fritsch, EF, and Maniatis, T (1989) Molecular cloning, a laboratory manual Cold Spring Harbor Laboratory, Cold Spring Harbor, NY.

Savas, Ü, Christou, M, and Jefcoate, CR (1993) Mouse endometrium stromal cells express a polycyclic aromatic hydrocarbon-inducible cytochrome P450 that closely resembles the novel P450 in mouse embryo fibroblasts (P450EF). *Carcinogenesis* **14**:2013-2018.

Savas, Ü, Carstens, C-P, and Jefcoate, CR (1997) Biological oxidations and P450 reactions. Recombinant mouse CYP1B1 expressed in *Escherichia coli* exhibits selective binding by polycyclic aromatic hydrocarbons and metabolism which parallels C3H10T1/2 cell microsomes, but differs from human recombinant CYP1B1. *Arch Biochem Biophys* **347**:181-192.

Schmidt, JV, Su, GH, Reddy, JK, Simon, MC, and Bradfield, CA (1996) Characterization of a murine Ahr null allele: involvement of the Ah receptor in hepatic growth and development. *Proc Natl Acad Sci USA* **93**:6731-6736.

Schoffelmeer, AN, De Vries, TJ, Vanderschuren, LJ, Tjon, GH, Nestby, P, Wardeh, G, and Mulder, AH (1995) Glucocorticoid receptor activation potentiates the morphine-induced adaptive increase in dopamine D-1 receptor efficacy in gamma-aminobutyric acid neurons of rat striatum/nucleus accumbens. *J Pharmacol Exper Therapeutics* **274**:1154-1160.

Swanson, HI, and Perdew, GH (1993) Half-life of aryl hydrocarbon receptor in Hepa 1 cells: evidence for ligand-dependent alterations in cytosolic receptor levels. *Arch Biochem Biophys* **302:**167-174.

Wallace, AD, Wheeler, TT, and Young, DA (1997) Inducibility of E4BP4 suggests a novel mechanism of negative gene regulation by glucocorticoids. *Biochem Biophys Res Comm* **232**:403-406.

Wanner, R, Brommer, S, Czarnetzki, BM, and Rosenbach, T (1995) The differentiation-related upregulation of aryl hydrocarbon receptor transcript levels is suppressed by retinoic acid. *Biochem Biophys Res Comm* **209**:706-711.

Weiss, C, Kolluri, SK, Kiefer, F, and Gottlicher, M (1996) Complementation of Ah receptor deficiency in hepatoma cells: negative feedback regulation and cell cycle control by the Ah receptor. *Exp Cell Res* **226**:154-163.

Whitlock, JP, Jr., Okino, ST, Dong, L, Ko, HP, Clarke-Katzenberg, R, Ma, Q, and Li, H (1996) Cytochromes P450 5: induction of cytochrome P4501A1: a model for analyzing mammalian gene transcription. *FASEB J* **10**:809-818.

Wiebel, FJ, and Cikryt, P (1990) Dexamethasone-mediated potentiation of P450IA1 induction in H4IIEC3/T hepatoma cells is dependent on a time-consuming process and associated with induction of the Ah receptor. *Chem Biol Interact* **76**:307-320.

Xiao, GH, Pinaire, JA, Rodrigues, AD, and Prough, RA (1995) Regulation of the Ah gene battery via Ah receptor-dependent and independent processes in cultured adult rat hepatocytes. *Drug Metabol Dispos* **23**:642-650.

Yang, Z, Lee, D, Huang, W, Copolov, DL, and Lim, AT (1994) Glucocorticoids potentiate the adenylyl cyclase-cAMP system mediated immunoreactive beta-endorphin production and secretion from hypothalamic neurons in culture. *Brain Res* **648**:99-108..

Zhang, L, Savas, Ü, Alexander, D, and Jefcoate, CR (1998) Characterization of the mouse CYP1B1 gene: identification of an enhancer region that directs aryl hydrocarbon receptor-mediated constitutive and induced expression. *J Biol Chem* **273**:5174-5183.

Footnotes:

This research was supported by NIEHS grant 144EN46 and DOD Breast Cancer Research Grant DAMD17-94-J-4054.

Reprints should be sent to: Dr. Colin R. Jefcoate
University of Wisconsin
Department of Pharmacology
3770 Medical Sciences Center
1300 University Avenue
Madison, WI 53706

Figure 1. Effect of DEX preincubation on constitutive and TCDD-induced CYP1B1 mRNA. Primary cultures of RMF were isolated and cultured until 75-80% confluent, then pretreated for 2 hr with 10^{-7} M DEX (D) alone or in combination with 10^{-6} M RU486 (R), before addition of 0.1% DMSO (Con, C) or 10^{-9} M TCDD (T) for 6 hr (A). The effect of a 2 hr preincubation with DEX on TCDD-induction of CYP1B1 was duplicated in REF (C). Messenger RNA levels were quantitated, normalized to TCDD-induced levels, and presented in graphical form below each blot for RMF (B) or REF (D). Values represent the mean ± SEM from three separate experiments. Poly(A)$^+$ RNA (5 µg/lane) was isolated and separated in 1% agarose/formaldehyde gels, transferred to nylon membranes, and probed by Northern hybridization analysis of CYP1B1, as described in materials and methods.

Figure 2. Dose-response relationship of DEX suppression of TCDD induction of CYP1B1 mRNA. Primary cultures of RMF (A) and REF (B) were isolated and cultured until 75-80% confluent, then pretreated 2 hr with various concentrations of DEX as indicated, before addition of 10^{-9} M TCDD for 6 hr. Poly(A)$^+$ RNA (5 μg/lane) was isolated and separated in 1% agarose/formaldehyde gels, transferred to nylon membranes, and probed by Northern hybridization analysis of CYP1B1, as described in materials and methods. Expression of CYP1B1 was normalized to ß-actin, quantitated, and displayed in graphical form as percent of TCDD-induced CYP1B1 mRNA (normalized as 100%) versus concentration of DEX. Values presented represent the mean and range of results from two experiments.

Figure 3. Effect of DEX on TCDD induction of CYP1B1 protein. RMF were isolated and cultured until 75-80% confluent, as described in materials and methods, then preincubated with 10^{-7} M DEX for times (hr, h) indicated (hr, h), or left untreated (-), before addition of 10^{-9} M TCDD for 12 hr to assess the effects of DEX pretreatment time on TCDD induction of CYP1B1 protein (A). After 12 hr of TCDD treatment, the cells were harvested and microsomal protein was isolated and probed for immunodetectable CYP1B1, as described in materials and methods. Protein loadings were 5 μg/lane for both (A) and (B). Shown are representative blots of repeated experiments. CYP1B1 protein levels were quantitated as described in materials and methods, and relative levels were determined from two separate experiments and presented in graphical form (B), as mean and range, for percent inhibition of TCDD-induced CYP1B1 protein versus preincubation times for DEX.

Figure 4. Effect of DEX on *CYP1B1* promoter-luciferase activity. RMF were isolated and cultured until 50% confluent, then transiently transfected with a number of *CYP1B1* promoter-luciferase constructs (A) and assessed for effects of DEX on TCDD-induced luciferase activities (B), as described in materials and methods. Luciferase activities (LUC, arbitrary units) were determined in response to 12 hr of 0.1% DMSO (Con) or 10^{-9} M TCDD treatment following a 2 hr preincubation with 10^{-7} M DEX alone, or in combination with 10^{-6} M RU486 (RU). In (C), a comparison of the effects of DEX on TCDD induction of two CYP1B1 constructs (p1075/+150 and p210/+124) that were repeated in another experiment in RMF. Values for (B) represent mean ± SEM for triplicate samples and values for (C) represent the means ± SEM of triplicate samples from two experiments (n=6).

† Significantly different from TCDD treatment ($p < 0.05$)

Significantly different from DEX treatment ($p < 0.05$)

Figure 5. Effect of DEX on AhR expression. RMF were isolated and cultured until 50% confluent, then pretreated with 10^{-7} M DEX for the times indicated (hr, h), and treated with 10^{-9} M TCDD for 0 hr and 1 hr. Cells were then harvested and cytosolic (C) and nuclear (N) proteins were isolated and probed for immunodetectable AhR (A), as described in materials and methods. Cytosolic and nuclear levels were quantitated, normalized to untreated (0 hr TCDD) samples, and presented in graphical form for the AhR (B). These samples were also probed for immunodetectable Arnt (C). Values presented represent the mean ± SEM for three experiments (B).

† Significantly different from No DEX treatment ($p < 0.05$)

Figure 6. Effect of DEX on cellular proliferation of RMF. Actively proliferating RMF (passage 3) were plated into a 96-well plate and allowed to attach for 3 hr. At this time the cells were treated with either 0.1% DMSO (Con), 10^{-9} M TCDD, or various concentrations of DEX for 24 hr, at which time actively growing cells were determined using a non-radioactive cellular proliferation assay kit based on reduction of a tetrazolium compound to formazan that can be measured by absorbance at 490 nm (Promega Corp., Madison, WI). The graphical representation compares proliferating activity (absorbance at 490 nm, arbitrary units) versus various concentrations of DEX. Values represent the mean ± SEM for triplicate samples (n=3).
† Significantly different from control ($p < 0.05$)

Index items: glucocorticoid
CYP1B1
Rat mammary fibroblasts
Dexamethasone
TCDD

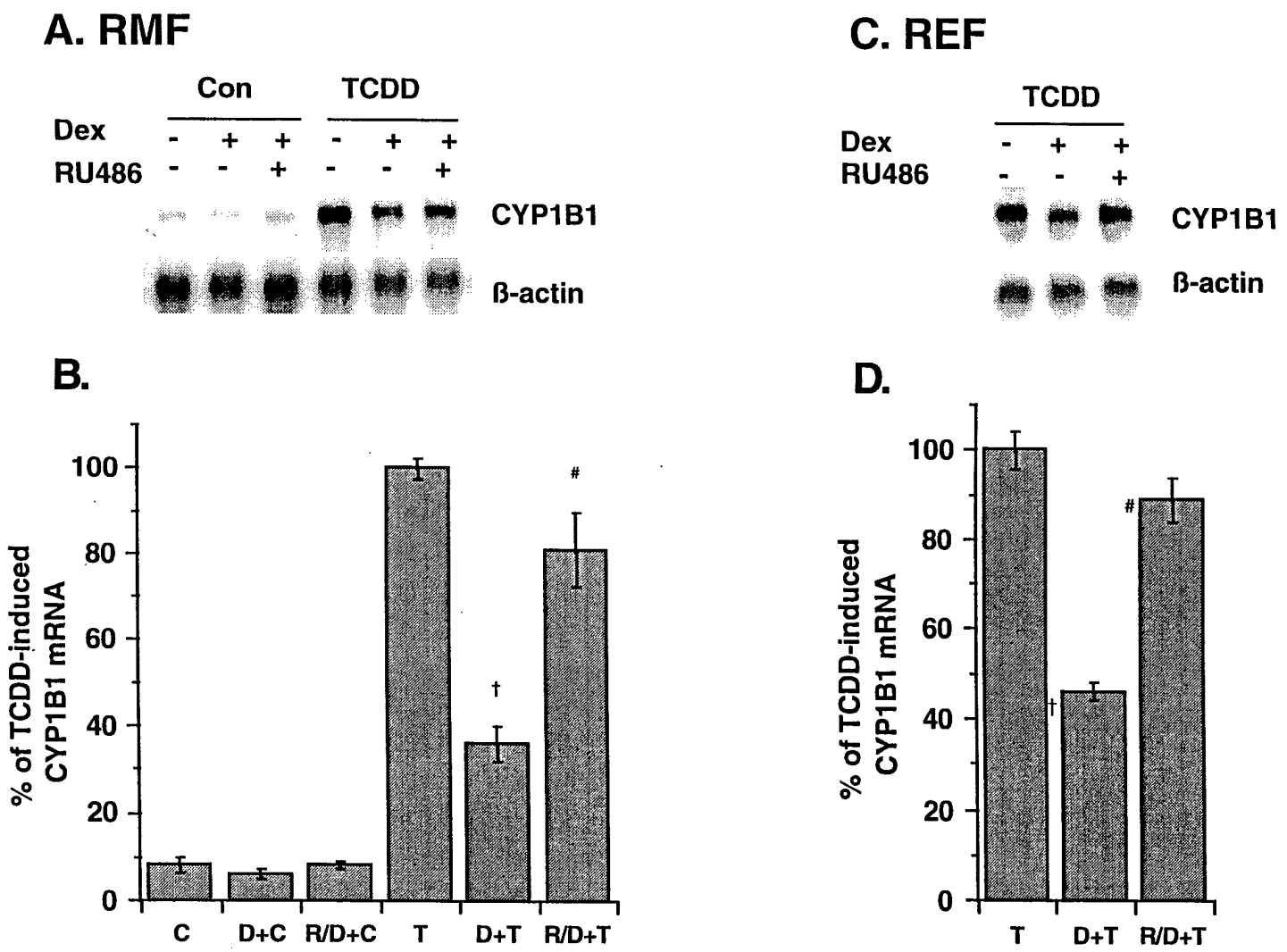
A. RMF
Con
TCDD
Dex
RU486
CYP1B1
ß-actin
B.
% of TCDD-induced CYP1B1 mRNA
C
D+C
R/D+C
T
D+T
R/D+T
C. REF
D.

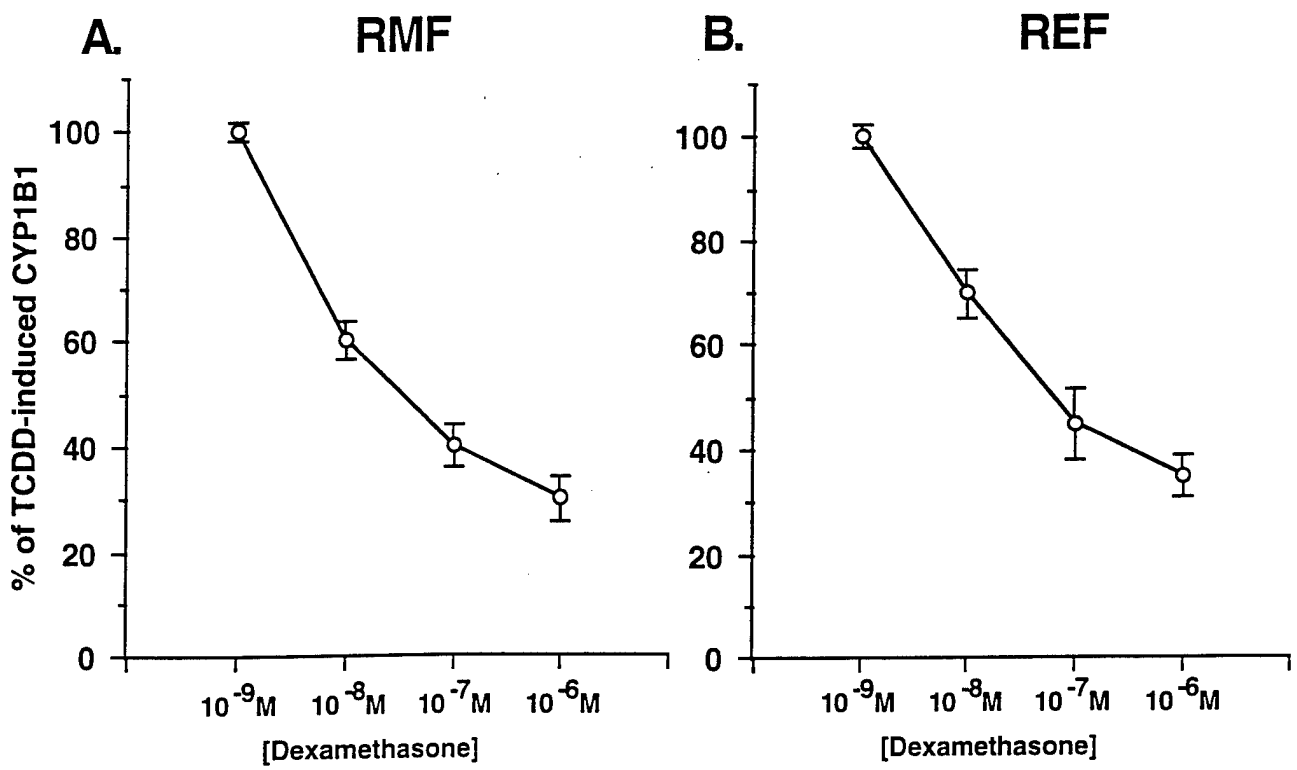
A.
RMF
B.
REF
% of TCDD-induced CYP1B1
100
80
60
40
20
0
10-9M
10-8M
10-7M
10-6M
[Dexamethasone]

A.

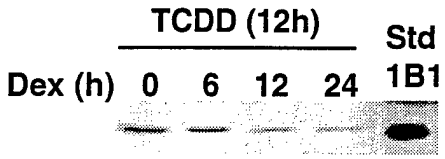
TCDD (12h)
Std
Dex (h) 0 6 12 24
1B1

B.

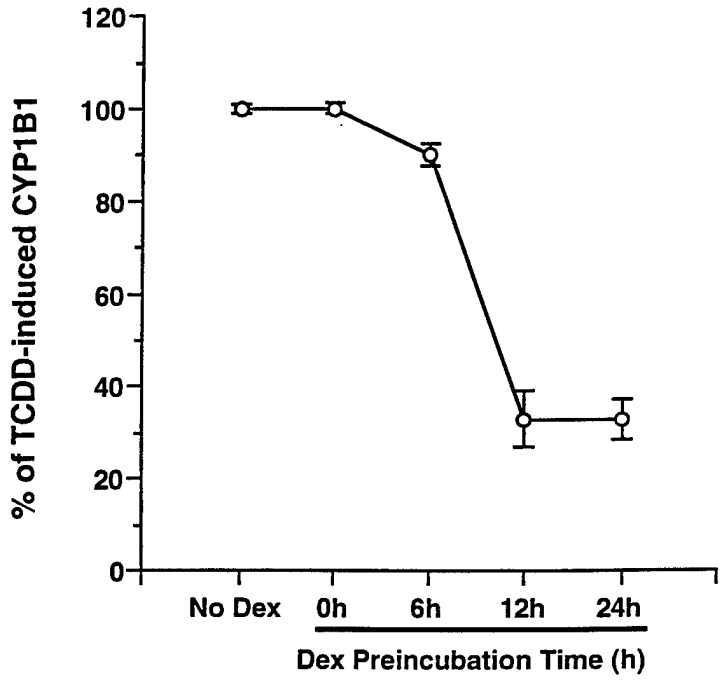
% of TCDD-induced CYP1B1
120
100
80
60
40
20
0
No Dex
0h
6h
12h
24h
Dex Preincubation Time (h)

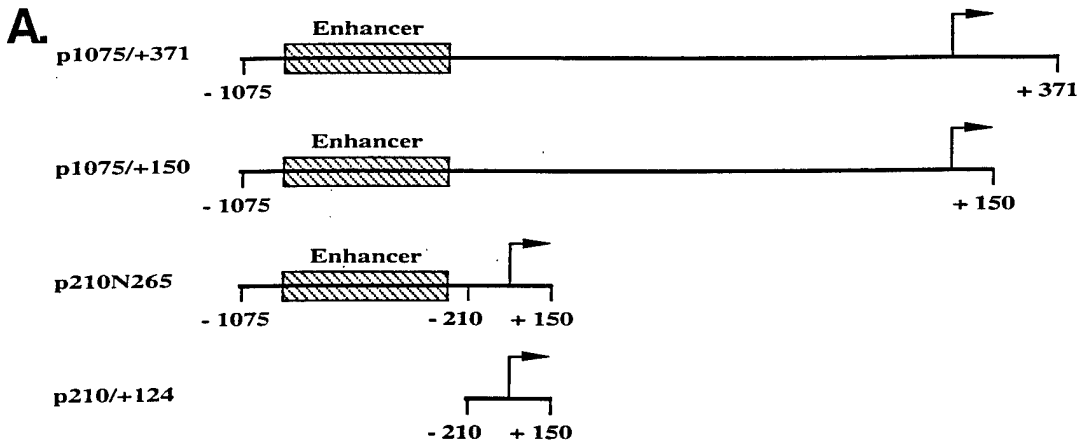
A.
p1075/+371
Enhancer
- 1075
+ 371
p1075/+150
Enhancer
- 1075
+ 150
p210N265
Enhancer
- 1075
- 210
+ 150
p210/+124
- 210
+ 150

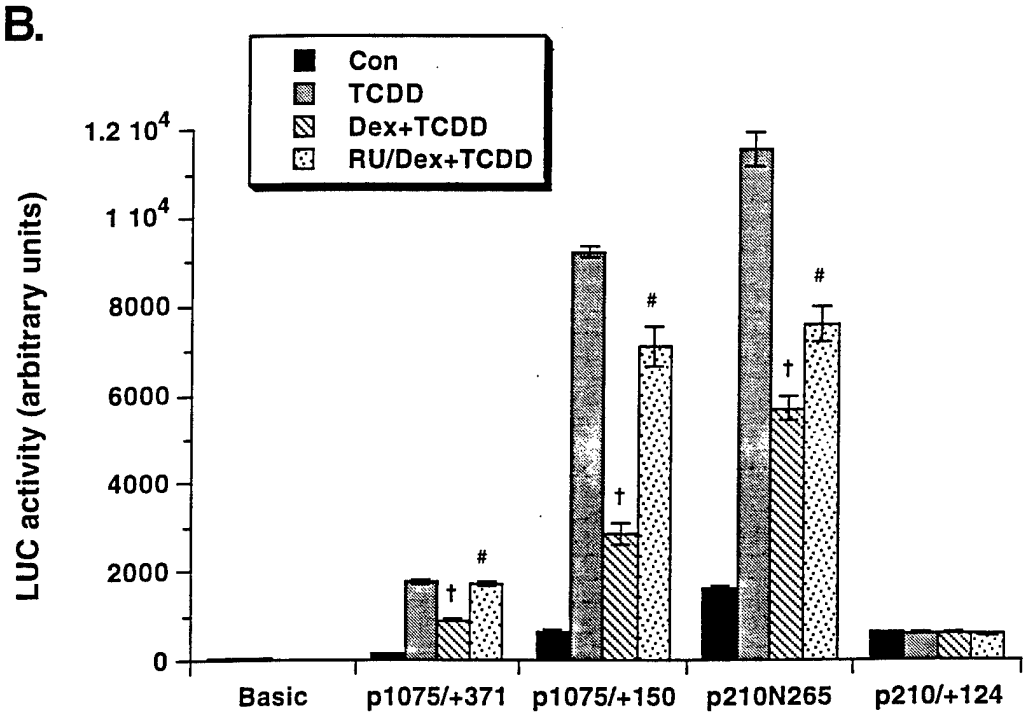
B.
Con
TCDD
Dex+TCDD
RU/Dex+TCDD
LUC activity (arbitrary units)
1.2 10^4
1 10^4
8000
6000
4000
2000
0
Basic
p1075/+371
p1075/+150
p210N265
p210/+124

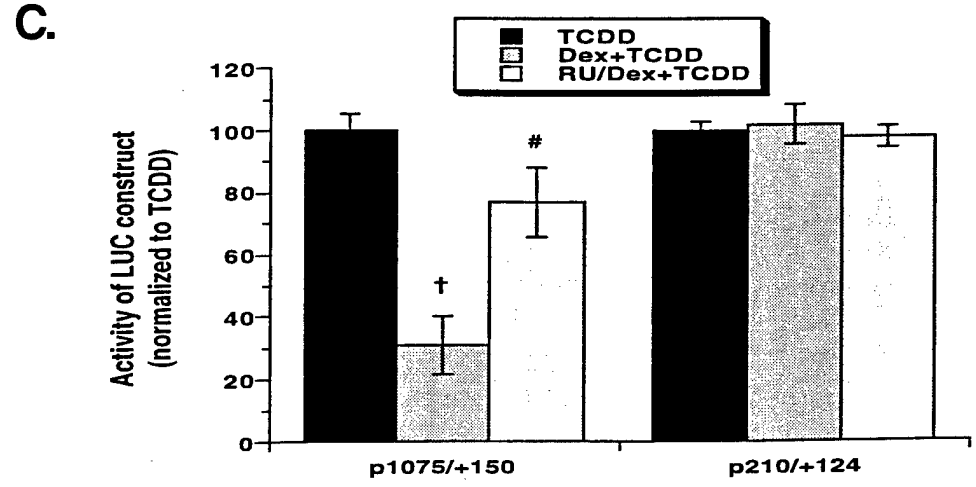
C.
TCDD
Dex+TCDD
RU/Dex+TCDD
Activity of LUC construct
(normalized to TCDD)
120
100
80
60
40
20
0
p1075/+150
p210/+124

A. AhR

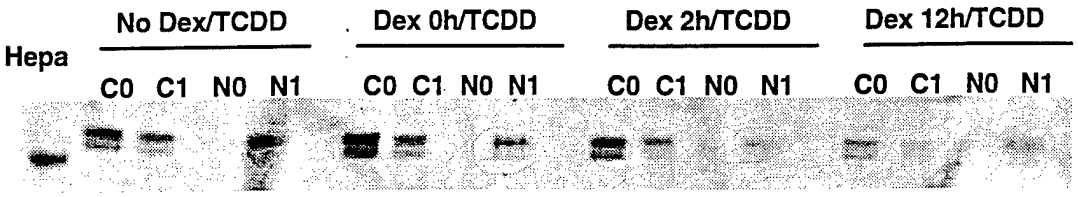
Hepa
No Dex/TCDD
Dex 0h/TCDD
Dex 2h/TCDD
Dex 12h/TCDD
C0 C1 N0 N1
C0 C1 N0 N1
C0 C1 N0 N1
C0 C1 N0 N1

B.

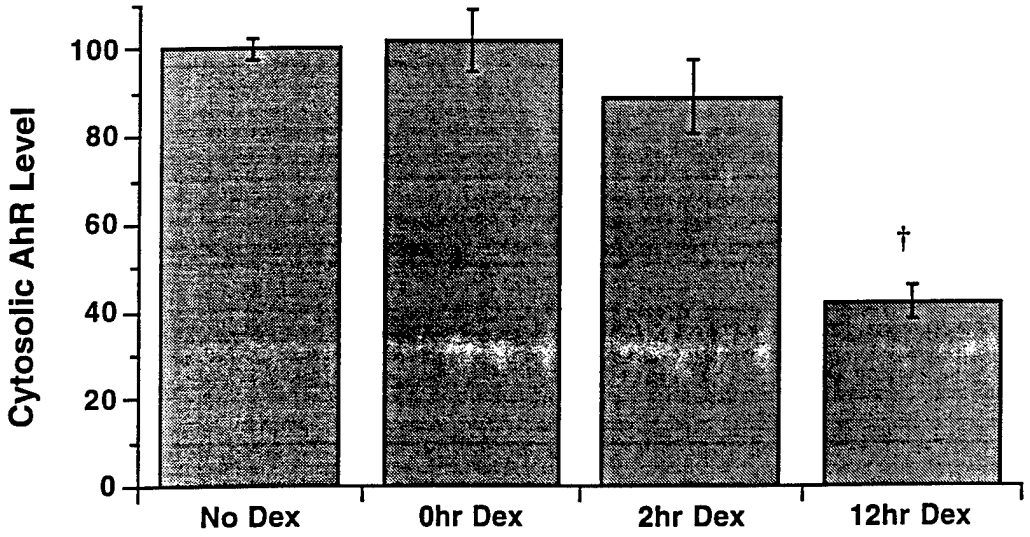
Cytosolic AhR Level
100
80
60
40
20
0
†
No Dex
0hr Dex
2hr Dex
12hr Dex

C. Arnt

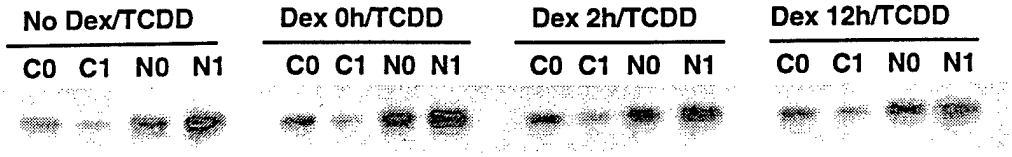
No Dex/TCDD
Dex 0h/TCDD
Dex 2h/TCDD
Dex 12h/TCDD
C0 C1 N0 N1
C0 C1 N0 N1
C0 C1 N0 N1
C0 C1 N0 N1

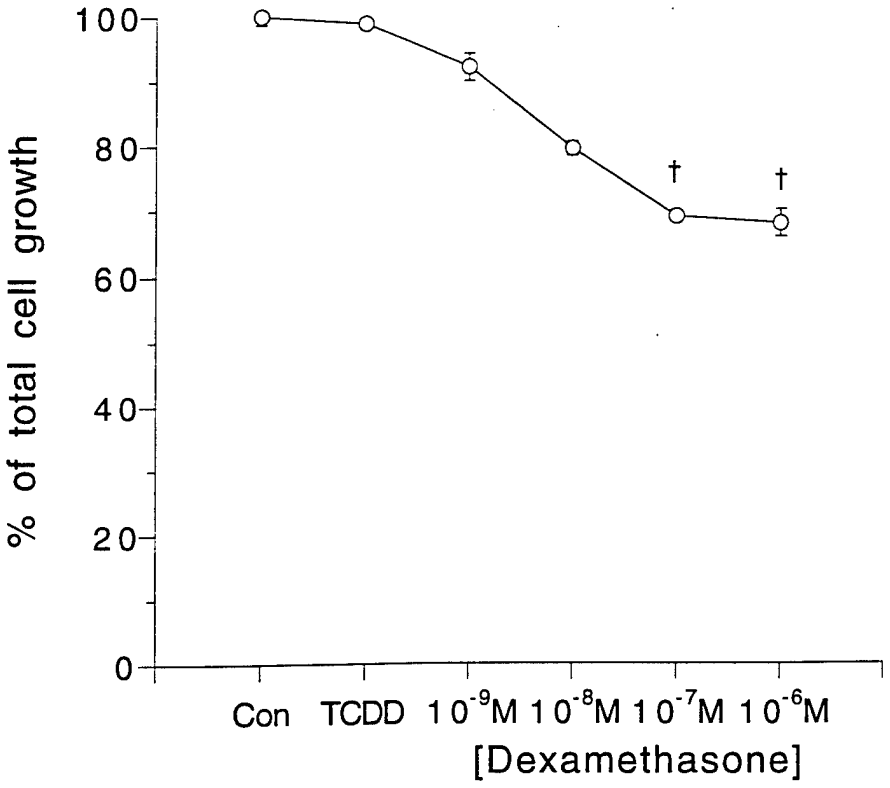
100
80
60
40
20
0
% of total cell growth
†
†
Con
TCDD
10-9M
10-8M
10-7M
10-6M
[Dexamethasone]

CRT IN PRESS

Revised Version March 23, 1

Stable Expression of Human Cytochrome P450 1B1 in V79 Chinese Hamster Cells and Metabolically Catalyzed DNA Adduct Formation of Dibenzo[*a*,*l*]pyrene

Andreas Luch,[†] Stephanie L. Coffing,[‡] Yong M. Tang,[§,¢] Anneliese Schneider,[†] Volker Soballa,[†] Helmut Greim,[†,¶] Colin R. Jefcoate,[¥] Albrecht Seidel,[◊] William F. Greenlee,[§] William M. Baird,[‡,fl] and Johannes Doehmer*,[†]

[†] Institute of Toxicology and Environmental Hygiene, Technical University of Munich, Lazarettstrasse 62, 80636 Munich, Germany;

[‡] Department of Medicinal Chemistry and Molecular Pharmacology, Hansen Life Sciences Research Building, Purdue University, West Lafayette, Indiana 47907, USA;

[§] Department of Pharmacology and Molecular Toxicology, University of Massachusetts Medical Center, Worcester, Massachusetts 01655, USA;

[¢] present address: National Center for Toxicological Research, Division of Molecular Epidemiology, Jefferson, Arkansas 72079, USA;

[¶] GSF - National Research Center for Environment and Health, Institute of Toxicology, 85764 Neuherberg, Germany;

[¥] Department of Pharmacology, University of Wisconsin Medical School, Madison, Wisconsin 53706, USA;

[◊] Institute of Toxicology, University of Mainz, 55131 Mainz, Germany;

[fl] present address: Environmental Health Sciences Center, 1011 Agricultural & Life Sciences Building, Oregon State University, Corvallis, Oregon 97331-7302, USA;

* Author to whom correspondance and reprint requests should be addressed:

Prof. Dr. Johannes Doehmer
Institute of Toxicology and Environmental Hygiene
Technical University of Munich
Lazarettstrasse 62
80636 Munich, Germany
phone: +49-89-3187-2973
fax: +49-89-3187-3449
e-mail: doehmer@gsf.de

Running title: Human P450 1B1 and DNA adducts of DB[*a*,*l*]P

Abstract

Chinese hamster V79 cell lines were constructed for stable expression of human cytochrome P450 1B1 (P450 1B1) in order to study its role in the metabolic activation of chemicals and toxicological consequences. The new V79 cell lines were applied to studies on DNA adduct formation of the polycyclic aromatic hydrocarbon (PAH) dibenzo[*a,l*]pyrene (DB[*a,l*]P). This compound has been found to be an environmental pollutant and in rodent bioassays it is the most carcinogenic PAH yet discovered. Activation of DB[*a,l*]P in various metabolizing systems occurs via fjord region DB[*a,l*]P-11,12-dihydrodiol 13,14-epoxides (DB[*a,l*]PDE): we found that DB[*a,l*]P is stereoselectively metabolized in human mammary carcinoma MCF-7 cells to the (–)-*anti*- and (+)-*syn*-DB[*a,l*]PDE which both bind extensively to cellular DNA. In order to follow up this study and to relate specific DNA adducts to activation by individual P450 isoforms, the newly established V79 cells stably expressing human P450 1B1 were compared with those expressing human P450 1A1. DNA adduct formation in both V79 cell lines differed distinctively after incubation with DB[*a,l*]P or its enantiomeric 11,12-dihydrodiols. Human P450 1A1 catalyzed the formation of DB[*a,l*]PDE-DNA adducts as well as several highly polar DNA adducts as yet unidentified. The proportion of these highly polar adducts to DB[*a,l*]PDE adducts was dependent upon both the concentration of DB[*a,l*]P and the time of exposure. In contrast, V79 cells stably expressing human P450 1B1 generated exclusively DB[*a,l*]PDE-DNA adducts. Differences in the total level of DNA binding were also observed. Exposure to 0.1 μM of DB[*a,l*]P for 6 h caused a significantly higher level of DNA adducts in V79 cells stably expressing human P450 1B1 (370 pmol/mg DNA) compared to those with human P450 1A1 (35 pmol/mg DNA). A 4-fold higher extent of DNA binding was catalyzed by human P450 1B1 (506 pmol/mg DNA) compared to human P450 1A1 (130 pmol adducts/mg DNA) 6 h after treatment with 0.05 μM (–)-(11*R*,12*R*)-dihydrodiol. In cells stably expressing human P450 1B1 the DNA adducts were derived exclusively from the (–)-*anti*-DB[*a,l*]PDE. These results indicate that human P450 1B1 and P450 1A1 differ in their regio- and stereochemical selectivity of activation of DB[*a,l*]P with P450 1B1 forming a higher proportion of the highly carcinogenic (–)-*anti*-(11*R*,12*S*,13*S*,14*R*)-DB[*a,l*]PDE metabolite.

Footnotes

[1] Abbreviations: B[*a*]P, benzo[*a*]pyrene; B[*c*]Ph, benzo[*c*]phenanthrene; DB[*a,h*]A, dibenz-[*a,h*]anthracene; DB[*a,l*]P, dibenzo[*a,l*]pyrene; (+)-*syn*-DB[*a,l*]PDE, (+)-*syn*-dibenzo[*a,l*]-pyrene-11*S*,12*R*-dihydrodiol 13*S*,14*R*-epoxide; (–)-*anti*-DB[*a,l*]PDE, (–)-*anti*-dibenzo[*a,l*]-pyrene-11*R*,12*S*-dihydrodiol 13*S*,14*R*-epoxide; DMBA, 7,12-dimethylbenz[*a*]anthracene; DMEM, Dulbecco Vogt's modified Eagle medium; EROD, ethoxyresorufin *O*-deethylation; FITC, fluorescein-isothiocyanate; IgG, immunoglobulines; MC, 3-methylcholanthrene; P450, cytochrome(s) P450; PAGE, polyacrylamide electrophoresis; PAH, polycyclic aromatic hydrocarbon(s); PBS, phosphate-buffered saline; SDS, sodium dodecyl sulfate; TBS, Tris-buffered saline; TCDD, 2,3,7,8-tetrachloro-dibenzo-*p*-dioxin.

[2] Baird, W. M., Ralston, S. L., Coffing, S. L., Luch, A., and Seidel, A., unpublished data

Introduction

Multiple isoforms of cytochrome P450 (P450)[1] play key roles in the metabolic activation of polycyclic aromatic hydrocarbons (PAH) by generating proximate and ultimate carcinogenic metabolites (*1-6*). Understanding the role of each of these isoforms is part of a rationale-based risk assessment. Several cellular systems have been developed to study P450-mediated metabolism and metabolite-dependent toxic effects (*7*). V79 Chinese hamster cells had been selected to serve as host cells for heterologous expression of P450, because these cells possess several biological characteristics which make them a valuable mammalian test system for various toxicological endpoints (*8*). At the same time, these cells lack detectable P450. Therefore, V79 cells genetically engineered for stable expression of a single P450 isoform allow evaluation of the role of the isoform in metabolite formation and the toxic effect observed under defined experimental conditions.

Recently, a new isoform P450 1B1 was detected, in mouse first (*9-11*), and subsequently in rat (*12,13*) and human tissues (*14,15*). P450 1B1 has been found in most extrahepatic human organs including fetal heart, brain, lung and kidney (*14,16*). This isoform is inducible in rodents by exposure to PAH (*9,17*) and its importance in the metabolic activation of various members of this group of chemicals has been already indicated by several studies (*16,18-20*). The metabolic activity of P450 1B1, together with the tissue specific expression pattern, may help to explain induction of human tumors of extrahepatic origin by procarcinogens activated by this isoform.

Due to its presence in various environmental sources (*21-25*) and its exceptionally high carcinogenic activity in rodent bioassays among all PAH tested so far (*26-28*), the hexacyclic dibenzo[*a,l*]pyrene (DB[*a,l*]P) (Scheme 1) must be considered as a potential risk for human health. Studies with mammalian cell cultures (*29,30*) and microsomal preparations (*31-33*) have demonstrated that this compound is metabolically activated via its 11,12-dihydrodiols (Scheme 1) to the fjord region *syn*- and *anti*-DB[*a,l*]P-11,12-dihydrodiol 13,14-epoxides (*syn*- and *anti*-DB[*a,l*]PDE), the most potent mutagenic metabolites of any PAH tested in the Ames assay and Chinese hamster V79 cell system, respectively (*34*). Moreover, both *syn*- and *anti*-

DB[*a,l*]PDE have been shown to be very potent carcinogens in newborn mice, mouse skin and rat mammary gland (*35-37*).

This exceptional biological activity prompted a number of investigations of DB[*a,l*]P. Studies using the human mammary carcinoma MCF-7 cells (*30*) and liver microsomes from rats pretreated with 3-methylcholanthrene (MC) (*31*) demonstrated that metabolic activation of this compound occurs with similar stereoselectivity characteristics as those found for other fjord or bay region PAH such as benzo[*c*]phenanthrene (B[*c*]Ph) or benzo[*a*]pyrene (B[*a*]P). DB[*a,l*]P is stereoselectively converted to the (–)-*anti*- and the (+)-*syn*-DB[*a,l*]PDE with 11*R*,12*S*,13*S*,14*R*- and 11*S*,12*R*,13*S*,14*R*-configuration, respectively. In addition, investigations on the metabolic activation of the two immediate precursors of both fjord region DB[*a,l*]PDE, the (–)-(11*R*,12*R*)- and (+)-(11*S*,12*S*)-dihydrodiols, respectively (Scheme 1), have revealed very high levels of DNA binding as well as mutagenic activity in V79 cells after metabolic activation of the (–)-dihydrodiol by MCF-7 cells (*38*) or liver preparations from rats pretreated with Aroclor 1254 (*32*). In contrast, the (+)-dihydrodiol bound only weakly to DNA and was not significantly mutagenic. In both test systems the (–)-dihydrodiol was stereoselectively transformed to the (–)-*anti*-(11*R*,12*S*,13*S*,14*R*)-DB[*a,l*]PDE in large amounts, whereas corresponding activation of the (+)-dihydrodiol to the (+)-*syn*-(11*S*,12*R*,13*S*,14*R*)-DB[*a,l*]PDE was virtually undetectable.

Two crucial steps in the metabolic activation of DB[*a,l*]P to its fjord region DB[*a,l*]PDE require oxidation by P450 enzymes (Scheme 1). Human mammary carcinoma MCF-7 cells express P450 1B1 constitutively and P450 1A1 upon induction (*18*). In order to assess the role of each P450 isoform for metabolic activation of DB[*a,l*]P and DNA adduct formation by its metabolites, the cell line V79MZ-h1A1, stably expressing human P450 1A1, and the newly constructed V79MZ-h1B1 cell line, stably expressing human P450 1B1, were exposed to DB[*a,l*]P and its enantiomeric 11,12-dihydrodiols and the DNA adducts formed were analyzed.

Experimental Procedures

Caution: Dibenzo[a,l]pyrene and its enantiomerically pure 11,12-dihydrodiols are mutagenic and carcinogenic and should be handled with care using the guidelines for carcinogenic chemicals of the National Cancer Institute.

Chemicals. Nuclease P1 (EC 3.1.30.1; from *Penicillium citrinum*), human prostatic acid phosphatase (EC 3.1.3.2; from human semen), apyrase (EC 3.6.1.5; from *Solanum tuberosum*), and phosphodiesterase I (EC 3.1.4.1; from *Crotalus atrox*) were purchased from Sigma Chemical Co. (St. Louis, MO). RNase T1 (EC 3.1.21.3; from *Aspergillus oryzae*) and RNase (DNase free) were obtained from Boehringer Mannheim Co. (Indianapolis, IN). T4 polynucleotide kinase was obtained from United States Biochemical (Cleveland, OH). [γ-^{33}P]ATP [3500 Ci (129.5 TBq)/mmol] was purchased from Amersham Corp. (Arlington Heights, IL). Proteinase K (EC 3.4.21.64; from *Tritirachium album*) was obtained from Merck (Darmstadt, Germany) or Sigma Chemical Co. (St. Louis, MO). Dulbecco's modified Eagle medium, high glucose type (DMEM with 4.5 g D-glucose/L) was obtained from Biochrom-Seromed (Berlin, Germany) or Gibco BRL (Grand Island, NY). Antibiotics (penicilline and streptomycin), L-glutamine, and phosphate-buffered saline (PBS without Ca^{2+} or Mg^{2+}; 3.0 mM KCl, 1.5 mM KH_2PO_4, 140 mM NaCl, 8.0 mM Na_2HPO_4, pH 7.0) were purchased from Biochrom-Seromed (Berlin, Germany). Fetal calf serum was obtained from Intergen (Purchase, NY). Antibiotic G418 (geneticin sulfate) was purchased from Calbiochem-Novabiochem Corp. (La Jolla, CA) or Gibco BRL. Synthesis of DB[*a,l*]P and its enantiomeric 11,12-dihydrodiols was described previously (*32,34,39*).

Cell Culture. The parental V79MZ cell line (*40*), the genetically engineered cell lines V79MZ-h1A1, expressing human P450 1A1, V79MZ-h3A4, expressing human P450 3A4, V79MZ-r1A1, expressing rat P450 1A1, V79MZ-r1A2, expressing rat P450 1A2 (*8*) and newly established V79 cell lines for human P450 1B1 (see paragraph below) were cultivated in Dulbecco's modified Eagle medium (DMEM), high glucose type, supplemented with 1 mM sodium pyruvate, 4 mM L-glutamine, 10 % fetal calf serum, 100 U penicillin/mL and 100 µg streptomycin/mL at 37 °C, 7 % CO_2, and 90 % saturated atmospheric humidity.

Construction of the pRC/CMV-h1B1 Expression Vector. Human P450 1B1 clone 128 (*14*) was used as the template to create a *Hind* III restriction site at the 5'-end and a *Xba* I restriction site at the 3'-end by performing the polymerase chain reaction in order to facilitate insertion of the cDNA into the expression vector pRC/CMV (Invitrogen, Carlsbad, CA). The resulting recombinant expression vector pRC/CMV-h1B1 is shown in Figure 1 with characteristic restriction sites and functions.

Genetical Engineering of V79 Cells for Human P450 1B1. The expression plasmid pRc/CMV-h1B1 linearized with *Pvu* I, and containing the neomycin-phosphotransferase gene as eukaryotic selection marker, was used for transfection of parental V79 cells. For coexpression with human NADPH-P450 reductase, cells were cotransfected with pSV-hCYPOR (*41,42*). Transfection was carried out according to the calcium phosphate coprecipitation method of Graham and Van der Eb (*41,43*). V79MZ parental cells were transfected with either of the following plasmid preparations: (1) 10 μg of *Pvu* I linearized pRc/CMV-h1B1 for 1 x 10^6 cells; (2) 20 μg of *Pvu* I linearized pRc/CMV-h1B1 for 8 x 10^5 cells; (3) 1 μg of *Pvu* I linearized pRc/CMV-h1B1 and 30 μg of pSV-hCYPOR for 8 x 10^5 cells. Cell clones resistant against 1 mM G418 appeared around 10 days after transfection and were picked the following day. Cell clones were expanded for another 5 days and aliquots were checked for expression of human P450 1B1 and human NADPH-P450 reductase by *in situ* immunofluorescence.

***In situ* Immunofluorescence.** *In situ* immunofluorescence was performed on tissue culture chambers ("Chamber Slide", Nunc, Naperville, USA) with 1 x 10^4 cells per well, cultivated for 24 h, washed with PBS, fixed with ice-cold methanol/aceton (1:1, v/v) for 7 min. Fixed cells were incubated with the immunoglobulines (IgG) anti-mouse P450 1B1-IgG from rabbit and anti-human NADPH-P450 reductase-IgG from rabbit (Amersham, Little Chalfont, UK) as primary antibodies at a dilution of 1 : 2000 in DMEM for 1 h at room temperature, followed by 3 washing cycles with PBS. Fluorescein-isothiocyanate (FITC)-conjugated anti-rabbit-IgG from goat (Dianova, Hamburg, Germany) served as secondary antibody. Plates were mounted with 100 mg *p*-phenylendiamin-dihydrochloride (Sigma) in a mixture of 10 mL PBS and 80 mL glycerol and covered with a cover slip. Fluorescence was obtained with a fluorescence microscope equipped with standard FITC filter sets (Zeiss Axioplan, Oberkochen,

Germany). Selected expressing clones were cultivated for another period of 3 months and periodically checked for expression of human P450 1B1 and human NADPH-P450 reductase by *in situ* immunfluorescence.

Western Blot Analysis. Cellular homogenates were separated by sodium dodecyl sulfate (SDS)/polyacrylamide gel electrophoresis (PAGE) (8.5 % polyacrylamide) according to Laemmli with some modifications (*41*) and transferred onto Immobilon-P protein-binding membrane (Millipore Corp., Bedford, MA). The presence of human P450 1B1 and human NADPH-P450 reductase protein on the Western blots was detected using the same antisera as in the *in situ* immunofluorescence assay. Finally, the specifically bound rabbit IgG was detected with a horseradish peroxidase-conjugated antiserum from pig (Dakopatts, Hamburg, Germany) by enhanced chemiluminescence (Amersham Int., Little Chalfont, UK).

Enzyme Assay. The ethoxyresorufin *O*-deethylation (EROD) assay was used to measure P450 1B1 or P450 1A1 activity. The enzyme assay was performed with total protein from cells harvested by scraping the cells from the Petri dishes with a rubber policeman. After centrifugation at 1500 x *g* the cell pellet was shock frozen in liquid N_2 and stored at -70 °C. The assay was performed as previously described (*44*).

Treatment of V79 Cells with DB[*a*,*l*]P and DB[*a*,*l*]P-11,12-Dihydrodiols. Prior to the treatment (24 h) V79 cell lines were seeded at a density of 1 x 10^6 to 3 x 10^6 cells/75 cm^2 cell culture flask and grown in a total volume of 30 mL DMEM, high glucose type, supplemented with 10 % fetal calf serum, and 400 µg/mL G418 at 37 °C, 5 % CO_2, and 90 % saturated atmospheric humidity. Then 10 µL of a Me_2SO-solution of DB[*a*,*l*]P or its enantiomerically pure 11,12-dihydrodiols were added.

Cell Harvesting and DNA Isolation. After an incubation period of 6 or 24 h the supernatant was removed and the cells were harvested by trypsinization with 0.025 % trypsin and 0.01 % EDTA in PBS. Equal volume of media supplemented with 10% fetal calf serum were added to stop trypsinization. Subsequently, centrifugation at 2000 rpm and two washing steps with PBS yielded a cell pellet which was stored at - 80 °C until DNA isolation. To isolate the DNA from V79 cells, the pellet was resuspended in a solution containing 10 mM Tris, 1 mM EDTA and 1 % (w/v) SDS (pH 8.0), homogenized and subsequently incubated for 1 h at 37 °C with RNase T1 (1000 units/mL) and RNase, DNase free (5 µg/mL) on a shaker (100

rpm). Then proteinase K (500 μg/mL) was added and the incubation continued (1 h at 37 °C). Purification of the DNA was achieved by successive extractions of the mixture with 1 volume Tris-saturated phenol/chloroform/*iso*-amyl alcohol (25:24:1, v/v/v; 3 times), followed by separation of the phases by centrifugation at 2000 rpm. Finally, the DNA was precipitated with twice the volume of ethanol, separated, dissolved in water and stored at -80 °C.

^{33}P-Postlabeling of DNA Adducts. The procedure used was as described previously (*30*). Briefly, 10 μg DNA isolated from V79 cells after treatment with DB[*a*,*l*]P or its enantiomeric 11,12-dihydrodiols was digested with Nuclease P1 and prostatic acid phosphatase, postlabeled with [γ-^{33}P]ATP [3500 Ci/mmol], cleaved to adducted mononucleotides with snake venom phosphodiesterase I, and prepurified with a Sep-Pak C_{18} cartridge (Waters Corp., Milford, MA). Subsequent separation by HPLC (Beckman HPLC system equipped with two 110B pumps and a Model 420 controller; Beckman Instruments Inc., St. Louis, MO) was carried out using a C_{18} reverse-phase column (5 μm Ultrasphere ODS, 4.6 x 250 mm; Beckman Instruments Inc.) and the radiolabeled nucleotides were detected by an on-line radioisotope flow-detector (Radiomatic FLO-ONE Beta; Packard Instruments, Downers Grove, IL) as described (*30*). The level of DB[*a*,*l*]P-DNA binding was calculated based on labeling of a [^{3}H]-benzo[*a*]pyrene-7,8-dihydrodiol 9,10-epoxide-DNA standard (*45*).

Results

Preparation and Characterization of V79 Cells Stably Expressing Human P450 1B1 and Human NADPH-P450 Reductase. Approximately 50 G418-resistant cell clones were obtained from the first transfection, 400 clones from the second transfection, and 50 clones from the third transfection. After repeated *in situ* immunofluorescence assays for checking the maintenance of P450 1B1 expression over a 3 months period, seven clones were selected for further investigation; six V79 clones with human P450 1B1 alone, and one V79 clone coexpressing human NADPH-P450 reductase. P450 1B1 and NADPH-P450 reductase expression in these clones was verified by Western blot analysis (Figure 2) and enzyme activity in each was verified by EROD activity (Table 1). The cell clone #6 (V79MZ-h1B1) expressing both human P450 1B1 and human NADPH-P450 reductase (Figure 2, Table 1) was selected for use in this study.

DNA Adducts from DB[*a,l*]P and its 11,12-Dihydrodiols in V79 Cells Stably Expressing a single P450 Isoform. The V79 cell lines stably expressing human P450 1A1, human P450 3A4, rat P450 1A1 and rat P450 1A2, respectively (*8*), in addition to the newly constructed V79MZ-h1B1 cell line, were exposed to DB[*a,l*]P and its 11,12-dihydrodiols in order to measure DNA adduct formation. The DNA was then isolated, postlabeled and analyzed by HPLC. The HPLC elution profiles of the ^{33}P-postlabeled DNA adducts formed in V79 cells stably expressing human P450 1B1 (V79MZ-h1B1) after treatment with DB[*a,l*]P contained four or six peaks, depending on the concentration of the PAH used (Figure 3). Treatment with low doses (0.1 μM) resulted in the formation of four adduct peaks 1, 2a, 2b, and 4 (Figure 3A) which are formed from (–)-*anti*-DB[*a,l*]PDE. These are identical to those identified previously from DB[*a,l*]P activated in the human mammary carcinoma cell line MCF-7 ((*30*); that peak numbering system was used to allow direct comparison with results presented in our earlier studies). At higher concentrations of DB[*a,l*]P (1 or 5 μM) two additional peaks (3 and 6) were detected in the adduct profile (Figure 3B). Both are due to covalent interaction of (+)-*syn*-DB[*a,l*]PDE with DNA (*30*). At all doses, no DNA adducts eluted with a retention time shorter than 30 min (Figure 3). In contrast to results with V79 cells stably expressing human P450 1B1, exposure of V79 cells stably expressing human P450 1A1

(V79MZ-h1A1) to DB[*a,l*]P resulted in the formation of several DNA adducts with highly polar character that eluted between 5 and 30 min under the HPLC conditions used (Figure 4A and 4B; polar adducts are labeled with Roman numerals). Treatment of the cells expressing human P450 1A1 with low concentrations of DB[*a,l*]P (0.1 μM) resulted in the formation of only these highly polar DNA adducts (Figure 4A). Treatment with higher doses of DB[*a,l*]P produced both highly polar adducts and DB[*a,l*]PDE-DNA adducts in considerable amounts (Figure 4B). Comparison of the total DNA binding measured in both cell lines after exposure to the lowest concentration (0.1 μM) of DB[*a,l*]P revealed a significantly higher level of DNA adducts after metabolic activation by human P450 1B1 irrespective of the time of incubation (Table 2). Levels of 370 pmol DB[*a,l*]PDE-DNA adducts/mg DNA were detected in V79MZ-h1B1 cells 6 h after treatment with 0.1 μM DB[*a,l*]P, whereas only 35 pmol adducts/mg DNA (highly polar as well as DB[*a,l*]PDE-DNA adducts) were found in V79MZ-h1A1 cells (Table 2). As the dose of DB[*a,l*]P increased, both cell lines formed comparable levels of adducts. At the highest dose tested, DNA modification levels were as great as 1 adduct per 6000 DNA bases. Interestingly, in the cells expressing human P450 1A1, the percentage of DB[*a,l*]PDE-DNA adducts increased from 17 % to 87 % at 6 h after treatment with increasing concentrations of DB[*a,l*]P from 0.1 to 5.0 μM .

To determine whether formation of highly polar DB[*a,l*]P-DNA adducts is also catalyzed by P450 1A1 from other species, V79 cells stably expressing rat P450 1A1 (V79MZ-r1A1) were exposed to DB[*a,l*]P. These cells formed similar highly polar DNA adducts (Figure 4C) to those in the cells expressing human P450 1A1 (Figure 4B). However, in comparison to the results obtained with V79MZ-h1A1 cells (Figure 4A, 4B) the amount and relative proportion of these highly polar adducts was much smaller than that of the DB[*a,l*]PDE-DNA adducts (Figure 4C, Table 2). The adduct profiles formed from the cells expressing rat P450 1A1 appeared to look like a composite of the profiles from cells expressing human P450 1B1 and human P450 1A1 (cf. Figures 3 and 4). Rat P450 1A1 catalyzed the formation of a higher proportion of DB[*a,l*]PDE-DNA adducts irrespective of the concentration of DB[*a,l*]P (Table 2).

The ability of these cells to metabolically activate DB[*a,l*]P was further characterized by examining the competence of each cell line for activation of the (–)-(11*R*,12*R*)-dihydrodiol, the immediate metabolic precursor of the (–)-*anti*-(11*R*,12*S*,13*S*,14*R*)-DB[*a,l*]PDE (Scheme 1).

After treatment of V79MZ-h1B1 cells with different doses of this compound and subsequent ^{33}P-postlabeling, the HPLC adduct patterns obtained consisted exclusively of DNA adducts 1, 2a, 2b, and 4 (Figure 5A), which resulted from formation of (–)-*anti*-(11*R*,12*S*,13*S*,14*S*)-DB[*a*,*l*]PDE (*30*,*38*). As was observed after exposure of these cells to the parent PAH (Figure 4A, 4B), metabolic activation of the (–)-dihydrodiol by human P450 1A1 resulted in the formation of several DNA adducts with highly polar character (Figure 5B, 5C). These adducts were the major adducts present after exposure to low concentrations of the (–)-dihydrodiol (0.05 μM, Figure 5B): the proportion of (–)-*anti*-DB[*a*,*l*]PDE-DNA adducts increased considerably after treatment with a high concentration (0.5 μM, Figure 5C). Comparison of the total DNA binding in V79 cells stably expressing human P450 1B1 or human P450 1A1 after exposure to the (–)-dihydrodiol also gave results consistent with those obtained with the parent compound (Table 2). Comparable levels of DNA binding were observed with both P450 isoforms at high concentrations, however, at the low concentration of 0.05 μM the human P450 1B1 isoform was more efficient in catalyzing the formation of DNA adducts than human P450 1A1 (506 compared to 130 pmol/mg DNA, respectively). In the cells expressing human P450 1A1 only 24 % (31 pmol/mg DNA) of the total DNA binding was caused by the (–)-*anti*-DB[*a*,*l*]PDE. At higher concentrations an increasing proportion of DB[*a*,*l*]PDE-DNA adducts (up to 91 % after exposure to 1 μM of the dihydrodiol for 6 h) was observed (Table 2). In cells expressing human P450 1B1 only the (–)-*anti*-DB[*a*,*l*]PDE-DNA adducts were detected at all times and concentrations tested (Table 2).

The HPLC adduct patterns obtained after incubation of V79 cells expressing rat P450 1A1 with different doses of the (–)-dihydrodiol contained two major polar adducts and the four (–)-*anti*-DB[*a*,*l*]PDE-DNA adducts peaks (1, 2a, 2b, and 4) which were detected in the human P450 expressing cells (data not shown, cf. Figure 4C). The rat P450 1A1 isoform activated the (–)-dihydrodiol to yield 35 and 310 pmol adducts/mg DNA after 6 h exposure to 0.005 and 0.05 μM, respectively. A further increase in the total DNA binding was detected after 24 h incubation (Table 2). At the 0.5 μM dose activation of the (–)-dihydrodiol by the V79 cells expressing rat P450 1A1 was comparable to that observed in cells expressing human P450 1A1 or human P450 1B1 (modification levels in the range of 1 adduct per 1000-2000 DNA bases).

Activation of the (+)-(11*S*,12*S*)-dihydrodiol, the precursor of the (+)-*syn*-(11*S*,12*R*,13*S*,14*R*)-DB[*a*,*l*]PDE (Scheme 1), was also examined. Low levels of formation of the (+)-*syn*-DB[*a*,*l*]PDE-DNA adducts were observed in the cells expressing human P450 1B1 and human P450 1A1 after exposure to high doses of DB[*a*,*l*]P (Figures 3B, 4B). In V79 cells stably expressing human or rat P450 1A1 only low levels of the (+)-dihydrodiol were activated to DNA binding intermediates even at the high concentration of 0.5 μM (Table 2). These P450 1A1 isoforms had much greater ability to activate the enantiomeric (–)-dihydrodiol than the (+)-dihydrodiol (Table 2). However, activation of the (+)-dihydrodiol could contribute to DNA binding for P450 isoforms which possess limited activity for the metabolic activation of parent PAH (e.g. human P450 3A4 or rat P450 1A2). Total DNA adduct levels of 6.5 and 1.8 pmol/mg DNA could be measured after exposure of V79 cells expressing human P450 3A4 to 0.5 μM (–)-dihydrodiol and its (+)-enantiomer, respectively. In contrast, this isoform activated DB[*a*,*l*]P itself only to a low extent (0.1 pmol adducts/mg DNA 24 h after treatment with 1 μM). Cells stably expressing the rat P450 1A2 isoform metabolically activated both enantiomeric dihydrodiols with comparable efficiency: the levels of binding were 6.0 and 4.0 pmol adducts/mg DNA after exposure to 0.5 μM (+)- and (–)-dihydrodiol, respectively (Table 2).

Discussion

Various P450 isoforms are responsible for the carcinogenic activity of a large number of PAH by catalyzing the formation of proximate and/or ultimate carcinogenic metabolites (*3-6,16*). Enzymatic activation of the potent carcinogen DB[*a,l*]P to its electrophilically reactive and DNA binding *syn*- and *anti*-DB[*a,l*]PDE requires two epoxidation steps by P450 enzymes (Scheme 1). Measurement of the formation of DB[*a,l*]P dihydrodiols by recombinant human P450 1A1 demonstrated that this isoform catalyzes considerable oxidation of DB[*a,l*]P at the 8,9-, 11,12- and 13,14-positions (*5*). The immediate metabolic precursor of the *syn*- and *anti*-DB[*a,l*]PDE, the 11,12-dihydrodiol, is also formed by rat liver microsomes of MC-treated animals (*46*) or by lung and liver microsomes of human donors in the age range of 18 to 60 years (*5*). Moreover, both *syn*- and *anti*-DB[*a,l*]PDE-DNA adducts have been detected after incubation of DB[*a,l*]P with liver microsomes of MC- (*31*) or Aroclor 1254-treated (*33*) rats in the presence of DNA. Administration of MC or Aroclor 1254 is known to significantly increase the level of P450 1A1 in the liver of the treated rodents (*47,48*). All together, these results suggested that P450 1A1 is capable of carrying out both epoxidation steps required for activation of DB[*a,l*]P to its fjord region DB[*a,l*]PDE (Scheme 1).

Exposure of human mammary carcinoma MCF-7 cells (*29*) or mouse embryo C3H10T1/2CL8 fibroblasts (*49*) to DB[*a,l*]P resulted in formation of both *syn*- and *anti*-DB[*a,l*]PDE-DNA adducts. This has also been verified in vivo by analyzing lung tissue of strain A/J mice after ip administration of DB[*a,l*]P (*50*). Moreover, it could be demonstrated that this bioactivation is highly stereoselective. MCF-7 cells exclusively generate (+)-*syn*- and (–)-*anti*-DB[*a,l*]PDE-DNA adducts which are formed from the respective precursors, the (+)-(11*S*,12*S*)- and (–)-(11*R*,12*R*)-dihydrodiols, respectively ((*30*); cf. Scheme 1). No formation of (+)-*anti*- or (–)-*syn*-DB[*a,l*]PDE was detected. Interestingly, human MCF-7 cells express P450 1A1 only upon induction, but P450 1B1 constitutively (*18*). Additional evidence suggesting an important role of human P450 1B1 during biotransformation of PAH was provided by studies of the induction of *umu* gene expression in bacteria after metabolic activation of various dihydrodiols of PAH by purified microsomal P450 1B1 (*16*). The present

study was designed to clarify the role of individual human P450 isoforms, especially P450 1B1 and P450 1A1, in the metabolic activation of DB[*a,l*]P.

Chinese hamster V79 cells stably expressing human P450 1A1 were treated with different doses of DB[*a,l*]P or its enantiomeric 11,12-dihydrodiols. Comparison to the corresponding turnover catalyzed by human P450 1B1 was feasible using the genetically engineered V79 cell lines stably expressing this P450 isoform. Results obtained from both cell lines are directly comparable. The P450 activities were found to be of the same order of magnitude (cf. Table 1) taking into account that the specific activity of human P450 1A1 for ethoxyresorufin is nearly 7-fold higher than for human P450 1B1 (*51*).

Exposure to different concentrations of DB[*a,l*]P revealed that V79 cells stably expressing human P450 1B1 exclusively generate (+)-*syn*- and (–)-*anti*-DB[*a,l*]PDE-DNA adducts (Figure 3, Table 2) and, thus form exactly the same adducts as previously detected in human MCF-7 cells (*29,30*). At low concentrations of DB[*a,l*]P (0.1 μM) only (–)-*anti*-DB[*a,l*]PDE-DNA adducts could be detected (Figure 3A) indicating either an exclusive generation of the respective *R,R*-configurated (–)-dihydrodiol precursor at low doses of the parent compound (cf. Scheme 1) or an increased sequestration of any (+)-*syn*-DB[*a,l*]PDE formed by water or other cellular nucleophiles. The latter explanation seems to be more likely in consideration of the finding that *syn*-DB[*a,l*]PDE preferentially adopts a conformation with pseudo-diequatorial oriented hydroxy groups (*aligned* conformation) (*34*) and the demonstration that vicinal *syn*-dihydrodiol epoxides prefering this conformation undergo significantly accelerated hydrolytic opening of their oxiranyl ring under neutral conditions compared to corresponding *anti*-diastereomers (*52,53*). The dose-dependency of the adduct pattern obtained in V79 cells expressing human P450 1B1 (Figure 3A and 3B) was also observed in MCF-7 cells. (+)-*syn*-DB[*a,l*]PDE-DNA adducts were only detected in MCF-7 cells after treatment with high doses of the parent PAH, e.g. 1-8 μM.[2] DNA adducts of (+)-*syn*-DB[*a,l*]PDE were virtually undetectable in MCF-7 cells after exposure to 0.05 μM (+)-11,12-dihydrodiol (*38*). These results suggest that nucleophilic sequestration of small amounts of intermediately formed (+)-*syn*-DB[*a,l*]PDE by water or cellular proteins rather than a limited metabolic conversion of DB[*a,l*]P to its (+)-11,12-dihydrodiol (cf. above) may account for the absence of (+)-*syn*-DB[*a,l*]PDE-DNA adducts in cells treated with small amounts of DB[*a,l*]P.

Treatment of V79 cells expressing human P450 1A1 with DB[*a,l*]P also resulted in the formation of large amounts of DB[*a,l*]PDE-DNA adducts (Figure 3A and 3B, Table 2). In addition, considerable amounts of earlier-eluting highly polar DNA adducts were detected (Figure 3A and 3B, Table 2). Since human P450 1A1 is able to generate 8,9-, 11,12- and 13,14-dihydrodiols during incubation of DB[*a,l*]P ((*5*); cf. above) it is possible that this P450 isoform catalyzes the formation of highly polar DB[*a,l*]P-DNA adducts via successive oxidations of different benzo rings in the peri-condensed hexacyclic molecule. Strong evidence in support of this conclusion is provided by a study recently presented by Nesnow et al. (*54*) that reported that human P450 1A1 is able to metabolically convert the 8,9-dihydrodiol of DB[*a,l*]P to a previously unknown tetrahydrotetrol. Furthermore, an unidentified tetrahydrotetrol epoxide-DNA adduct was detected after coincubation of human P450 1A1 with DB[*a,l*]P-8,9-dihydrodiol in the presence of DNA (*54*). Involvement of multiple sites of metabolic activation of the hexacyclic DB[*a,l*]P could be anticipated based on similar findings during activation of certain other penta- or hexacyclic PAH such as B[*a*]P (*55*), dibenz[*a,h*]anthracene (DB[*a,h*]A) (*56,57*) and dibenzo[*a,h*]pyrene (*58*). These PAH have been shown to be capable of undergoing further oxidation after intermediate formation of vicinal dihydrodiol epoxides or to be electrophilically activated as tetrahydrotetrol epoxides via the formation of corresponding tetrahydrotetrol precursors.

Incubation of the immediate metabolic precursor of (–)-*anti*-DB[*a,l*]PDE, the (–)-(11*R*,12*R*)-dihydrodiol (Scheme 1), with V79 cells expressing human P450 1B1 indicated that this isoform metabolically generates (–)-*anti*-DB[*a,l*]PDE-DNA adducts (Figure 5A) in extraordinary large amounts (Table 2). No other adducts have been detected. In contrast, V79 cells expressing human P450 1A1 are able to produce (–)-*anti*-DB[*a,l*]PDE- as well as the highly polar DNA adducts (Figure 5B) previously detected after incubation of the parent compound. The similar HPLC patterns of highly polar DNA adducts obtained after incubation of DB[*a,l*]P or (–)-DB[*a,l*]P-11,12-dihydrodiol with V79 cells stably expressing human P450 1A1 (cf. Figures 4A, 4B and 5B) provide strong evidence that the pathway(s) of successive oxidations at multiple sites of DB[*a,l*]P to form these polar DNA-binding metabolites include an epoxidation step at the 11,12-position.

The presence of highly polar DNA adducts together with DB[*a,l*]PDE-DNA adducts in V79 cells expressing human P450 1A1 (Figures 4A, 4B and 5B) and the absence of these polar DNA adducts in MCF-7 cells (*29,30*) and V79 cells expressing human P450 1B1 after exposure to DB[*a,l*]P or its 11,12-dihydrodiol (Figures 3B and 5A) suggests that human P450 1A1 is not induced in MCF-7 cells by treatment with low doses of DB[*a,l*]P and that the DB[*a,l*]PDE-DNA adducts found in MCF-7 cells result from activation of DB[*a,l*]P by human P450 1B1 which is constitutively expressed (*18*). Cai et al. (*59*) found that treatment of MCF-7 cells with DB[*a,l*]P increased the level of P450 1B1, but not the level of P450 1A1. The same result was obtained previously after incubation of MCF-7 cells or treatment of mouse skin with B[*c*]Ph (*60*). In contrast, treatment of MCF-7 cells with B[*a*]P induced both P450 1B1 and P450 1A1 (*59*). Typical inducers of P450 1A isoforms have been demonstrated to possess a large molecular area/depth ratio as a requirement for sufficient binding of the Ah receptor to cause induction of P450 1A enzymes (*61,62*). This requirement is fulfilled by compounds like 2,3,7,8-tetrachloro-dibenzo-*p*-dioxin (TCDD), MC or planar PAH like B[*a*]P or DB[*a,h*]A (*61,62*). In contrast, non-planar compounds with a small area/depth ratio have limited ability to induce P450 1A1; however, they have been shown to induce other P450 isoforms via an Ah receptor-independent pathway, e.g. members of the P450 2B subfamily which are preferentially involved in biotransformation of non-planar bulky compounds (*61,62*). Molecules containing a sterically hindered fjord region such as B[*c*]Ph and DB[*a,l*]P exhibit an out-of plane distortion due to repulsive hydrogen interactions (*63*), thus, differences in the induction of P450 1A1 by B[*a*]P and DB[*a,l*]P might be due to their different ability to bind the Ah receptor. Further investigations are needed to clarify this point.

In conclusion, the present study demonstrates that the potent carcinogen DB[*a,l*]P is metabolically activated by human P450 1B1 very effectively via its (–)-(11*R*,12*R*)-dihydrodiol to the DNA-binding fjord region (–)-*anti*-DB[*a,l*]PDE. Small amounts of (+)-*syn*-DB[*a,l*]PDE-DNA adducts are detectable only after exposure to high concentrations of the parent compound. Studies of V79 cells expressing human P450 1A1 have demonstrated that this isoform is also able to catalyze the formation of large amounts of DB[*a,l*]PDE-DNA adducts as well as highly polar DNA adducts which may result from oxidations at both the 8,9- and 11,12-positions of the parent PAH. However, taking into account that P450 1A1 is virtually inactive in human

tissues in the absence of inducers (*64,65*), the similar DB[*a,l*]P-DNA adduct profiles obtained in V79 cells expressing human P450 1B1 and in human mammary carcinoma MCF-7 cells suggests that P450 1B1 may be responsible for activation of DB[*a,l*]P at low levels at which human exposure occurs.

Acknowledgements

This work was financially supported by the Deutsche Forschungsgemeinschaft grants DO 242/6 (J.D.) and SFB 302 (A.S.) and by NCI grants CA40228 and CA28825 (W.M.B.).

References

(1) Thakker, D. R., Levin, W., Yagi, H., Wood, A. W., Conney, A. H., and Jerina, D. M. (1988) Stereoselective biotransformation of polycyclic aromatic hydrocarbons to ultimate carcinogens. In *Stereochemical Aspects of Pharmacologically Active Compounds* (Wainer, A.W. and Dryer, D., Eds) pp 271-296, Marcel Dekker, New York.

(2) Jacob, J., Raab, G., Soballa, V., Schmalix, W. A., Grimmer, G., Greim, H., Doehmer, J., and Seidel, A. (1996) Cytochrome P450-mediated activation of phenanthrene in genetically engineered V79 Chinese hamster cells. *Environ. Toxicol. Pharmacol.* **1**, 1-11.

(3) Shimada, T., Martin, M. V., Pruess-Schwartz, D., Marnett, L., and Guengerich, F. P. (1989) Roles of individual human cytochrome P-450 enzymes in the bioactivation of benzo[*a*]pyrene, 7,8-dihydroxy-7,8-dihydrobenzo[*a*]pyrene, and other dihydrodiol derivatives of polycyclic aromatic hydrocarbons. *Cancer Res.* **49**, 6304-6312.

(4) Shou, M., Korzekwa, K. R., Crespi, C. L., Gonzalez, F. J., and Gelboin, H. V. (1994) The role of 12 cDNA-expressed human, rodent, and rabbit cytochromes P450 in the metabolism of benzo[*a*]pyrene and benzo[*a*]pyrene *trans*-7,8-dihydrodiol. *Mol. Carcinog.* **10**, 159-168.

(5) Shou, M., Krausz, K. W., Gonzalez, F. J., and Gelboin, H. V. (1996) Metabolic activation of the potent carcinogen dibenzo[*a,l*]pyrene by human recombinant cytochromes P450, lung and liver microsomes. *Carcinogenesis (London)* **17**, 2429-2433.

(6) Shou, M., Krausz, K. W., Gonzalez, F. J., and Gelboin, H. V. (1996) Metabolic activation of the potent carcinogen dibenz[*a,h*]anthracene by cDNA-expressed human cytochromes P450. *Arch. Biochem. Biophys.* **328**, 201-207.

(7) Doehmer, J., and Greim, H. (1993) Cytochromes P450 in genetically engineered cell cultures: the gene technological approach. In *Cytochrome P450* (Schenkman, J.B. and Greim, H., Eds) pp 415-425, Springer-Verlag, Berlin.

(8) Doehmer, J. (1993) V79 Chinese hamster cells genetically engineered for cytochrome P450 and their use in mutagenicity and metabolism studies. *Toxicology* **82**, 105-118.

(9) Shen, Z., Liu, J., Wells, R. L., and Elkind, M. M. (1994) cDNA cloning, sequence analysis, and induction by aryl hydrocarbons of a murine cytochrome P450 gene, Cyp1b1. *DNA Cell Biol.* **13**, 763-769.

(10) Savas, U., Bhattacharyya, K. K., Christou, M., Alexander, D. L., and Jefcoate, C. R. (1994) Mouse cytochrome P450EF, representative of a new 1B subfamily of cytochrome P-450s: cloning, sequence determination, and tissue expression. *J. Biol. Chem.* **269**, 14905-14911.

(11) Pottenger, L. H., and Jefcoate, C. R. (1990) Characterization of a novel cytochrome P450 from the transformable cell line, C3H/10T1/2. *Carcinogenesis (London)* **11**, 321-327.

(12) Bhattacharyya, K. K., Brake, P. B., Eltom, S. E., Otto, S. A., and Jefcoate, C. R. (1995) Identification of a rat adrenal cytochrome P450 active in polycyclic aromatic hydrocarbon metabolism as rat CYP1B1: demonstration of a unique tissue specific pattern of hormonal and aryl hydrocarbon receptor-linked regulation. *J. Biol. Chem.* **270**, 11595-11602.

(13) Walker, N., Gastel, J. A., Costa, L. T., Clark, G. C., Lucier, G. W., and Sutter, T. (1995) Rat CYP1B1: an adrenal cytochrome P450 that exhibits sex-dependent expression in livers and kidneys of TCDD-treated animals. *Carcinogenesis (London)* **16**, 1319-1327.

(14) Sutter, T. R., Tang, Y. M., Hayes, C. L., Wo, Y. Y. P., Jabs, E. W., Li, X., Yin, H., Cody, C. W., and Greenlee, W. F. (1994) Complete cDNA sequence of a human dioxin-inducible mRNA identifies a new gene subfamily of cytochrome P450 that maps to chromosome 2. *J. Biol. Chem.* **269**, 13092-13099.

(15) Tang, Y. M., Wo, Y.-Y. P., Stewart, J., Hawkins, A. L., Griffin, C. A., Sutter, T. R., and Greenlee, W. F. (1996) Isolation and characterization of the human cytochrome P450 CYP1B1 gene. *J. Biol. Chem.* **271**, 28324-28330.

(16) Shimada, T., Hayes, C. L., Yamazaki, H., Amin, S., Hecht, S. S., and Guengerich, F. P. (1996) Activation of chemically diverse procarcinogens by human cytochrome P-450 1B1. *Cancer Res.* **56**, 2979-2984.

(17) Christou, M., Savas, U., Schroeder, S., Shen, X., Thompson, T., Gould, M. N., and Jefcoate, C. R. (1995) Cytochromes CYP1A1 and CYP1B1 in the rat mammary gland:

Cell-specific expression and regulation by polycyclic aromatic hydrocarbons and hormones. *Mol. Cell. Endocrinology* **115**, 41-50.

(18) Christou, M., Savas, Ü., Spink, D. C., Gierthy, J. F., and Jecoate, C. R. (1994) Co-expression of human CYP1A1 and human analog of cytochrome P450-EF in response to 2,3,7,8-tetrachloro-dibenzo-p-dioxin in the human mammary carcinoma-derived MCF-7 cells. *Carcinogenesis (London)* **15**, 725-732.

(19) Otto, S., Bhattacharyya, K. K., and Jefcoate, C. R. (1995) Polycyclic aromatic hydrocarbon metabolism in rat adrenal, ovary, and testis microsomes is catalyzed by the same novel cytochrome P450 (P450RAP). *Endocrinology* **131**, 3067-3076.

(20) Seidel, A., Soballa, V. J., Raab, G., Frank, H., Greim, H., Grimmer, G., Jacob, J., and Doehmer, J. (1997) Regio- and stereoselectivity in the metabolism of benzo[*c*]phenanthrene mediated by genetically engineered V79 Chinese hamster cells expressing rat and human cytochromes P450. *Environ. Toxicol. Pharmacol.*, in press.

(21) Snook, M. E., Severson, R. F., Arrendale, R. F., Higman, H. C., and Chortyk, O. T. (1977) The identification of high molecular weight polynuclear aromatic hydrocarbons in a biologically active fraction of cigarette smoke condensate. *Beitr. Tabakforsch.* **9**, 79-101.

(22) Kozin, I. S., Gooijer, C., and Velthorst, N. H. (1995) Direct determination of dibenzo[*a,l*]pyrene in crude extracts of environmental samples by laser excited Shpol'skii spectroscopy. *Anal. Chem.* **67**, 1623-1626.

(23) DeRatt, W. K., Kooijman, S. A. L. M., and Gielen, J. W. J. (1987) Concentrations of polycyclic hydrocarbons in airborne particles in Netherlands and their correlation with mutagenicity. *Sci. Total. Environ.* **66**, 95-114.

(24) Mumford, J. L., Harris, D. B., Williams, K., Chuang, J. C., and Cooke, M. (1987) Indoor air samling and mutagenicity studies of emissions from unvented coal combustion. *Environ. Sci. Technol.* **21**, 308-311.

(25) Mumford, J. L., Xueming, L., Fuding, H., Xu, B. L., and Chuang, J. C. (1995) Human exposure and dosimetry of polycyclic aromatic hydrocarbons in urine from Xuan Wei, China with high lung cancer mortality associated with exposure to unvented coal smoke. *Carcinogenesis (London)* **16**, 3031-3036.

(26) Cavalieri, E. L., Higginbotham, S., RamaKrishna, N. V. S., Devanesan, P. D., Todorovic, R., Rogan, E. G., and Salmasi, S. (1991) Comparative dose-response tumorigenicity studies of dibenzo[*a,l*]pyrene versus 7,12-dimethylbenz[*a*]anthracene, benzo[*a*]pyrene and two dibenzo[*a,l*]pyrene dihydrodiols in mouse skin and rat mammary gland. *Carcinogenesis (London)* **12**, 1939-1944.

(27) Higginbotham, S., RamaKrishna, N. V. S., Johansson, S. L., Rogan, E. G., and Cavalieri, E. L. (1993) Tumor-initiating activity and carcinogenicity of dibenzo[*a,l*]pyrene versus 7,12-dimethylbenz[*a*]anthracene and benzo[*a*]pyrene at low doses in mouse skin. *Carcinogenesis (London)* **14**, 875-878.

(28) LaVoie, E. J., He, Z.-M., Meegalla, R. L., and Weyand, E. H. (1993) Exceptional tumor-initiating activity of 4-fluorobenzo[*j*]fluoranthene on mouse skin: comparison with benzo[*j*]fluoranthene, 10-fluorobenzo[*j*]fluoranthene, benzo[*a*]pyrene, dibenzo[*a,l*]pyrene and 7,12-dimethylbenz[*a*]anthracene. *Cancer Lett.* **70**, 7-14.

(29) Ralston, S. L., Lau, H. H. S., Seidel, A., Luch, A., Platt, K. L., and Baird, W. M. (1994) The potent carcinogen dibenzo[*a,l*]pyrene is metabolically activated to fjord-region 11,12-diol 13,14-epoxides in human mammary carcinoma MCF-7 cell cultures. *Cancer Res.* **54**, 887-890.

(30) Ralston, S. L., Seidel, A., Luch, A., Platt, K. L., and Baird, W. M. (1995) Stereoselective activation of dibenzo[*a,l*]pyrene to (–)-*anti*(11*R*,12*S*,13*S*,14*R*)- and (+)-*syn*(11*S*,12*R*,13*S*,14*R*)-11,12-diol-13,14-epoxides which bind extensively to deoxyadenosine residues of DNA in the human mammary carcinoma cell line MCF-7. *Carcinogenesis (London)* **16**, 2899-2907.

(31) Li, K.-M., Todorovic, R., Rogan, E. G., Cavalieri, E. L., Ariese, F., Suh, M., Jankowiak, R., and Small, G. J. (1995) Identification and quantitation of dibenzo[*a,l*]pyrene-DNA adducts formed by rat liver microsomes *in vitro*: preponderance of depurination adducts. *Biochemistry* **34**, 8043-8049.

(32) Luch, A., Seidel, A., Glatt, H.-R., and Platt, K. L. (1997) Metabolic activation of the (+)-*S,S*- and (–)-*R,R*-enantiomers of *trans*-11,12-dihydroxy-11,12-dihydrodibenzo[*a,l*]-pyrene: stereoselectivity, DNA adduct formation, and mutagenicity in Chinese hamster V79 cells. *Chem. Res. Toxicol.* **10**, 1161-1170.

(33) Arif, J. M., and Gupta, R. C. (1997) Microsome-mediated bioactivation of dibenzo[*a,l*]pyrene and identification of DNA adducts by ^{32}P-postlabeling. *Carcinogenesis (London)* **18**, 1999-2007.

(34) Luch, A., Glatt, H.-R., Platt, K. L., Oesch, F., and Seidel, A. (1994) Synthesis and mutagenicity of the diastereomeric fjord-region 11,12-dihydrodiol 13,14-epoxides of dibenzo[*a,l*]pyrene. *Carcinogenesis (London)* **15**, 2507-2516.

(35) Amin, S., Desai, D., Dai, W., Harvey, R. G., and Hecht, S. S. (1995) Tumorigenicity in newborn mice of fjord region and other sterically hindered diol epoxides of benzo[*g*]chrysene, dibenzo[*a,l*]pyrene (dibenzo[*def,p*]chrysene), 4H-cyclopenta[*def*]-chrysene and fluoranthene. *Carcinogenesis (London)* **16**, 2813-2817.

(36) Amin, S., Krzeminski, J., Rivenson, A., Kurtzke, C., Hecht, S. S., and El-Bayoumy, K. (1995) Mammary carcinogenicity in female CD rats of fjord region diol epoxides of benzo[*c*]phenanthrene, benzo[*g*]chrysene and dibenzo[*a,l*]pyrene. *Carcinogenesis (London)* **16**, 1971-1974.

(37) Gill, H. S., Kole, P. L., Wiley, J. C., Li, K. M., Higginbotham, S., Rogan, E. G., and Cavalieri, E. L. (1994) Synthesis and tumor-initiating activity in mouse skin of dibenzo[*a,l*]pyrene *syn*- and *anti*-fjord-region diolepoxides. *Carcinogenesis (London)* **15**, 2455-2460.

(38) Ralston, S. L., Coffing, S. L., Seidel, A., Luch, A., Platt, K. L., and Baird, W. M. (1997) Stereoselective activation of dibenzo[*a,l*]pyrene and its *trans*-11,12-dihydrodiol to fjord region 11,12-diol 13,14-epoxides in a human mammary carcinoma MCF-7 cell-mediated V79 cell mutation assay. *Chem. Res. Toxicol.* **10**, 687-693.

(39) Frank, H., Luch, A., Oesch, F., and Seidel, A. (1996) 4-[4-(Dimethylamino)-phenylazo]benzoate, a new red-shifted chromophore for use in the exciton chirality method: assignment of absolute configuration to fjord-region metabolites of dibenzo[*a,l*]pyrene. *Polycycl. Aromat. Compd.* **10**, 109-116.

(40) Glatt, H.-R., Gemperlein, I., Turchi, G., Heinritz, H., Doehmer, J., and Oesch, F. (1987) Search for cell culture systems with diverse xenobiotic-metabolizing activities and their use in toxicological studies. *Mol. Toxicol.* **1**, 313-334.

(41) Doehmer, J., Dogra, S., Friedberg, T., Monier, S., Adesnik, M., Glatt, H.-R., and Oesch, F. (1988) Stable expression of rat cytochrome P-450IIB1 cDNA in Chinese hamster cells (V79) and metabolic activation of aflatoxin B_1. *Proc. Natl. Acad. Sci. USA* **85**, 5769-5773.

(42) Schneider, A., Schmalix, W. A., Siruguri, V., de Groene, E. M., Horbach, G. J., Kleingeist, B., Lang, D., Boecker, R., Belloc, C., Beaune, P., Greim, H., and Doehmer, J. (1996) Stable expression of human cytochrome P450 3A4 in conjunction with human NADPH-cytochrom P450 oxidoreductase in V79 Chinese hamster cells. *Arch. Biochem. Biophys.* **332**, 295-304.

(43) Graham, F. L., and Van der Eb, A. J. (1973) A new technique for the assay of infectivity of human adenovirus 5 DNA. *Virology* **52**, 456-467.

(44) Schmalix, W. A., Lang, D., Schneider, A., Bocker, R., Greim, H., and Doehmer, J. (1996) Stable expression and coexpression of human cytochrome P450 oxidoreductase and cytochrome P450 1A2 in V79 Chinese hamster cells: sensitivity to quinons and biotransformation of 7-alkoxyresorufins and triazines. *Drug Metab. Disp.* **24**, 1314-1319.

(45) Lau, H. H. S., and Baird, W. M. (1991) Detection and identification of benzo[*a*]pyrene-DNA adducts by [^{35}S]phosphorothioate labeling and HPLC. *Carcinogenesis (London)* **12**, 885-893.

(46) Devanesan, P. D., Cremonesi, P., Nunnally, J. E., Rogan, E. G., and Cavalieri, E. L. (1990) Metabolism and mutagenicity of dibenzo[*a,e*]pyrene and the very potent environmental carcinogen dibenzo[*a,l*]pyrene. *Chem. Res. Toxicol.* **3**, 580-586.

(47) Parkinson, A., Safe, S. H., Robertson, L. W., Thomas, P. E., Ryan, D. E., Reik, L. M., and Levin, W. (1983) Immunochemical quantitation of cytochrome P-450 isozymes and epoxide hydrolase in liver microsomes from polychlorinated or polybrominated biphenyl-treated rats. *J. Biol. Chem.* **258**, 5967-5976.

(48) Thomas, P. E., Reik, L. M., Ryan, D. E., and Levin, W. (1983) Induction of two immunochemically related rat liver cytochrome P-450 isozymes, cytochromes P-450c and P-450d, by structurally diverse xenobiotics. *J. Biol. Chem.* **258**, 4590-4598.

(49) Nesnow, S., Davis, C., Nelson, G., Ross, J. A., Allison, J., Adams, L., and King, L. C. (1997) Comparison of the morphological transforming activities of dibenzo[*a,l*]pyrene and benzo[*a*]pyrene in C3H10T1/2CL8 cells and characterization of the dibenzo[*a,l*]-pyrene-DNA adducts. *Carcinogenesis (London)* **18**, 1973-1978.

(50) Prahalad, A. K., Ross, J. A., Nelson, G. B., Roop, B. C., King, L. C., Nesnow, S., and Mass, M. J. (1997) Dibenzo[*a,l*]pyrene-induced DNA adduction, tumorigenicity, and Ki-*ras* oncogene mutations in strain A/J mouse lung. *Carcinogenesis (London)* **18**, 1955-1963.

(51) Crespi, C. L., Penman, B. W., Steimel, D. T., Smith, T., Yang, C. S., and Sutter, T. R. (1997) Development of a human lymphoblastoid cell line constitutively expressing human CYP1B1 cDNA: substrate specificity with model substrates and promutagens. *Mutagenesis* **12**, 83-89.

(52) Sayer, J. M., Yagi, H., Silverton, J. V., Friedman, S. L., Whalen, D. L., and Jerina, D. M. (1982) Conformational effects in the hydrolyses of rigid benzylic epoxides: implications for diol epoxides of polycyclic hydrocarbons. *J. Am. Chem. Soc.* **104**, 1972-1978.

(53) Sayer, J. M., Whalen, D. L., Friedman, S. L., Paik, A., Yagi, H., Vyas, K. P., and Jerina, D. M. (1984) Conformational effects in the hydrolysis of benzo-ring diol epoxides that have bay-region diol groups. *J. Am. Chem. Soc.* **106**, 226-233.

(54) Nesnow, S., Davis, C., Padgett, W., George, M., Lambert, G., Adams, L., and King, L. (1997) Biotransformation and DNA adduct formation of 8,9-dihydroxy-8,9-dihydrodibenzo[*a,l*]pyrene by induced rat liver and human CYP1A1 and CYP1B1 microsomes. *16th International Symposium on Polycyclic Aromatic Compounds*, November 4-8, Charlotte, North Carolina, USA.

(55) Dock, L., Waern, F., Martinez, M., Grover, P. L., and Jernstrom, B. (1986) Studies on the further activation of benzo[*a*]pyrene diol epoxides by rat liver microsomes and nuclei. *Chem.-Biol. Interact.* **58**, 301-318.

(56) Carmichael, P. L., Platt, K. L., Shé, M. N., Lecoq, S., Oesch, F., Phillips, D. H., and Grover, P. L. (1993) Evidence for the involvement of a bis-diol-epoxide in the metabolic activation of dibenz[*a,h*]anthracene. *Cancer Res.* **53**, 944-948.

(57) Fuchs, J., Mlcoch, J., Platt, K. L., and Oesch, F. (1993) Characterization of highly polar bis-dihydrodiol epoxide-DNA adducts formed after metabolic activation of dibenz[*a,h*]-anthracene. *Carcinogenesis (London)* **14**, 863-867.

(58) Marsch, G. A., Jankowiak, R., Small, G. J., Hughes, N. C., and Phillips, D. H. (1992) Evidence of involvement of multiple sites of metabolism in the in vivo covalent binding of dibenzo[*a,h*]pyrene to DNA. *Chem. Res. Toxicol.* **5**, 765-772.

(59) Cai, Y., Marcus, C., Guengerich, F. P., Gelboin, H. V., and Baird, W. M. (1997) Roles of cytochrome P450 1A1 and 1B1 in metabolic activation of dibenzo[*a,l*]pyrene by microsomes from the human mammary carcinoma cell line MCF-7. *16th International Symposium on Polycyclic Aromatic Compounds*, November 4-8, Charlotte, North Carolina, USA.

(60) Einolf, H. J., Story, W. T., Marcus, C. B., Larsen, M. C., Jefcoate, C. R., Greenlee, W. F., Yagi, H., Jerina, D. M., Amin, S., Park, S. S., Gelboin, H. V., and Baird, W. M. (1997) Role of cytochrome P450 enzyme induction in the metabolic activation of benzo[*c*]phenanthrene in human cell lines and mouse epidermis. *Chem. Res. Toxicol.* **10**, 609-617.

(61) Ioannides, C., and Parke, D. V. (1993) Induction of cytochrome P4501 as an indicator of potential chemical carcinogenesis. *Drug Metab. Rev.* **25**, 485-501.

(62) Ioannides, C., and Parke, D. V. (1990) The cytochrome P450 I gene familiy of microsomal hemoproteins and their role in the metabolic activation of chemicals. *Drug Metab. Rev.* **22**, 1-85.

(63) Hirshfeld, F. L. (1963) The structure of overcrowded aromatic compounds. Part VII. Out-of plane deformation in benzo[*c*]phenanthrene and 1,12-dimethylbenzo[*c*]-phenanthrene. *J. Chem. Soc.* 2126-2135.

(64) Guengerich, F. P., and Shimada, T. (1991) Oxidation of toxic and carcinogenic chemicals by human cytochrome P-450 enzymes. *Chem. Res. Toxicol.* **4**, 391-407.

(65) Gonzalez, F. J. (1993) Cytochromes P450 in humans. In *Cytochrome P450* (Schenkman, J.B. and Greim, H., Eds) pp 239-257, Springer-Verlag, Berlin.

(66) Döhr, O., Vogel, C., and Abel, J. (1995) Different response of 2,3,7,8-tetrachloro-dibenzo-*p*-dioxin (TCDD)-sensitive genes in human breast cancer MCF-7 and MDA-MB 231 cells. *Arch. Biochem. Biophys.* **321**, 405-412.

Table 1. EROD Activities in Lysates from Parental V79 Cells and Newly Constructed V79 Cell Clones Stably Expressing Human P450 1B1 Alone or Together With Human NADPH-P450 Reductase (cf. Figure 2).[a]

V79 cell clone	EROD pmol/min/mg
parental V79 cells	0
V79 cell clone #1	1.83 ± 0.03
V79 cell clone #2	3.59 ± 0.15
V79 cell clone #3	3.15 ± 0.16
V79 cell clone #4	8.06 ± 0.32
V79 cell clone #5	11.5 ± 0.9
V79 cell clone #6*	5.11 ± 0.36
V79 cell clone #7	3.24 ± 0.10
V79Mz-h1A1*	22.0 ± 0.9
MCF-7 cells**	11.3 ± 4.7

[a] EROD data represent the mean of three experiments ± difference of single measurements from the mean. They were calculated from the fluorescence after 30 minutes of incubation. *These clones have been used in the present study. **EROD activity was detectable after induction with 10 nM TCDD only (*66*).

Table 2. Total DNA Binding in V79 Chinese Hamster Cells Stably Expressing one Cytochrome P450 6 h or 24 h after Exposure to DB[*a*,*l*]P, (–)-(11*R*,12*R*)-DB[*a*,*l*]P-Dihydrodiol, or (+)-(11*S*,12*S*)-DB[*a*,*l*]P-Dihydrodiol.[a]

compound [μM]	human P450 1B1		human P450 1A1		rat P450 1A1		human P450 3A4	rat P450 1A2
	6 h	24 h	6 h	24 h	6 h	24 h	24 h	24 h
DB[*a*,*l*]P								
0.01					1.5 (1.7)	4.8 (5.0)		
0.1	370	350	6.0 (35)	6.8 (27)	7.9 (9.0)	23 (28)		
1.0	430	280	142 (232)	127 (169)	9.6 (9.6)	140 (145)	0.1	17
5.0	84	433	522 (602)	1380 (1560)	n.t.	n.t.		
(–)-(11*R*,12*R*)-dihydrodiol								
0.005	18	22	n.t.	n.t.	28 (35)	34 (40)		
0.05	506	1010	31 (130)	49 (175)	252 (310)	393 (490)		
0.5	1650	1680	1560 (1990)	2430 (3000)	929 (1000)	1340 (1350)	6.5	4.0
1.0	n.t.	n.t.	2180 (2400)	3250 (3560)	n.t.	n.t.		
(+)-(11*S*,12*S*)-dihydrodiol								
0.5	n.t.	n.t.	n.t.	4.4	n.t.	2.5	1.8	6.0

[a] All data presented are reported in pmol adducts/mg DNA. Values represent adducts of DB[*a*,*l*]PDE; values in parenthesis represent all adducts found including both those of DB[*a*,*l*]PDE and those of more polar character (see Figures 4 and 5). n.t. not tested

Legends

Scheme 1. Stereoselective Bioactivation of Dibenzo[*a,l*]pyrene to the Fjord Region 11,12-Dihydrodiol 13,14-Epoxides, Catalyzed by Cytochromes P450 (P450) and Microsomal Epoxide Hydrolase (mEH).[a]

[a] The picture includes activation to the diastereomeric (+)-*syn*- and (–)-*anti*-11,12-dihydrodiol 13,14-epoxides, which are exclusively formed during metabolism of dibenzo[*a,l*]pyrene in MCF-7 cells via the enantiomeric (+)-(11*S*,12*S*)- and (–)-(11*R*,12*R*)-dihydrodiols, respectively (*30*). Arrow indicates the sterically hindered fjord region of the parent compound.

Figure 1. Recombinant eukaryotic expression vector pRC/CMV-h1B1, containing the cytomegalo virus (CMV) promotor attached to the human P450 1B1 cDNA (h1B1) and the selectable marker gene neomycin phosphotransferase (neo).

Figure 2. Western blot analysis of the V79 cell clones obtained after individual transfection or cotransfection with plasmid sequences containing the human P450 1B1 and human NADPH-P450 reductase gene, respectively (cf. Table 1). Experimental conditions are described in Experimental Procedures. Lane 1: positive control for human P450 1B1; Lane 2: parental V79 cell line (*40*); Lanes 3-7 and 9: different V79 cell clones (#1-5 and #7) stably expressing human P450 1B1; Lane 8: V79 cell clone (#6: V79MZ-h1B1) stably coexpressing human P450 1B1 and human NADPH-P450 reductase; Lane 10: positive control for human NADPH-P450 reductase.

Figure 3. HPLC elution profiles of ^{33}P-labeled DNA adducts of DB[*a,l*]P formed in V79 Chinese hamster cells stably expressing the human P450 1B1 enzyme (V79MZ-h1B1) 6 h after treatment with 0.1 μM (A) or 1.0 μM (B) of DB[*a,l*]P. DNA adducts of the (–)-*anti*-DB[*a,l*]PDE (peaks 1, 2a, 2b, and 4) and (+)-*syn*-DB[*a,l*]PDE (peaks 3 and 6) were previously identified by cochromatography with authentic standards (*30*). HPLC conditions are described in Experimental Procedures.

Figure 4. HPLC elution profiles of ^{33}P-labeled DNA adducts of DB[*a*,*l*]P formed in V79 Chinese hamster cells stably expressing the human P450 1A1 enzyme (V79MZ-h1A1) or the rat P450 1A1 enzyme (V79MZ-r1A1). (A) DNA adducts formed in V79MZ-h1A1 cells 6 h after treatment with 0.1 μM DB[*a*,*l*]P. (B) DNA adducts formed in V79MZ-h1A1 cells 6 h after treatment with 1.0 μM DB[*a*,*l*]P. (C) DNA adducts formed in V79MZ-r1A1 cells 6 h after treatment with 0.1 μM DB[*a*,*l*]P. Highly polar unidentified DB[*a*,*l*]P-DNA adducts are labeled with Roman numerals. HPLC conditions are described in Experimental Procedures.

Figure 5. HPLC elution profiles of ^{33}P-labeled DNA adducts of the (–)-(11*R*,12*R*)-dihydrodiol of DB[*a*,*l*]P formed in V79 Chinese hamster cells stably expressing the human P450 1B1 enzyme (V79MZ-h1B1) or the human P450 1A1 enzyme (V79MZ-h1A1). (A) DNA adducts formed in V79MZ-h1B1 cells 6 h after treatment with 0.005 μM (–)-DB[*a*,*l*]P-11,12-dihydrodiol. (B) DNA adducts formed in V79MZ-h1A1 cells 6 h after treatment with 0.05 μM (–)-DB[*a*,*l*]P-11,12-dihydrodiol. (C) DNA adducts formed in V79MZ-h1A1 cells 6 h after treatment with 0.5 μM (–)-DB[*a*,*l*]P-11,12-dihydrodiol. Highly polar unidentified DB[*a*,*l*]P-DNA adducts are labeled with Roman numerals. HPLC conditions are described in Experimental Procedures.

Scheme 1

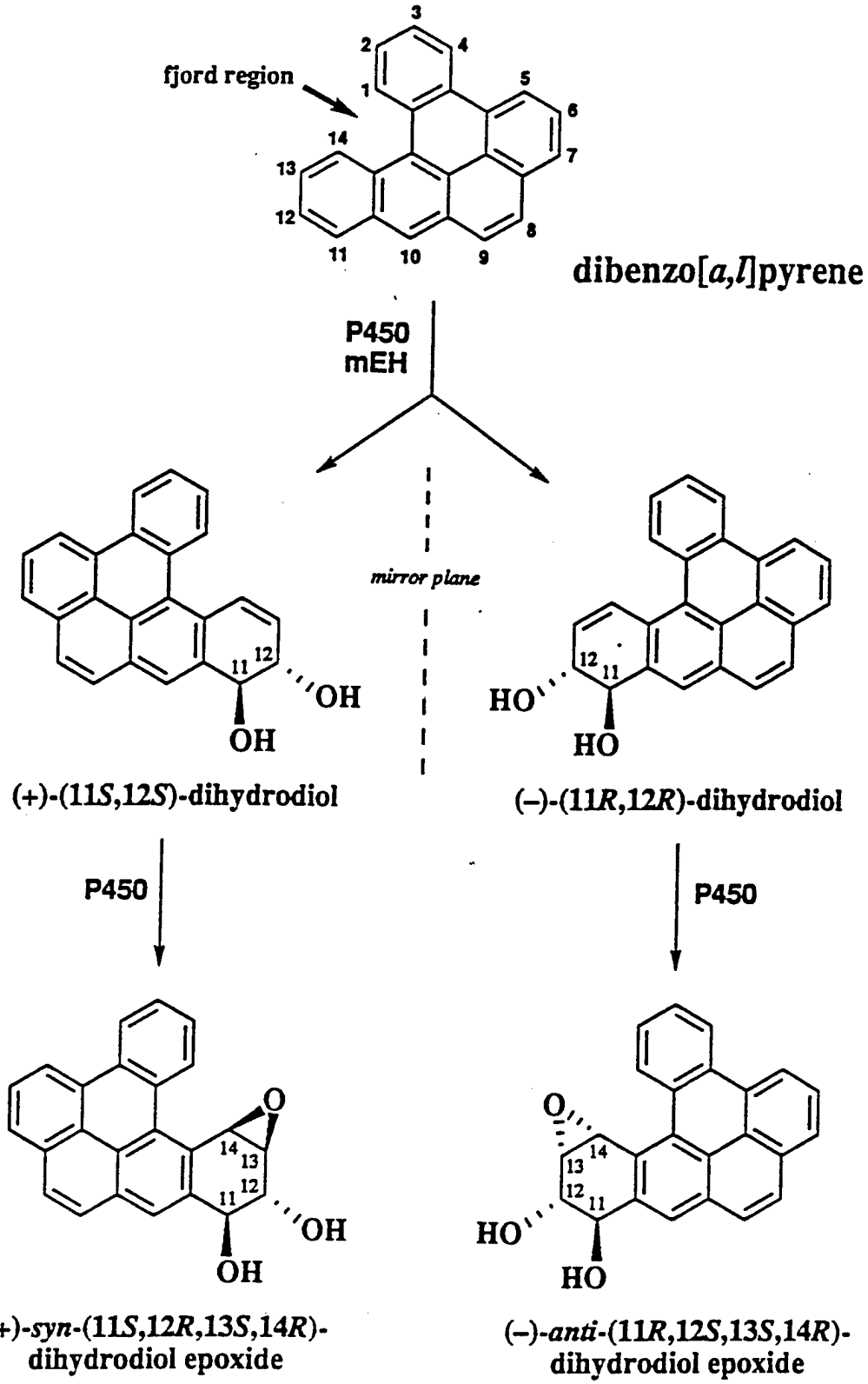
fjord region
dibenzo[a,l]pyrene
P450
mEH
mirror plane
(+)-(11S,12S)-dihydrodiol
(–)-(11R,12R)-dihydrodiol
P450
P450
(+)-syn-(11S,12R,13S,14R)-
dihydrodiol epoxide
(–)-anti-(11R,12S,13S,14R)-
dihydrodiol epoxide

Fig 1

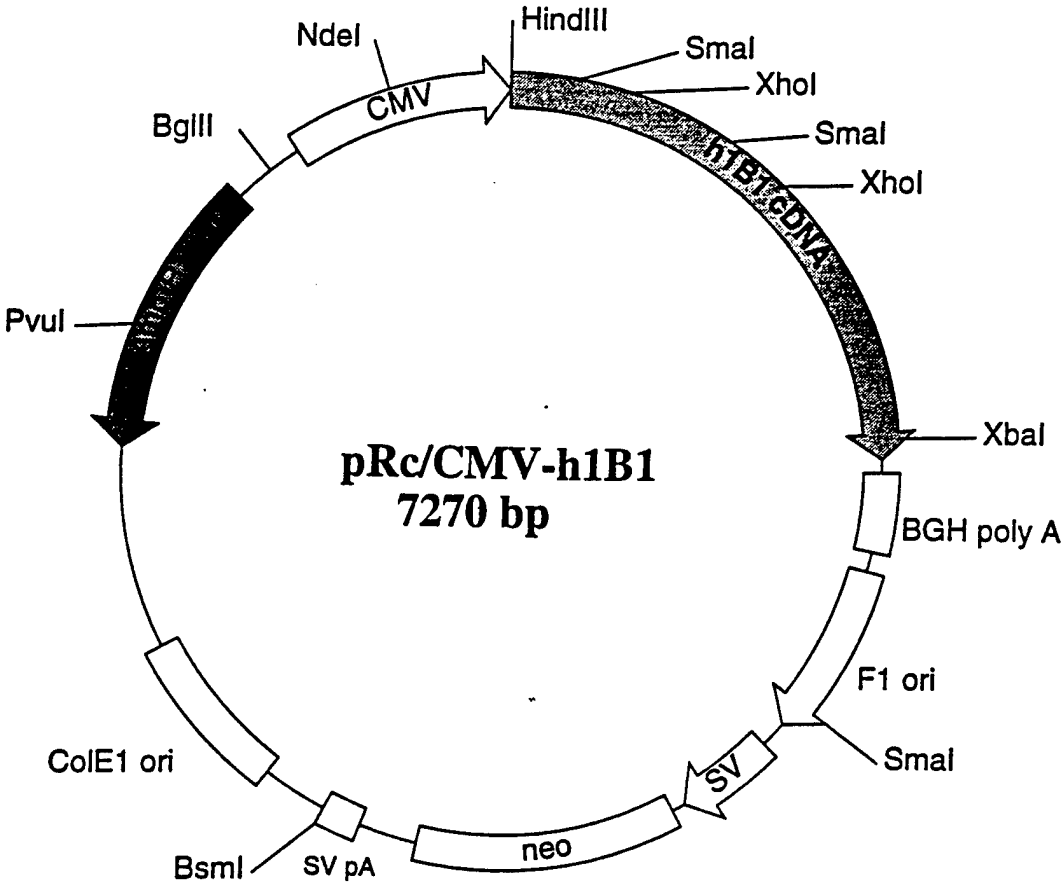
NdeI
HindIII
SmaI
XhoI
BglII
CMV
SmaI
h1B1 cDNA
XhoI
PvuI
XbaI
pRc/CMV-h1B1
7270 bp
BGH poly A
F1 ori
SmaI
SV
ColE1 ori
neo
BsmI
SV pA

Fig. 2

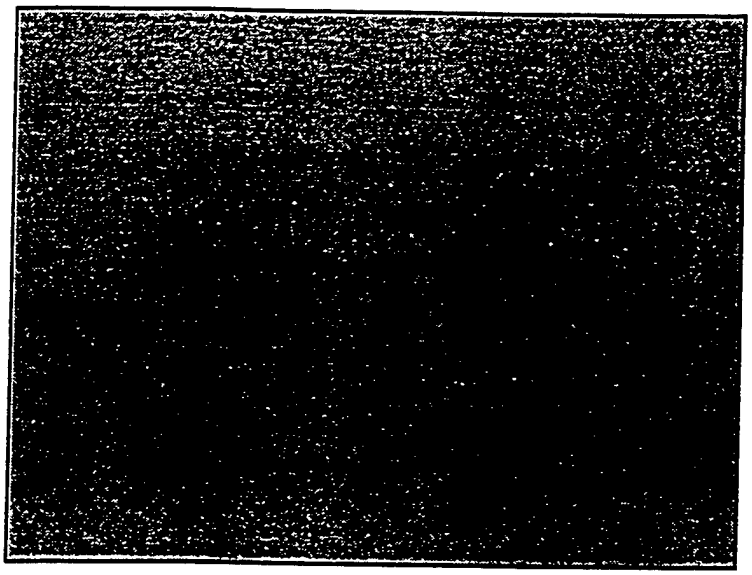

Fig. 3

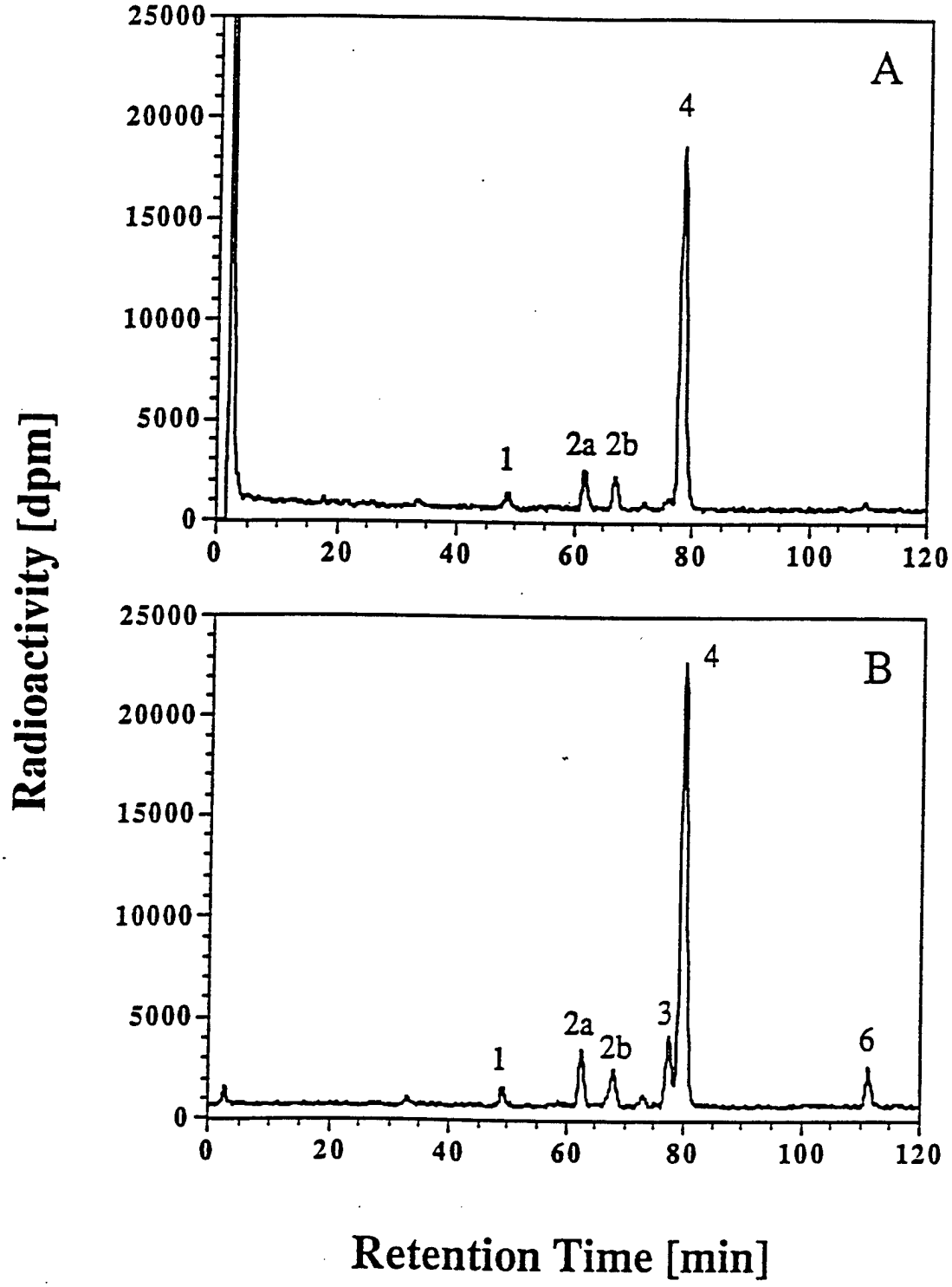
A
B
1
2a
2b
3
4
6
Radioactivity [dpm]
Retention Time [min]
0
5000
10000
15000
20000
25000
0
20
40
60
80
100
120

Fig. 4

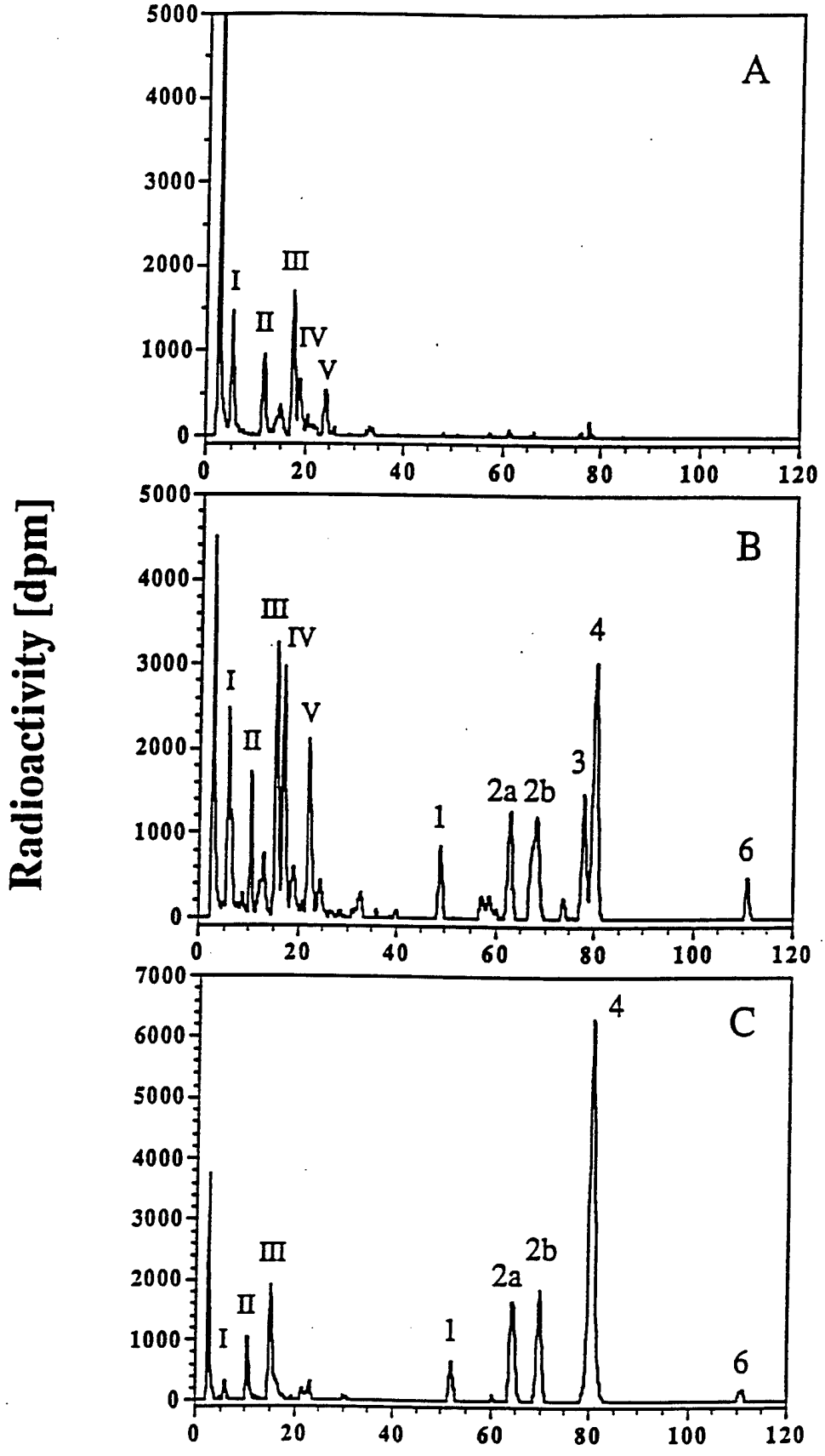
A
B
C
I
II
III
IV
V
1
2a
2b
3
4
6
Radioactivity [dpm]
Retention Time [min]

Fig. 5

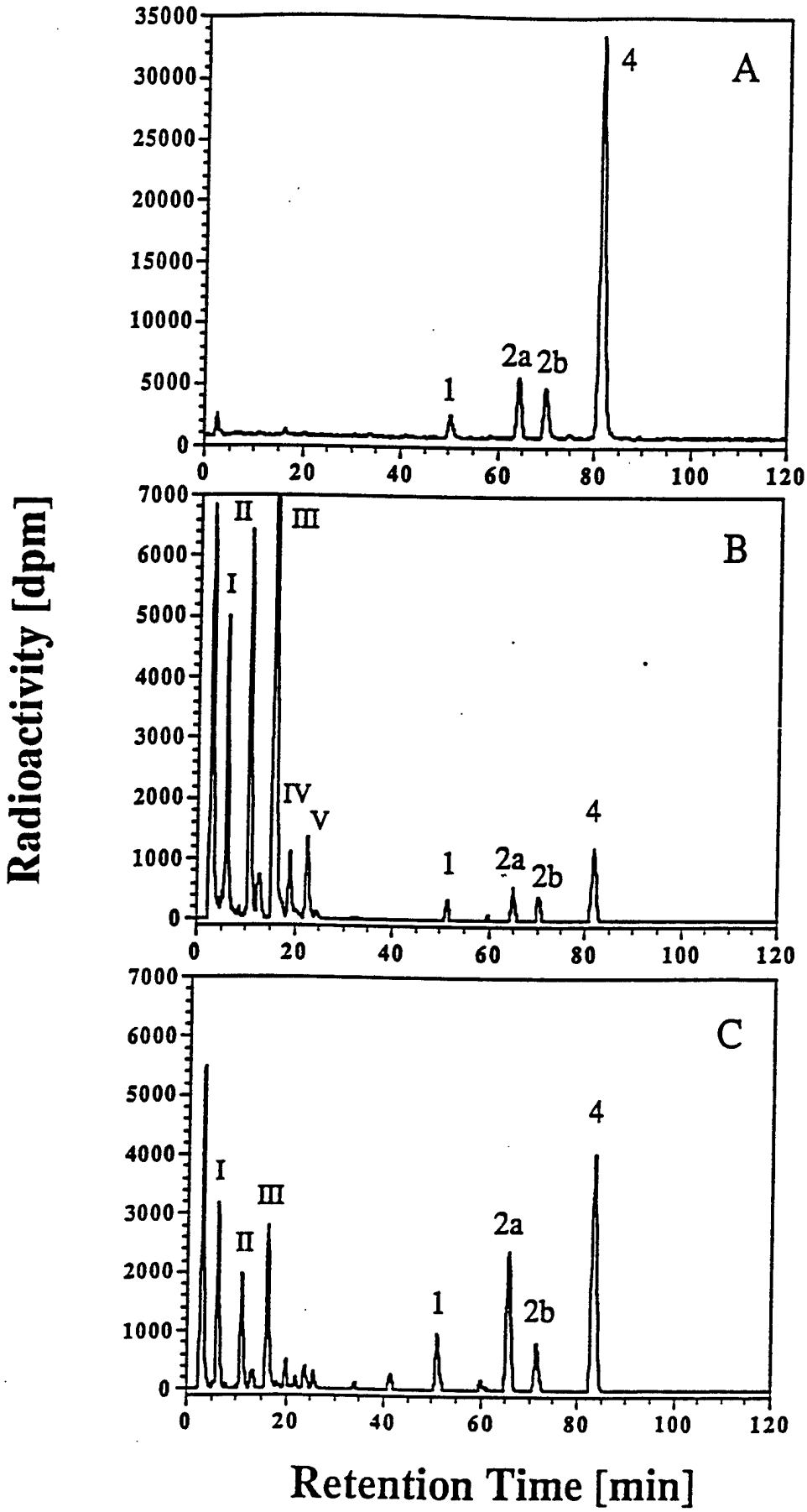
A
4
2a
2b
1
B
I
II
III
IV
V
1
2a
2b
4
C
I
II
III
1
2a
2b
4
Radioactivity [dpm]
Retention Time [min]